University of Balearic Islands
Research Institute on Health Sciences

ON THE ROLE AND POTENTIAL USE OF PROLINE-RICH PEPTIDES IN BONE REGENERATION

Doctoral Thesis to achieve the Degree of

Doctor by the *University of Balearic Islands*

Programa de Doctorat de Ciències Biosociosanitàries
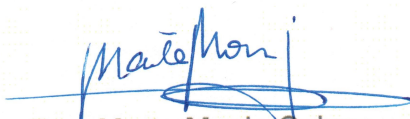*del Institut Universitari d'Investigació en Ciències de la Salut*

Presented by:
Marina Rubert Femenias

Palma, November 2012

Amb el vist-i-plau dels Directors

With the approval of the supervisors

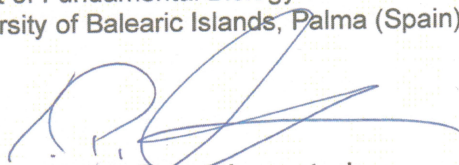Dra. Marta Monjo Cabrer
Ramón y Cajal researcher
Department of Fundamental Biology and Health Sciences
University of Balearic Islands, Palma (Spain)

Dra. Joana Mª Ramis Morey
Assistant professor,
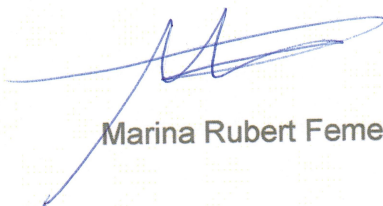Department of Fundamental Biology and Health Sciences
University of Balearic Islands, Palma (Spain)

Dr. Staale Petter Lyngstadaas
Prof., Head of Department of Biomaterials,
University of Oslo (Norway)

La interessada,

Marina Rubert Femenias

Agraïments/*Acknowledgments*

Els estudis presentats en aquesta tesi han estat duits a terme al Grup de Terapia Cel·lular i Enginyeria Tissular de l'Institut Universitari d'Investigació en Ciències de la Salut a la Universitat de les Illes Balears i al Departament de Biomaterials de la Facultat d'Odontologia a la Universitat d'Oslo. Vull agrair a totes aquelles persones que al llarg d'aquests anys han contribuït d'una manera o altra a aquesta feina.

En primer lloc, vull expressar la meva més sincera gratitud a les meves directores de tesi, la Dra. Marta Monjo i la Dra. Joana Mª Ramis per donar-me la oportunitat a embarcar-me dins el món de la ciència, per ensenyar-me ciència, per la seva gran competència científica i per transmetrer-me uns bons ideals de feina i de progrés. També els hi vull agraïr el seu suport i la confiança que han dipositat en jo, així com la oportunitat que m'han donat de participar en diversos estudis que han resultat en la publicació de varis articles i la assistència a diverses comunicacions orals. Tot això ha contribuït molt positivament en la meva trajectòria científica fet que m'ha aportat una major maduresa tant profesional com personal.

Thanks to my supervisor Prof. Dr. Staale Petter Lyngstadaas, for giving me the opportunity to work at his group in Oslo, for the welcoming and fruitful stay at his lab, that encouraged me to start a PhD program and further for his good ideas to improve and get a potential studies during my thesis.

I would like to thank the co-authors who contributed to my thesis: Antoni Gayà, Christiane Petzold, Haavard Haugen, Hanna Tianinen, Helen Pullisaar, Jiri Vondrasek, Manuel Gómez-Florit and Maria Alonso-Sande. Als meus companys Alba, Manu, Mar i Maria, per tot el que he après d'ells, per intercanviar coneixements i maneres de fer estudis i de treballar. En general a tots el companys de l'Edifici Científico-tècnic i del IUNICS per el seu suport científic per un bon desenvolupament dels estudis i per fer que les estonetes del dinar servissin d'un momentet de desconnexió. A na Marga, una bona amiga amb qui sempre he pogut comptar.

Vull agrair als meus pares i germans per animar-me a iniciar un doctorat i a continuar la meva trajectòria en investigació, tot i que això signifiqui estar lluny des meu redol. Al meu al·lot Michel pels seus bons consells i els seus ànims per afrontar nous reptes. Per sempre tenir un gran somriure que m'anima i em dóna energia, per la seva paciència i comprenssió i per respectar sempre amb bona cara la meva gran dedicació a la investigació.

A tots voltros, moltes gràcies.

Index

Abbreviations

Alkaline phosphatase	ALP
Ameloblastin	AMBN
Amelogenin	AMEL
Arg-gly-asp	RGD
Back-scattered electron detector	BSED
Bone morphogenic protein	BMP
Bone sialoprotein	BSP
Bromo-2'-deoxyuridine	BrdU
Cbfa-1	Core binding α-1
Collagen type I	Coll-I
Complementary deoxyribonucleic acid	cDNA
Confocal laser scanning microscopy	CLSM
Contact angle	CA
Crossing-point	Cp
Deionized	DI
Demineralized bone matrix	DBM
Deoxynucleotides triphosphates	dNTPs
Deoxyribonucleic acid	DNA
Diffuse reflectance infrared fourier transform spectroscopy	DRIFT
Double-strand DNA	dsDNA
Emdogain	EMD
Energy-dispersive X-Ray spectroscopy	EDS
Enzyme-Linked ImmunoSorbent Assay	ELISA
Extracellular matrix	ECM
Fibroblast growth factors	FGFs
Fibronectin	Fn
Fluorescein isothiocyanate	FITC
Fourier transform infrared spectroscopy	FTIR
Glyceraldehyede-3-phosphate dehydrogenase	GAPDH
Guluronic monomers	G monomers
Human umbilical cord mesenchymal stem cell	hUCMSC
Hyaluronic acid	HA
Inductively coupled atomic plasma emission spectroscopy	ICP-AES
Insulin-like growth factor	IGF
Integrin α8	Itga8
Integrin β1	Itgb1
Integrin β3	Itgb3

Interleukine-1	IL-1
Interleukine-10	IL-10
Interleukine-6	IL-6
Lactate dehydrogenase	LDH
Leucine-rich amelogenin peptide	LRAP
Macrophage stimulating colony factor	M-CSF
Mesenchymal stem cell	MSC
Microcomputed tomography	micro-CT
Minimum Information for Publication of Quantitative Real-Time PCR Experiments	MIQE
Osteoblast stimulating factor 1	OSF-1
Osteocalcin	OC
Osteonectin	ON
Osteopontin	OPN
Osterix	Osx
Phosphate buffer saline	PBS
Platelet derived growth factor	PDGF
p-Nitrophenyl phosphate	pNPP
Polymerase chain reaction	PCR
Polyproline II helical	PPII
Quantitative PCR	qPCR
Receptor activator NFκBLigand	RANKL
Reverse transcription polymerase chain reaction	RT-PCR
Ribonucleases protective assay	RPA
Ribonucleic acid	RNA
Ribosomal RNA 18S	18S
Room temperature	RT
Runt related gene	Runx2
Scaffold	SC
Scanning electron microscope	SEM
Secondary electron detector	ESED
Tartrate-resistant acid phosphatase	TRAP
Three-dimensional	3D
Tissue culture plastic	TCP
Titanium	Ti
Titanium dioxide	TiO_2
Tumor necrosis factor alpha	TNF-α
Ultraviolet	UV
Ultraviolet-visible	UV-Vis
Vascular endothelial growth factor	VEGF

ON THE ROLE AND POTENTIAL USE OF PROLINE-RICH PEPTIDES IN BONE REGENERATION

PhD thesis, Marina Rubert Femenias, Institut Universitari d'Investigació en Ciències de la Salut (IUNICS), Universitat de les Illes Balears, Palma de Mallorca, Spain

Abstract

Hard tissue formation is a process mediated by extracellular matrix proteins that often exhibit proline-rich regions. With the aim to find new treatments for bone repair, in this thesis we designed synthetic peptides based on consensus polyproline sequences of hard tissue extracellular matrix proteins involved in the regulation of biomineralization processes and evaluated their three dimensional structure *in silico*, determined their effect *in vitro,* alone or in combination with different biomaterials, and studied their performance *in vivo* on coated titanium implants.

The obtained results prove that synthetic proline-rich peptides have no toxic effects and stimulate osteoblast differentiation regardless to the means of administration or the cell type used. We hypothesized that synthetic proline-rich peptides might interact with a receptor (e.g. integrins) capable for influencing intracellular signaling cascades at the initial stages of cell differentiation to finally stimulate their differentiation. Among all the synthetic peptides, peptide 2 showed to exert the better biological activity, which might be due to the accessibility of the PPLPP sequences present at the C-terminal.

Furthermore, the synthetic peptides were used to coat different biomaterials, including hydrogels, scaffolds and endosseous titanium implants. The results derived from this thesis have demonstrated that synthetic peptides improve the osteogenic properties of those biomaterials either *in vitro* (alginate hydrogel, alginate-coated TiO_2 scaffolds) or *in vivo* (Ti implants). More specifically, synthetic peptides have shown to improve alginate properties for cell adhesion and, in consequence, cell proliferation and differentiation of cells cultured either onto an alginate hydrogel or alginate-coated TiO_2 scaffolds. Likewise, a higher percentage of new bone formation accompanied by decreased bone resorption was observed in peptide 2-modified Ti implants *in vivo*. Consequently, peptide 2-modified Ti implants have shown improved osseointegration properties *in vivo.*

All in all, results from this thesis prove that synthetic proline-rich peptides are osteopromotive when used in combination with alginate hydrogels, when contained into alginate-coated TiO_2 scaffolds or when coated on titanium implant surfaces. Thus, the designed synthetic peptides may represent a new strategy for bone regeneration treatment in different applications.

FUNCIÓ I ÚS POTENCIAL DE PÈPTIDS RICS EN PROLINES EN LA REGENERACIÓ ÒSSIA

Tesi doctoral, Marina Rubert Femenias, Institut Universitari d'Investigació en Ciències de la Salut (IUNICS), Universitat de les Illes Balears, Palma de Mallorca, Spain

Resum

La formació dels teixits durs és un procés regulat per proteïnes de la matriu extracel·lular, comunment riques en prolines. Amb l'objectiu de trobar noves estratègies per a la regeneració òssia, en aquesta tesi es dissenyaren pèptids sintètics amb una seqüència consens rica en prolines anàloga a diferents proteïnes de la matriu extracel·lular de teixits durs implicades en la regulació dels processos de biomineralització; i es determinà la seva estructura tridimensional *in silico*, el seu efecte *"in vitro"*, individual o en combinació amb diferents biomaterials, i l'efecte *"in vivo"* en implants de titani.

Els resultats d'aquesta tesi demostren que els pèptids sintètics rics en prolines són segurs i estimulen la diferenciació dels osteoblasts, independentment de la forma d'administració i del tipus cel·lular emprat. A més a més, els resultats obtinguts permeten hipotetitzar que els pèptids sintètics rics en prolines podrien actuar per mitjà de la seva interacció amb un receptor (per exemple, integrines) desencadenant una via de transducció de senyal específica en estadis inicials de la diferenciació cel·lular que, finalment, estimularia la diferenciació dels osteoblasts. Entre les diferents variants dels pèptids sintètics investigats, el pèptid 2 ha estat el que ha presentat millor activitat biològica, fet que es podria relacionar amb l'accessibilitat de la seqüència PPLPP present en l'extrem C-terminal del pèptid.

A més, els pèptids sintètics s'han combinat amb diversos biomaterials, incloent hidrogels, substituts ossis sintètics de TiO_2 i implants de titani. Els resultats obtinguts demostren que els pèptids sintètics milloren les propietats osteogèniques dels biomaterials tant "*in vitro*" (hidrogels d'alginat, substituts ossis sintètics de TiO_2 recoberts amb alginat) com "*in vivo*" (implants de titani). Més concretament, els pèptids sintètics milloren les propietats de l'alginat per a l'adhesió i, en conseqüència, per a la proliferació i la diferenciació de les cèlules sembrades dels diferents biomaterials analitzats *in vitro*. De la mateixa manera, en els estudis *"in vivo"* s'ha observat un major percentatge de formació de nou òs acompanyat d'una disminució en la quantitat d'òs resorbit en aquells implants de Ti recoberts amb pèptid 2. Conseqüentment, els implants de Ti modificats amb pèptid 2 han demostrat millorar les propietats osseointegratives *"in vivo"*.

En conjunt, els resultats d'aquesta tesi demostren que els pèptids sintètics rics en prolines són osteopromotors quan s'utilitzen en combinació amb hidrogels d'alginat, tant sols com recobrint substituts ossis sintètics de TiO_2 o recobrint superficies d'implants de titani. En conclusió, els pèptids sintètics dissenyats podrien representar una nova estratègia per tractaments de regeneració òssia en diverses aplicacions.

List of publications

This thesis is based on the following papers:

Paper 1. Rubert, M.; Ramis, J.M.; Vondrasek, J.; Gayà, A.; Lyngstadaas, S.P.; Monjo, M. Synthetic peptides analogue to enamel proteins promote osteogenic differentiation of MC3T3-E1 and mesenchymal stem cells. *Journal of Biomaterials and Tissue Engineering 1 (2): 198 - 209, 2011.*

Paper 2. Ramis, J.M.; Rubert, M.; Vondrasek, J.; Gayà, A.; Lyngstadaas, S.P.; Monjo, M. Effect of enamel matrix derivative and of proline-rich synthetic peptides on the differentiation of human mesenchymal stem cells towards the osteogenic lineage. *Tissue Engineering Part A 18 (1-2): 1-11, 2012.*

Paper 3. Rubert, M.; Alonso-Sande, M.; Monjo, M.; Ramis, J.M. Evaluation of alginate and hyaluronic acid for their use in bone tissue engineering. *Biointerphases 7:44, 2012. DOI: 10.1007/s13758-012-0044-8.*

Paper 4. Rubert, M.; Monjo, M.; Lyngstadaas; S.P.; Ramis, J.M. Effect of alginate hydrogel containing polyproline-rich peptides on osteoblast differentiation. *Biomedical Materials 7 (5): 055003, 2012. DOI: 10.1088/1748-6041/7/5/055003.*

Paper 5. Gómez-Florit, M.; Rubert, M.; Ramis, J.M.; Haugen, H.J.; Tiainen, H.; Lyngstadaas, S.P; Monjo, M. TiO_2 scaffolds sustain differentiation of MC3T3-E1 cells. *Journal of Biomaterials and Tissue Engineering 2: 1-8, 2012.*

Paper 6. Rubert, M.; Pullisaar, H.; Gómez-Florit, M.; Ramis, J.M.; Tiainen, H.; Haugen, H.J.; Lyngstadaas S.P.; Monjo, M. Effect of TiO_2 scaffolds coated with alginate hydrogel containing a proline-rich peptide on osteoblast growth and differentiation in vitro. *Journal of Biomedical Materials Research part A*, *In press.*

Paper 7. Petzold, C.; Monjo, M.; Rubert, M.; Gómez-Florit, M.; Ramis, J.M.; Ellingsen, J.E.; Lyngstadaas, S.P. Effect of Proline-Rich Synthetic Peptide–Coated Titanium Implants on Bone Healing in a Rabbit Model. *Oral and Craniofacial Tissue Engineering 2: 35-43, 2012.*

1. Introduction

1. Introduction

1.1. Background of the study

Bone is a dynamic tissue with capacity for regeneration as part of the repair process in response to injury, as well as during the skeletal development or continuous remodeling throughout adult life (Dimitriou et al., 2011). However, under certain circumstances such as a traumatic fracture, pathological defects (osteogenesis imperfecta, osteoporosis, osteonecrosis) or large bone defects, the ability of bone to self-repair can be impaired leading to nonunion or mal-unions. An attractive way of promoting bone regeneration is to try to mimic the events that take place during the development of the bone tissues (Heijl et al., 1997; Sculean et al., 1999). For many years, autologous bone grafts was the only available choice to restore bone structure and functionality. However, several drawbacks have been associated to their use, such as the risk of infection, hemorrhage, nerve damage and loss of function together with limitation of suitable bone and its collection which is painful and limited. To overcome those limitations, nowadays several strategies based on the use of cells, growth factors, extracellular matrix proteins or several types of biomaterials (either alone or combined) are being developed to restore the architecture and function of loss or damaged bone tissue.

For many years it was believed that biological treatments for hard tissue diseases would be based on growth factors. However, these are inherently unstable and short-lived and their use as reliable hard tissue inducers has been hampered due to several problems regarding stability, administration, bioactivity and availability. Genetic engineering of artificial polypeptides based on proteins sequences of hard tissue extracellular matrix offers a novel method for developing materials for bone regeneration (Bhatnagar et al., 1999; Lutolf et al., 2003; Thorwarth et al., 2005). Due to their shorter length, compared to natural proteins, the artificial peptides are easier to produce and allow the use of amino acid analogues, which may improve the stability; moreover, they are cheaper and avoid the problems related to immunogenicity and disease transmission.

The following sections give an overview of the bone as a fully functional organ, the process of bone formation and remodeling, followed by a description of the current strategies used to promote bone regeneration.

1.2. Bone as an organ

Bone is a specialized connective tissue that makes up, together with the cartilage, the skeletal system. The skeletal system is a multifunctional tissue that provides structural support for the whole body, permits movement and locomotion by levers for the muscles, protects internal organs and acts as a reservoir of mineral content, thus contributing to the homeostasis maintenance (Baron, 2003).

Bone organization

Bone can be divided into an outer part called cortical or compact bone and by an inner part named cancellous, trabecular or spongy bone. In whole, this structure allows optimal structural properties to support mechanical stress (Fleisch, 2000).

Although they are made of the same cells and same matrix components, cortical and trabecular bone differ at structural and functional level:

▪ **Cortical bone** (or compact bone) represents the 80% of bone volume and is calcified in an 80-90% of the bone volume. Cortical bone is formed by osteons, by an intersticial lamellae (in between the osteons) and by a periosteum at the outer and inner surfaces of cortical bone. The primary anatomical and functional unit of bone are the osteons, which consists of a lamellae of bone matrix concentrically orientated around a central channel (harvesian canal) containing blood vessels, nerves and connective tissue. Cortical bone is dense and has a strength of 100-200 MPa (Bose et al., 2012). The compact structure leads cortical bone to fulfill mainly a mechanical and protective function (Baron, 2003; Mackiewicz et al., 2011). Cortical bone is produced by intramembranous ossification (Baroli, 2009) and comprises long bones, flat bones and short bones (Salgado et al., 2004).

▪ In contrast, **trabecular bone** (or cancellous bone) is calcified only in a 15-25% of the bone volume, and constitutes a highly porous structure characterized by a thin calcified network surrounded by hematopoietic bone marrow and embryonic connective tissue. Due to its high porosity, trabecular bone is a weak structure with a compressive strength between 2 and 20 MPa (Bose et al., 2012). This spongeous structure ensures the elasticity and stability of the skeleton and counters for the main part of bone metabolism (Mackiewicz et al., 2011). It is commonly found in the methaphysis of long bones, covered by cortical bone, and in the vertebral bodies (Salgado et al., 2004).

The adult skeleton of bone is composed of 213 bones, excluding the sesamoid bones, and makes up about 20% of body mass. There are four categories of bones on the basis of their shape: long bones (tibia, femur, humerous…); short bones (wrist and ankle appear cubelike in shape); flat bones (flat bones includes skull bones, scapula, mandibula and ileum) and irregular bones (bones of the spinal column).

Microscopically, woven and lamellar bone can be distinguished. Woven bone is the type formed initially in the embryo and during growth, and is characterized by an irregular array of loosely packed collagen fibrils. It is then replaced by lamellar bone, so that woven bone is practically absent from the adult skeleton, except under pathological conditions of rapid bone formation, such as fracture healing. In contrast, lamellar bone is the form present in the adult, both in cortical and in cancellous bone. It is made of well-ordered parallel collagen fibers organized in a lamellar pattern (Fleisch, 2000).

Bone composition

Like any other connective tissue, bone is made up of an extracellular matrix (ECM), cells and water. Table 1 summarizes the composition of bone.

Table 1. Composition of bone (Baron, 2003; Fleisch, 2000).

Composition of bone
ECM   *Ions (2%):* Na^+, Mg^{2+}, HCO_3.
Mineral (65%): Hydroxyapatite.
Organic (33%): Collagen (90%), non-collagen proteins (BSP, OC, ON …), lipids.
Cells   Osteoblasts (<5% of total amount of cells), osteocytes (90-95% of total amount of cells), lining cells, osteoclasts (<1% of total amount of cells), other (lymphocytes, mesenchymal stem cells).
Water

▪ **The bone extracellular matrix** (ECM) is composed of an organic component (33%) and a mineral component (65%). The organic matrix is mainly composed of collagen (90%) that provides flexibility to the bone and non-collagen proteins (10%), of which bone sialoprotein (BSP), osteocalcin (OC) and osteonectin (ON) are predominant. Non-collagen proteins exert important roles such as the modulation of calcification and tissue repair, cell attachment and binding of growth factors. The mineral component is mainly made up of hydroxyapatite crystals (insoluble salt of calcium and phosphorous), which are located within and between the collagen fibrils (Fleisch, 2000). ECM also contains small amounts of magnesium, sodium and bicarbonate (2%).

▪ **Cell types**

There are two categories of bone cells (Figure 1), those involved in the bone formation (osteoblasts, osteocytes and lining cells) and those responsible of bone resorption (osteoclasts).

Osteoblasts originate from mesenchymal stem cells under the influence of local growth factors such as fibroblast growth factors (FGFs), bone morphogenetic proteins (BMPs) and Wnt proteins and require of Runt related transcription factor 2 (Runx2) and Osterix (Osx) transcriptional factors (Baron, 2003). Development of pre-osteoblasts into fully functional osteoblasts occurs by achievement of sequential stages characterized by an initial cell growth and cell proliferation followed by the development and acquisition of a matured ECM and culminates with the matrix mineralization. Each stage is characterized by specific changes in gene expression (Stein et al., 1996). Mature osteoblasts are the bone cells responsible for the production and maintenance of the bone architecture, since they are responsible for the synthesis of the bone ECM, the control of the mineralization and the regulation of the osteoclast activity by secretion of Receptor Activator of Nuclear factor Kappa-β Ligand (RANKL). These cells can remain entrapped into the bone matrix and differentiate to osteocytes (Bronner and Farach-Carson, 2004; Currey, 2002); or remain on bone surface differentiating to bone lining cells (Currey, 2002).

At a certain moment some of the osteoblasts stop synthesizing matrix and become embedded within bone. They are then called **osteocytes**. After local damage or local mechanical stress, osteocytes present at bone matrix are activated and may stimulate osteoblast recruitment and differentiation by

the expression of osteoblast stimulating factor 1 (OSF-1) (Klein-Nulend and Bonewald, 2008). Osteocytes are stellate cells, with long, slender cytoplasmatic processes ("fingers") that radiate in all directions (Klein-Nulend and Bonewald, 2008). Mature osteocytes connect through small canals (canaliculi) present into bone matrix with other osteocytes and cells in the bone surface (lining cells or osteoblast). The organization of osteocytes as a network gap junction-coupled cell suggests that they may play an important role in the metabolism and maintenance of bone. The cell processes orientated to the bone surface offers a tremendous cell-bone surface, suggesting that osteocytes are involved in the phosphate and blood-calcium homeostasis, facilitating the diffusion of calcium in and out of the bone. In addition, they are spaced regularly and also well located into the mineralized matrix for responding to mechanical strain that seems to play a role in transducing mechanical loads into changes in bone formation and bone resorption. Thus, osteocytes act as mechanosensor cells that send signals directing both osteoclast and osteoblast activity during bone remodeling (Fleisch, 2000; Sela and Bab, 2012)

Bone lining cells are flat cells that cover the bone tissue surface acting as a blood-bone barrier (Fleisch, 2000) and being responsible for bone protection (Currey, 2002). Bone lining cells also participate in the control of the flux of ions from the organism to bone and are responsible for the immediate calcium release in a low calcium blood levels situation.

Besides of bone forming cells (osteoblast, osteocytes and bone lining cells), bone is also constituted by cells involved in bone resorption processes. **Osteoclasts** are multinucleated cells derived from hematopoietic stem cells and are formed by fusion of precursor monocytes. During bone remodeling or following a bone fracture, cells from the osteoblast lineage and as well immune cells, express macrophage stimulating colony factor (M-CSF) or RANKL that induce mononuclear cells to fuse and form osteoclasts (Sela and Bab, 2012). Osteoclasts are situated on the bone surface and are responsible for bone resorption. They secrete acids and enzymes close to the bone surface to dissolve the mineral content and degrade the organic matrix. Like other cells, once bone resorption has finished they undergo apoptosis (Fleisch, 2000).
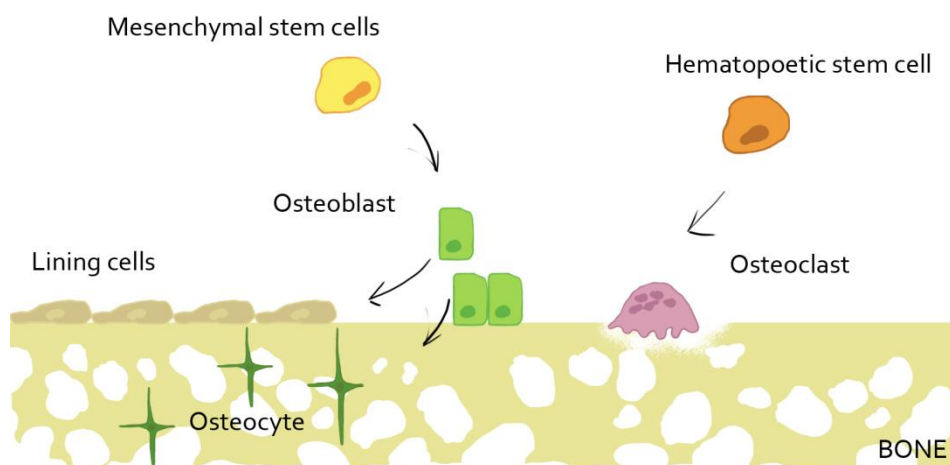

Figure 1. Cells involved in bone formation and bone remodeling.

1.3. Bone formation and remodeling

Bone is built during embryogenesis, youth and adolescence by two fundamental mechanisms: endochondral ossification, whereby bone is built on a cartilaginous scaffold, and intramembranous ossification where it is formed directly without the latter. Once formed, the shape and structure of the bones is continuously renovated and modified by the two processes of modeling and remodeling. In the modeling, which takes place principally during growth, new bone is formed at a location different from the one destroyed resulting in a change in the shape of the skeleton. In remodeling, which is the main process in the adult, the two processes are coupled in space and time, so that no change occurs in the shape of the bone. Both modeling and remodeling, however, result in the replacement of old bone by new bone. This allows the maintenance of the mechanical integrity of the skeleton. The turnover also allows the bone to play its role as an ion bank (Fleisch, 2000).

- **Bone formation** (osteogenesis)

Bone formation occurs throughout life and is involved in bone remodeling in adults. It is an active process initiated by local mesenchymal stem cells (bone marrow stromal cells or connective tissue mesenchymal stem cells) and depends on the cooperation of several types of cells (osteoblast or osteoclasts), which are under the influence of local growth factors, extracellular matrix proteins, cytokines, hormones, ions or vitamins (Baron, 2003; Deschaseaux et al., 2009).

Bone formation occurs by two types of processes of bone development: *intramembranous ossification*, that will origin flat bones, and by *endochondral ossification*, that will origin long bones. The main difference is that while for intramembranous ossification MSCs differentiate directly to osteoblasts, for endochondral ossification there is an intermediate stage that involves differentiation of MSCs to chondroblasts, instead of osteoblasts. These chondroblasts synthesize a cartilaginous matrix that will regulate growth and act as a template for later skeleton development (Baron, 2003; Deschaseaux et al., 2009). Endochondral ossification is the process associated with fetal bone development, day-to-day growth and to a certain extent with fracture repair.

- **Bone remodeling**

Bone is a dynamic tissue that suffers a continuous and a compensated process of bone formation and bone resorption, namely **bone remodeling** (Figure 2). Bone remodeling occurs at many sites throughout the body where bone is experiencing growth, mechanical stress, microfractures or breaks. Bone remodeling is a tightly regulated process securing repair of microdamage and replacement of old bone with new bone through sequential osteoblastic resorption and osteoblastic bone formation (Sela and Bab, 2012).

Bone remodeling is activated as a result of RANKL secretion by cells from the osteoblast lineage in response to a hormonal stimulus or to growth factors. The interaction of RANKL with its receptor (RANK), an osteoclast protein, induces pre-osteoclast migration at the remodeling site promoting

osteoclast differentiation and maturation with bone resorption capacity (Mandalunis, 2006). Bone resorption occurs by the mineral solubilization as a result of bone acidification. In addition, bone resorption is also mediated by the increased local production of pro-inflammatory cytokines, such as tumor necrosis factor-alpha (TNFα), which stimulates differentiation and maturation of osteoclasts (Boyce et al., 2005; Vitale and Ribeiro, 2007). Therefore, osteoclast function is increased by cooperation mechanism between TNFα and RANKL (Vitale and Ribeiro, 2007). Activity of other pro-inflammatory cytokines such as interleukin 1 and 6 (IL-1 and IL-6) contributes as well to bone resorption (Tamura et al., 1993).

Once bone has been resorbed, osteoclasts enter into apoptosis. At this time, osteoblasts are attracted by several growth factors at the bone remodeling site and start synthesizing new matrix that in the end it will mineralize. The bone remodeling process is finished at the dormancy stage when some osteoblast cells involved in bone remodeling are embedded into the matrix and differentiates to osteocytes, others suffer apoptosis and others remain onto the bone surface as a bone lining cells until the next activation cycle of bone remodeling starts (Figure 2).
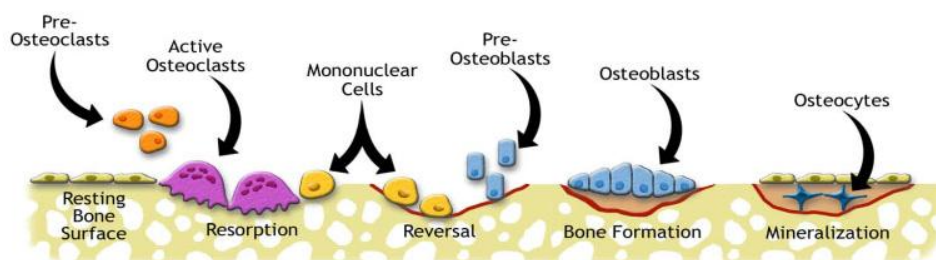
Figure 2. Scheme of the bone remodeling cycle (adapted from http://www.ns.umich.edu/Releases/2005/Feb05/bone.html).

1.4. Bone regeneration and repair

Bone repair in adults closely resembles bone formation during embriogenesis (Deschaseaux et al., 2009) and involves a complex interplay of cells, growth factors and extracellular matrix (Maes et al., 2006; Schindeler et al., 2008).

The process of bone repair is characterized by an initial inflammatory response, followed by granulation tissue formation (or primary soft callus formation) that will be replaced by mineralized callus (hard callus formation) and it will finalize with the callus remodeling (substitution of hard callus with lamellar bone) (Baroli, 2009) (Figure 3).

Figure 3. Schematic representation of the sequential fracture healing stages (Baroli, 2009).

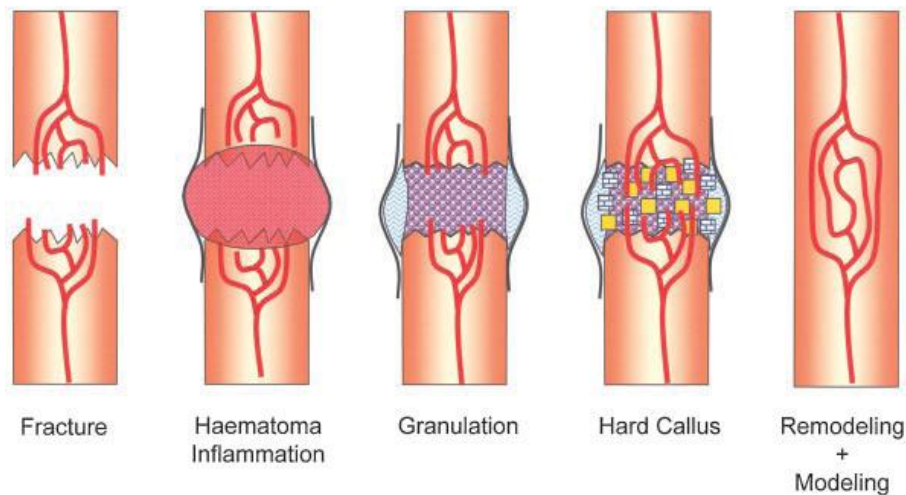Immediately after bone is fractured, trauma results in a hemorrhage that leads to an inflammation at the fracture site. Macrophages and other inflammatory cells colonize the area and combat the infection, secrete cytokines and growth factors and advance clotting into a fibrinous thrombus (Schindeler et al., 2008). Cytokine and growth factor secretion will set up a chemotactic gradient causing the migration of endothelial and MSCs to the healing site. The repair process then starts with the formation of new blood vessels (angiogenesis) that will maintain cellular activity during the repair process. At this stage, growth factors released by macrophages will stimulate fibroblasts to synthesize a provisional connective tissue matrix, which in turn will support cell and vascular growth. This cartilaginous callus will provide fracture stability and will act as a template. As the wound healing progresses, the matrix will be replaced by a collagen rich matrix. The connective tissue is subsequently replaced by endochondral ossification in new bone and that will be later followed with an intramembranous ossification. Hard callus will then be formed in the absence of a cartilaginous template in intramembranous bone formation. In the final stage of fracture repair encompasses the remodeling of the woven bone hard callus into the original cortical and/or trabecular bone configuration (Schindeler et al., 2008), and it reflects the functional adaptation of bone structure.

Although bone has the ability to self-renew by a rapid and efficient process, under certain circumstances such as a traumatic fracture, a pathological defect (osteogenesis imperfecta, osteoporosis, osteonecrosis) or large bone defects, the fracture healing fails and delayed unions or non-unions develop. There are millions of cases of skeletal defects a year that require bone-graft procedures to achieve union. For many years, the gold standard choice to repair a bone defect was based on the transplantation of tissue from another part of the patient's own body (autologous bone grafts) or bone taken from a donor (allograft). However, the lack of bone tissue available for transplantation and several limitations associated to their use, such as donor site morbidity or inmuno-rejection, led the emergence of other alternatives. Therefore, several strategies have been developed to restore the architecture and function of loss or damaged bone tissue, such as the use of cells,

growth factors, extracellular matrix proteins and several types of biomaterials. They are being used as adjuncts or alternatives to these traditional bone regeneration methods.

In the following sections the different strategies used for bone regeneration will be discussed.

1.4.1. Cells for bone regeneration

An alternative for bone regeneration involves the use of cells combined with a specific matrix or scaffold, frequently associated to growth factors (Boeckel et al., 2012). The use of cells for tissue engineering represents an important component in building and maintaining tissue function (Shi, 2006). In order to achieve efficacy and long-lasting repair of the damaged tissue, an important starting point is the selection of the correct cells (cell type, quantity, source and quality) (Shi, 2006). In order to regenerate the lost or damaged tissue, the ideal cell source should be easily expandable to higher passages, be non-immunogenic and should have a protein expression pattern similar to that tissue to be regenerated (Salgado et al., 2004).

Several types of cells are being used for tissue engineering applications such as mature cells or stem cells. Following, the origin and the advantages or disadvantages of different cell types are briefly described:

- Osteoblastic cells isolated from bone biopsies of the patient (autograft) represent a good choice because of their non-immunogenicity. However, their extraction is time-consuming and the amount of cells that can be harvested is limited. Non-human donors (xenogenic cells) offer an alternative to yield higher amount of available cells, however, problems related to immunogenicity and transmission of infectious agents together with ethical and social problems has refrained their use for bone tissue engineering purposes (Salgado et al., 2004).

- Stem cells represent the most valid and promising cell source for bone tissue engineering. They are undifferentiated cells with unique capabilities to self-renew and with potential to differentiate into all cell types. In addition, they have a high proliferative potential, keep their osteogenic properties and are able to adhere easily on plastic surfaces. The origin of the stem cells can be embryonic or adult.

  - Embryonic cells are found in the blastocyt and primordial germ cells. These cells are characterized by their high plasticity, and therefore they possess a great potential to differentiate into all type of cells (Boeckel et al., 2012). Although their excellent properties as a cell source for tissue engineering, legal regulatory policies and ethical considerations limit their current use in clinical and research applications.

  - Adult stem cells reside in the fully differentiated or adult tissue. They are restricted to differentiate only into certain cell lines (Boeckel et al., 2012). Adult cells include: hematopoietic stem cells, bone marrow stem cells, neural stem cells, dermal stem cells and several others (Dinopoulos et al., 2012). Stem cells located in the bone marrow are of special interest for bone tissue engineering. Bone marrow cells can yield two different types of cells, the hematopoietic stem cells which give rise to the entire blood cell lineage and the mesenchymal stem cells (MSC). MSC are pluripotential cells

with the capacity to differentiate into osteoblasts, chondroblasts, adipocytes and myoblasts. Besides its differentiation potential they can also be extensively expanded *in vitro* and possess immunosuppressive effects which would make them suitable for allogenic or xenogenic transplantation (Dinopoulos et al., 2012; Salgado et al., 2004).

1.4.2. Growth factors for bone regeneration

In 1965, Urist reported the ability of devitalized, demineralized bone to induce ectopic bone formation and the recognition that bone morphogenetic proteins were the responsible for this bone induction (Urist, 1965). Since then, the use of bioactive molecules has emerged as a promising alternative to induce bone regeneration. With improved understanding of fracture healing and bone regeneration at molecular levels, a number of growth factors and other molecules that regulate this complex physiology, including BMPs, transforming growth factor (TGF-β), insulin-like growth factor (IGF), fibroblast-like growth factor (FGF), platelet derived growth factor (PDGF) and vascular endothelial growth factor (VEGF), have been identified, isolated and investigated for their therapeutic potential in bone regeneration (Dimitriou et al., 2011; Kempen et al., 2010). Encapsulation of growth factors into a scaffold provides a suitable method for a sustained release of the growth factors overtime.

Following, the main growth factors used in bone regeneration are briefly described.

Bone morphogenetic proteins (BMPs)

BMPs are members of the transforming growth factor (TGF-β) family and are involved in the cascade of cellular events during bone tissue formation and regeneration. They are potent osteoinductive factors involved in the differentiation of MSC towards the osteogenic lineage and in osteoblast proliferation and differentiation (Bose et al., 2012). In bone, they are synthesized by skeletal cells such as osteoblasts and sequestered in the extracellular matrix (Kempen et al., 2010). Among the different types of BMPs, BMP2 and BMP7 are those mainly involved in osteogenesis. BMP2 and BMP7 have shown to be safe and effective in improving and accelerating bone healing in a variety of clinical conditions including non-unions, open fractures, joint fusions, aseptic bone necrosis and critical bone defects (Dimitriou et al., 2011).

*Transforming growth factor (*TGF-β)

TGF-βs are multifunctional growth factors related to bone that stimulate recruitment and proliferation of mesenchymal stem cells, their differentiation to osteoblasts and/or chondrocytes and ECM production (Bose et al., 2012). In osteoblastic cells, TGF-β stimulates cell growth and synthesis of collagen and non-collagenous extracellular matrix proteins (Issa et al., 2006; Salgado et al., 2004), while inhibits some features of the fully differentiated osteoblast phenotype such as the alkaline phosphatase activity and the osteocalcin synthesis (Issa et al., 2006). In an attempt to enhance bone regeneration, several studies have combined TGF-β and BMPs and have demonstrated a synergistic effect of the growth factors combination (Kempen et al., 2010).

Insulin-like growth factor (IGF)

IGF is a small single-chain polypeptide that plays an important role in bone metabolism and is essential for the skeletal growth and maintenance of bone mass (Kempen et al., 2010). IGF acts as an autocrine, endocrine or a paracrine inductive molecule by mediating the effects of hormones, growth factors, cytokines or morphogens during wound healing (Lee and Shin, 2007). IGF regulates several key cellular processes, including proliferation, by stimulating synthesis of collagen, movement, and inhibition of apoptosis (Bose et al., 2012; Salgado et al., 2004). *In vivo*, systemic IGF infusion showed an increase in bone formation, bone volume and bone turnover in animal models and clinical trials for osteoporosis (Kempen et al., 2010).

Fibroblast-like growth factor (FGF)

FGF are glycoproteins secreted from the ECM by heparinases, with diverse biological activity and expression profile. In bone, they are produced by various cells, including osteoblasts, macrophages and endothelial cells. FGFs are released from the ECM and regulate cellular proliferation, survival migration and differentiation (Bose et al., 2012). They are involved in bone remodeling processes probably through their regulation on the balance between bone forming and bone resorbing cells. In addition, they also promote the development of new blood vessels and have a role on the stimulation of the osteoblastic phenotype through the activation of Runx2 transcription factor (Salgado et al., 2004).

Platelet derived growth factor (PDGF)

PDGF is a peptide signaling molecule produced by platelets, monocytes and osteoblasts. In connective tissue, PDGF increases collagen synthesis and enhances the tensile strength at the wound sites (Einhorn, 1995). PDGF also acts stimulating the migration and proliferation of MSC cells (Issa et al., 2006).

Vascular endothelial growth factor (VEGF)

VEGF is a potent angiogenic factor responsible for the generation of new blood vessels in the tissue. It is commonly found in the bone fracture healing sites and the plate growth, where regulates vascularization through the recruitment of endothelial cells at the healing site (Salgado et al., 2004). In addition, VEGF also stimulates migration and differentiation of primary human osteoblasts and mediates the activity of various osteoinductive factors such as $TFG\beta1$, IGF, FGF-2 (Lee and Shin, 2007).

1.4.3. Extracellular matrix proteins for bone regeneration

Bone is mainly composed by an extracellular matrix that surrounds and supports cells in the tissue. ECM of hard tissues is a natural and highly organized structure that is composed by various proteoglycans, polysaccharides and proteins, including collagen, elastin, fibronectin, laminin, bone

sialoprotein, osteopontin, amelogenin and ameloblastin. Protein composition confers to the bone ECM a role in the regulation of cell behavior such as morphogenesis, migration, proliferation and differentiation (Shi, 2006). In addition, non-collagenous ECM proteins control hydroxyapatite crystal nucleation, growth, shape and size as well as facilitate the attachment between the major organic (collagen) and inorganic (hydroxyapatite) components (Thurner et al., 2010).

Additionally, ECM proteins have shown to stabilize and pattern the mineral-tissue interface in bone and to control the formation and stability of the tissue-mineral complex (Ellingsen et al., 2006). Therefore, the incorporation of ECM molecules/proteins, either alone or combined such as with hydroxyapatite or polymeric scaffolds, represent a promising strategy in the development of functional tissues.

Following is presented a brief description of some of the main proteins present in the bone ECM.

Collagen (Coll)

It is the main organic component of the extracellular matrix and is synthesized by a variety of cells such as chondrocytes, osteoblasts and adipocytes (Shi, 2006). Coll gives to bone tissue its tensile strength (Fleisch, 2000). In addition, Coll contributes to vascular ingrowth, growth factor binding, enhanced cell proliferation and to mineral deposition, thus providing a favorable environment for bone regeneration (Giannoudis et al., 2005; Shi, 2006).

Elastin

Elastin is a chemotactic and an adhesive protein (Shi, 2006) found in a relatively large amount of elastic tissues and connective tissues (Park and Lakes, 1992). In addition, elastin is also a structural protein that functions together with collagen; and whereas collagen provides rigidity, elastin gives elasticity to connective tissue (Shi, 2006).

Fibronectin (Fn)

Fn can be found in a soluble form, that circulates in the body fluids to enhance blood clotting and fagocytosis, or in insoluble form. The insoluble fibronectin is a dimeric protein with more than six highly folded domains, which acts as a cell adhesion molecule binding to cell surface through its arginine-glycine-aspartate (RGD) sequence and deposits at the interstitial spaces, such as the ECM. Fn participates in osteoblast cell growth, migration and differentiation during cell development (Shi, 2006).

Laminin (Ln)

Laminin is a high-molecular weight extracellular glycoprotein present in the basement membranes that it plays a role in determining the architecture and integrity of various tissues (Kamegai et al., 1994). Laminin binds to cell surface through integrin interaction and participates in the regulation of cell migration, development and differentiation of cells (Shi, 2006).

Bone sialoprotein (BSP)

BSP is a major non-collagenous protein in mineralizing connective tissues such as dentin, cementum and calcified cartilage tissues. The RGD sequence near the carboxy-terminus of BSP protein is a cell attachment site recognized by $\alpha v \beta 3$ integrin receptor, while polyglutamic acid regions in the amino terminus mediate the binding of BSP to hydroxyapatite (Zhang et al., 2009). In fact, BSP induces osteoblast cell attachment and differentiation *in vitro* (Mizuno et al., 2000). Furthermore, BSP is also responsible for the deposition of calcium phosphate in bone tissues, especially after association with collagen type I (Gomes et al., 2011).

Osteopontin (OPN)

OPN represents together with the BSP the major non-collagenous proteins secreted by the osteoblasts and deposited into the ECM (Lekic et al., 1996). It is involved in many diverse functions, such as binding to cells via their integrin receptors or regulation of the formation and remodeling of mineralized tissues. In osteogenesis, OPN mRNA is up-regulated during matrix formation (Lekic et al., 1996; Sommer et al., 1996).

Amelogenin and ameloblastin (AMEL and AMBN)

AMEL and AMBN are two major enamel matrix hydrophobic proteins rich in proline aminoacid that regulate initiation and growth of hydroxyapatite during enamel formation (Eastoe, 1965; Lang, 2006; Mazzey et al., 2006). In addition, ameloblastin and amelogenin expression have also been detected in mesenchymal cells during embryogenesis or tissue repair, suggesting that enamel matrix proteins also have roles outside enamel tissue and that these molecules could play an active role in bone formation and remodeling (Deutsch et al., 2006; Fong et al., 1998; Haze et al., 2007; Spahr et al., 2006; Tamburstuen et al., 2010).

Amelogenin is well characterized from aminoacid sequencing data, the gene structure and from the construction and identification of amelogenin clones (Bonass et al., 1994; Gibson et al., 1992; Lau et al., 1992; Shimokawa et al., 1987; Snead et al., 1983; Takagi et al., 1984). Its structure and function has remained remarkably well-conserved through evolution (Fincham et al., 1994), suggesting that they may have great functional importance (Lyngstadaas et al., 1990). Several studies have focused on the study of different forms of amelogenin (Emdogain®, LRAP) on mineralization in different cell types and have shown to induce bone tissue regeneration *in vitro* and in animal models. A summary of several *in vitro* and *in vivo* studies performed are detailed below:

Table 2. Effects of different forms of amelogenin on different cell types.

Amelogenin form/Description	Cell culture model (specie/cell model type)	Cell response	References
Leucine-rich amelogenin peptide	Mouse embryonic stem cell (RW4)	Increase cell differentiation	(Warotayanont et al., 2008)
EMD	Human periodontal ligament cells (RN6)	Increase cell adhesion, growth and metabolism	(Lyngstadaas et al., 2001)
EMD	Human epithelial cells (HeLa)	Inhibit cell proliferation and growth	(Lyngstadaas et al., 2001)
EMD	Epithelial cells	Increase cell adhesion	(Kawase et al., 2001)
EMD	Primary human osteoblasts (NHOst)	Increase cell differentiation; increase cell proliferation	(Reseland et al., 2006; Schwartz et al., 2000)
EMD	Primary human osteoblasts (human alveolar bone)	Increase cell proliferation; Reduced cell differentiation	(Palioto et al., 2011)
EMD	Human primary osteoblasts	Induce cell proliferation; Do not induce matrix mineralization	(Pischon et al., 2006)
EMD	Primary osteoblasts mouse calvaria	Regulate gene expression during periodontal tissue	(Jiang et al., 2001)
EMD	Mouse transgenic pre-oblast cell line (2T9)	Increase cell proliferation	(Schwartz et al., 2000)
EMD	Human osteoblast-like osteosarcoma cells (MG63)	Decrease cell proliferation, increase cell differentiation	(Schwartz et al., 2000)
EMD	Rat bone marrow stromal cells (BMSCs)	Increase osteoblast differentiation and cell proliferation	(Keila et al., 2004)
EMD	Rat bone marrow cells	Not significant effect on cell growth and cell differentiation	(van den Dolder et al., 2006)
EMD	Rat bone marrow cells	Increase cell proliferation; Decrease osteogenic differentiation	(Guida et al., 2007)
Amelogenin fragment 25kDa	Rat bone marrow mesenchymal stem cells	Promote differentiation and mineralization; No effects on cell proliferation and cell morphology	(Izumikawa et al., 2012)
EMD	Rat gingival fibroblasts (GF)	Do not induce osteoblast differentiation	(Keila et al., 2004)
EMD	Mouse osteoblast (KUSA/A1)	Increase cell differentiation	(Yoneda et al., 2003)
EMD	Mouse osteoblast (ST2)	Do not induce osteoblast proliferation; induce cell differentiation	(Yoneda et al., 2003)
EMD	Mouse pre-oblast cell line (MC3T3-E1)	Increase cell proliferation and cell differentiation Inhibits osteoclastogenesis and osteoclast function	(He et al., 2004)
EMD	Mouse pre-oblast cell line (MC3T3-E1)	Increase cell differentiation	(Weishaupt et al., 2008)
EMD	PDL	Induce cell proliferation; Do not induce matrix mineralization	(Pischon et al., 2006)
Fractions of enamel proteins	human periodontal ligament (PDL)	Osteoinductive activity	(Nagano et al., 2006)
EMD	In vivo (Wistar rats)	Accelerate new bone formation	(Yoneda et al., 2003)
EMD	In vivo (rat calvaria)	New bone formation	(Potijanyakul et al., 2010)
EMD	In vivo (rat femur)	New trabecular bone formation	(Kawana et al., 2001)

Emdogain, is a purified acid extract of proteins from pig enamel matrix extracted from developing porcine teeth, commercialized as Emdogain® (EMD, Biora AB, Malmö, Suecia), that has been approved for clinical use in the regeneration of periodontal attachment and bone. EMD mimics the biological process of natural tooth development and thus enables the regeneration of new periodontal tissue. In 1997, Hammarstrom *et al* (Hammarstrom, 1997) found that EMD promoted the reformation of acellular cementum and alveolar bone in a dehiscent model and in a replantation model in monkeys, and since then a multitude of case reports and clinical studies are now published confirming the clinical effect of EMD. The major constituent of Emdogain® is amelogenins. Amelogenins self-assemble into supramolecular aggregates and precipitate to form an extra cellular matrix layer with a hydrophobic surface (Fincham et al., 1994) that acts as an extracellular matrix scaffold for the growing crystallites. As it has been presented in Table 2, experimental studies have demonstrated the capacity of EMD inducing bone tissue regeneration *in vitro* and in animal models.

In vitro differences in amelogenin effects have been suggested to be dependent on cell type, culture condition, maturation state of cells and exposure time of treatment. *In vivo*, the bioactive effects of Emdogain® (EMD, Biora AB, Malmö, Suecia) on bone wound healing and mineralized tissue formation depend, at least in part, on the local osseous environment in which EMD has been applied (Sawae et al., 2002).

The major drawback of using extracellular matrix proteins is their immunogenicity that can cause inflammation or even rejection. A solution is to identify short functional peptides sequences from the ECM and then synthesize these short peptides for their use either alone or combined with a non-immunogenic scaffold to function as an artificial ECM.

1.4.3.1. The role of polyproline sequences in bone mineralization

Several extracellular matrix proteins involved in hard tissue formation (such as Coll-I, BSP, OPN, amelogenin or ameloblastin) are rich in proline sequences. Interestingly, polyproline sequences are well-conserved through evolution, suggesting that they may have great functional importance (Lyngstadaas et al., 1990). As observed in
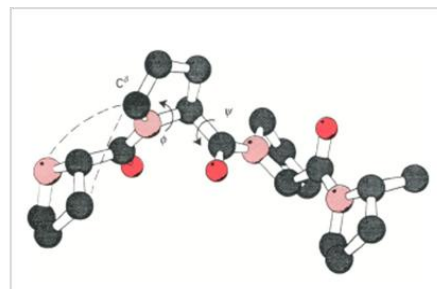

figure 4, proline is an unusual aminoacid in that the side-chain is cyclized back on to the backbone amide position (Williamson, 1994). The cyclic structure of the proline's side chain give this residue exceptional conformational rigidity compared to other aminoacids (Biedermannova et al., 2008). In addition, the bulkiness of the N-CH$_2$ group places restrictions

Figure 4. Part of a polyproline II helix. The helix is extended and repeats every three residues. Nitrogen atoms are shown in pink, and oxygen atoms in red. Figure extracted from Williamson *et al.* (Williamson, 1994).

on the conformation of the residue preceding proline (disfavoring the α‑helix conformation), and the replacement of the amide proton by a CH_2 group (that unables proline to act as a hydrogen bond donor) produces a potent α-helix and β-sheets breaker (Fincham et al., 1994; Williamson, 1994).

Actually, many proline-rich proteins contain repetitive proline motifs and adopt left-handed polyproline II helical conformations (PPII) (Jin et al., 2009; Stapley and Creamer, 1999), an extended and more restricted structure than α-helix and β-sheets with three residues per turn. This well-defined mobile and semi-flexible structure of PPII structure has been demonstrated to be essential to biological activities such as signal transduction, transcription, cell motility, and immune response (Bochicchio and Tamburro, 2002). A typical feature of PPII structure is the absence of any intramolecular hydrogen bonds that renders the PPII structure indistinguishable from an irregular backbone structure by H-NMR spectroscopy (Bochicchio and Tamburro, 2002). It has been reported that there is a very strong correlation between structural disorder of proteins, biomineralization and particular sequence features indicating that regulated growth of mineral phase in biology can only be achieved by the assistance of highly disordered proteins (Kalmar et al., 2012). Indeed, structure of proline-rich proteins has led to hypothesize that such proteins may function as mineral-binding domains, protein-protein interaction domains or internal molecular spacers during the formation of biological minerals and other biocomposites (Jin et al., 2009).

1.4.4. Biomaterials for bone regeneration

Another alternative to promote bone regeneration is through the use of biomaterials to assist, replace or repair damaged or missing bone tissue. Up to now several materials such as metals (stainless steel, titanium or titanium alloys), ceramics (coralline hydroxylapatite, hydroxyapatite or β-tricalcium phosphate) and polymer (collagen, fibrinogen, chitosan, alginate, hyaluronic acid, poly(α-hydroxyacids), poly(propylene fumaretes)) from both natural or synthetic origins have been proposed for bone replacement. Biomaterial selection depends on each specific application.

1.4.4.1. Hydrogels

Hydrogels are a highly hydrated class of polymers (Gkioni et al., 2010) widely used in bone regeneration. They are nontoxic, typically degradable, can be processed under relative mild conditions and can be delivered in a minimally invasive manner (Drury and Mooney, 2003). Their high water content provides a suitable environment for cells and drugs to be incorporated in the network for a controlled delivery at the site of injury and it allows transportation of substances such as nutrients and products from cell metabolism in and out of the hydrogels (Gkioni et al., 2010). Therefore, hydrogels have many different functions in the field of bone regeneration. They are applied as a space filling agents, as delivery vehicles for bioactive molecules, and as three-dimensional structures that organize cells and present stimuli to direct the formation of a desired tissue (Drury and Mooney, 2003).

Both synthetic and natural polymers are being used to form hydrogels. While synthetic hydrogels are appealing for bone regeneration because of their chemistry and properties are controllable and reproducible, natural polymers have been frequently used due to their inherent biocompatibility, biodegradability and bioactive properties (Lin and Metters, 2006), as they are either components of or have macromolecular properties similar to natural ECM and have also shown to interact in a favorable manner *in vivo* (Drury and Mooney, 2003). Natural polymers and synthetic monomers currently used for hydrogels fabrication are listed in Table 3:

Table 3. Natural polymer and synthetic monomers used in hydrogel fabrication. Table adapted from Lin *et al*. (Lin and Metters, 2006).

Natural polymers	Alginate, chitosan, collagen, dextran, fibrin, gelatin
Synthetic monomers	Acrylic acid, hydroxyethyl methacrylate, methacrylic acid, *N*-(2-hydroxypropyl) methacrylate, *N*-vinyl-2-pyrrolidone, *N*-isopropyl acrylamide, polyethylene glycol acrylate/methacrylate, polyethylene glycol diacrylate/dimethacrylate, Vinyl acetate, Poly(ethylene glycol), Poly(L-lactic acid)

Hydrogels can act as carriers of bioactive molecules or cells supporting bone formation. Moreover, hydrogels are versatile materials that allow their use in different forms depending on their function and the site to be placed. Thus, hydrogels with low viscosity are used as injectable hydrogels, which allow the administration of the material through minimally invasive techniques and possess good malleability allowing the filling of any area with the desired shape (Gutowska et al., 2001; Martinez-Sanz et al., 2011; Tan et al., 2009; Tan et al., 2011). In contrast, hydrogels with high viscosity are used for coating biomaterials (e.g. ceramic scaffolds and metal implants) to act as cell/bioactive molecule carriers. To provide stiffness and high compressive strength, hydrogels can be cross-linked either chemically or physically (Gkioni et al., 2010; Shi, 2006)

Therefore, the selection and fabrication of the appropriate hydrogel polymer is governed by the physical property (mechanical strength), the mass transport property (diffusion) and the biological interaction requirements of each specific application (Drury and Mooney, 2003).

- *Mechanical strength*: depends on elasticity, compressibility, visco-elastic behavior, tensile strength and failure strain. These properties are affected by polymer and cross-linker characteristics, gelling conditions (pH, temperature), swelling and degradation properties. Compression modulus of polymers and viscosity can be increased by increasing *polymer concentration* (Liew et al., 2006). The mechanical properties are also affected by the cross-linker type and density. There are many methods of preparing cross-linking hydrogels. Alginate can be easily cross-linked with calcium ions but also covalently cross-linked with carbodiimide (Shi, 2006). For other polymers, various chemical cross-linkers (carbodiimide, dyepoxi glutaraldehyde, dydrazides derivatives (Bergman et al., 2009; Rault et al., 1996; Vercruysse et al., 1997)), physical treatments (UV irradiation (Ono et al., 2000), freeze-

drying, heating) or blending with other polymers have been used to enhance mechanical strength (Bernhardt et al., 2009; Patterson et al., 2010).

▪ *Mass transport*: is governed by the hydrogel matrix characteristics. Hydrogel properties such as polymer fraction, polymer size, polymer concentration and cross-linking concentration determine the gels nanoporous structure. As a consequence, diffusion rates will be affected by the molecular weight and size of the diffusion species compared to the pores. In addition, hydrogel viscosity may play a role influencing biomolecule release (Liew et al., 2006), in which an increase in gel matrix viscosity may be translated with a reduction in the effective diffusion of the biomolecule (Skoug et al., 1993).

▪ *Biological parameters*: are defined by the hydrogel composition that must support cell function and tissue development. Cell interactions with the hydrogel affect significantly on the cell adhesion, migration and differentiation. Cell-hydrogel specific interactions occur through cell membrane receptors with ligands that are a component or adsorbed onto the material (Giancotti and Ruoslahti, 1999). While many hydrogels are not toxic and do not activate an immune response, alginate and other hydrogels lack receptors by which cells can interact, thus cells are not able to adhere on it (Alsberg et al., 2001). Therefore, a common approach to design a highly specific adhesive surface is to covalently couple an entire ECM protein, or a peptide sequence (RGD) capable of binding to cellular receptors to the polymer.

1.4.4.1.1. Alginate

Alginate is a natural and linear unbranched polysaccharide composed of 1,4-linked β-D-mannuronic acid (M-block) and α-L-guluronic acid (G-block) (Chung et al., 2002), with the capacity to gel in the presence of calcium ions, which is a mild method to create cross-links into an organic matrix (George and Abraham, 2006). Alginate has been used in a variety of bone regeneration applications, including the regeneration of skin, cartilage, bone, liver and cardiac tissue (Barbetta et al., 2009).

Mechanical strength and compression modulus can be increased either by selection of alginate polymers, with increasing ratios of *Guluronic (G)/Mannuronic (M) monomers,* or as well with increased lengths of G blocks. The structural integrity of hydrogels also depends on the *cross-linking type* (via various chemical bonds or physical interactions) and *cross-linking density* (Lee et al., 2000); thus, strength of ionically cross-linked alginate hydrogels increases at higher ion concentration and when divalent ions that have a higher affinity for alginate (e.g. Ca^{2+}). Regarding to the biomolecule transport, the rate diffusion depends on the molecular weight and size of the diffusion species (defined by Stroke radii) compared to the pore size of the hydrogel. Further, for higher molecular weight molecules, mass transport is negatively affected by increases in alginate concentration, in Ca^{2+} concentration and/or in extent gellation. For alginate and other charged polymers the diffusion rates are not solely size-dependent but also affected by the charge interactions with the negatively charged polymer chains (Drury and Mooney, 2003).

Potential of modified alginate hydrogels to induce bone formation has been demonstrated *in vitro* and *in vivo* (Lee et al., 2007; Li et al., 2005). Due to the inert properties for cell adhesion, alginate is commonly used in a modified manner with RGD-sequences, with immobilization of osteogenic peptides, with BMP-2 or in combination with other polymers and it has shown to support cell attachment, cell proliferation, osteogenic differentiation and mineral deposition *in vitro* (Alsberg et al., 2001; Lee et al., 2007; Li et al., 2005). *In vivo,* alginate has demonstrated to conduct cell differentiation and an early calcification when used in combination with chitosan gel or encapsulating MSC cells and BMP-2 or containing modified-peptides (Lee et al., 2007; Li et al., 2005; Park et al., 2005).

1.4.4.1.2. *Hyaluronic Acid*

Hyaluronic acid (HA) is a natural and linear polymer of altering disaccharide units of D-glucuronic and N-acetyl-D-glucosamine that is normally present in tissue as sodium hyaluronate (Schmut and Hofmann, 1982). Although HA occurs typically as a high molecular-size polymer of the extracellular matrix of up to $2x10^4$ kDa, HA is susceptible to fragmentation. Polymer size appears to confer specific functions to the HA fragments. The large hyaluronan polymers are space-filling, anti-angiogenic, immunosuppressive and impede differentiation, possibly by suppressing cell-cell interactions, or ligand access to cell surface receptors. Smaller polysaccharide fragments are inflammatory, immuno-stimulatory and angiogenic (Maharjan et al., 2011; Stern et al., 2006). In aqueous solution, hydrogen bonding occurs between adjacent carboxyl and N-acetyl groups; theses feature allows HA to maintain conformation stiffness and to retain water (Ballini et al., 2009). Although hyaluronate forms a visco-elastic solution in water, even at high concentrations of HA, the solution lacks gel-like properties at physiological pH (Schmut and Hofmann, 1982). Thus, HA gelation can be induced by acidification and subsequent dialysis against ethanol (Schmut and Hofmann, 1982) or by reaction with Cu^{2+} ions. The gelation degree also depends on the molecular weight of the hyaluronate (Schmut and Hofmann, 1982).

Hyaluronate has shown excellent potential for tissue engineering applications such as wound healing (Price et al., 2005), artificial skin (Murashita et al., 1996), soft (Duranti et al., 1998) and bone tissue augmentation (Martinez-Sanz et al., 2011). *In vitro* studies using derivatized hyaluronic acid (Hyffa-11) containing rhBMP2 have shown to support cell attachment and growth, increased ALP activity and osteocalcin expression in a murine fibroblast cell line (Kim and Valentini, 2002), and to enhance calcium content, osteopontin and BSP expression and to decrease ALP activity in rat bone marrow stromal cell when combined with FGF (Lisignoli et al., 2001). *In vivo*, HA hydrogels containing BMP2 showed to support newly bone formation (Bergman et al., 2009; Patterson et al., 2010).

1.4.4.2. Bone graft materials

Bone grafting is used in bone injuries, genetic malformations and bone diseases in which filling a defect is required (Dinopoulos et al., 2012; Giannoudis et al., 2005; Janicki and Schmidmaier, 2011).

Depending on the origin, bone grafts can be divided in autografts, allografts, xenografts and alloplasts. Their advantages and inconvenient are briefly described in the following table:

Table 4. Characteristics of the different types of bone grafts used for filling bone defects. Table adapted from (Bartold et al., 2006; Bashutski and Wang, 2009; Dinopoulos et al., 2012; Salgado et al., 2004).

Origin	Type	Source	Properties	
			Advantages	**Disadvantages**
Natural	Autograft	Host	Osteogenic, osteoconductive, osteoinductive Minimum immunological reaction	Limited amount of graft, morbidity
	Allograft	Different individuals of the same species (human cadavers or living donors)	Osteoconductive, non-limited avaliability No donor-site morbidity	Reduced osteoinductive properties Immune rejection Cost
	Xenograft	Different species	Osteoconductive, some osteoinductive	Risk of infections
Synthetic	Alloplast	Synthetic	Osteoconductive	Do not increase substantially bone formation

Although autologous bone graft is considered to be the "gold standard" bone grafting material to enhance bone regeneration and to repair bone defects, the supply of suitable bone is limited and its collection is painful, with a risk of infection, hemorrhage, nerve damage and loss of function (Dinopoulos et al., 2012; Janicki and Schmidmaier, 2011; Petite et al., 2000).

To overcome the aforementioned limitations of bone grafts, a promising alternative are tissue-engineered bone graft substitutes (Janicki and Schmidmaier, 2011). Several materials have been developed to be used instead of the transplanted bone. These include demineralized bone matrix (DBM), polymer-based bone graft substitutes, ceramics (synthetic scaffolds like hydroxyapatite, calcium phosphate or oxide ceramics (Al_2O_3, TiO_2)), growth factor-based graft substitutes and cell-based bone graft substitutes (Dinopoulos et al., 2012). They vary in composition and mechanism of action (Giannoudis et al., 2005). Thus, depending on the surgical indication for bone grafting, the properties of the bone graft substitute will be different.

To fully restore the structure and functionality of bone, the ideal bone graft substitute would combine the following properties:

▪ Biocompatibility: do not elicit an immune response after placement into the host tissue (Salgado et al., 2004) and allow cell attachment, differentiation and proliferation.

- Osseointegration: ability to adhere to the surface of bone without an interfering layer of fibrous tissue.

- Osteoinduction: ability to stimulate and activate host mesenchymal stem cells or osteoprogenitor cells from the surrounding tissue to differentiate into bone-forming osteoblasts (Giannoudis et al., 2005).

- Osteoconduction: ability to act as a scaffold to direct and support bone growth over its surface. In this sense, surface properties (chemical, physical and topographical) will control and affect the ability of cells to adhere to the biomaterial and to proliferate (Dinopoulos et al., 2012; Salgado et al., 2004).

- Interconnected and porous structure: Pore size is important for bone ingrowth and to provide internal surface area for cell attachment (Haugen et al., 2004). Porosity higher than 90% with open and large pores greater than 300-500µm allow cell penetration, migration and vascularization (Mohamad Yunos et al., 2008; Rezwan et al., 2006). In addition, diffusion of nutrients, waste removal and protein transport is obtained with a well interconnected network scaffold (Haugen et al., 2004). However, the porosity and pore size of the scaffolds for bone formation are compromised between the suitability of cells to migrate and grow with the mechanical stability of the scaffold.

- Mechanical competence: sufficient strength to provide mechanical stability in load bearing sites.

- Bio-resorbable: replaced over time by the new bone formed (Janicki and Schmidmaier, 2011).

Therefore, the success of the scaffold/bone graft substitute to induce bone regeneration depends primarily on the nature and properties of the biomaterial and the fabrication process. Consequently, structural (mechanical properties or the degradation behavior) and surface properties (affecting to the biological interactions) will determine the selection of the material for each application (Hutmacher et al., 2007).

Bioactive ceramics represent one type the bone graft substitutes currently used to promote bone regeneration. Bioactive ceramics have chemical composition resembling that of natural bone, allow osteogenesis to occur and provide bonds with host bone (Fostad et al., 2009a; Li et al., 2005). Bioactive TiO_2 ceramics has proven to be one of the most promising biomaterials that satisfy most of the properties described above. TiO_2 is a biocompatible material that does not induce an inflammatory response or encapsulation (Haugen et al., 2004), induces bone-like apatite formation *in vitro,* stimulates osteoconductivity *in vivo* (Marchi et al., 2010) and supports formation of a strong bond to bone upon implantation via the formation of hydroxyapatite (Novak et al., 2009).

In addition, mechanically loadable TiO_2 scaffolds with a compressive strength exceeding 1.5MPa and with porosity above 85% have been produced (Fostad et al., 2009b). These scaffolds allow cell attachment, proliferation and differentiation *in vitro* (Fostad et al., 2009b; Sabetrasekh et al., 2011; Sabetrasekh et al., 2010) and promote new bone formation and vascularization *in vivo* (Haugen et al., 2012; Tiainen et al., 2010).

1.4.4.3. Metal implants

Metal implants are a good material of choice when mechanical and biological implant stability is necessary to direct function in heavily loaded positions, such as in joints and jaws. Thus, metals are used for fracture fixation devices in orthopedic surgery and for endosseous dental implants (Ellingsen et al., 2006; Karageorgiou and Kaplan, 2005).

Stainless steel, pure titanium (Ti) or titanium alloys are the materials that usually comprise the basis of metal implants for bone regeneration (Moradian-Oldak et al., 2006). Lightness, lower modulus of elasticity, and better corrosion has increased the use of commercially pure titanium, at different grades, and its alloys compared to stainless steel implants (Acero et al., 1999; Liu et al., 2004). Ti can be used pure or as alloy when mixed with other metals and metalloids (Schweitzer, 2007) depending on the requested properties. Pure Ti has a high corrosion resistance (Taki et al., 2002), while Ti alloys have an extremely high strength to weight ratio (Elias et al., 2008; Niinomi, 1998). There are four grades of unalloyed Ti used in medical applications, separated by their impurity contents (Table 5). Its mechanical properties including strength, ductability, formability and weldability vary with their content in iron and oxygen.

Table 5. Titanium implant compositions and properties. Adapted from Donachie, Jr. *et al* 2000. (Donachie, 2000).

	Impurity limits, wt% (max)					Tensile strength (min)
Designation	N	C	H	Fe	O	MPa
ASTM grade 1	0.03	0.08	0.015	0.20	0.18	240
ASTM grade 2	0.03	0.08	0.015	0.30	0.25	340
ASTM grade 3	0.05	0.08	0.015	0.30	0.35	450
ASTM grade 4	0.05	0.08	0.015	0.50	0.40	550

Natural or non-modified chemically pure Ti is normally covered by a 2-6 nm thick oxide layer, spontaneously formed in presence of oxygen molecules (Kasemo, 1983; Nygren et al., 1997a). This titanium dioxide (TiO_2) surface layer is believed to be the reason for Ti biocompatibility since the oxide layer protects Ti from corroding, and thus hinders metallic cation release into the human body (Watson, 1985). It has been suggested that varying the thickness of this oxide layer and surface topography may influence the interaction between the implant surface and the surrounding tissue (Larsson et al., 1996; Larsson et al., 1994; Sul et al., 2002).

Implanted metal based biomaterials often induce formation of a poorly vascularized collagenous capsule that can eventually lead to implant failure. Several strategies have been used to improve the biocompatibility and osteogenic capacity of metal implants, with the aim of making the metal surface more acceptable to bone cells and, by doing so, trick the body into rapid integration of the implanted structure rather than fibrous encapsulation. This process, often referred to as foreign body reaction, develops in response to almost all implanted biomaterials and consists of overlapping phases similar

to those in wound healing and tissue repair processes (Ellingsen et al., 2006). The use of micro threads for proper load distribution and micro-rough surface topography have reduced the extent of fibrous encapsulation of implants, and increased the biomechanical properties of the implant-bone interface (Rønold et al., 2003). Therefore, a variety of surface modification technologies for manufacturing rough implants, e.g. grinding (Pavón et al., 2012), polishing (Lucchini et al., 1996), machining (Henry, 1987; Orsini et al., 2000; Sutherland et al., 1993) or blasting (Baleani et al., 2000; Buser et al., 1999), are often used in order to improve the osseointegration of Ti implants (Liu et al., 2004), but also to remove surface contamination (Liu et al., 2004). However, even though reduced in size, the problem of foreign body reaction still have a major clinical impact, and is considered an important issue in all implant treatment strategies, including orthopedics and dentistry. Other strategies for improving biocompatibility and osteoconductive capacity of metal implants in bone include surface modification by non-biological coatings, such as carbide, fluorine, calcium, hydroxyl apatite or calcium phosphate coatings (Brama and Rhodes, 2007; Chetty et al., 2008; Ichikawa et al., 1995; Lamolle et al., 2009; Leeuwenburgh et al., 2006; Sul, 2003), or coatings that aim at mimicking the biological surfaces using lipid mono- or bilayers (Iwasaki et al., 2003; Kim et al., 2005; Svedhem et al., 2003; Tegoulia et al., 2001; Willumeit et al., 2003), thin layers of fatty acids (FAs) (Biesalski et al., 2006; Lee and Chen, 2003), amino acids (Zhao et al., 2008), growth factors or peptides (Rammelt et al., 2006), and proteins (Scheideler L et al., 2007). The idea behind all of these strategies is to make the metal surface look more like bone, and by doing so, trick the body into integrate the implanted structure in the surrounding bone rather than to isolate the structure by encapsulation.

2. Aims & Experimental design

2. Aims & Experimental design

The overall aim of the present thesis was the research of novel treatments for bone regeneration. The results presented in this study were achieved by using short synthetic peptides containing consensus polyproline sequences of hard tissue extracellular matrix proteins involved in the regulation of biomineralization processes. The work can be divided in three sections: the design and evaluation of the three dimensional structure of the synthetic peptides, the determination of their effect *in vitro,* alone or in combination with different biomaterials, and the study of their performance *in vivo* on coated titanium implants. The following specific aims were defined:

Peptide design

Regulation of biomineralization processes are mediated by extracellular matrix proteins that often exhibit proline-rich regions (Jin et al., 2009). First, we designed the sequence of short synthetic peptides based on proline-rich regions of hard tissue extracellular matrix proteins. We used advanced bioinformatics methods for alignment of protein sequences involved in biomineralization processes **(papers 1 and 2)**. Computational simulation methods were utilized to explore correlation between the structure and biological response for a particular synthetic peptide.

Characterization of the biological effects of synthetic proline-rich peptides *in vitro*

After the peptide design and evaluation of the three dimensional structure, we first hypothesized whether those proline-rich peptides would maintain or induce higher osteoblast differentiation compared to the effect of the commercially available amelogenin formulation (Emdogain®) (EMD), which is clinically used for periodontal and bone regeneration. We aimed at evaluating the effects of the designed synthetic peptides **(paper 1)** on MC3T3-E1 and human umbilical cord mesenchymal stem cells (hUCMSC) by assessing toxicity, proliferation, differentiation and mineralization. The effect of synthetic peptides on the differentiation of hUCMSC cells towards the osteogenic lineage with or without and osteogenic media was also studied using new peptide variants **(paper 2).** After confirming the osteopromotive effect of the designed synthetic peptides on MC3T3-E1 cells and on hUCMSC cells, we further aimed at finding a formulation to facilitate their use for bone regeneration. Hydrogels have been widely used in many applications in tissue engineering (Mann, 2003). Sodium alginate and hyaluronic acid are two natural polymers that have been widely used for this purpose; however, to the best of our knowledge, a comparison of the effect of those polymers on osteoblast differentiation has never been reported before. Thus, we studied and compared (1) their structural and physico-chemical properties and (2) their biocompatibility and bioactivity **(paper 3)**, to select the one that better supported osteoblast cell differentiation for later studies. From this study, alginate was selected as a carrier for synthetic proline-rich peptides and their effect was tested *in vitro* **(paper 4).** We next aimed at translating the use of synthetic peptide 2 to bone regeneration applications using biomaterials in parts of the body subjected to mechanical stress, such as scaffolds and Ti implants. TiO_2 scaffolds

have been shown to be a good alternative to autografts, though the behavior over time of MC3T3-E1 osteoblasts on highly porous TiO_2 scaffolds has never been reported before. Therefore, we first set the osteoblast cell culture conditions and we characterized osteoblast cell behavior on highly porous TiO_2 scaffolds **(paper 5)**. Next, TiO_2 scaffolds were coated with an alginate hydrogel containing synthetic peptide 2 and their effect was investigated *in vitro* with MC3T3-E1 osteoblasts. Our hypothesis was that the combination of the osteoconductive properties of TiO_2 SC with the osteogenic effects of proline-rich peptides could represent a new strategy for bone tissue regeneration in load-bearing applications **(paper 6)**.

Evaluation of the effects of peptide-coated Ti implants *in vivo*

Finally, the best variant of our designed synthetic proline-rich peptide tested earlier *in vitro* was selected to functionalize implant surfaces to favor osseointegration. The peptide was used to coat Ti implants and its bone forming abilities was investigated in an animal *in vivo* model after 4 weeks of healing **(Paper 7)**.

The experimental work presented in this thesis was carried out in the Group of Cell Therapy and Tissue Engineering at the Research Institute on Health Science (IUNICS) at the University of Balearic Islands, except the experimental work presented in paper 7, which was performed at the laboratory of Professor S.P. Lyngstadaas at the University of Oslo. Advanced bioinformatics analysis of the different synthetic peptides was carried out in collaboration with the University of Biotechnology (Czech Academy of Sciences, Prague) and with the Institute of Organic Chemistry and Biochemistry (Czech Academy of Sciences, Prague). Human umbilical cord mesenchymal stem cells were a donation from the "Fundació del Banc i Teixits de les Illes Balears", who also collaborated in the characterization of hUCMSC cell surface profile.

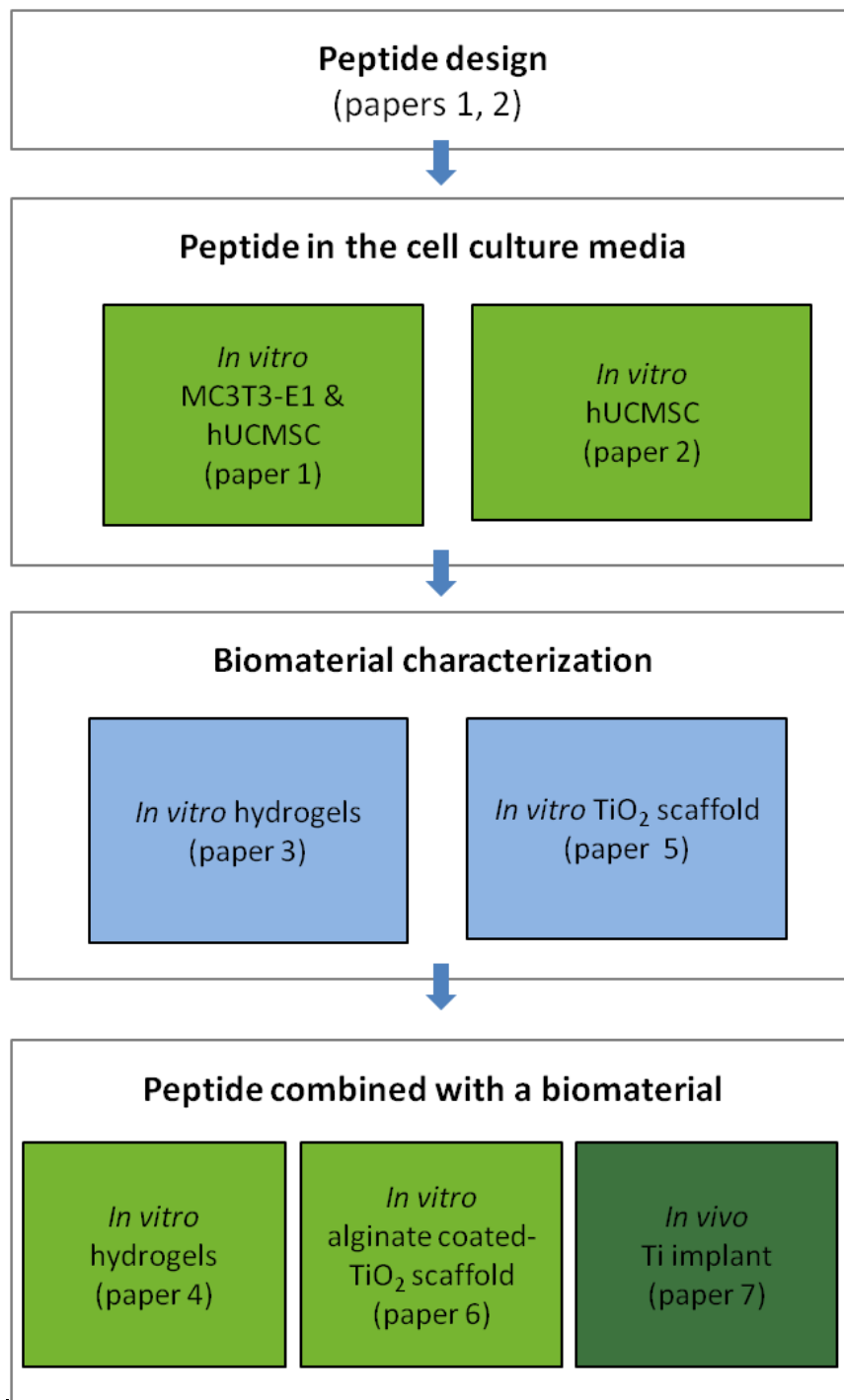An overview of the steps followed throughout this thesis for the methodological approach is provided in Figure 5.

Peptide design
(papers 1, 2)

Peptide in the cell culture media

In vitro
MC3T3-E1 &
hUCMSC
(paper 1)

In vitro
hUCMSC
(paper 2)

Biomaterial characterization

In vitro hydrogels
(paper 3)

In vitro TiO$_2$ scaffold
(paper 5)

Peptide combined with a biomaterial

In vitro
hydrogels
(paper 4)

In vitro
alginate coated-
TiO$_2$ scaffold
(paper 6)

In vivo
Ti implant
(paper 7)

Figure 5. Chart illustrating how the aims of this thesis were approached. Green boxes represent studies using the synthetic peptides (light green for the *in vitro* and in dark green for the *in vivo* study). Blue boxes indicate preliminary studies to set material and culture conditions. In parentheses are indicated the numbers of the respective papers.

2.1. Methods

This chapter provides an overview of the different methods used during this thesis. Advantages or disadvantages of the methods and instruments used are considered. For a detailed description of the methods we refer to the Material and Methods sections of the papers. Figure 6 gives an overview of the different methods used for the methodological approach.
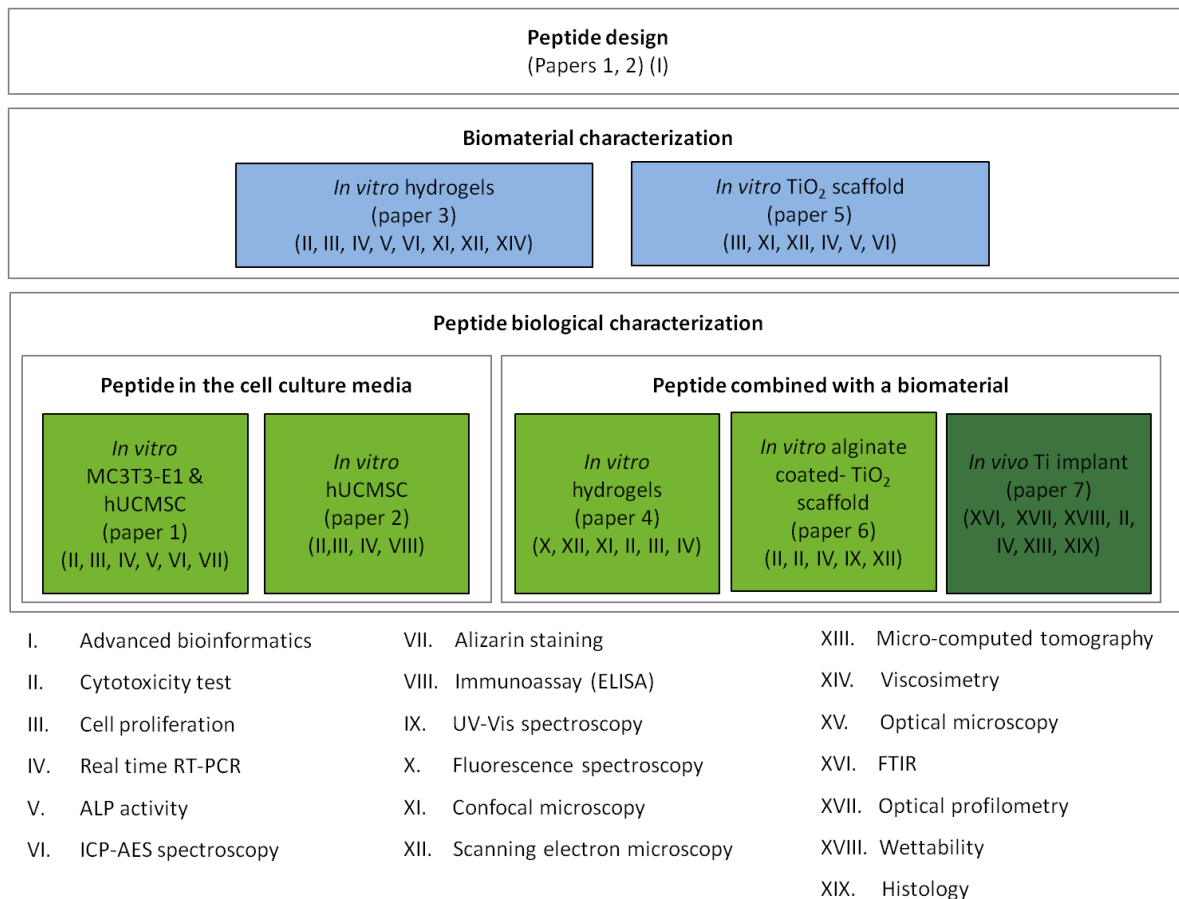

I.	Advanced bioinformatics	VII.	Alizarin staining
II.	Cytotoxicity test	VIII.	Immunoassay (ELISA)
III.	Cell proliferation	IX.	UV-Vis spectroscopy
IV.	Real time RT-PCR	X.	Fluorescence spectroscopy
V.	ALP activity	XI.	Confocal microscopy
VI.	ICP-AES spectroscopy	XII.	Scanning electron microscopy

XIII. Micro-computed tomography
XIV. Viscosimetry
XV. Optical microscopy
XVI. FTIR
XVII. Optical profilometry
XVIII. Wettability
XIX. Histology

Figure 6. Overview of the methods used. The Roman numbers refer to the methods and the latin numbers to the papers. Green boxes represent studies using the synthetic peptides (light green for the *in vitro* studies and dark green for the *in vivo* study). Blue boxes indicate preliminary studies to set material and culture conditions.

2.1.1. Peptide design, bioinformatics

The EMBOSS pairwise sequence alignment algorithm freely available at EBI (http://www.ebi.ac.uk) was applied simultaneously on pairs of sequences of amelogenins and ameloblastins (from human, mouse and rat), two major proteins involved in regulation of biomineralization processes. By increasing the penalty for gap opening to value 100, continuous aligned sequences were identified. Short peptides were designed with constraints on length (25 aminoacids), conservation of proline positions and with systematic variation of the rest of aminoacids.

The different peptides should differ in their physical, chemical, and structural properties due to their different amino acid compositions, except the conserved proline positions in the sequence. The sequences of the designed peptides were modeled by MOBYLE server (Maupetit et al., 2009). This bioinformatic method provides variable conformational orientation of peptides. The best energy conformer of each peptide was subsequently used for analysis and further optimization. Structural stability of the modeled peptides was further explored by molecular dynamic by AMBER package (Cornell et al., 1995) using ff99SB force field (Hornak et al., 2006) in TIP3 (Jorgensen et al., 1983) explicit water environment. The predicted 3D structure obtained for the different peptides are shown Figure 7.
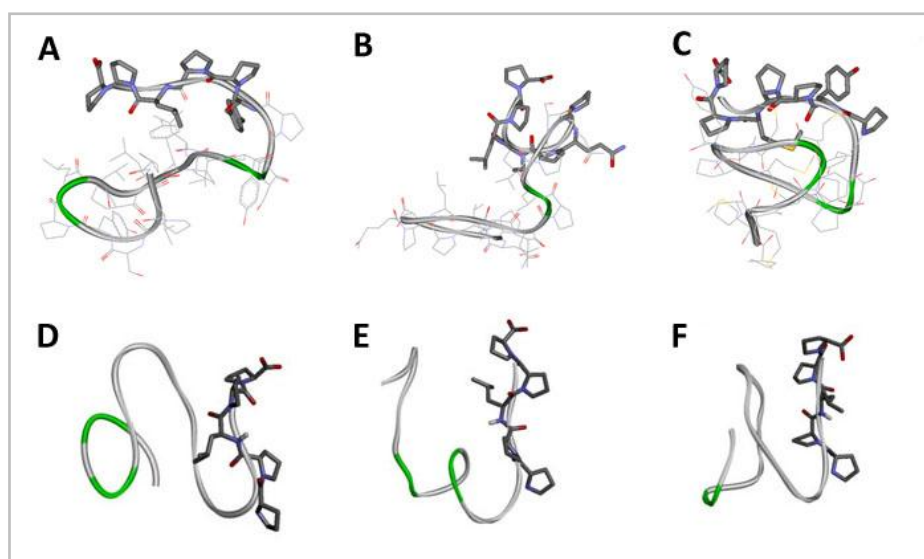

Figure 7. PepFold predicted 3D structures of peptide 1 (A), peptide 2 (B), peptide 3 (C), peptide 4 (D), peptide 5 (E) and peptide 6 (F). C terminal sequence of peptides (PPXPP) is accented by using of stick representation for corresponding amino acids.

2.1.2. Production of biomaterials

2.1.2.1. Hydrogels

As mentioned in the introduction chapter, hydrogels are widely used for many applications in bone tissue engineering (Mann, 2003). A hydrogel formulation is dependent of each specific application.

Hydrogel features are governed by the physical properties (e.g. mechanics, degradation, gel formation), the mass transport properties (e.g. diffusion) and the biological interaction requirements (e.g. cell adhesion and signaling) (Drury and Mooney, 2003). Hence, the type of polymers, the concentrations used and procedure of its preparation has been optimized throughout the present work depending on each specific application (Table 6). In this section, the criteria for selection of type of natural polymers, concentrations used and the modifications followed on the procedure for the hydrogel production in the course of the different studies are described.

Table 6. Polymers used in the different studies.

	Paper 3		Paper 4	Paper 6
Application	Injectable		Coating of biomaterials	Coating of biomaterials
Polymer type	Alginate	Hyaluronic acid	Alginate	Alginate
G monomer content	35-45%	High Mw[*] (800-1200KDa)	≥60%	≥60%
Polymer concentration	1%, 2%, 3%	1%, 2%, 3%	2%	2%
Polymerization	Non cross-linked hydrogels	Non cross-linked hydrogels	Cross-linked hydrogels with $CaCl_2$	Cross-linked hydrogels with $CaCl_2$
$CaCl_2$ concentration	-	-	300mM	50mM

*Mw: molecular weight

2.1.2.1.1.Hydrogel preparation

Alginate or high molecular weight hyaluronic acid (HA, Mw 800-1200 KDa) were dissolved in Phosphate Buffer Saline (PBS) (papers 3 and 4) or distilled water (paper 6), obtaining a solution close to the physiological pH, that was vigorously stirred to avoid formation of polymer grains that are hard to dissolve. The subsequent agitation overnight at 180rpm provided a completely homogenous solution with minimized bubble formation.

In paper 3, with the aim to select the most suitable polymer and its concentration to be used as carrier of peptides in bone regeneration, three different polymer concentrations (1%, 2% and 3%) of alginate and high molecular weight HA were characterized for their physico-chemical and structural properties as well as for their biocompatibility and bioactivity on osteoblasts. 2% alginate resulted to be the most suitable formulation to act as peptide vehicle and to better support osteoblast differentiation. Thus, 2% alginate was selected for further studies.

Additionally, different types of alginate were selected to perform the different studies, since the cross-linking degree of alginate matrices increases with higher G monomers content (Goh et al.). The alginate with a low (35-45%) α-L-guluronic acid content (Protanal LF 200M,) used in paper 3 for the

development of a more elastic injectable hydrogel was replaced in papers 4 and 6 by a sodium alginate containing a minimum 60% of guluronate monomers (NovaMatrix, FMC BioPolymer AS, Norway) with the aim of using an alginate hydrogel with higher consistency for coating different biomaterials.

2.1.2.1.2. Alginate polymerization

Alginate polymerization occurs by the establishment of ionic bridges between the G monomers of alginate and divalent cations, such as Ca^{2+} (Figure 8). The increase in the gel strength depends on the amount of polymer and also on the cross-linking ions. By increasing $CaCl_2$ molarity the compressive strength increases, presumably by an increase in the cross-linking density. Thus, with increasing $CaCl_2$ ions a more compact microstructure of the alginate with a decrease in pore size should be expected.
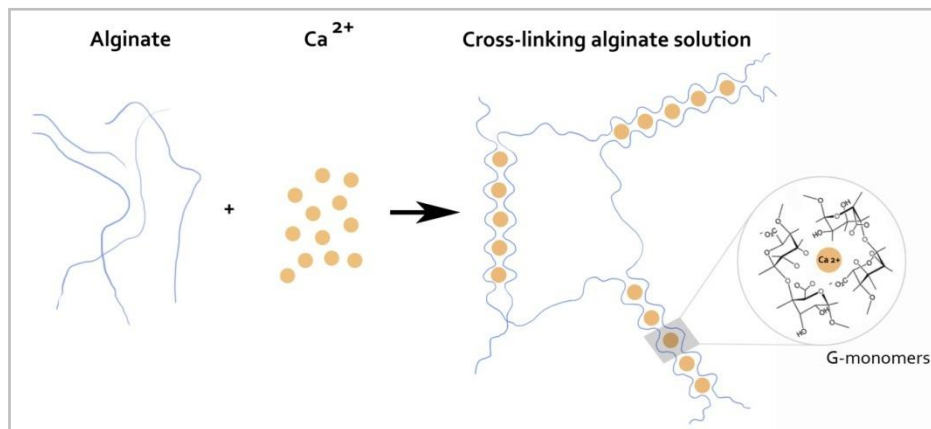
Figure 8. Structure of an alginate gel polymerized by the formation of ionic bridges between Ca^{2+} and G-monomers.

In the different studies, some changes have been introduced in the fabrication of a cross-linked alginate hydrogel depending on each specific application (Figure 3 and Figure 4).

■ For the development of an alginate hydrogel for their stand-alone or their use as coating on biomaterials (paper 4) (Figure 9), the solution of alginate containing synthetic peptides/EMD was distributed into 24-well culture plates and sprayed with 300mM $CaCl_2$. An Aerograph paint atomizer (Precisso®, Madrid, Spain) was used to add a thin layer of $CaCl_2$ for an adequate polymerization and to get a coin-shaped hydrogel. This shape was convenient since it provided a plane disk to perform the *in vitro* studies. Prior to use, alginate hydrogels were kept for 1-2 hours at room temperature to allow complete gelation and were subsequently washed with cell culture media in order to remove the excess of $CaCl_2$.
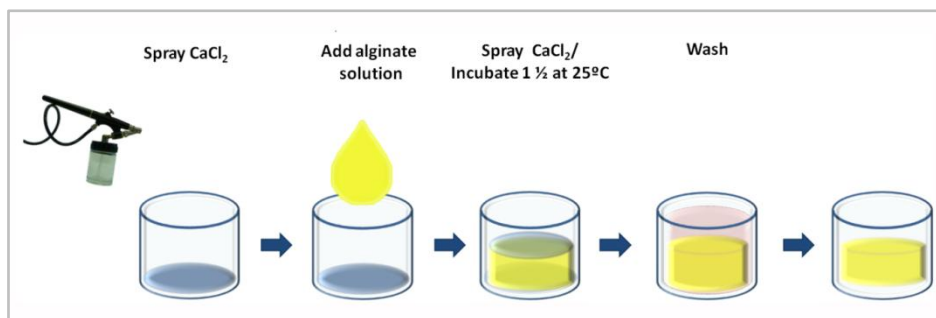
Figure 9. Schematic overview for the preparation of alginate hydrogels. Alginate gelation was obtained after spraying with 300mM CaCl$_2$.

■ For coating TiO$_2$ scaffolds with a layer of alginate (paper 6) (Figure 10), scaffolds were submerged into 2% alginate solution with or without P2 under agitation at 100rpm on an orbital shaker (IKA Vibrax VXR basic, Staufen, Germany) for 1 h at room temperature (RT) to ensure the complete coating of the 3D structure with alginate and were subsequently centrifuged at 252xg for 1 min to remove the excess of alginate. To allow alginate gelation, sample was immersed into 50mM CaCl$_2$ for 30 minutes. Prior to their final use, the scaffolds were rinsed with distilled water to ensure the removal of residual CaCl$_2$ present on the surface, and samples were let to dry overnight at room temperature.
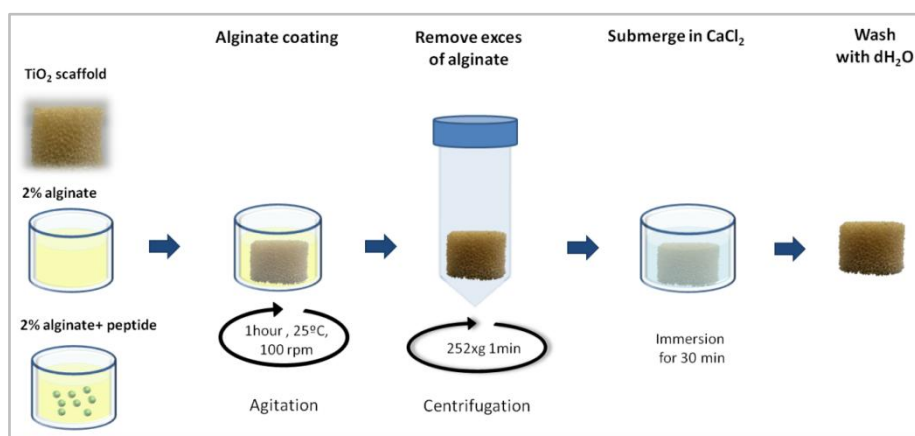

Figure 10. Schematic overview of coating TiO$_2$ scaffolds with alginate. Alginate gelation was obtained by submersion into 50mM CaCl$_2$.

2.1.2.2. TiO$_2$ scaffolds

High porous TiO$_2$ scaffolds, with a size of 9 mm of diameter and 8 mm high, were produced by a polymer sponge replication process (Figure 11) (Tiainen et al., 2010). TiO$_2$ was chosen since it has proven to be a biocompatible material with bioactive properties promoting good cell adhesion and growth of mouse osteoblast cells and human mesenchymal stem cells (Fostad et al., 2009b; Nygren et al., 1997b; Rincon et al., 2005). Briefly, polyurethane foam templates were infiltrated with ceramic TiO$_2$ slurry. Excess slurry was squeezed out, to ensure that only a thin layer of slurry covered uniformly the entire surface area of the polymer template without blocking the pores, and subsequently let to dry. Then, for the burnout of the polymer, the scaffolds were slowly heated thus

minimizing the damage to the porous coating. Once the polymer was removed, the ceramic was sintered to the desired density. Through this process, the macrostructure of the polymer was replicated.
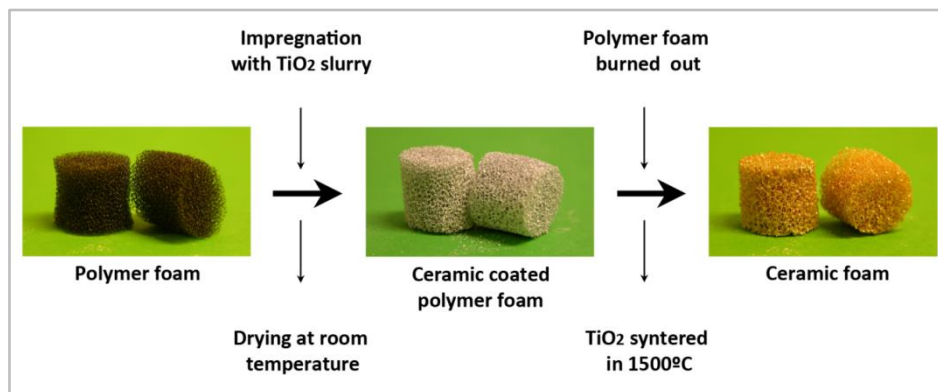

Figure 11. Overview of the production of TiO$_2$ scaffolds by the polymer sponge method. With the permission of Hanna Tiainen (Department of Biomaterials, University of Oslo).

Following, scaffolds were coated with 2% alginate containing synthetic peptide P2. Due to the fact that scaffold porosity and pore network interconnectivity of the surface determines cell migration and differentiation, bone ingrowth, vascularization and mass transfer between the cells and the environment (Hutmacher, 2000), the coating with alginate should avoid the blocking of scaffold pores to allow cell migration and nutrient flow in- and out- the three dimensional structure. The procedure followed for coating the scaffolds with alginate has been described in section 2.1.2.1.2.

2.1.2.3. Ti implants

Pure machined Ti disks of grade 4 with a diameter of 6.25 mm and a height of 1.95mm were selected for studying the effect of synthetic peptide P2 adsorbed on- Ti implant surfaces on osseointegration and bone healing using a rabbit model.

Commercially pure machined Ti disks were cleaned to completely remove debris from machining. Briefly, implants were washed in a glass beaker with deionized (DI) water for 30 s, with 70% ethanol for 30s, and in an ultrasonic bath in DI water at 40ºC for 5 min. The implants were subsequently placed in 40% NaOH solution in a water bath at 40ºC for 10 min, sonicated in DI water for 5 min and then washed with DI water until pH reached six. Afterwards, the implants were sonicated in DI water at 50ºC for 5 min, placed in 50% HNO$_3$ solution at 50ºC for 10 min and sonicated in DI water for another 5 min. The implants were then washed with DI water until pH reached six and stored in 70% ethanol until use. Before use, the disks were rinsed with water, rinsed with ethanol, sonicated in DI water for 5 min at RT and subsequently rinsed with DI water. The Ti disks were subsequently sterilized by autoclaving at 121ºC for 15 min. Before peptide coating, the implants were washed for 10s in autoclaved DI water, rinsed with acetone/water (50:50 by volume) and with 100% acetone, air dried and packed individually in microcentrifuge sterile tubes until their use. Special care in the quality of

water and the final pH value of water was needed to avoid the staining of the device or for a proper cleaning of the implants.

For peptide coating of Ti disks, synthetic peptide 2 solution (10µL of 100µg/mL) was applied to the surface and incubated at 37ºC for 24 hours. Ti implants were subsequently rinsed with sterile DI water, dried in a desiccator, packed and stored at 4ºC until use. Peptides were physically adsorbed onto the Ti surface through interaction of the negatively charged carboxilic groups of peptide with the metal oxide of Ti surfaces (Figure 12).
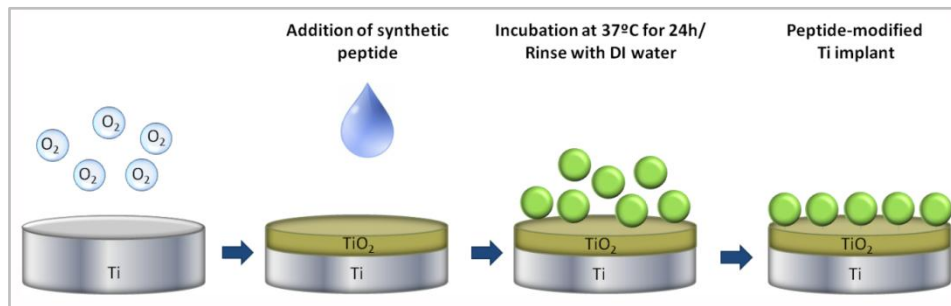
Figure 12. Schematic overview of the peptide coating of Ti implants used in the rabbit study.

2.1.3. Physico-chemical characterization

2.1.3.1. Scanning electron microscope (SEM)

Scanning electron microscope *(SEM)* is a fast qualitative method that provides information about sample surface topography or composition at high magnification. Secondary electron imaging (ESED) produce a very high-resolution images with a large depth of field revealing tiny details and thus providing a three dimensional appearance useful for understanding the surface structure of the sample. Alternatively, by back-scattered electron detector (BSED), images appear with different intensity of grey values depending on the different atomic number of the material, thus, being useful to visualize the distribution of different elements (TiO_2, alginate or cells) in the sample (Krinsley et al., 1998). Energy-dispersive x-ray spectroscopy (EDS) can be coupled to SEM for analytical analyses of specific areas of the sample (Reimer, 1998). SEM was used in this thesis for imaging the changes in the gel network (papers 3 and 4), the morphology of TiO_2 scaffolds (papers 5 and 6) and the amount of cells adhered onto three dimensional structures (papers 5 and 6) (Figure 13). EDS analysis was also performed to confirm the presence or absence of alginate coating and of a cell monolayer in TiO_2 scaffolds (data not presented). Biological samples containing cells need to be fixed and to be completely dry to preserve its structure under the high vacuum conditions of the chamber specimen. Hydrogels, characterized by high water content, must be dried by lyophilisation to prevent artifacts from vapor coming out of the sample that spreads and attenuate electron beams. Thus, the hydrogel morphology in wet state cannot be assessed by SEM.
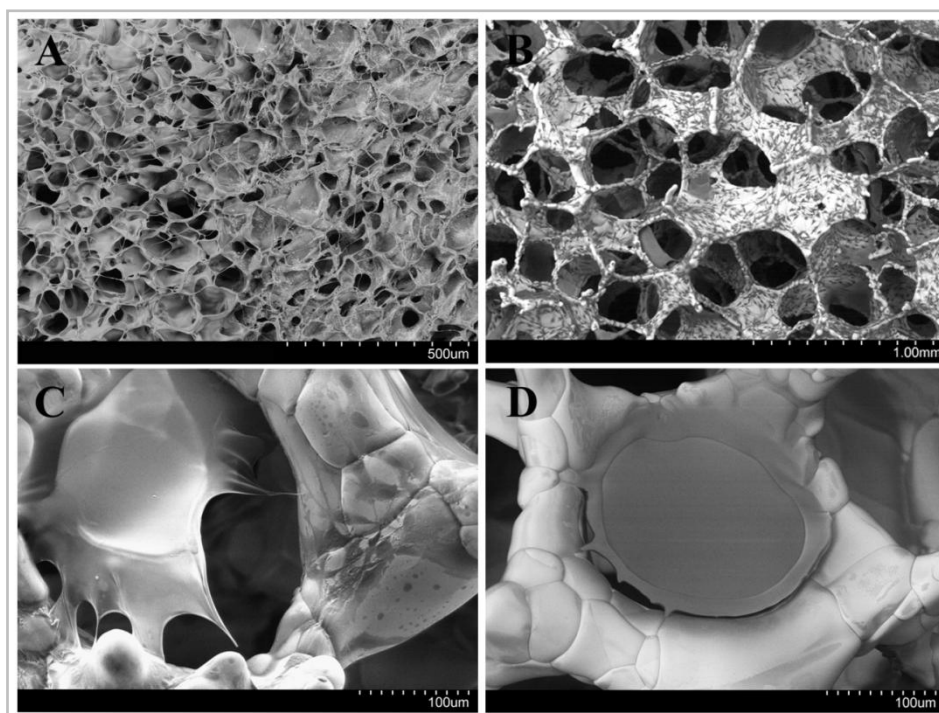
Figure 13. SEM was used in this thesis for imaging the changes in the hydrogel network (A), the morphology of TiO$_2$ scaffolds (B, C and D), and the amount of cells adhered onto three dimensional structures (B, C). Two different detectors were used. ESED detector (A, C) was useful to get an overview of the material topography, while BSED detector was used to differentiate TiO$_2$ scaffolds from alginate coating and/or to easily visualize cells adhered on the TiO$_2$ scaffold (B, D).

2.1.3.2. Optical profilometry

Optical profilometry is a method of great value to measure the surface's profile and to give information on material roughness before and after bioactive surface coatings at high resolution. An optical profilometer is a non-contact profiler that can measure small vertical features ranging in the nanometer level but with a poor lateral resolution (Mix, 2010). Thus, an optical profilometer (PLµ 2300, Sensofar, Terrassa, Spain) was used to visualize Ti implants surfaces coated with the peptide P2 (paper 7).

2.1.3.3. Fourier transform infrared spectroscopy (FTIR)

Chemical changes in molecular structure can be detected by molecular spectroscopy methods such as fourier transform infrared spectroscopy (FTIR). This technique measures the absorption of infrared radiation by the sample material versus wavelength. The FTIR spectra allow the identification of molecular components and structures (Smith, 2011). In this thesis (paper 7), FTIR spectroscopy was used to verify the presence of attached peptide on the sample surface and to analyze structural changes upon adsorption (measured with the diffuse reflectance unit (DRIFT). The FTIR spectrum of the attached peptide was compared with the spectrum of the peptide dissolved in PBS (collected with ATR with a resolution of 4 cm^{-1}). The spectrum were baseline corrected, deconvoluted (γ=1.5,

length=75%), and normalized with spectrum (version 6.3.2.0151, PerkinElmer, inc., Waltham, USA). Details in the shape of the amide 1 peak (~ 1,740 to ~1,580 cm-1) of proteins and polypeptides by FTIR allowed the analysis of its secondary structure (Barth, 2007) and thus gave indications of conformational changes of peptide upon adsorption on the surfaces of Ti implants. In addition, the size of the peak in the spectrum was directly related to the amount of the peptide adsorbed.

2.1.3.4. Contact angle

Contact angle is a direct measure of the ability of a liquid to spread on a surface (surface wettability). If the liquid completely spreads out on the solid surface, the contact angle will be close to 0°; this means that it is a hydrophilic surface. On the contrary, if the surface is hydrophobic, the contact angle will be larger than 90° (Figure 14). Surface wettability is a physico-chemical property of all surfaces that influences the adhesion and proliferation of different types of cells (Lee et al., 1997; Lim et al., 2005). Several studies have reported that cells preferentially adhere to surfaces with a low contact angle (of about 50º) (Lee et al., 1997). Contact angle is a highly sensitive method, being useful for evaluating cleanness of solid surfaces, as it can show different results even with small amount of contamination. In order to avoid contamination coming from external factors such as environmental factor (temperature, humidity), it is very important to work in a controlled environment when performing the surface modification of Ti implants. In paper 7, the water contact angle of the surfaces of different Ti implants were measured using a video based contact angle system (OCA 20, DataPhysics Instruments).
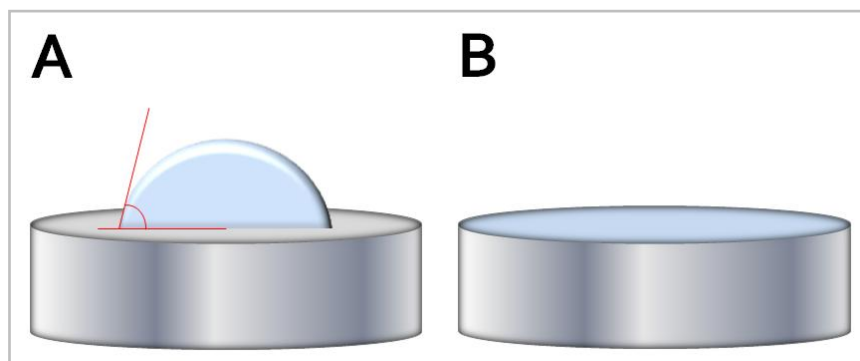

Figure 14. Scheme of a water drop on a hydrophobic (A) or hydrophilic (B) surface.

2.1.3.5. UV-Vis spectroscopy

UV-Vis spectroscopy is an easy and quick method that can be used for example to quantify protein content by measuring the absorbance of ultraviolet light by peptide bonds (Simonian, 2002). Absorbance into the UV-Vis range can be measured by means of different equipments, e.g. by using conventional UV spectroscopy (UV Quartz cuvettes), by using a NanoDrop spectrophotometer or by means of a microplate spectrophotometer reader. Based on the absorbance of the peptide bond, peptide 2 released from 2% alginate gel coated TiO_2 scaffolds (paper 6) was measured at 206nm with a conventional UV spectrophotometer using Quartz cuvettes. As it will be commented further in this

thesis, alginate can interfere with synthetic peptide quantification when using UV-VIS spectroscopy. However, in the experiments performed in paper 6 no artefacts were obtained from alginate; probably due to the thin layer of alginate produced for coating the TiO$_2$ scaffolds.

2.1.3.6. Fluorescence spectroscopy

Fluorescence spectroscopy is a spectrochemical method that analyses the fluorescence of a sample that is based on the capacity of certain molecules (fluorophores) to emit light. When light of an appropriate wavelength is absorbed by a fluorophore (i.e., excitation), the electronic state of the molecule changes from the ground state to one of many vibrational levels in one of the excited electronic states. Fluorescence corresponds to the relaxation of the molecule from the singlet excited state to the singlet ground state with emission of light. The fluorescence spectroscopy gives emission spectra of the fluorescence intensity versus the wavelength, which vary widely and is dependent upon the chemical structure of the fluorophore and the solvent in which it is dissolved (Lakowicz, 2006; Sauer et al., 2011). In this thesis, this method was used to quantify the release of peptide 2 labeled with FITC (a fluorophore) contained into 2% alginate hydrogels (paper 4). This method was developed since an interference of the alginate was found when using UV-VIS spectroscopy in paper 4. This interference resulted from the biodegradation of alginate (Drury and Mooney, 2003) after being incubated at 37ºC for a long period, and since an alginate waste was generated and interfered with the quantification of the peptide at 206 nm. Thus, the labeling of peptide with a fluorophore (FITC) was a useful and trustworthy method to get a quantifiable peptide avoiding alginate artifacts. Then, the peptide release (P2-FITC) was quantified by fluorescence spectroscopy (λex 490 nm and λem 525 nm). Relative fluorescence units were correlated with the amount of peptide released using a linear standard curve for each time point.

2.1.4. Biological characterization *in vitro* and *in vivo*

2.1.4.1. Cell culture

In vivo research poses a beneficial model for gaining immediate and direct knowledge of human exposure to a certain treatment (Clift et al., 2011). However, the complexity of this system, the ethical issues for using animals together with the costs associated to this research, limits their use for a first screening and characterization of cell response to a certain stimuli (Habibovic et al., 2007). *In vitro* models provide an inexpensive and high-throughput alternative to *in vivo* research strategies (Clift et al., 2011). *In vitro* assays give a simplified reflection of the *in vivo* situation in controlled and well defined conditions. Therefore, the establishment of an *in vitro* model is attractive and useful for a first characterization of the biological effects of a specific biomolecule or a new biomaterial. Once it is established the cell behavior in front of a certain treatment, an intermediate step prior to clinical use in humans is to test the effects of the specific treatment *in vivo*.

In this thesis two types of *in vitro* cell culture models have been used: primary cultures and cell lines.

▪ *Primary cell culture* refers to cells that are placed in culture directly from the tissue of origin. Although functionally differentiated primary cell cultures have a limited life span compared to cell lines, the use of primary cell cultures reflects better the *in vivo* situation. In this thesis, mesenchymal stem cells (MSC) were selected as *in vitro* model. MSC cells are multipotent cells that can differentiate along a variety of cell lineages, such as chondrocytes, osteoblasts, adipocytes, myocytes, neurons and hepatocytes (Bobis et al., 2006). Mesenchymal stem cells are the main source of osteoprogenitor cells, being involved in normal skeletal homeostasis (Deschaseaux et al., 2009) and in bone regeneration mechanisms (Bielby et al., 2007). When cultured with osteogenic supplements (ascorbic acid, β-glycerolphosphate and hydrocortisone) (Jaiswal et al., 1997) (Figure 15), MSC cells are capable to differentiate to osteoblastic cells. The main properties of those osteogenic supplements are detailed next:

- Ascorbic acid (AA) or vitamin C: is an essential component for the synthesis of hydroxyproline, which is essential to stabilize the collagen triple helix (Murad et al., 1981). Consequently, AA has been described to play an important role in the production of a collagenous bone extracellular matrix (Coelho et al., 2000). AA is generally used at a working concentration of 50 µg/ml in isolated cell culture systems, at which concentration it is not toxic nor does it lead to ectopic mineralization (Hughes and Aubin, 1998).

- β-Glycerophosphate (βGP): is an organic phosphate source that, in osteogenic cells acts as a substrate for ALP resulting in an increased concentration of inorganic phosphate and subsequent mineral deposition. β-GP is usually used to a final concentration of 10 mM and, as with AA, a 100x stock solution can conveniently be prepared, with PBS as diluent, and stored in single-use aliquots at -20°C (Hughes and Aubin, 1998).

- Hydrocortisone hemisuccinate: glucocorticoids such as hydrocortisone hemisuccinate have complex effects on osteoblast metabolism, which may include increased expression of a differentiated phenotype, together with suppression of production of a number of extracellular signaling molecules such as interleukin 1, prostaglandins and nitric oxide. It is a glucocorticoid produced by the adrenal gland (Hughes and Aubin, 1998). Glucocorticoids affect cell proliferation indirectly by altering cell responsiveness to growth factors (Baker et al., 1978). In a number of cell systems, glucocorticoids have been shown to be an important medium supplement to achieve expression of a recognizably osteoblastic phenotype. In addition the beneficial effects of hydrocortisone in culture are its ability to promote differentiation and to prolong the life of the cultures (Hanks, 1979; Hughes and Aubin, 1998). Glucocorticoids are usually used to a final concentration of 200nM.

In this thesis, human umbilical cord mesenchymal stem cells (hUCMSCs) were isolated from umbilical cords obtained in the process of human umbilical cord blood donations under the Concordia Cord Blood Donation Program. When using primary cultures, variables among different donors must be taken into account; to overcome this problem and to improve validity of our data, we used three

different donors. We used standard flow cytometry techniques to determine the cell surface profile and to confirm that the resulting cells isolated fulfilled the criteria of a MSCs population established by Mesenchymal and Tissue Stem Cell Committee of the International Society for Cellular Therapy (Dominici et al., 2006).
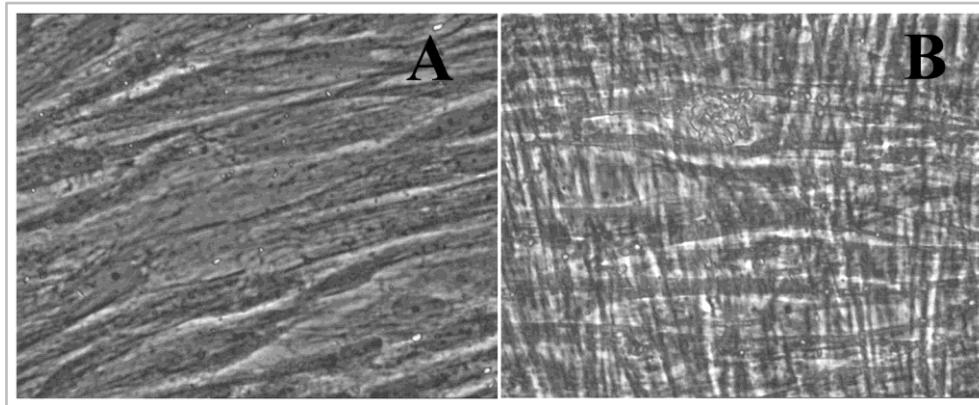

Figure 15. Human UC-MSC cell morphology in cells cultured with growth media (A) or media with osteogenic supplements (B). Visualization by optical microscope at 32x of magnification.

Since MSCs are directly involved in the bone regenerative process and are capable of propagating along the osteogenic lineage, hUCMSCs were chosen to evaluate the effects of synthetic peptides on the differentiation of hUCMSCs towards the osteogenic lineage, either when cultured in a growing or in an osteogenic media.

- *Cell lines* are derived and developed as a subculture from a primary cell culture. The advantages of immortal cell lines over primary cells are the ease of culture and increased phenotypic stability with serial passages, which results in increased reproducibility of results in independently conducted experiments, and therefore present the advantage of the comparability between different experiments. Donor variations are diminished. However, immortal cell lines might show characteristics less close to actual *in vivo* situations. It should also be taken into account that there might be differences between species, even when conducting *in vitro* experiments. Immortal cell lines might show abnormal behavior compared to primary cell lines.

MC3T3-E1 pre-osteoblastic cells (Figure 16), derived from mouse calvarial cells, have been widely used to study bone tissue development *in vitro* because, under appropriate conditions, this cell line undergoes a developmental sequence of proliferation and differentiation similar to primary cells in culture (He et al., 2004; Peterson et al., 2004). In addition, MC3T3-E1 cells are often chosen as *in vitro* model for the cell-material interaction studies (Czekanska et al., 2012). Thus, MC3T3-E1 cells were chosen as an *in vitro* model for studying the stimulatory
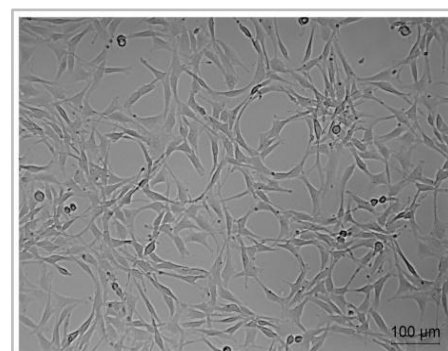

Figure 16. MC3T3-E1 cell morphology. Optical microscope 10x of magnification.

effect of synthetic peptides, either alone or in combination with different biomaterials, on osteoblast differentiation and mineralization. Cells were cultured in alpha-MEM culture media that includes both ascorbic acid and a phosphate source available to cells for mineralization.

In papers 1 and 2, the osteogenic effect of synthetic peptides when administered in the cell culture media was tested either in a pre-defined osteoblastic cell line (MC3T3-E1 cells) or in human umbilical cord mesenchymal stem cells (hUCMSCs) cultured either with or without osteogenic supplements. Equally interesting would be to test the response of hUCMSCs to synthetic peptides when they are administered as a hydrogel form or loading alginate-coated TiO_2 scaffolds.

2.1.4.2. Animal model

Female New Zealand White rabbits were used for *in vivo* testing of the effect of peptide-modified Ti implants on osseointegration. The animal model used is a standardized and validated model that have been established for studying bone attachment to Ti implant surfaces (Ronold and Ellingsen, 2002). Ti implants with a coin-shaped design enables the possibility of performing a molecular analysis of the peri-implant bone attached to the extracted implants, the enzymatic analysis of ALP and LDH activity in the wound fluid present at the implant site and the micro-CT analysis of the intact bone; giving together very valuable information on the nature of the biological factors in the bone bonding and mineralization at the interface. In this model, polytetrafluoroethylene (PTFE) caps are used to cover the back side of the implants in order to prevent bone formation around and on the back side of the implants, which would influence the measurements of the direct bonding between the bone and the test surface (Monjo et al., 2008; Monjo et al., 2012). This animal model is well established and frequently used in the laboratory of Prof. Lyngstadaas at the University of Oslo.

We used a limited number of animals, according to the 3 R's rule for good animal practice. Thus, three female New Zealand White rabbits, all from the same age and weighing 3.0 to 3.5kg, were used. Animals were housed together in one cage before surgery and during healing period. Animals were maintained at 19°C ± 1°C of temperature with a humidity of 55% ± 10%. Room was lightened from 8 am to 8pm, in accordance with the Animal Welfare Act of December 20th 1974, Nº 73, Chapter VI, Section 20-22 and Regulation on Animal Experimentation of January 15th 1996. The experiments had been approved by the Norwegian Animal Research Authority (NARA) and registered by this authority.

Four Ti implants were placed in the tibiae of each rabbit, two on the left side and two on the right side, according to the predetermined randomization protocol. The surgical method was based on the standardized and validated method developed by Rønold *et al* (Rønold and Ellingsen, 2002). Four weeks after surgery, the animals were sacrificed and the effect of peptide-modified Ti implants on bone formation was evaluated by analysing gene expression of osteoblast markers, osteoclast markers and inflammatory markers using real time RT-PCR. In addition, the morphometry of the peri-implant cortical bone tissue was evaluated by micro-CT and histology. Finally, tissue fluid from the

implant site was collected to measure tissue necrosis (LDH activity) and ALP activity and total protein content (Figure 17).
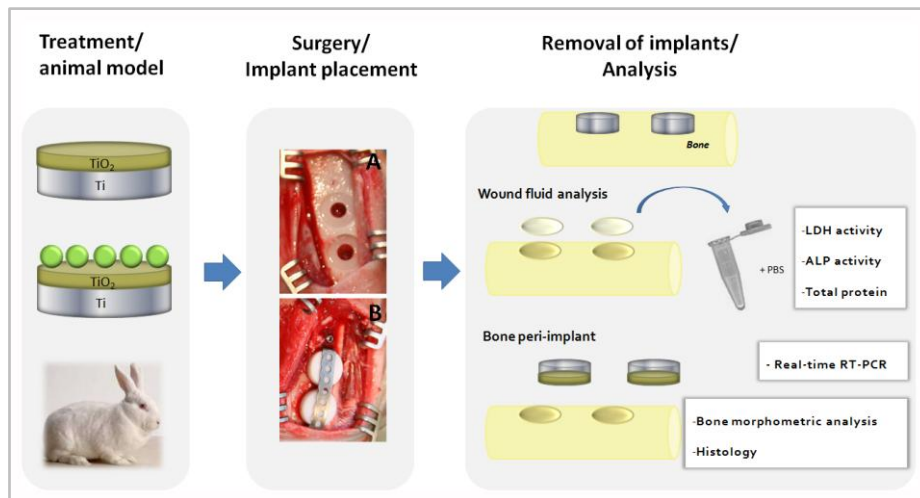

Figure 17. Schematic overview of the steps and analysis performed in the animal model. Figure adapted from Monjo *et al* (Monjo et al., 2010b).

2.1.4.3. Cell toxicity: Lactate dehydrogenase (LDH) activity

One of the important prerequisites for the use of a biomaterial is a high level of biocompatibility (Van Tienhoven et al., 2006). Lactate dehydrogenase (LDH) is an oxidoreductase that catalyzes the conversion of lactate to piruvate. LDH is a stable cytoplasmatic enzyme present in all cells, which is rapidly released into the cell supernatant upon damage of the plasma membrane. The release of the LDH in the cell culture media can be used to quantify cytotoxicity in cell cultures *in vitro* and the release of LDH to the wound fluid to assess tissue necrosis at the bone-implant interface *in vivo*. It is a simple colorimetric assay that measures the lactate dehydrogenase by assessing spectroscopically the rate of oxidation of NADH at 490nm in the presence of piruvate. The intensity of color of the product is directly related to the enzymatic activity. By performing this assay, it is possible to measure the adverse effects induced by different treatments and/or by a biomaterial when are in contact with the cells, either *in vitro* or *in vivo*. In this thesis we have assessed the biocompatibility, in terms of cell viability, of the synthetic peptides (paper 1, 2, 4, 6) but also of the different materials used (alginate or hyaluronic acid hydrogels (paper 3 and 4), alginate-coated TiO_2 scaffolds (paper 6). Moreover, tissue necrosis upon placement of peptide-modified Ti implants in the rabbit tibiae was also assessed (paper 7).

Alternatively, the cytotoxicity of biomaterials can be measured through assessment of changes in membrane integrity by tripan blue exclusion or by nucleic acid staining using propidium iodide or through assessment of the metabolic activity by the tetrazodium salt (MTT) assay.

Aims & Experimental design

2.1.4.4. Cell morphology, attachment and proliferation

Cell attachment and cell growth is a direct result of the stimulatory or inhibitory growth signals received by the cells (Barnes and Gillet, 1995). Physico-chemical properties of biomaterials determine cell behavior, affecting their ability to adhere and to proliferate on the surface and regulating cytoskeletal organization with long-term effects on osteoblast cell maturation and mineralization (Shah et al., 1999).

In this thesis, incorporation of bromo-2'-deoxyuridine (BrdU) into the DNA was used to determine the effect of synthetic peptides on cell proliferation compared to EMD in hUCMSC and MC3T3-E1 cells cultured on tissue culture plastic dishes (TCP) (papers 1 and 2). In later studies, total DNA content quantification (papers 3, 4, 5 and 6), determination of the number of cells attached onto the surface by confocal microscopy (paper 4 and 5) or by scanning electron microscope (paper 5 and 6) were used to assess the ability of cells to attach and spread onto alginate hydrogels (paper 3 and 4), TiO_2 scaffolds (paper 5) or alginate-coated TiO_2 scaffolds (paper 6).

2.1.4.4.1. Confocal laser scanning microscopy (CLSM)

Fluorescence imaging is one of the most basic tools used in biological sciences for the visualization of cells and tissues (Wu et al., 2008). In fluorescence imaging, specimens are labeled with fluorophores. Fluorescence imaging can be performed with conventional fluorescence microscopy or with confocal microscopy (Figure 18). Whereas the first is most commonly used for fluorescence microscopy of thin fixed samples, confocal microscopy is more appropriate for thicker samples (Wu et al., 2008). The most important feature of a confocal microscope is the capability of isolating and collecting only light from a focal plane within a sample, allowing image capture at higher quality and with a less out-of-focus blur compared to conventional fluorescent microscopy. In addition, fine detail is often obscured by the haze and cannot be detected in a non-confocal, fluorescent microscope (Corle and Kino, 1996). Moreover, by CLSM it is also possible to carry out serial optical slices that can then be combined into one single image or to produce a 3D image. In this thesis, cell morphology and the amount of cells attached to alginate hydrogels were visualized by confocal microscopy (paper 3, 4 and 5). Combination of serial images was useful for imaging cells growing onto alginate hydrogels (paper 4) and on TiO_2 scaffolds (paper 5), where not all cells were at the same plane.
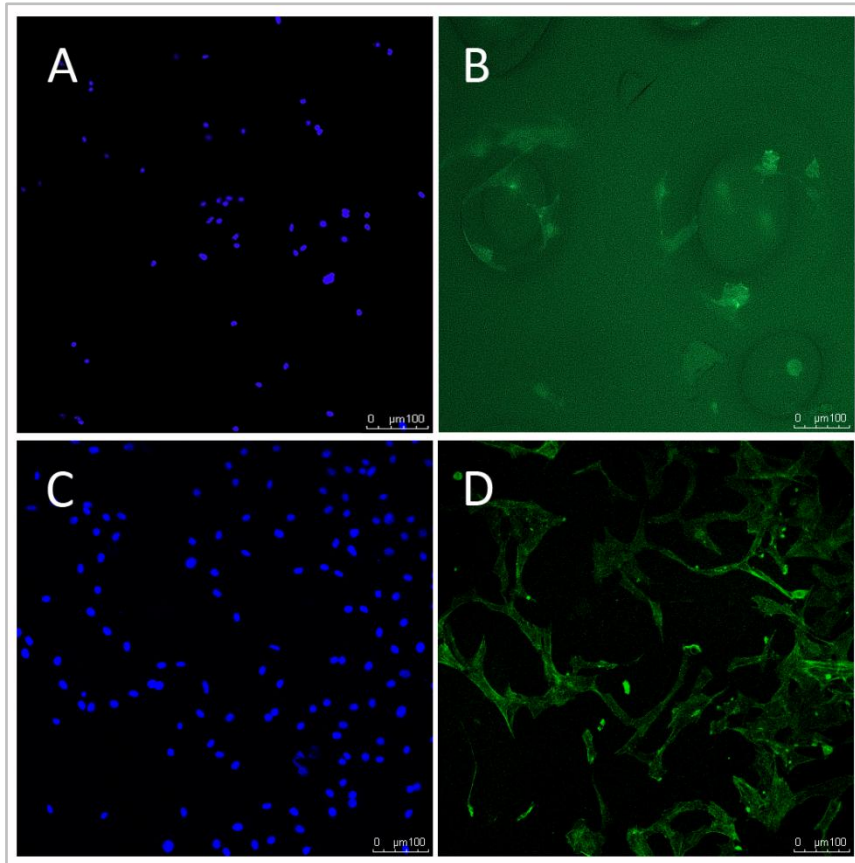
Figure 18. Visualization of MC3T3-E1 cells growing on 2% alginate hydrogels. Images represent observation of the same sample preparation by a conventional fluorescence microscope (A and B) or by a confocal microscope (C and D). Cell nuclei are shown in blue (DAPI staining) and actin filaments are shown in green (phalloidin-FITC staining).

2.1.4.4.2. Bromo-2'-deoxyuridine (BrdU)

Determination of bromo-2'-deoxyuridine (BrdU) incorporation into the DNA is used as a parameter of DNA synthesis and cell proliferation. It is a quantitative method in which cells are cultured in a 96-well plate and the BrdU added to the culture medium is incorporated into cellular DNA. This constitutes a safer alternative to the use of radioactive labeled or radioisotopes, and it is easier and faster than immunohistochemistry/cytochemistry and fluorescence activated cell sorter analysis. Nevertheless, by using this method we have been unable to appreciate differences on cell proliferation of MC3T3-E1 and hUCMSCs cells cultured with different treatments (papers 1 and 2). Although it could be expected that treatments lacked an effect on cell proliferation, it should also be considered that this lack of differences on cell proliferation might be due to: i) the addition of the BrdU was not well adjusted to cell division, ii) the time or BrdU incubation was not enough to allow its incorporation into the cellular DNA, iii) or to the combination of both. So, further experiments should be performed to better define the rate of cell division for the establishment of "*when*" and "for *how long*" adding BrdU. Therefore, total DNA content quantification (paper 3, 4, 5 and 6), determination of the number of cells attached onto the surface by confocal microscopy (paper 4 and 5) or by scanning electron microscope (paper 5 and 6) were alternatively used for the following studies as an indicator of cell growth.

2.1.4.4.3. DNA content

By quantification of the DNA content it is possible to get an estimation of the number of cells, thus we can know the rate of proliferation at a specific time point since we know the amount of cells initially seeded. Among the different methods used for DNA content quantification, in this thesis we used phenol-chloroform extraction (paper 3) and DNA staining using Hoechst dye after cell lysis (papers 4, 5 and 6).

Phenol-chloroform extraction is a common method used for nucleic acid isolation. This method is based on the differential solubility among RNA, DNA and proteins in the two immiscible liquids for its separation. In this method, cells are first lysated by guanidine thiocyanate which disrupts cells and denatures endogenous nucleases. By the addition of chloroform the sample separates into three phases: 1) an aqueous phase that contains RNA, 2) a white interphase containing the DNA and 3) an organic phase with the total protein. For DNA isolation, the interphase and organic phase are selected and ethanol is added to allow precipitation of DNA. Although this method allows the isolation of RNA, DNA and total protein content from the same sample, is a long protocol with several washing steps that introduces high variability/error. Therefore, phenol-chloroform DNA extraction with the subsequent alcohol precipitation steps was only used in paper 3, and in further studies of this thesis (papers 4, 5 and 6), DNA was quantified by a more accurate, sensitive, specific and faster method based on DNA staining by Hoechst (Rao and Otto, 1992). In this case, the cells are lysed by freezing in distilled water and DNA is subsequently stained with Hoechst that rapidly access DNA. Fluorescence is measured at $\lambda_{excitation}$= 356 nm and $\lambda_{emission}$= 465 nm, then, the relative fluorescence units are correlated with the cell number using a linear standard curve. In paper 4 the number of cells attached to each alginate hydrogel were measured 24h and 5 days after seeding by Hoechst staining. It was a useful method to determine the optimal seeding density of cells onto alginate hydrogels. This quantitative method was supplemented with imaging of cell spreading by confocal microscopy after nuclei and actin filaments staining. This method was also used in papers 5 and 6 to assess the progression of cells in the 3D structure of TiO_2 scaffolds and to study the effect of synthetic peptides on cell spreading, reinforcing the images obtained by SEM.

2.1.4.5. *Cell differentiation and mineralization*

2.1.4.5.1. Real time reverse transcription polymerase chain reaction (Real-time RT-PCR)

Specific mRNA sequences can be detected by northern blot, by in situ hybridization techniques, by conventional reverse transcription polymerase chain reaction (RT-PCR) or by real-time reverse transcription polymerase chain reaction (real-time RT-PCR). Among them, real-time RT-PCR provides a quantitative, sensitive and fast technique for detection of specific mRNA sequences. Opposite to northern blot and ribonucleases protective assay (RPA), the amplification cycles of DNA obtained by real-time RT-PCR allow detection of mRNA sequences from very tiny amounts of sample (nanogram level). In addition, some of the limitations of end-point detection in RT-PCR have been diminished by

Aims & Experimental design

the use of real-time PCR systems. These systems offer many general technical advantages, including reduced probabilities of variability and contamination, as well as online monitoring and the lack of need for post-reaction analyses (http://qpcr.gene-quantification.info/). Taking all together, real-time RT-PCR is a reliable method for determining the effects of the synthetic peptides on mRNA expression levels of different osteogenic markers.

Before performing a gene expression measurement by real-time RT-PCR, total RNA from tissues (*in vivo*) or from cells (*in vitro*) is first isolated by using the guanidine thiocyanate method (Sambrook J et al., 1989). Guanidine thiocyanate is a method widely used to isolate of RNA and DNA that is based on different solubilities of RNA and DNA in two different immiscible liquids. The basis of the method has been described in more detail in section 2.1.4.4.3. After RNA isolation, the same amount of total RNA is retro-transcribed to its complementary DNA chain (cDNA). The cDNA synthesized is then used as template for real-time RT-PCR using gene specific primers (Figure 19).
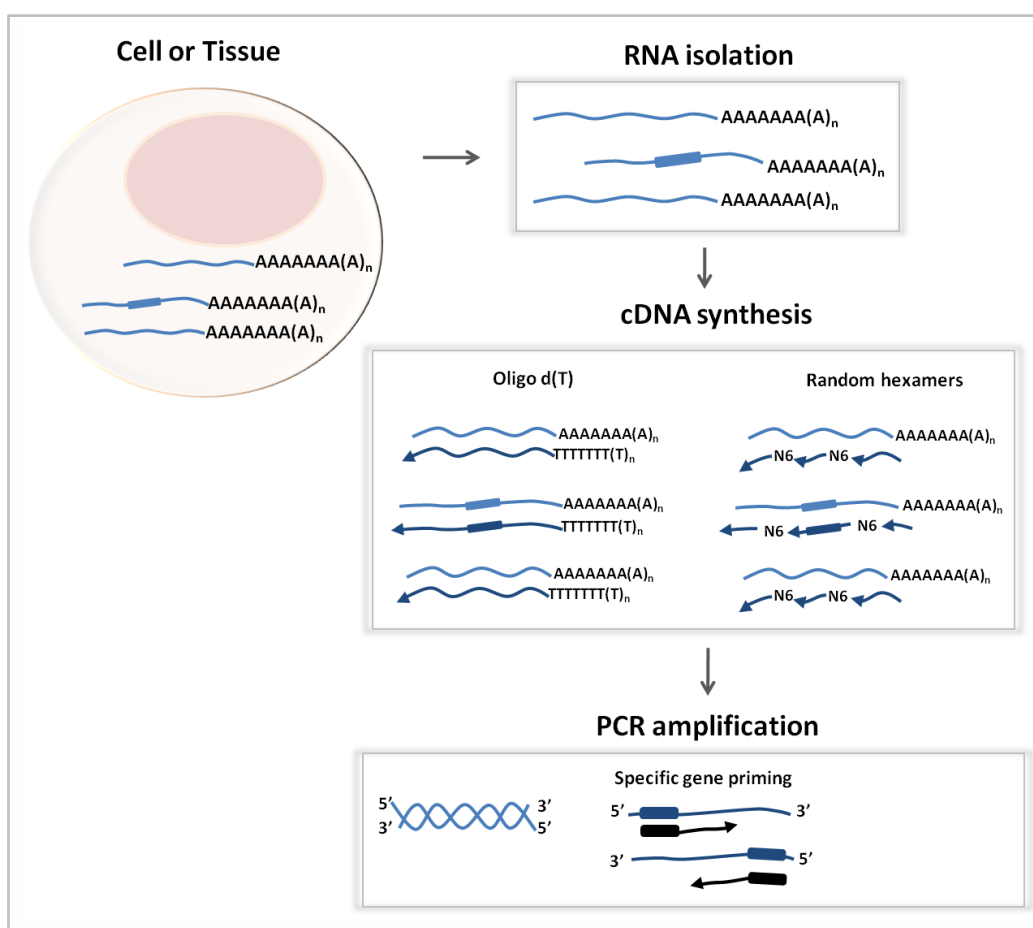
Figure 19. Steps in real-time RT-PCR. Total RNA from cells (*in vitro*) or bone tissue (*in vivo*) in contact with Ti implants was first isolated and quantified. This step was followed by cDNA synthesis using random hexamers and oligo d(T) priming strategy, and PCR amplification of selected target genes.

Retro-transcription of RNA to its cDNA can be primed by (1) oligo (dT) primers, which hybridizes to the poly(A) tail of eukaryotic mRNAs (2) random hexamer primers, which prime the reverse transcription

(RT) at multiples origins along every RNA template or (3) gene-specific primers, which hybridizes to a known sequence within the RNA template. Selection of the appropriate primers for RT depends on the target abundance and the interest to obtain a faithful cDNA representation of the mRNA pool. Table 7 summarizes the advantages and inconvenient of using each type of primers.

Table 7. Schematic description of the advantages and inconvenients of using different types of primers for RNA retro-transcription. Adapted from Bustin *et al* (Bustin et al., 2005).

Type of primer	Advantage	Disadvantage
Oligo (dT)	Faithful cDNA representation of the mRNA pool Allow to study different targets from the same cDNA pool	Requires full-length RNA Secondary structure of RNA may lead to incomplete cDNA synthesis
Random hexamer	Synthesis of large pools of cDNA	If mRNA target of interest is at low levels, amplification may not be quantitative
Gene specific	The most specific cDNA and greatest sensitivity for the quantitative assay	Requires separate priming reactions for each target

Thus, RT using specific primers may be appropriate for a very abundant target, but random primers maybe better if the target is present at very low copy numbers. To guarantee synthesis of a cDNA from RNA template from tiny samples (isolated from *in vitro* cultures or from the bone in contact to implants), a mixture of random primers and oligo(dT) primers for the *in vitro* studies and random primers in the *in vivo* study were used. Next, a specific cDNA-sequence is amplified in a cyclic process by **polymerase chain reaction** (PCR), to a large number of copies. The PCR step requires the use of target-specific primers.

Design of good primers is indispensable to guarantee the success in the amplification. When designing primers for real-time PCR one has to keep in consideration:

- Length of primers between 18-24pb: long enough to be specific but short enough to bind easily to the template.
- Product size between 100-200pb, to give enough time to polymerase to finish each amplification cycle.
- A maximum G+C content around 40-60%.
- Primer melting temperature around 52-58ºC, to guarantee dsDNA stability.

- In order to avoid false positive signals from amplification of the gene or pseudo-gene in genomic DNA quantification, primers must be designed hybridizing two different exons, hence having at least one intron in between, or spanning across an exon/exon boundary.

In the present thesis, specific primers of each target gene were designed by using a *Primer-Blast* tool (http://www.ncbi.nlm.nih.gov/tools/primer-blast/index.cgi?LINK_LOC=BlastHome).

In real time RT-PCR, the amount of product formed is monitored during the course of the reaction by monitoring the fluorescence of dyes or probes introduced into the reaction. By real-time RT- PCR techniques, signals are monitored as they are generated and are tracked after they rise above background but before the reaction reaches a plateau. The increase in fluorescent signal is proportional to the amount of DNA synthesized during each amplification cycle. Each reaction is characterized by the cycle fraction at which fluorescence first arise above defined background fluorescence, a parameter known as the crossing point (Cp), and correlates with the initial amount of DNA target -low Cp values are correlated to high levels of DNA template. There are three main types of fluorescent probes used for real-time RT-PCR applications:

1. *Intercalating dyes* such as SYBR-Green. It is the simplest method to detect the amplified product and uses a fluorescent dye that binds specifically to double-stranded-DNA (dsDNA). The unbound dye exhibits little fluorescence in solution, but during each elongation cycle the number of dsDNA formed is increased and thus also increases the amount of SYBR-Green that binds to the nascent double-stranded DNA. SYBR-Green generates a fluorescence signal that reflects the amount of product formed. The specificity of this method is determined entirely by its primers. These are cheap, easy to use and RT-PCR product verification can be achieved by assessing the melting curves of the products amplified. The inconvenient is that it will bind to any dsDNA in the reactions, including primer-dimer and other non-specific reaction products (contaminating DNA and PCR product from misannealed primer) (Bustin, 2000).

2. *Fluorophores attached to primers* e.g. Invitrogen's Lux or Promega's Plexor primers. These are relatively inexpensive and amplification products can be verified by melting curves. Specificity depends on the primers and usually company-specific design software needs to be used for optimal performance. This is not necessarily a bad thing (indeed the Plexor software is very useful), but it is not always possible to change primer design parameters.

3. *Hybridisation-probe based methods*, e.g. hydrolysis (TaqMan) or Molecular Beacons. Unlike intercalating dyes methods that detect all dsDNA, e.g. SYBR-Green, probe-based qPCR relies on the sequence-specific detection of a desire product, through using a dual-labeled target-specific fluorescent probe, increasing specificity and sensitivity detection. During amplification, annealing of the probe to its specific target generates a substrate that is cleaved by the 5' nuclease activity of the Taq polymerase when the enzyme extents from an upstream primer into the region of the probe. This ensures that the cleavage of the probe occurs only if the target sequence is being amplified and thus, only specific amplified products is detected. Additionally, fluorogenic probes can be labeled with

different and reporter dyes so that multiple primers can be used to simultaneously amplify many sequences. The main drawback is that the different probes must be synthetized to detect different sequences and the occasional fragility of the probes synthesized together with the associated higher costs (Bustin, 2000).

In this thesis SYBR-Green dye was used to monitor the amount product formed. To allow relative quantification after PCR, standard curves are constructed from the standard reactions for each target and reference genes by Cp values versus log cDNA dilution. The Cp readings for each of the unknown samples are used to calculate the amount of either the target or the reference relative to a standard curve, using the second derivative maximum method. Relative mRNA levels are calculated as the ratio of relative concentration for the target genes relative to that for the mean between the different reference genes.

Comparing samples requires normalization of gene expression data against reference genes (housekeeping or internal control genes) to minimize differences in the amount of biological material in the tested samples. Normalization is an essential component of a reliable real-time PCR assay because this process controls for variations in extraction yield, and efficacy of amplification, thus enabling comparisons of mRNA concentrations across different samples (Bustin et al., 2009). This provides an accurate and reliable gene expression analysis. By definition, a reference gene is a constitutive gene that is required for the maintenance of basic cellular functions and expressed in all cells of the organism under normal and pathological conditions. These genes should have similar mRNA levels in all samples analyzed and they should not vary by the experimental treatment. Although some reference genes are expressed at constant levels, others may vary depending on the experimental conditions. Therefore, selection of appropriated reference genes with stability in gene expression levels is essential for an appropriate interpretation of the results (De Jonge et al., 2007). Along the analysis on gene expression performed through this thesis three "classical" and well described reference genes (ribosomal RNA 18S (18S) and glyceraldehyde-3-phosphate dehydrogenase (GAPDH) β-actin) (Willems et al., 2006) have been used for normalization of gene expression.

It is interesting to point out that to overcome the currently lack of consensus on how best to performe and interpret quantitative real time PCR (qPCR) experiments, in this thesis we followed the considerations the Minimum information for Publication of Quantitative Real-Time PCR Experiments (MIQE) guidelines for a more reliable and unequivocal interpretation of the qPCR results. The MIQE guidelines is a set of guidelines that describe the minimum information necessary for evaluation qPCR experiments in terms of standardization of the nomenclature, accuracy in the assay performance and how to perform the data analysis.

Two different cell types were used in the course of the present studies (Papers 1, 2, 3, 4, 5 and 6), and each of them was characterized with an array of genes related to osteoblast proliferation, differentiation and mineralization by real-time RT-PCR. This technique was also used to assess cell

adhesion markers (paper 4, 5 and 6) and different markers for bone formation, resorption and inflammation in the peri-implant bone tissue attached to the Ti implants (Paper 7). Thus real-time RT-PCR was used as reliable assay to understand how synthetic peptides influence on osteoblast differentiation (*in vitro*) and on bone formation and mineralization (*in vivo*).

The function and importance of the different marker genes analyzed through the different studies is described next:

▪ Runx2 (Runt related gene) also called Cbfa-1 (Core binding α-1): Is an early and a key transcriptional factor involved in the mesenchymal stem cell differentiation towards the osteogenic lineage, while inhibits adipogenic or chondrogenic differentiation (Yamaguchi et al., 2000). It is also essential for osteoblast differentiation and skeletal development during the early stages of embryogenesis. Runx2 regulates the expression of bone extracellular matrix protein genes that encode for bone sialoprotein, osteocalcin and collagen type I (Komori et al., 1997) and also influences on the signaling pathways and transcriptional factors which regulate osteoblastogenesis (Jensen et al., 2010). In this thesis, mRNA expression of Runx2 was analyzed in pluripotential hUCMSC cells, since its expression indicates that MSC cells are committed to the osteogenic lineage; whereas, when the studies were carried on MC3T3-E1 cells, *Runx2* mRNA expression was not analyzed, since these cells are already committed to the osteogenic lineage (pre-osteoblasts) and its expression is steady during differentiation.

▪ Wnts: Are key signaling regulators of the MSC maintenance and differentiation. Wnts bind to serpentine receptors of the Frizzled (FZD) family on the plasma membrane to initiate several distinct cascades classified as either canonical (Wnt1, 2, 3 and 3a, 8 and 8b) or non-canonical (Wnt4, 5a, 5b, 6, 7a and 11) depending on whether β-catenin is involved (Ling et al., 2009). In paper 2, we studied the expression of Wnt 7b, which activates the canonical pathway (Davis et al., 2008). Canonical Wnt signaling maintains an undifferentiated proliferative state of MSC, although the effects of Wnt signaling are context-dependent (Baksh et al., 2007).

▪ Osterix: is a specific osteogenic zinc finger transcription factor that acts down-stream of Runx2 to induce differentiation of pre-osteoblasts into fully functional osteoblasts (Tu et al., 2006).

▪ Decorin: is a small leucine rich proteoglycan highly expressed in extracellular bone matrix. It is capable of forming a dimeric structure facilitating protein-protein interaction with a range of other matrix components (collagen, fibronectin) (Ungefroren et al., 1995) and with the mineral phase in the formation of calcified tissues. Thus, decorin is involved in cell adhesion, matrix assembly and in either the inhibition or controlled deposition of mineral crystal (Waddington et al., 2003)

▪ BMPs (Bone morphogenic protein): BMPs are a potent growth/differentiation factor that induces differentiation of undifferentiated mesenchymal cells, bone marrow cells, myoblast cell lines and preosteoblasts into the osteogenic lineage (Xiao et al., 2002). Among the different types of BMPs,

BMP2 plays an important role in osteogenesis. BMP2 regulates osteoblast phenotype development at different stages, stimulates osteoblast cell adhesion and migration, but also osteoblast differentiation and bone matrix mineralization (Lai and Cheng, 2005).

- Coll-I (collagen type I): is the most abundant of all collagen types. Collagen-I contributes to bone strength (Viguet-Carrin et al., 2006) providing a binding site for mineral components. Biosynthesis of collagen occurs at early stages supporting cell proliferation (Stein et al., 1996).

- ALP (alkaline phosphatase): is a membrane bound enzyme contained in matrix vesicles that contributes to rendering the extracellular matrix competent for mineralization (Stein et al., 1996). Alkaline phosphatase is an early marker of osteoblast differentiation that is involved in hydroxyapatite crystal deposition, its expression increases during extracellular matrix maturation and decreases when mineralization is well progressed (Guida et al., 2007).

- BSP (bone sialoprotein): constitutes an 8-12% of the total non-collagen proteins in bone and cementum (Ganss et al., 1999). Is a highly sulfated, phosphorylated, and glycosylated protein that mediates cell attachment to extracellular matrices through an RGD motif. BSP also nucleates hydroxyapatite crystal formation (Sila-Asna et al., 2007), having a role in the initial mineralization of bone.

- OC (osteocalcin): is a major non-collagen protein component of bone extracellular matrix which is synthesized and secreted exclusively by differentiated osteoblasts at the late stage of cell maturation. OC is considered to be the most specific bone marker playing a positive role in cell mineralization through binding with high affinity to hydroxyapatite crystals, the key mineral component of bone and regulates bone crystal growth (Boskey et al., 1998).

- OPN (osteopontin): is a sialoprotein secreted by osteoblasts that mediate hydroxyapatite binding. Moreover, through interaction with integring subunits $\alpha v \beta_{1,3,5}$, $\alpha 9 \beta_1$, $\alpha 8 \beta_1$ (Bueno Rde et al.; Sodek et al., 1995), also mediates cell adhesion, cell attachment, chemotaxis and intracellular signaling in various cell types. OPN is produced early in the differentiation of bone cells with higher expression levels after mineralization has been initiated (McKee and Nanci, 1995; Sodek et al., 1995).

- IL-6 (interleukine-6): is one of the essential factors in the acute-phase systemic reaction to inflammatory stimuli or tissue injury (Tilg et al., 1994). IL-6 is a pleiotropic cytokine that stimulates bone resorption by recruiting mature osteoclasts and by activating them through an autocrine mechanism (Fiorito et al., 2003; Tilg et al., 1994) and also stimulates osteoblast differentiation and bone formation (Taguchi et al., 1998) .

- Itgb1 (integrin β1): is an integrin subunit found in the bone receptors for collagen, fibronectin, laminin and vitronectin (Gronowicz and McCarthy, 1996). It is expressed during the first 24 hours after cell seeding, playing a role on osteoblast cell adhesion (Anselme, 2000; Gronowicz and McCarthy, 1996), while when cells are already attached and are spreading its expression is down-regulated.

- Itgb3 (integrin β3): mediates the adhesion to a variety of cells to osteopontin, BSP, vitronectin and fibronectin (Cheng et al., 2001). Cheng *et al* (Cheng et al., 2001) reported that Itgb3 stimulates cell proliferation while when osteoblast cell differentiation starts its expression is significantly reduced and kept at basal levels during cell maturation.

- Itga8 (integrin α8): plays a role during the osteoblast mineralization phase through interaction with Fn1 (Moursi et al., 1997). Up-regulation of Itga8 also occurs by interaction with osteopontin (Opn) (Denda et al., 1998).

- Fn1 (fibronectin 1): is a glycoprotein present in dimeric form in plasma and represents a major component of the extracellular matrix (ECM) (Muller et al., 1995). Several integrins serve as a receptor for Fn1 (Muller et al., 1995), however the function of Fn1 and how it affects osteoblast development is ambiguous. Whereas some authors state that Fn1 is up-regulated at the early stages of cell differentiation and reduced during cell maturation (Moursi et al., 1997), others postulate that Fn1 regulates osteoblast differentiation by regulating ECM assembly and mineralization (Daculsi et al., 1999).

- TRAP (tartrate-resistant acid phosphatase): is highly expressed in differentiated osteoclast cells, and is commonly used as a indicator of bone resorption (Minkin, 1982). In addition, TRAP also prompts the dephosphorylation of bone matrix phosphoproteins like osteopontin and bone sialoprotein and has originally shown to be important for a normal endochondral bone formation (Blumer et al., 2012).

- IL-10 (interleukine-10): is a cytokine with pleitropic activities. It is an anti-inflammatory cytokine that suppresses cytokine synthesis by murine Type 1 helper T cells and macrophage functions. In addition, IL-10 has shown to inhibits the potential of mouse bone marrow to synthesize bone-related and specific proteins, including ALP, Coll-I and OC, and to mineralize by interfering with early steps of osteogenic differentiation (Van Vlasselaer et al., 1994).

- TNF-alpha (tumor necrosis factor alpha): is secreted by macrophages, lymphocytes and monocytes and it is considered one of the main cytokines related to inflammation and immune processes. In addition to its role on inflammation, TNF-alpha is also involved on bone resorption by stimulating the differentiation and maturation of osteoclasts (Vitale and Ribeiro, 2007).

Following are listed the different markers genes analyzed through the different studies:

Table 8. List of bone marker genes and integrins analysed in the different studies.

Markers related to	In vitro studies		In vivo studies
	Pre-osteoblast MC3T3-E1 cells	hUCMSC cells	
Adhesion and osteogenic differentiation	Osx	Runx2	Runx2
	BMP2	BMP2, Wn7b	
	Coll-I, Fn1, Itgb1, Itgb3	Coll-I decorin	Coll-I
	BSP, ALP, OC, OPN, Itga8	ALP, OC	OC
Osteoclast differentiation			TRAP
Inflammation	IL-6		IL-6, IL-10, TNF-α

To provide a better understanding of the effects of synthetic peptides on cells, the temporal expression of the makers during MC3T3-E1 and hUCMSC cell differentiation on TCP are depicted in Figure 20 and Figure 21, respectively.
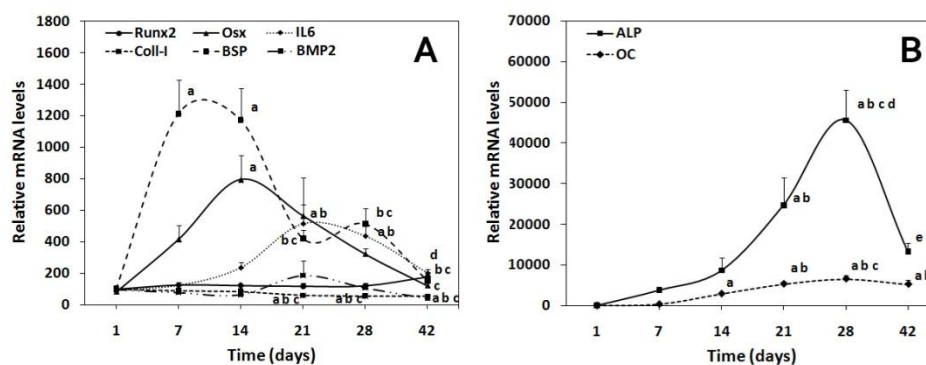

Figure 20. Temporal expression of markers related to the osteoblast phenotype in pre-osteoblast MC3T3-E1 cells cultured on TCP. Figure A represents relative mRNA levels of Runx2, Coll-I, Osx, IL-6, BSP and BMP2. Figure B shows relative mRNA levels of ALP and OC. Figures are adapted from Monjo *et al* (Monjo et al., 2010a). Data represent fold changes of target genes normalized with reference genes (18S and GAPDH), expressed as a percentage of cells after 1 day of cell culture, which were set to 100%. Values represent the mean ± SEM. Differences over time were assessed by Student's *t*-test post hoc analysis, p≤0.05; (a) versus day 1, (b) versus day 7, (c) versus day 14, (d) versus day 21, (e) versus day 28.
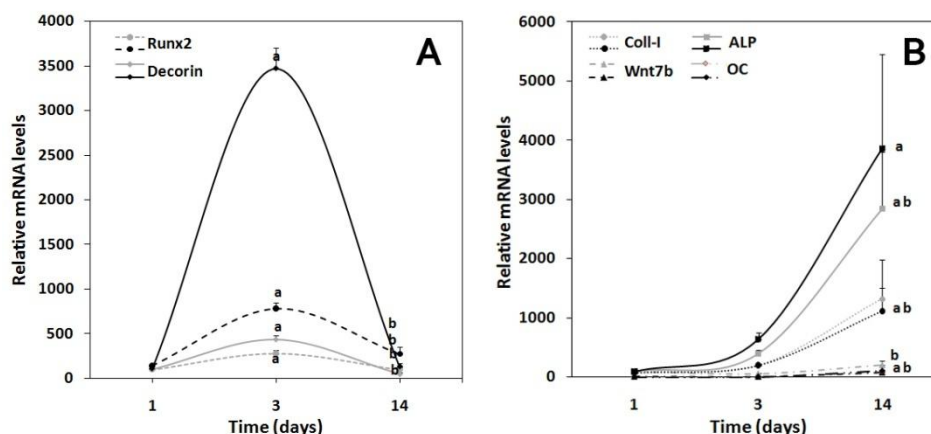
Figure 21. Temporal gene expression levels of Runx2 and Decorin (A) and Coll-I, Wnt7b, ALP and OC (B) markers in human umbilical cord mesenchymal stem cells (hUC-MSCs) cultured with growing media (grey lines) or with growing media with osteogenic supplements (black lines). Data represent fold changes of target genes normalized with reference genes (beta-actin and GAPDH), expressed as a percentage of cells at day 1, which were set to 100%. Values represent the mean ± SEM. Differences over time were assessed by Student's *t*-test post hoc analysis, p≤0.05; (a) versus day 1 for each growth media, (b) versus day 3 for each growth media.

2.1.4.5.2. Enzyme-Linked ImmunoSorbent Assay (ELISA)

Enzyme-Linked ImmunoSorbent Assay (ELISA) is a sensitive immunoassay that uses an enzyme linked to an antibody or antigen as a marker for the detection of a specific protein. It consists on the immobilization of the protein of interest (antigen) through its interaction with a specific antibody that is attached to a solid. Its further detection occurs by means of a secondary antibody that has a linked enzyme. This enzyme reacts with a colorless substrate giving an end product that can be measured spectrophotometrically. To allow quantification, a standard curve with known amounts of the protein of interest is run in every assay. Thus, it is an accurate method for a quantitative determination of a specific protein. However, it requires a proper selection of the reagents (range of detection, sensibility…) and to adjust the volume and dilution of sample to get a successful detection. Quantification of the amount of secreted proteins involved in bone formation processes is, as well, a reliable method to assess the osteogenic effect of synthetic peptides. BMP2 is an important growth factor for osteoblast cell differentiation that mediates mesenchymal stem cell differentiation towards the ostegenic phenotype through the Wnt-signaling pathway (Verrier et al., 2010). In paper 2, the amount of BMP2 secreted in hUCMSCs treated either with or without osteogenic supplements was quantified by ELISA.

2.1.4.5.3. Alkaline phosphatase activity

Alkaline phosphatase is an ectoenzyme attached to the osteoblast cell membrane by a glycosyl-phosphatidylinositol anchor and its expression is necessary for initiating bone mineralization (Golub et al., 1992). The determination of ALP activity is based on a colorimetric method that follows the

hydrolization of p-Nitrophenyl phosphate (pNPP) with the formation of a yellow end product that can be measured spectrophotometrically at 405nm. Determination of ALP activity from cell monolayer implies a previous step of cell membrane disruption with 0.1% of Triton X-100 followed by three freeze-thaw cycles. In this thesis, ALP activity was determined from cell monolayers in the *in vitro* studies (papers 1, 3 and 5) or from the wound fluid (paper 7) in the *in vivo* study in order to get an estimation of cell differentiation or bone formation.

2.1.4.5.4.Alizarin red staining

Mineralization is considered a functional end-point reflecting advanced cell differentiation (Hoemann et al., 2009). Different methods were used to measure the mineralization of MC3T3-E1 cells treated with the synthetic peptides.

A simple and rapid screening method to directly visualize calcium deposition is by alizarin red staining of the calcium present in the cell monolayer. This is a common method used to detect and quantify calcium, within the deposited mineral (Gregory et al., 2004; Hale et al., 2000). Although alizarin red staining has been described to be a versatile method in that the dye can be extracted from the stained monolayer using acetic acid followed by colorimetric detection at 405nm (Gregory et al., 2004), we did not obtain quantitative results from the colorimetric detection. Our lack of quantitative measurements can be due to: i) inefficiency of the dye extraction, and ii) that minor differences in the dye recovering are translated into big differences in the colorimetric values. Thus, this method was only used to qualitatively detect calcium deposition (paper 1). Alternatively, calcein staining could also be used as a highly sensitive semi-quantitative method for rapid measurement of mineralization (Hale et al., 2000).

2.1.4.5.5.Inductively coupled atomic plasma emission spectroscopy (ICP-AES)

Inductively coupled atomic plasma emission spectroscopy (ICP-AES) is a highly sensitive and precise analytical technique for detection of the concentration of a wide range of elements present in a solution, principally the alkali metals (Li-Rb), alkaline earth metals (Be, Mg, Ca, Sr, Ba), transition metals (Sc-Mo; Al) and metalloids and non-metals (Si, P, S, As), based in the emission of electromagnetic radiation at wavelengths characteristic of each particular element from excited atoms by inductively coupled plasma. ICP-AES was chosen to quantify the total calcium content extracted from cell monolayers (papers 1, 3, 5). The concentration of calcium was calculated correlating the intensity of the emission to a standard curve. For this method, it is necessary to take special care to do not contaminate the samples with calcium from other sources, to use material not autoclaved and to avoid glass labware. In those studies using alginate hydrogels as a carrier for synthetic peptide delivery (papers 4 and 6), we could not quantify calcium deposition, as it was hampered by the use of $CaCl_2$ for alginate gelification. Furthermore, a methodological interference in the determination of calcium content was also observed in cells cultured in direct contact with HA (paper 3).

Figure 22. Photograph of the inductively coupled atomic plasma emission spectrometer (ICP-AES Optima 5300DV, PerkinElmer, Massachusetts, USA) used to quantify calcium content.

2.1.4.6. Bone tissue response

2.1.4.6.1. Wound fluid analysis

For the *in vivo* experiments, tissue fluid at the implant site was collected for determination of the adverse tissue response upon implantation by quantification of the LDH activity and for assessing osteoblast differentiation at the bone implant interface by quantification of the ALP activity. Right after implant detachment, sterilized filter paper of the same size of the implant coins was placed for 1 min in each drilled hole (proximal and distal) to absorb the wound fluid and then transferred to microcentrifuge tubes containing 200 µl of phosphate-buffered saline (PBS). A vigorous stirring of the tubes was then applied to release the wound fluid absorbed to the sterilized filter paper followed by a centrifugation of tubes at 250xg for 5 min at 4 ºC to remove tissue remains. LDH activity and ALP activity determination was performed as described above (section 2.1.4.3 and section 2.1.4.5.3, respectively). It is important that LDH and ALP activity analysis are performed during the first 48h after sample collection and that samples are kept at 4 ºC (freezing of samples leads to inactivation of the enzymes).

2.1.4.6.2. Micro-CT analysis

Microcomputed tomography (micro-CT) is a non-invasive technique that provides qualitative and quantitative analysis of the sample morphology and of the internal microstructure at high spatial resolution (sub-micron level). By performing a micro-CT analysis, virtual cross-sections of an object are generated and later reconstructed in a 3D model based on the bone density. In paper 6, bone sample scanning with a SkyScan 1172 tabletop µCT scanner (SkyScan) was used to study bone architecture and for bone morphometric analysis. For bone samples, scans need to be performed with 100kV, a current of 100µA and using an aluminum filter of 0.5mm.

2.1.4.6.3.Histology

Histological analysis is a semi-quantitative method to examine or to differentially identify tissues at microscopic level. Tissue is first protected by fixation. Then, thin sections are cut and stained for further examination under light or electron microscope. Hematoxilin/eosin staining represents the most common staining method in histology, in which hematoxilin stains in purple the acid structures (e.g. cell nucleus), and eosin stains in pink-orange the basic structures (e.g cytoplasm, collagen fibers). In paper 7, histological analysis of bone samples were preserved in formalin, decalcifiied in 7% etylenediaminetetraacetic acid and embedded in paraffin. Four sections per defect were then stained with hematoxilin/ eosin and new bone, fibrous tissue formation and their distribution around the implant were examined under a light microscope.

Histological analysis was used as a complementary method to the micro-CT analysis. While by using micro-CT the mineralization of the newly healed bone can be determined, histological analysis provides information with respect to the percentages of bone and new bone and fibrous tissue encapsulation at the interface between bone and metal implant. Also if there is any inflammatory reaction at the bone-implant interphase.

2.1.5. Statistical analysis

For the data analysis Excel, GraphPad Prism and SPSS were used. Data are mainly presented as mean values ± SEM (standard deviation of the mean), but for the in vivo experiments data are presented as mean values ± SD (standard deviation). Kolmogorov-Smirnov test was done to assume parametric or non-parametric distributions for the normality tests, differences between groups were assessed by Mann-Whitney-test or by Student t-test depending on their normal distribution. Results were considered statistically significant at p-values ≤ 0.05.

3. Results

Paper 1

Synthetic peptides analogue to enamel proteins promote osteogenic differentiation of MC3T3-E1 and mesenchymal stem cells.

Rubert, M.; Ramis, J.M.; Vondrasek, J.; Gayà, A.; Lyngstadaas, S.P.; Monjo, M.

Synthetic Peptides Analogue to Enamel Proteins Promote Osteogenic Differentiation of MC3T3-E1 and Mesenchymal Stem Cells

Marina Rubert[1, 2], Joana Maria Ramis[2], Jiri Vondrasek[3, 4], Antoni Gayà[5], Staale Petter Lyngstadaas[1, *], and Marta Monjo[1, 2]

[1] *Department of Biomaterials, Institute for Clinical Dentistry, University of Oslo, Oslo, N-0317, Norway*
[2] *Group of Cell Therapy and Tissue Engineering, Research Institute on Health Sciences (IUNICS)*
Group of Biomaterials, University of Balearic Islands, Palma De Mallorca, E-07122, Spain
[3] *Institute of Biotechnology Czech Academy of Sciences, Videnska 1083, 142 00 Prague 4, Czech Republic*
[4] *Institute of Organic Chemistry and Biochemistry, Czech Academy of Sciences,*
Flemingovo namesti 2, 166 10 Prague 6, Czech Republic
[5] *Fundació Banc De Sang i Teixits De Les Illes Balears, Palma De Mallorca, E-07004, Spain*

Regulation of biomineralization processes are mediated by extracellular matrix proteins that often exhibit proline-rich regions. Advanced bioinformatic methods were used to design the structure of artificial peptides (P1, P2, P3) based on proline-rich domains of extracellular proteins. Their effect on osteoblast differentiation and *in vitro* biomineralization was tested on MC3T3-E1 and human umbilical cord mesenchymal stem cells (hUCMSCs) and compared to the commercially available enamel matrix derivative (EMD). MC3T3-E1 and hUCMSCs treated with the synthetic peptides showed a decreased cytotoxicity after 24–48 h of treatment compared to control. MC3T3-E1 cells treated with EMD showed lower expression of osteoblast markers genes than cells treated with P2, except for collagen type I. In hUCMSCs, OC gene expression was higher in P2-treated cells compared to those treated with EMD or control. ALP activity was markedly increased in MC3T3-E1 cells incubated with P2 compared to other treatments. Similar results were observed in hUCMSCs. Further, P2 increased calcium deposition rate compared to EMD or control either in MC3T3-E1 or hUCMSCs. The observed effects of proline-rich peptides hold potential for both clinical applications and as a research tool in further investigations of the molecular basis of induced osteogenic cell differentiation.

Keywords: Proline-Rich Regions, Synthetic Peptides, Bone Formation, Mineralization, *In Vitro.*

1. INTRODUCTION

Vertebrate hard tissue formation occurs by a process of matrix-mediated biomineralization in which intracellular and extracellular organic proteins regulate the initiation, growth and deposition of mineral crystals.[1] Among the extracellular proteins that regulate biomineralization are several molecules that exhibit proline-rich regions, like collagens, amelogenins, ameloblastin and sialoproteins.[2] The proline-rich regions have remained remarkably well-conserved through evolution, suggesting that they may have functional importance. In fact, the well defined mobile and semi-flexible structure of polyprolines-rich proteins has led to hypothesize that such proteins may function as mineral-binding domains, protein–protein interaction domains or internal molecular spacers during the formation of biological minerals and other biocomposites. Thus, polyproline repeats may exert their control over biological events by altering the length of their central domain.[2]

Amelogenin and ameloblastin, two major enamel matrix proteins, are important for enamel mineralization.[3] Both amelogenin and ameloblastin contain proline enriched regions at the level which emerges a question of their dominant role in the organism. Polyproline repeats in amelogenin were studied for their effect to matrix assembly and apatite crystal growth and it was shown that the increase of the proline repeats influenced compaction of protein matrix, conformational variability, increase of polyproline II helices and last but not least the apatite crystal length.[2] Except the specific role of proline-rich motifs

---

in aggregation and adhesion there is one important factor reflecting the unique structural and interaction properties of these motives. Proline-rich sequences are often bound to protein domains frequently involved in signaling events.[4] The structural as well chemical properties of proline helps to promote high structural selectivity of such sequences often accompanied by high binding affinity towards a target.[5]

For decades, amelogenins and ameloblastin were thought to be tissue-specific and exclusively expressed by the ectodermal enamel-producing ameloblast cells. However, in 2006 amelogenin expression was described in mesenchymal mineralizing tissues such as alveolar bone, long bone and cartilage and also in cranio-facial soft tissues such as brain and salivary gland.[6, 7] Ameloblastin expression was also detected in developing mesenchymal dental hard tissues, during early odontogenesis as well as in differentiating odontoblasts prior to mantle dentin mineralization[8] and during early craniofacial bone formation.[9] Recent studies have also confirmed a role of ameloblastin in bone formation and repair also in adult tissues.[10]

The finding of amelogenin and ameloblastin expression in mineralizing tissues suggests that they are active in bone formation and remodeling. Actually, experiments using different forms of amelogenin[11–17] have shown induction of bone tissue regeneration *in vitro* and in animal models.[18–20] *In vitro* experiments in bone cells have shown that amelogenins can induce the expression of specific bone markers such as collagen type I,[11, 21–23] alkaline phosphatase,[11, 24–26] osteocalcin[11, 21, 23–26] or bone sialoprotein.[12, 21, 24, 27, 28] Moreover, they can induce expression profiles in bone cells similar to that of growing bone,[23] cell growth,[26, 29] and the formation of the mineralized nodules.[24, 30, 31] In rats, amelogenins have been shown to promote new bone regeneration in femurs[19, 31, 32] to enhance formation of new alveolar bone,[19–21] and new root cementum either in long bones, rat parietal bones and maxillary rat molars.[20]

The use of natural proteins in tissue engineering and regenerative medicine has some associated disadvantages including immunogenicity, relatively high cost, large molecular weight (100–200 amino acids), instability *in vivo*, and difficulty in sterilization.[33] Genetic engineering of artificial peptides offers a novel method of developing biomaterials for tissue regeneration.[34, 35] Synthetic peptides are advantageous due to their ease of synthesis and handling, as well as their low immunogenic activity.[33] Biological activity of matrix derived synthetic peptides has already been described.[33, 36, 37]

Our aim was to design an artificial peptide based on the common characteristics of the proline-rich region in hard tissue extracellular matrix proteins to see if such peptides can be used for induction of bone formation and biomineralization in regenerative medicine. In our study, we have designed three artificial peptides and tested their activity on

osteoblast-like cells (MC3T3-E1) compared to the effect of the commercially available enamel matrix derivative (EMD). To evaluate the potential induction of those synthetic peptides on bone formation and biomineralization, we also studied the effect of synthetic peptides on the differentiation of human umbilical cord mesenchymal stem cells (hUCMSCs) stimulated to the osteogenic lineage.

2. MATERIALS AND METHODS

2.1. Peptide Design

With the aim to provide an artificial peptide with improved properties for induction of bone formation and biomineralization we designed an artificial consensus peptide. We used the EMBOSS pairwise sequence alignment algorithm freely available at EBI (http://www.ebi.ac.uk) and applied it simultaneously on pairs of sequences of amelogenins (Q99217|AMELX_HUMAN Amelogenin, X isoform OS = Homo sapiens, |AMELX_MOUSE Amelogenin, X isoform OS = Mus musculus, P63278|AMELX_RAT Amelogenin, X isoform OS = Rattus norvegicus) and ameloblastins (Q9NP70, AMBN_HUMAN Ameloblastin OS = Homo sapiens GN = AMBN, O55189, AMBN_MOUSE Ameloblastin OS = Mus musculus GN = Ambn, Q62840 AMBN_RAT Ameloblastin OS = Rattus norvegicus GN = Ambn). We explored two alignment options – global pairwise alignment (Needleman–Wunsch) and local pairwise alignment (Smith-Watterman) with default parameters (Blosum62, gap open penalty = 10, gap extension = 0.5). To identify continuous aligned sequences of AMELX and AMBN we had to dramatically increase the penalty for gap opening to value 100. The pairwise alignment of human amelogenin and ameloblastin identified region 107–151 on human amelogenin and region 77–121 on human ameloblastin rich in prolines. These regions were analysed and more amino acids were taken into account: amino acids 120–160 on amelogenin and 77–127 on ameloblastin. This alignment provided 6 different pairs of amelogenin-ameloblastin sequences which we limited to length of 25 AA rich of conserved proline positions. We designed our peptides with constraints on a length (25 AA), conservation of proline positions and with systematic variation of other composition aminoacids, which resulted in 3 final peptide sequences shown in Table I.

2.2. 3D Models of the Designed Peptides

The designed peptides (P1, P2 and P3) should differ in their structures because of the different amino acids between proline residues in the sequence. We utilized a recently introduced method of peptide design[38] to explore possible correlation between the structure and biological response for particular peptide. The sequences of three designed peptides were sent to MOBYLE server[39] and only the best energy conformer of each peptide was used

J. Biomater. Tissue Eng. 1, 198–209, **2011**

199

Table I. Aminoacidic sequence of recombinant peptides.

| | | N° of aminoacids | | |
Peptide	Sequence	Charged	Polars	Hydrophobic aminoacids
P1	H$_2$N-PLV PSY PLV PSY PLV PSY PYP PLP P-COOH	0	3	22
P2	H$_2$N -PLV PSQ PLV PSQ PLV PSQ PQP PLP P-COOH	0	7	18
P3	H$_2$N-PMM PSY PMM PSY PMM PSY PYP PMP P-COOH	0	3	22

Peptide 1 (P1), peptide 2 (P2), peptide 3 (P3).

for analysis and further optimization. These three resulted peptides were further explored by molecular dynamic (MD) by AMBER package[40] using ff99SB force field[41] in TIP3[42] explicit water environment to get insight of structural stability of the modeled molecules.

2.3. Preparation of Peptides and Enamel Matrix Derivative (EMD)

EMD was kindly supplied by Straumann GMbH (Basel, Switzerland). EMD was dissolved to 10 mg/ml in 0.1% acetic acid in phosphate-buffered saline (PBS). Aliquots were prepared and stored at -20 °C until use. The three synthetic peptides were designed and purchased from Eurogentec (Seraing, Belgium). One vial containing 10–21 mg of the selected synthetic peptides was delivered in a freeze-dried pellet form and dissolved to 10 mg/ml (peptide 1 (P1) and peptide 3 (P3)) and to 20 mg/ml (peptide 2 (P2)) in 0.1% acetic acid in phosphate-buffered saline (PBS). For P1, 6.6% of dimethyl sulfoxide (DMSO) was added to the mix due to its higher hydrophobicity and thus lower solubility. Peptides were incubated at 50 °C for 30 min and sonicated shortly. Final concentrations of 50 μg/ml for peptides and EMD were used, *in vitro,* to assay their effect on cytotoxicity, proliferation and differentiation (gene expression, ALP activity and calcium content) of MC3T3-E1 osteoblastic cells and hUCMSCs.

2.4. Cell Culture of MC3T3-E1 Cells

Mouse preosteoblast MC3T3-E1 cells (DSMZ, Braunschweig, Germany) were selected as an *in vitro* model. Cells were routinely cultured in α-MEM (PAA Laboratories GmbH, Pasching, Austria), which contains ascorbic acid (45 μg/ml) and sodium dihydrogen phosphate (140 mg/l), and supplemented with 10% fetal bovine serum (FBS) (PAA Laboratories GmbH, Pasching, Austria) and antibiotics (50 IU penicillin/ml and 50 μg streptomycin/ml) (Sigma, St. Louis, MO, USA) under standard cell culture conditions (at 37 °C in a humidified atmosphere of 5% CO$_2$). Under these conditions, these cells are able to differentiate and mineralize. Cells were subcultured 1:4 before reaching confluence using PBS and trypsin/EDTA. All experiments were performed after 9 passages of the MC3T3-E1 cells.

Cells were seeded in 24-well plates and they were maintained in α-MEM supplemented with 10% FBS, antibiotics and in presence of synthetic peptides (50 μg/ml) and EMD (50 μg/ml). Cells cultured in α-MEM supplemented with 10% FBS and treated with 0.1% acetic acid-PBS that served as control. Media was changed every 2–3 days. Treatments were added after changing the media to keep the concentration of peptides and EMD in solution throughout the whole experiment. Culture media was collected after treatment for 24 hours and 48 hours, to test cytotoxicity. The effect of P2 (50 μg/ml) and EMD (50 μg/ml) on cell toxicity was also assessed after a longer time period of 14, 21 and 28 days. Cells were harvested after 14 days using Trizol reagent (Invitrogen Life Technologies, Carlsbad, CA, USA), to analyse gene expression of several osteoblast differentiation markers using real-time RT-PCR. In parallel, cells were cultured to days for 28 days to analyse calcium content and ALP activity in the cell monolayer.

2.5. hUCMSCs Isolation

Human umbilical cord derived mesenquimal stem cells (hUCMSCs) were isolated from umbilical cords obtained in the process of human umbilical cord blood donation under the Concordia Cord Blood Donation Program. The samples were obtained after informed consent and with the approval of the Ethical Committee of Balearic Islands (CEIC-IB).

To isolate hUCMSCs, the cord was rinsed several times with sterile saline, the cord blood was drained and clots flushed from the vessels. Next, the cord was cut into small pieces and incubated with 0.075% collagenase type IA (Sigma, St. Louis, MO, USA) for 2 h. Then, 0.125% trypsin was added for 30 min with gentle agitation at 37 °C. The digested mixture was then passed through a 100 μm filter to obtain cell suspensions. Cell pellets were resuspended in NH$_4$Cl-based erythrocyte lysis buffer, incubated for 10 min at room temperature and washed in PBS. Finally, the cells were resuspended in Dubelcco's modified Eagle's medium with low glucose and Gluta-max (DMEM-LG; Gibco, Grand Island, NY, USA) and 20% FBS (HyClone, Thermo Scientific, Logan, USA) and plated in non-coated 25 cm^2 cell culture flask. Cultures were maintained in a humidified atmosphere with 5% CO$_2$ at 37 °C. After 3 days of culture the medium was replaced and non-adherent cells were removed. The medium was changed twice weekly thereafter. Once 80% confluence had been reached, adherent cells were replated at a density of 1×10^4 cells/cm^2.

2.6. Immunophenotyping Using FACS

Standard flow cytometry techniques were used to determine the cell surface profile (CD105, CD73, CD90, CD45, CD34, CD31, HLA-DR) of hUCMSCs. Briefly,

hUCMSCs were immunolabeled with saturating concentrations of conjugated mouse monoclonal antibodies to human CD105-phycoeritrin (PE), CD90-fluorescein (FITC), CD73-PE, CD34-PE, CD45-FITC, CD31-PE and HLA-DR-FITC (BD Biosciences). Cells were stained in single label and then analysed by flow cytometry with a FACScan (Becton Dickinson, MD, USA). The hUCMSCs used for the studies did no express CD34, CD45, CD31 and HLA-DR, whereas were positive for CD105, CD90 and CD73, a typical profile of MSCs.[43]

2.7. Cell Culture of hUCMSCs

hUCMSCs from three different donors were seeded (in duplicate) in 24-well plates and grown to confluence in a "growing media" consisting of DMEM-LG supplemented with penicillin (50 IU/ml), streptomycin (50 μg streptomycin/ml) and 20% FBS (HyClone). Cells were cultured at 37 °C in a humidified atmosphere of 5% CO_2. At confluence (designated as day 0), cells were grown in "differentiation media" consisting of growing media supplemented with hydrocortisone (200 nM), ascorbic acid (50 μg/ml) and β-glycerophosphate (10 mM) and treated with 0.1% acetic acid-PBS (control), with P2 (50 μg/ml) or with EMD (50 μg/ml). Media was replaced twice weekly. Treatments were added after changing the media to keep the concentration of peptides and EMD in solution throughout the whole experiment. Culture media was collected after 1, 14 and 21 days of treatment to test cytotoxicity. Cells were harvested at day 14 to analyse gene expression of several osteoblast differentiation markers using real-time RT-PCR, and after 21days to analyze calcium content and ALP activity in the cell monolayer.

2.8. Cell Toxicity

The LDH activity in the culture media was taken as an indicator of membrane leakage or cell lysis. The activity of the cytosolic enzyme was estimated according to the manufacturer's kit instructions (Roche Diagnostics, Mannheim, Germany), by assessing the rate of oxidation of NADH at 490 nm in presence of piruvate. After removing the background in the absorbances of the culture media without cells, results from all the samples were presented relative to the LDH activity in the medium of cells treated with 0.1% acetic acid-PBS (low control, 0% of cell death) and of cells treated with 1% Triton X-100 (high control, 100% cell death). The percentage of LDH activity was calculated using the equation:

$$Cytotoxicity\ (\%) = (exp.value - lowcontrol)/$$
$$(highcontrol - lowcontrol)*100. \quad (1)$$

2.9. Cell proliferation

Proliferation rate was analysed after the incorporation of bromodeoxyuridine (BrdU) as described by the manufacturer (Roche Diagnostics, Mannheim, Germany). To test the effect of the different synthetic peptides and EMD on osteoblast proliferation, 2×10^3 cells were seeded in each well (96-well plate) for 24 h. After cell attachment, culture medium was changed and synthetic peptides (50 μg/ml) and EMD (50 μg/ml) and BrdU were added to the wells. Cells were cultured for additional 24 h (MC3T3-E1) or 4 days (hUCMSCs) to allow the incorporation of BrdU to the proliferating cells.

2.10. RNA Isolation and Real-Time RT-PCR Analysis

The effect of synthetic peptides and EMD on gene expression was studied after 14 days of treatment on pre-osteoblast MC3T3-E1 cells and hUCMSCs.

Total RNA was isolated from cells using Trizol reagent (Invitrogen Life Technologies, Carlsbad, CA, USA) according to the manufacturer's protocol. Total RNA was quantified at 260 nm using a Nanodrop spectrophotometer (NanoDrop Technologies, Wilmington, DE, USA). Same amount of RNA (0.75 μg and 0.27 μg, for MC3T3-E1 and hUCMSCs, respectively) was reverse transcribed to cDNA at 42 °C for 60 min using iScript cDNA Synthesis kit (BioRad, Hercules, CA, USA) that contains both oligo(dT) and random hexamers for MC3T3-E1 cells, and using High Capacity RNA-to-cDNA kit (Applied Biosystems, Foster City, CA) for hUCMSCs, according to the protocol of the supplier. Aliquots of each cDNA were frozen (-20 °C) until the PCR reactions were carried out.

Real-time PCR was performed in the Lightcycler 480® (Roche Diagnostics, Mannheim, Germany) using SYBR green detection. For MC3T3-E1 cells, real time PCR was done for two housekeeping genes (18S and glyceraldehyde-3-phosphate dehydrogenase (GAPDH)) and seven target genes (bone morphogenetic protein 2 (BMP-2), osterix (Osx), bone sialoprotein (BSP), alkaline phosphatase (ALP), collagen type I (Coll-I), osteocalcin (OC), and interleukin-6 (IL-6)). For hUCMSC cells, real-time PCR was done for two housekeeping genes (GAPDH and β-actin) and four target genes (ALP, Coll-I, OC and runt-related transcription factor 2 (RUNX2)).

The primer sequences were as follows for mouse (m) and human (h): m-18s rRNA-F: 5'-GTAACCCGTTGAA CCCCATT-3'; m-18s rRNA-R: 5'-CCATCCAATCGGTAG TAGCG-3'; m-GAPDH-F: 5'-ACCCAGAAGACTGTG-GATGG-3'; m-GAPDH-R: 5'-CACATTGGG-GGTAGGA ACAC-3'; m-Coll-I-F: 5'-AGAGC-ATGACCGATGGAT TC-3'; m-Coll-I-R: 5'-CCTTCTTGAGGTTGCCAGTC-3'; m-BSP-F: 5'-GAAAATGGAGACGGCGATAG-3'; m-BSP-R: 5'-ACCCGAGAGTGTGGAAAGTG-3'; m-ALP-F: 5'-AACCCAGACACAAGCATT-CC-3'; m-ALP-R: 5'-GA GAGCGAAGGGTC-AGTCAG-3'; m-OC-F: 5'-CCGGGA GCAG-TGTGAGCTTA-3'; m-OC-R: 5'-TAGATGC-GTTT GTAGGCGGTC-3'; m-Osx-F: 5'-AC-TGGCTAGGTGGT GGTCAG-3';m-Osx-R:5'-GGTAGGGAGCTGGGTTAAG-G-3'; m-BMP2-F:5'-GCTCCACAAACGAGAAAAG-C-3';

RESEARCH ARTICLE

m-BMP2-R: 5′-AGCAAGGGGAAAAG-GACACT-3′; m-IL6-F: 5′-ACTTCCATCCAG-TTGCCTTC-3′; m-IL6-R: 5′-TTTCCACGTT-TCCCAGAGA-3′; h-β-actin-F: 5′-AAGG GAC-TTCCTGTAACAATGCA-3′; h-β-actin-R: 5′-CTGG AACGGTGAAGGTGACA-3′; hGAPDH-F: 5′-TGCACCA CCAACTGCTTA-GC-3′; hGAPDH-R: 5′-GGCATGGACT GTGG-TCATGAG-3′; h-ALP-F: 5′-CCGCTATCC-TGGC TCCGTGC-3′; h-ALP-R: 5′-GGTGGGC-TGGCAGTGGT CAG-3′; h-Coll-I-F: 5-CC-TGACGCACGGCCAAGA GG-3′; h-Coll-I-R: 5′-GGCAGGGCTCGGGTTTCCAC-3′; h-OC-F: 5′-GAAGCCCAGCGGTGCA-3′; h-OC-R: 5′-CA CTACCTCGCTGCCCTCC-3′; h-Runx2-F: 5′-CTGTGCT CGGTGCTGCCCTC-3′; h-Runx2-R: 5′-CGTTACCCGCC ATGACAG-TA-3′.

Each reaction contained 7 μl Lightcycler-FastStart DNA MasterPLUS SYBR Green I (containing Fast Start Taq polymerase, reaction buffer, dNTPs mix, SYBRGreen I dye and MgCl2), 0.5 μM of each, the sense and the anti-sense specific primers and 3 μl of the cDNA dilution in a final volume of 10 μl. The amplification program consisted of a preincubation step for denaturation of the template cDNA (10 min 95 °C), followed by 45 cycles consisting of a denaturation step (10 s 95 °C), an annealing step (8–10 s 60 °C, except for mALP that was 8 s 65 °C and for hALP and hOC that was 5 s 68 °C) and an extension step (10 s 72 °C). After each cycle, fluorescence was measured at 72 °C (λex 470 nm, λem 530 nm). A negative control without cDNA template was run in each assay.

Real-time efficiencies were calculated from the given slopes in the LightCycler 480 software using serial dilutions, showing all the investigated transcripts high real-time PCR efficiency rates, and high linearity when different concentrations are used. PCR products were subjected to a melting curve analysis on the LightCycler and subsequently 2% agarose/TAE gel electrophoresis to confirm amplification specificity, Tm and amplicon size, respectively.

Relative quantification after PCR was calculated by dividing the concentration of the target gene in each sample by the mean of the concentration of the two reference genes (housekeeping genes) in the same sample using the Advanced relative quantification method provided by the LightCycler 480 analysis software version 1.5 (Roche Diagnostics, Mannheim, Germany).

2.11. Determination of ALP Activity

ALP activity was determined from cell monolayers after 21 days (hUCMSCs) and 28 days (MC3T3-E1 cells) of cell culture, as described previously by Hinoi et al.[44] Briefly, cells were washed twice in PBS, solubilized with 0.1% Triton X-100. Then, samples were incubated with an assay mixture of p-Nitrophenyl Phosphate. Cleavage of p-Nitrophenyl Phosphate (pNPP) (Sigma, Saint Louis, Missouri, USA) in a soluble yellow end product which

absorb at 405 nm was used to assess ALP activity. In parallel to the samples, a standard curve with calf intestinal alkaline phosphatase (CIAP) (Promega, Madison, USA) was constructed; 1 μl from the stock CIAP was mixed with 5 ml of alkaline phosphatase buffer (1:5000 dilution), and subsequently diluted 1:5.

2.12. Alizarin-Red Staining in MC3T3-E1 Cells

The alizarin red (ARS) staining was used to visually detect the presence of mineralization nodules *in vitro*. MC3T3-E1 cells were trypsinized and 2×10^4 cells/well were seeded into 24-well culture plates. Confluent control and treated cells were cultured for 14, 21 and 28 days.

After removing culture media, cells were washed with 500 μl PBS and fixed in 10% (v/v) folmaldehyde 37% (Sigma-Aldrich, St. Louis, USA) at room temperature for 15 min. Then, fixed cells were washed with dH$_2$O ($\times$3) prior to addition of 500 μl of 40 mM ARS (Sigma-Aldrich, St. Louis, USA) (pH 4.1) per each well. The plates were incubated at room temperature for 1 hour. After removal of incorporated dye, the wells were washed three times with dH$_2$O to remove the excess of dye. For ARS visualization, 500 μl of dH$_2$O were added to each well to prevent damage of cell's monolayer. Plates with stained monolayers were photographed.

2.13. Determination of Calcium Content

Total calcium content was quantified on day 21 (hUCM-SCs) and 28 (MC3T3-E1 cells). Cells were washed twice in PBS and solubilized with 0.1% Triton X-100. Lysates were also treated with 0.5N hydrochloric acid overnight, followed by centrifugation at $500 \times$ g for 2 minutes for the subsequent determination of Ca^{2+} content in the supernatant by inductively coupled plasma atomic emission spectrometer (ICP-AES) Optima 5300 DV (PerkinElmer, Massachusetts, USA). Data were compared with CaCl$_2$ standards included in the assay.

2.14. Statistical Analyses

All data are presented as mean values $\pm$ SEM. Differences between groups were assessed by Mann-Whitney-test or by Student *t*-test depending on their normal distribution; The SPSS$^\circledR$ program for Windows, version 17.0 was used. Results were considered statistically significant at the *p*-values ≤ 0.05.

3. RESULTS

3.1. Peptide Structures

Lack of stable 3D structure is a usual problem in peptides with limited length or low complexity sequence. The full atom structure information we can obtain comes

from NMR (nuclear magnetic resonance) experiment or 3D structure prediction. Recently, improved methods for structure prediction of peptides provide only qualitative tool for finding of structure-activity relationships. Models of all 3 studied peptides showed signature of compact, well packed structures without any secondary structure elements, as expected due to the rich content of prolines. From this point of view, only the C termini exhibited structural features that can be related to the function of the particular peptide. Based on the expected mechanism of action, e.g., peptide molecule bearing a signal recognizable by a receptor, we can classify the predicted structures by the following scheme: according to analysis of backbone torsions of the PPXPP C-terminal sequence, P1 has preferential helical conformation only on proline 22 and the rest of prolines is in polypro II conformation, which results in rather extended type of structure (Fig. 1(a)). P2 is the only peptide that forms preoriented C terminal sequence known from crystal structures of proteins binding proline-rich regions. The regular repetition of polypro and α-helical torsions is characteristics for this peptide (Fig. 1(b)). Just opposite to the P1 is P3, where only the Pro 22 shows preferences for poly Pro II conformation while the other prolines are in helical conformation, which results in some conformational restraints probably not ideal for fast recognition as the P2 but still more suitable than P1 (Fig. 1(c)). We cannot unambiguously state that the described structural features are directly responsible for the effect of the peptides in question but they tell us about certain level of structural stability in otherwise non rigid molecules.

3.2. Cell Toxicity

The lactate dehydrogenase (LDH) activity in the culture media was used as an index of toxicity. After treatment of MC3T3-E1 cells for 24–48 h (Fig. 2(a)), P2 significantly increased cell viability in a short-term period (compared to untreated cells and EMD). Similar results to P2 were obtained for P1 and P3, compared to untreated cells and EMD (data not shown). The effect of P2 and EMD on cell viability was also tested after long-term of cell culture (Fig. 2(a)). EMD induced higher cell toxicity up to 14 days of cell treatment compared to untreated cells, whereas a decrease in LDH activity was observed after this time period, with a significant decrease in cell toxicity after 21 days compared to untreated cells and P2. After 28 days of treatment, no differences were observed among the groups. We verified these results in hUCMSCs (Fig. 2(b)) and found that, after 24 hours of treatment, P2 improved cell viability in hUCMSCs cells compared to control cells. No toxic effects were detected after treatment with P2 and EMD for 14 and 21 days compared to untreated cells. No differences were observed among the groups thereafter.
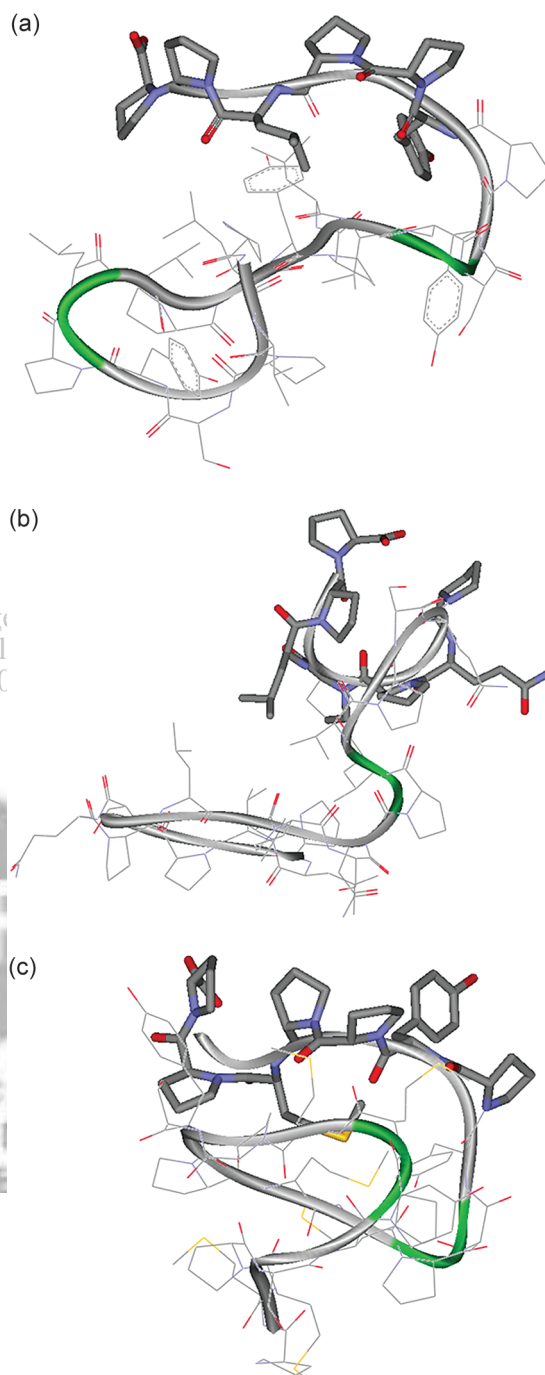
Fig. 1. PepFold predicted 3D structures of peptide 1 (a), 2 (b) and 3 (c). C terminal sequence of peptides (PPXPP) is accented by using of stick representation for corresponding amino acids.

3.3. Cell Proliferation

The effect of synthetic peptides on cell proliferation was assessed and compared to cells treated with EMD and control. No significant differences were found in the proliferation of MC3T3-E1 cells incubated with P2 compared to EMD or untreated cells (Fig. 3(a)). In contrast, P3 treatment at 50 μg/ml showed an increase of 40.6% in cell
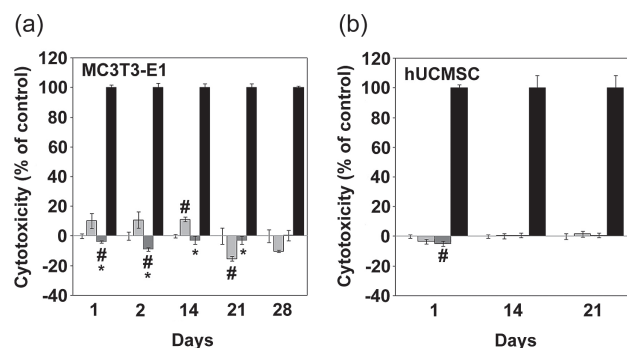
(a)   (b)

Fig. 2. LDH activity measured from culture media collected after treatment of MC3T3-E1 cells (a) and hUCMSCs (b) with P2 (50 μg/ml) or EMD (50 μg/ml) at different time points. Values represent the mean $\pm$ SEM. Mann-Withney test: (#) $p \leq 0.05$ versus control, (*) $p \leq 0.05$ versus EMD. (□ negative control (no treatment), ■ positive control (1% triton X-100), ■ EMD, ■ P2).

Table II. Gene expression of several osteoblast markers after 14 days of treatment in MC3T3-E1 and hUCMSCs. Data represent relative mRNA levels of target genes normalized with housekeeping genes, expressed as a percentage of control cells, which were set to 100%. Values represent the mean $\pm$ SEM. Differences between groups were assessed by Mann-Whitney-test or by Student t-test depending on their normal distribution; (#) $p \leq 0.05$ versus control (*), $p \leq 0.05$ versus EMD.

	Control	EMD	P2
MC3T3-E1			
Coll-I	100.0 ± 14.97	275.64 ± 74.47 (#)	152.11 ± 40.49
BSP	100.0 ± 21.64	127.20 ± 26.19	253.16 ± 90.21
ALP	100.0 ± 32.49	23.97 ± 3.40 (#)	187.26 ± 38.23 (*)
OC	100.0 ± 15.94	32.96 ± 4.97 (#)	97.25 ± 13.89 (*)
Osx	100.0 ± 22.13	44.36 ± 18.05	123.11 ± 64.62
BMP2	100.0 ± 18.44	54.84 ± 18.95	193.53 ± 95.80
IL-6	100.0 ± 16.61	17.75 ± 4.68 (#)	134.22 ± 33.45 (*)
hUCMSC			
Runx-2	100.0 ± 6.2	81.7 ± 3.3 (#)	97.8 ± 18.9
Coll-1	100.0 ± 5.7	105.0 ± 27.0	189.4 ± 85.6
ALP	100.0 ± 30.7	90.4 ± 8.1	124.6 ± 8.1
OC	100.0 ± 9.6	135.0 ± 30.5	163.8 ± 15.0 (#)

proliferation ($p = 0.045$), while no effects were found with P1 (data not shown). In hUCMSCs, treatment with P2 for 4 days displayed a reduced cell proliferation compared to control cells (Fig. 3(b)). No differences were seen in proliferation compared to EMD-treated cells.

3.4. Expression of Osteoblast Differentiation and Inflammation Related Genes

The effect of P2 or EMD treatment (50 μg/ml) on mRNA levels of marker genes was analysed after 14 days in MC3T3-E1 and hUCMSC cell cultures.

As shown in Table II, P2 treatment for 14 days of MC3T3-E1 cells induced an up-regulation of the osteoblast differentiation markers ALP and OC compared to EMD treatment (8-fold and 3-fold over EMD, respectively). Similar results to P2 were observed for P1 and P3 compared to EMD (data not shown). On the other hand, the expression of the differentiation markers ALP, OC and IL-6 was significantly decreased in cells treated with EMD compared to untreated cells. However, EMD treatment induced gene
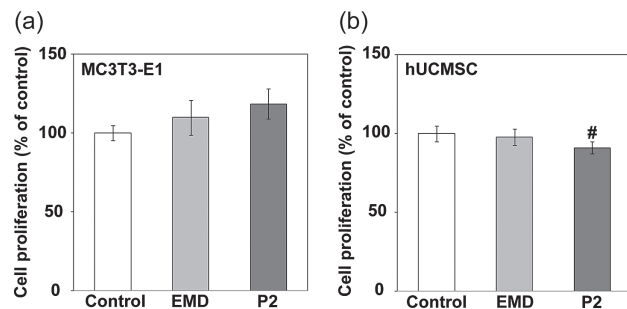
expression of the early stage marker of osteoblast differentiation, Coll-I.

In hUCMSCs, P2 treatment induced OC gene expression compared to untreated cells after 14 days of cell culture. No effects on Coll-I gene expression were observed in hUCMSCs cells treated with EMD (differing from MC3T3-E1 cells). Runx-2 mRNA levels showed a significant decrease in cells treated with EMD compared to untreated cells.

3.5. ALP Activity

To examine the effect on osteoblast differentiation, ALP activity was measured in the cell monolayer after incubation with 50 μg/ml P2 or EMD for 21 days in hUCMSCs, and for 28 days in MC3T3-E1 cells (Fig. 4). In both types of cells, P2 treatment induced a higher ALP activity compared to untreated or to EMD-treated cells. In MC3T3-E1 cells, P2 significantly increased ALP activity compared to EMD ($p = 0.002$) (Fig. 4(a)). The above results are in accordance with ALP mRNA levels in MC3T3-E1 cells. In hUCMSCs (Fig. 4(b)), P2 treatment increased ALP activity over cells treated with EMD ($+37\%$) or untreated cells ($+76\%$); however, differences were not statistically significant.

3.6. Extracellular Matrix Mineralization

In order to assess the stimulation of mineral nodule formation, the calcium deposition was observed in MC3T3-E1 cells by alizarin red staining. Mineral deposition was increased in a time-dependent manner from 14 to 28 days of cell culturing. Qualitatively, EMD and P2-treated cells increased alizarin red staining after 28 days of cell culture
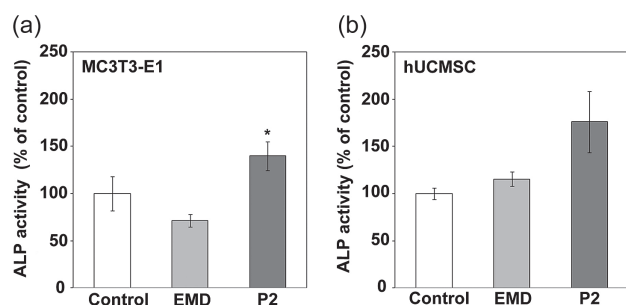
(a)   (b)

Fig. 3. Cell proliferation was measured by BrdU incorporation into the cells incubated with P2 (50 μg/ml) or EMD (50 μg/ml) for 24 hours in MC3T3-E1 cells (a) or for 4 days hUCMSCs cells (b). Values were expressed as a percentage of control, which were set to 100%. Values represent the mean $\pm$ SEM. Student t- test: (#) $p \leq 0.05$ versus control, (*) $p \leq 0.05$ versus EMD.

Fig. 4. (a) Alkaline phosphatase (ALP) activity measured from MC3T3-E1 cell monolayer after incubation with 50 μg/ml of P2 or EMD for 28 days. (b) ALP activity of hUCMSCs treated with 50 μg/ml of P2 or EMD for 21 days. Values were expressed as a percentage of untreated control cells, which were assigned as 100%. Values represent the mean $\pm$ SEM. Mann-Withney test: (#) $p \leq 0.05$ versus control, (*) $p \leq 0.05$ versus EMD.

against the control, with the formation of mineral nodules (Fig. 5(a)).

The calcium content in the cell monolayer after treatments with EMD and P2 was quantified by inductively coupled plasma atomic emission spectrometer (ICP-AES) in MC3T3-E1 and hUCMSC cells (Fig. 5(b)). Both types of cells studied showed higher calcium content in cells treated with P2 compared to EMD and untreated cells. As shown in Figure 5(b), P2 increased by 47% the calcium content of MC3T3-E1 cells compared to untreated cells, although data did not reach statistical significance ($p = 0.09$). Likewise, hUCMSCs showed higher calcium content in cells treated with P2 and EMD, however values were not statistically different compared to untreated cells ($p = 0.083$ and $p = 0.16$, respectively). While EMD
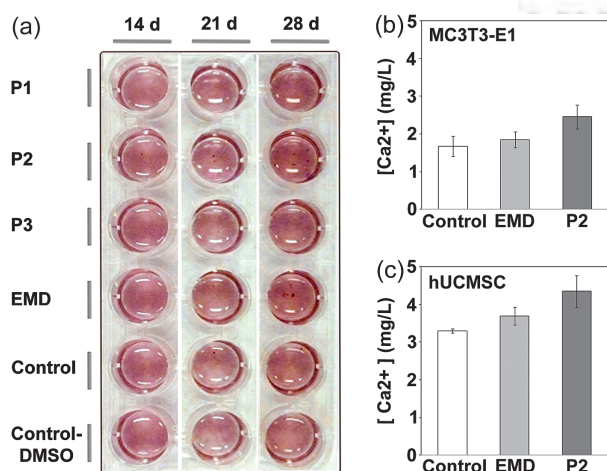
Fig. 5. Extracelular matrix mineralization after incubation with synthetic peptides or EMD (50 μg/ml). (a) Representative stained wells with Alizarin red S method in MC3T3-E1 cell cultures treated with synthetic peptides/EMD at 50 μg/ml or control after 14, 21 and 28 days. (b) Calcium content quantified with inductively coupled plasma atomic emission spectrometer after treatment with P2 or EMD (50 μg/ml) in MC3T3-E1 cells for 28 days and in hUCMSC cells for 21 days. Values represent the mean $\pm$ SEM, expressed in mg/L of calcium.

and P2 showed similar mineral nodule formation by qualitative alizarin red staining, the calcium content measured from cell monolayer in EMD was lower than in those treated with P2 when a quantitative ICP-AES method was used.

4. DISCUSSION

The present study demonstrates that the synthetic proline-rich peptides had no toxic effects and stimulated osteoblast differentiation *in vitro* either in MC3T3-E1 cells or in hUCMSCs. Among the 3 synthetic peptides tested, P2 showed the best structural and biological activity. Thus, P2 induced gene expression of differentiation markers in a higher degree than EMD, in both MC3T3-E1 and hUCMSC cells. Further, P2 exhibited greater effects at functional level on ALP activity and mineral content compared to the other treatments.

MC3T3-E1 osteoblast-like cells were chosen as an *in vitro* model for studying the stimulatory effects of synthetic proline-rich peptides on bone formation and biomineralization. This cell line, under appropriate conditions, undergoes a developmental sequence of proliferation and differentiation similar to primary cells in culture; as shown by the expression of osteoblast differentiation markers.[21, 45] To evaluate the potential induction of those synthetic peptides on bone formation and biomineralization, the effect of synthetic peptides was also studied in hUCMSCs. These cells are multipotent, differentiating along a variety of cell lineages, such as chondrocytes, osteoblasts, adipocytes, myocytes, neurons and hepatocytes.[46] In the present study, these cells were stimulated to the osteoblastic lineage using a combination of osteogenic supplements, exhibiting the ability to produce and mineralize the extracellular matrix.

Our first goal in the present investigation was to check whether the synthetic peptides had any negative effect on cell viability. They were found to be safe after short and long-time period of treatment either in MC3T3-E1 cells and hUCMSCs. EMD significantly increased cytotoxicity after 14 days of cell culture in MC3T3-E1 cells, but decreased thereafter. It has previously been shown that doses of EMD higher than 50 μg/ml are toxic for periodontal ligament cells (PDL).[47] However, other studies have reported that in human gingival cells, doses of 100 μg/ml of EMD had no effect on cell viability, while protected against TNF-induced apoptosis.[48]

Second, no significant effects on cell growth were found after one day of treatment either with P1, P2 or with EMD in MC3T3-E1 cells, only for P3 that increased cell proliferation by 41%. In hUCMSCs, P2 decreased by 9% cell proliferation after four days. There are controversial results as regards to the effect of EMD on cell proliferation, some studies have shown that EMD only stimulates cell proliferation after two days of treatment,[21, 26, 49, 50, 51] while others

have reported an enhancement of cell proliferation after one day of treatment.[52] It has been suggested that these differences are dependent on cell type,[31] culture conditions,[21] the maturation state of the cells[51] and exposure time of treatment.

We also studied the effect of proline-rich synthetic peptides on the differentiation of MC3T3-E1 and hUCMSCs. Formation and biomineralization of bone requires an integrated cascade of gene expression that initially supports proliferation and further a sequential expression of genes associated with the biosynthesis, organization, maturation and mineralization of the bone extracellular matrix.[53] Modulation of these expression genes is subjected to a transcriptional control regulated by growth factors and cytokines.[18, 53, 54] IL-6 is a pleiotropic cytokine that, on the one hand stimulates the formation of osteoclasts,[55] and on the other hand, stimulates osteoblast differentiation and bone formation.[56] IL-6 mRNA levels were increased significantly after treatment with P2 compared to EMD. Other studies have found an stimulation of IL-6 secretion[13, 22, 23] and IL-6 mRNA expression[22] by EMD. Numerous studies have reported that EMD enhances osteoblastic differentiation by increasing the expression of transcriptional factors. However, the underlying mechanisms by which EMD produces these effects are unknown.[57] We found that EMD decreased ALP, OC and IL-6 mRNA levels in MC3T3-E1 cells and Runx-2 in hUCMSCs. Several studies have reported increased osteocalcin mRNA levels[21, 23, 26, 31] with EMD. In the present study, we did not find such effects after EMD treatment, in accordance to other reports.[22,52] In contrast, treatment with P2 induced gene expression of differentiation markers ALP, OC and IL-6 compared to EMD in MC3T3-E1 cells and OC in hUCMSCs. Our results suggest that P2 could increase the expression of transcriptional factors at the initial states of cell differentiation and then undergo a cascade of signals to finally stimulate expression of osteoblast-differentiation specific markers. Coll-I mRNA levels, an early osteoblast marker which supports the cell proliferation stage,[53] was not induced by P2 after 14 days of incubation in MC3T3-E1 cells or hUCMSCs. In contrast, in accordance with our results, a few studies have documented that EMD induces Coll-I gene expression in primary osteoblasts.[21, 22, 23] Here we found that Coll-I was increased with EMD in MC3T3-E1 cells and not in hUCMSCs. This could be due to the fact that the latter studies used osteogenic supplements to facilitate differentiation and mineralization.

After synthesis of a collagenous network, a sequential expression of genes related with maturation and organization of the bone matrix are up-regulated, contributing to rendering an extracellular matrix competent for mineralization.[53] ALP is a membrane bound enzyme contained in matrix vesicles involved in hydroxyapatite crystal deposition and, commonly, is considered an early marker of osteogenic differentiation.[52] Consistent with the

increase in gene expression of differentiation markers by P2 treatment, the ALP activity in the MC3T3-E1 and hUCMSC cell monolayer was also enhanced. These results are in line with the increasing tendency of calcium deposition observed after treatment with P2. *In vitro* studies using osteogenic cultures, mineralization is considered a functional end-point reflecting advanced cell differentiation.[58] Alizarin red staining is commonly used to detect and quantify calcium, within the deposited mineral. It is interesting to note that although EMD decreased gene expression of ALP, OC in MC3T3-E1 cells and Runx-2 in hUCMSCs and no effects were found on ALP activity, cell monolayers after EMD treatment appeared more densely stained with alizarin than the control, and similar to P2. The same pattern was found when the calcium content was quantified with ICP-AES, with calcium content of EMD-treated cells lower than P2. This could be explained by the capacity of amelogenins to bind calcium.

EMD is mainly composed by amelogenins and processing products thereof.[59] The primary structure of amelogenin, which has a bipolar nature (hydrophobic–hydrophilic),[60] self-assembles through functional motifs of the protein primary structure generating specific supramolecular aggregates.[61] Formation of these nanospheres are found to be crucial for the regulatory function of amelogenins, possibly creating a hydrophobic core and leaving charged residues found in the NH_2 and COOH terminus covering the surface of the sphere.[62] The C-terminal region is composed of a sequence of hydrophilic and charged amino acids.[63] The capacity of amelogenins to bind calcium has been suggested to be mediated by ion interactions between the calcium and the charged acidic groups of aminoacids in the C-terminal region.[64] Further, current literature has reported that structural differences in different forms of amelogenins may be responsible for their ultimate differences in biological activities and functions in enamel biomineralization.[64] The secondary structure containing repetitive β-turns, forming an internal β-spiral channel, suggests a potential function facilitating calcium ion passage to regulate mineralization while the secondary structure in random coil of the LRAP could explain the role of LRAP on cell signalling. Therefore, given that our synthetic peptides are uncharged and their pattern rich in proline does not contain the classical secondary structure of β-sheet motif, structural differences between our synthetic peptides and EMD may be responsible for their ultimate differences in biological activities and functions in biomineralization. Furthermore, it has been described that the short sequence of PPXPP in the C-terminal region of peptides participate in the transactivation activity of transcription factors and/or co-activators.[65] The sequence PPXP is present on both amelogenin and ameloblastin molecules, suggesting that this short consensus sequence may be of importance in the signalling activity of these molecules. Structural differences between peptides may also explain

different mechanism of their action. Among the three peptides designed and tested, P2 was the peptide sequence that showed best structural characteristics and biological activity in MC3T3-E1 cells and hUCMSCs. The higher accessibility and structural rigidity of the C-terminus PPLPP in P2 suggest that this particular stretch of amino acids could act as a better signal sequence for proteins connected with signaling events. Further, the promoting effect of P2 on biomineralization might be due to its higher polar amino acids composition compared to P1 and P3.

These results suggest a more specific mechanism of action for the synthetic proline-rich peptides than for EMD, possibly involving intracellular signalling pathways for osteogenic differentiation of pre-osteoblastic cells. In contrast EMD, being a mix of mostly amelogenin derived peptides, is less specific in its actions combining the effect of several peptides, both proline-rich and not, that influence several processes including cell growth, inflammatory responses and repair mechanisms and also work as a modulator of crystal deposition and growth. The observed effect of the proline-rich peptides holds potential use for both clinical applications and as research tool for further investigations of the molecular basis of induced osteogenic cell differentiation. Further work on peptide primary and secondary structure for effect optimization, and isolation and characterisation of possible receptors for poly proline motifs are needed to clarify the biological importance of this intriguing molecule family in the development, growth and repair of hard tissues. Bioinformatics methods available at EBI (Proteins Functional Analysis) has been used to analyze the sequences of our synthetic peptides in order to find their cellular analogs our counterparts (FingerPRINT) and to identify putative functional sites identified by patterns (ELM) (see Supplementary Material). At this moment it is not possible to evaluate significancy of the localized motifs but they will be used in further studies.

References and Notes

1. S. Weiner, I. Sagi, and L. Addadi, Structural biology. Choosing the crystallization path less traveled. *Science* 309, 1027 (**2005**).

2. T. Jin, Y. Ito, X. Luan, S. Dangaria, C. Walker, M. Allen, A. Kulkarni, C. Gibson, R. Braatz, X. Liao, and T. G. Diekwisch, Elongated polyproline motifs facilitate enamel evolution through matrix subunit compaction. *PLoS Biol.* 7, e1000262 (**2009**).

3. J. Hatakeyama, S. Fukumoto, T. Nakamura, N. Haruyama, S. Suzuki, Y. Hatakeyama, L. Shum, C. W. Gibson, Y. Yamada, and A. B. Kulkarni, Synergistic roles of amelogenin and ameloblastin. *Journal of Dental Research* 88, 318 (**2009**).

4. L. J. Ball, R. Kuhne, J. Schneider-Mergener, and H. Oschkinat, Recognition of proline-rich motifs by protein-protein-interaction domains. *Angew Chem. Int. Ed. Engl.* 44, 2852 (**2005**).

5. L. Biedermannova, K. E. Riley, K. Berka, P. Hobza, and J. Vondrasek, Another role of proline: Stabilization interactions in proteins and protein complexes concerning proline and tryptophane. *Phys. Chem. Chem. Phys.* 10, 6350 (**2008**).

6. D. Deutsch, A. Haze-Filderman, A. Blumenfeld, L. Dafni, Y. Leiser, B. Shay, Y. Gruenbaum-Cohen, E. Rosenfeld, E. Fermon, B. Zimmermann, S. Haegewald, J. P. Bernimoulin, and A. L. Taylor, Amelogenin, a major structural protein in mineralizing enamel, is also expressed in soft tissues: brain and cells of the hematopoietic system. *Eur. J. Oral. Sci.* 114, 183 (**2006**).

7. A. Haze, A. L. Taylor, A. Blumenfeld, E. Rosenfeld, Y. Leiser, L. Dafni, B. Shay, Y. Gruenbaum-Cohen, E. Fermon, S. Haegewald, J. P. Bernimoulin, and D. Deutsch, Amelogenin expression in long bone and cartilage cells and in bone marrow progenitor cells. *Anat Rec (Hoboken)* 290, 455 (**2007**).

8. C. D. Fong, R. Cerny, L. Hammarstrom, and I. Slaby, Sequential expression of an amelin gene in mesenchymal and epithelial cells during odontogenesis in rats. *Eur. J. Oral. Sci.* 106, 324 (**1998**).

9. A. Spahr, S. P. Lyngstadaas, I. Slaby, and G. Pezeshki, Ameloblastin expression during craniofacial bone formation in rats. *Eur. J. Oral. Sci.* 114, 504 (**2006**).

10. M. V. Tamburstuen, J. E. Reseland, A. Spahr, S. J. Brookes, G. Kvalheim, I. Slaby, M. L. Snead, and S. P. Lyngstadaas, Ameloblastin expression and putative autoregulation in mesenchymal cells suggest a role in early bone formation and repair. *Bone* 48, 406 (**2011**).

11. C. Du, G. B. Schneider, R. Zaharias, C. Abbott, D. Seabold, C. Stanford, and J. Moradian-Oldak, Apatite/amelogenin coating on titanium promotes osteogenic gene expression. *Journal of Dental Research* 84, 1070 (**2005**).

12. S. Lacerda-Pinheiro, D. Septier, K. Tompkins, A. Veis, M. Goldberg, and H. Chardin, Amelogenin gene splice products A+4 and A−4 implanted in soft tissue determine the reorientation of CD45-positive cells to an osteo-chondrogenic lineage. *Journal of Biomedical Materials Research* 79, 1015 (**2006**).

13. S. P. Lyngstadaas, E. Lundberg, H. Ekdahl, C. Andersson, and S. Gestrelius, Autocrine growth factors in human periodontal ligament cells cultured on enamel matrix derivative. *J. Clin. Periodontol.* 28, 181 (**2001**).

14. T. Nagano, S. Oida, S. Suzuki, T. Iwata, Y. Yamakoshi, Y. Ogata, K. Gomi, T. Arai, and M. Fukae, Porcine enamel protein fractions contain transforming growth factor-beta1. *Journal of Periodontology* 77, 1688 (**2006**).

15. J. Svensson, C. Andersson, J. E. Reseland, P. Lyngstadaas, and L. Bulow, Histidine tag fusion increases expression levels of active recombinant amelogenin in Escherichia coli. *Protein Expression and Purification* 48, 134 (**2006**).

16. A. Veis, K. Tompkins, K. Alvares, K. Wei, L. Wang, X. S. Wang, A. G. Brownell, S. M. Jengh, and K. E. Healy, Specific amelogenin gene splice products have signaling effects on cells in culture and in implants *in vivo*. *J. Biol. Chem.* 275, 41263 (**2000**).

RESEARCH ARTICLE

J. Biomater. Tissue Eng. 1, 198–209, 2011

207

17. R. Warotayanont, D. Zhu, M. L. Snead, and Y. Zhou, Leucine-rich amelogenin peptide induces osteogenesis in mouse embryonic stem cells. *Biochemical and Biophysical Research Communications* 367, 1 (**2008**).

18. D. D. Bosshardt, Biological mediators and periodontal regeneration: A review of enamel matrix proteins at the cellular and molecular levels. *J. Clin. Periodontol.* 35, 87 (**2008**).

19. S. P. Lyngstadaas, J. C. Wohlfahrt, S. J. Brookes, M. L. Paine, M. L. Snead, and J. E. Reseland, Enamel matrix proteins; old molecules for new applications. *Orthodontics & Craniofacial Research* 12, 243 (**2009**).

20. A. Sculean, F. Schwarz, J. Becker, and M. Brecx, The application of an enamel matrix protein derivative (Emdogain) in regenerative periodontal therapy: A review. *Med. Princ. Pract.* 16, 167 (**2007**).

21. J. He, J. Jiang, K. E. Safavi, L. S. Spangberg, and Q. Zhu, Emdogain promotes osteoblast proliferation and differentiation and stimulates osteoprotegerin expression. *Oral Surgery, Oral Medicine, Oral Pathology, Oral Radiology, and Endodontics* 97, 239 (**2004**).

22. J. Jiang, A. F. Fouad, K. E. Safavi, L. S. Spangberg, and Q. Zhu, Effects of enamel matrix derivative on gene expression of primary osteoblasts. *Oral Surgery, Oral Medicine, Oral Pathology, Oral Radiology, and Endodontics* 91, 95 (**2001**).

23. J. E. Reseland, S. Reppe, A. M. Larsen, H. S. Berner, F. P. Reinholt, K. M. Gautvik, I. Slaby, and S. P. Lyngstadaas, The effect of enamel matrix derivative on gene expression in osteoblasts. *Eur. J. Oral. Sci.* 114, 205 (**2006**).

24. T. Iwata, Y. Morotome, T. Tanabe, M. Fukae, I. Ishikawa, and S. Oida, Noggin blocks osteoinductive activity of porcine enamel extracts. *Journal of Dental Research* 81, 387 (**2002**).

25. M. Ohyama, N. Suzuki, Y. Yamaguchi, M. Maeno, K. Otsuka, and K. Ito, Effect of enamel matrix derivative on the differentiation of C2C12 cells. *Journal of Periodontology* 73, 543 (**2002**).

26. Z. Schwartz, D. L. Carnes, Jr., R. Pulliam, C. H. Lohmann, V. L. Sylvia, Y. Liu, D. D. Dean, D. L. Cochran, and B. D. Boyan, Porcine fetal enamel matrix derivative stimulates proliferation but not differentiation of pre-osteoblastic 2T9 cells, inhibits proliferation and stimulates differentiation of osteoblast-like MG63 cells, and increases proliferation and differentiation of normal human osteoblast NHOst cells. *Journal of Periodontology* 71, 1287 (**2000**).

27. J. C. Rincon, Y. Xiao, W. G. Young, and P. M. Bartold, Enhanced proliferation, attachment and osteopontin expression by porcine periodontal cells exposed to Emdogain. *Archives of Oral Biology* 50, 1047 (**2005**).

28. E. Shimizu, R. Saito, Y. Nakayama, Y. Nakajima, N. Kato, H. Takai, D. S. Kim, M. Arai, J. Simmer, and Y. Ogata, Amelogenin stimulates bone sialoprotein (BSP) expression through fibroblast growth factor 2 response element and transforming growth factor-beta1 activation element in the promoter of the BSP gene. *Journal of Periodontology* 76, 1482 (**2005**).

29. Y. Tokiyasu, T. Takata, E. Saygin, and M. Somerman, Enamel factors regulate expression of genes associated with cementoblasts. *Journal of Periodontology* 71, 1829 (**2000**).

30. S. Keila, C. E. Nemcovsky, O. Moses, Z. Artzi, and M. Weinreb, *In vitro* effects of enamel matrix proteins on rat bone marrow cells and gingival fibroblasts. *Journal of Dental Research* 83, 134 (**2004**).

31. S. Yoneda, D. Itoh, S. Kuroda, H. Kondo, A. Umezawa, K. Ohya, T. Ohyama, and S. Kasugai, The effects of enamel matrix derivative (EMD) on osteoblastic cells in culture and bone regeneration in a rat skull defect. *Journal of Periodontal Research* 38, 333 (**2003**).

32. F. Rathe, R. Junker, B. M. Chesnutt, and J. A. Jansen, The effect of enamel matrix derivative (Emdogain) on bone formation: A systematic review. *Tissue Engineering* 15, 215 (**2009**).

33. M. Kantlehner, P. Schaffner, D. Finsinger, J. Meyer, A. Jonczyk, B. Diefenbach, B. Nies, G. Holzemann, S. L. Goodman, and H. Kessler, Surface coating with cyclic RGD peptides stimulates osteoblast adhesion and proliferation as well as bone formation. *Chembiochem* 1, 107 (**2000**).

34. R. S. Bhatnagar, J. J. Qian, A. Wedrychowska, M. Sadeghi, Y. M. Wu, and N. Smith, Design of biomimetic habitats for tissue engineering with P-15, a synthetic peptide analogue of collagen. *Tissue Eng.* 5, 53 (**1999**).

35. M. Thorwarth, S. Schultze-Mosgau, F. Wehrhan, S. Srour, J. Wiltfang, F. W. Neukam, and K. A. Schlegel, Enhanced bone regeneration with a synthetic cell-binding peptide—*in vivo* results. *Biochemical and Biophysical Research Communications* 329, 789 (**2005**).

36. D. Itoh, S. Yoneda, S. Kuroda, H. Kondo, A. Umezawa, K. Ohya, T. Ohyama, and S. Kasugai, Enhancement of osteogenesis on hydroxyapatite surface coated with synthetic peptide (EEEEEEP-RGDT) *in vitro*. *Journal of Biomedical Materials Research* 62, 292 (**2002**).

37. C. D. Reyes, T. A. Petrie, K. L. Burns, Z. Schwartz, and A. J. Garcia, Biomolecular surface coating to enhance orthopaedic tissue healing and integration. *Biomaterials* 28, 3228 (**2007**).

38. J. Maupetit, P. Derreumaux, and P. Tuffery, A fast method for large-scale de novo peptide and miniprotein structure prediction. *J. Comput. Chem.* 31, 726 (**2010**).

39. J. Maupetit, P. Derreumaux, and P. Tuffery, PEP-FOLD: an online resource for de novo peptide structure prediction. *Nucleic Acids Res.* 37, W498 (**2009**).

40. W. D. Cornell, P. Cieplak, C. I. Bayly, I. R. Gould, K. M. Merz, D. M. Ferguson, D. C. Spellmeyer, T. Fox, J. W. Caldwell, and P. A. Kollman, A second generation force field for the simulation of proteins, nucleic acids, and organic molecules. *Journal of the American Chemical Society* 117, 5179 (**1995**).

41. V. Hornak, R. Abel, A. Okur, B. Strockbine, A. Roitberg, and C. Simmerling, Comparison of multiple Amber force fields and development of improved protein backbone parameters. *Proteins* 65, 712 (**2006**).

42. W. L. Jorgensen, J. Chandrasekhar, J. D. Madura, R. W. Impey, and M. L. Klein, Comparison of simple potential functions for simulating liquid water. *The Journal of Chemical Physics* 79, 926 (**1983**).

43. M. Dominici, K. Le Blanc, I. Mueller, I. Slaper-Cortenbach, F. Marini, D. Krause, R. Deans, A. Keating, D. Prockop, and E. Horwitz, Minimal criteria for defining multipotent mesenchymal stromal cells. The international society for cellular therapy position statement. *Cytotherapy* 8, 315 (**2006**).

44. E. Hinoi, S. Fujimori, and Y. Yoneda, Modulation of cellular differentiation by N-methyl-D-aspartate receptors in osteoblasts. *FASEB J.* 17, 1532 (**2003**).

45. W. J. Peterson, K. H. Tachiki, and D. T. Yamaguchi, Serial passage of MC3T3-E1 cells down-regulates proliferation during osteogenesis *in vitro*. *Cell Prolif.* 37, 325 (**2004**).

46. S. Bobis, D. Jarocha, and M. Majka, Mesenchymal stem cells: Characteristics and clinical applications. *Folia Histochem Cytobiol.* 44, 215 (**2006**).

47. D. R. Davenport, J. M. Mailhot, J. C. Wataha, M. A. Billman, M. M. Sharawy, and M. K. Shrout, Effects of enamel matrix protein application on the viability, proliferation, and attachment of human periodontal ligament fibroblasts to diseased root surfaces *in vitro*. *J. Clin. Periodontol.* 30, 125 (**2003**).

48. E. Zeldich, R. Koren, C. Nemcovsky, and M. Weinreb, Enamel matrix derivative stimulates human gingival fibroblast proliferation via ERK. *Journal of Dental Research* 86, 41 (**2007**).

49. S. Gestrelius, C. Andersson, D. Lidstrom, L. Hammarstrom, and M. Somerman, *In vitro* studies on periodontal ligament cells and enamel matrix derivative. *J. Clin. Periodontol.* 24, 685 (**1997**).

50. A. Gurpinar, M. A. Onur, Z. C. Cehreli, and F. Tasman, Effect of enamel matrix derivative on mouse fibroblasts and marrow stromal osteoblasts. *Journal of Biomaterials Applications* 18, 25 (**2003**).

51. N. Pischon, B. Zimmermann, J. P. Bernimoulin, and S. Hagewald, Effects of an enamel matrix derivative on human osteoblasts and

PDL cells grown in organoid cultures. *Oral Surgery, Oral Medicine, Oral Pathology, Oral Radiology, and Endodontics* 102, 551 (**2006**).

52. L. Guida, M. Annunziata, F. Carinci, A. Di Feo, I. Passaro, and A. Oliva, *In vitro* biologic response of human bone marrow stromal cells to enamel matrix derivative. *Journal of Periodontology* 78, 2190 (**2007**).

53. G. S. Stein, J. B. Lian, J. L. Stein, A. J. Van Wijnen, and M. Montecino, Transcriptional control of osteoblast growth and differentiation. *Physiological Reviews* 76, 593 (**1996**).

54. J. E. Aubin, Advances in the osteoblast lineage. *Biochem Cell Biol.* 76, 899 (**1998**).

55. T. Tamura, N. Udagawa, N. Takahashi, C. Miyaura, S. Tanaka, Y. Yamada, Y. Koishihara, Y. Ohsugi, K. Kumaki, T. Taga, et al., Soluble interleukin-6 receptor triggers osteoclast formation by interleukin 6. *Proc. Natl. Acad. Sci. USA* 90, 11924 (**1993**).

56. Y. Taguchi, M. Yamamoto, T. Yamate, S. C. Lin, H. Mocharla, P. DeTogni, N. Nakayama, B. F. Boyce, E. Abe, and S. C. Manolagas, Interleukin-6-type cytokines stimulate mesenchymal progenitor differentiation toward the osteoblastic lineage. *Proc. Assoc. Am. Physicians* 110, 559 (**1998**).

57. A. Ulsamer, M. J. Ortuno, S. Ruiz, A. R. Susperregui, N. Osses, J. L. Rosa, and F. Ventura, BMP-2 induces Osterix expression through up-regulation of Dlx5 and its phosphorylation by p38. *J. Biol. Chem.* 283, 3816 (**2008**).

58. C. D. Hoemann, H. El-Gabalawy, and M. D. McKee, *In vitro* osteogenesis assays: Influence of the primary cell source on alkaline

phosphatase activity and mineralization. *Pathol. Biol. (Paris)* 57, 318 (**2009**).

59. S. Gestrelius, S. P. Lyngstadaas, and L. Hammarstrom, Emdogain–periodontal regeneration based on biomimicry. *Clinical Oral Investigations* 4, 120 (**2000**).

60. R. Lakshminarayanan, D. Fan, C. Du, and J. Moradian-Oldak, The role of secondary structure in the entropically driven amelogenin self-assembly. *Biophys. J.* 93, 3664 (**2007**).

61. A. G. Fincham, J. Moradian-Oldak, J. P. Simmer, P. Sarte, E. C. Lau, T. Diekwisch, and H. C. Slavkin, Self-assembly of a recombinant amelogenin protein generates supramolecular structures. *Journal of Structural Biology* 112, 103 (**1994**).

62. W. J. Shaw, A. A. Campbell, M. L. Paine, and M. L. Snead, The COOH terminus of the amelogenin, LRAP, is oriented next to the hydroxyapatite surface. *J. Biol. Chem.* 279, 40263 (**2004**).

63. J. Moradian-Oldak, N. Bouropoulos, L. Wang, and N. Gharakhanian, Analysis of self-assembly and apatite binding properties of amelogenin proteins lacking the hydrophilic C-terminal. *Matrix Biol.* 21, 197 (**2002**).

64. B. T. Le and I. Woo, Alveolar cleft repair in adults using guided bone regeneration with mineralized allograft for dental implant site development: A report of 2 cases. *J. Oral Maxillofac Surg.* 67, 1716 (**2009**).

65. Z. Wang and S. Melmed, Pituitary tumor transforming gene (PTTG) transforming and transactivation activity. *J. Biol. Chem.* 275, 7459 (**2000**).

RESEARCH ARTICLE

Paper 2

Effect of enamel matrix derivative and of proline-rich synthetic peptides on the differentiation of human mesenchymal stem cells towards the osteogenic lineage.

Ramis, J.M.; Rubert, M.; Vondrasek, J.; Gayà, A.; Lyngstadaas, S.P.; Monjo, M.

Original Article

Effect of Enamel Matrix Derivative and of Proline-Rich Synthetic Peptides on the Differentiation of Human Mesenchymal Stem Cells Toward the Osteogenic Lineage

Joana Maria Ramis, Ph.D.,[1] Marina Rubert, M.Sc.,[1] Jiri Vondrasek, Ph.D.,[2,3] Antoni Gayà, M.D., Ph.D.,[1,4] Staale Petter Lyngstadaas, B.Eng., D.D.S., Ph.D.,[5] and Marta Monjo, Ph.D.[1]

With the aim of discovering new molecules for induction of bone formation and biomineralization, combination of bioinformatics and simulation methods were used to design the structure of artificial peptides based on proline-rich domains of enamel matrix proteins. In this study, the effect of such peptides on the differentiation toward the osteogenic lineage of human umbilical cord mesenchymal stem cells (hUCMSCs) was evaluated with or without osteogenic supplements (hydrocortisone, β-glycerol phosphate, and ascorbic acid) and compared to the effect of the commercially available enamel matrix derivative (EMD). It was hypothesized that the differentiation toward the osteogenic lineage of hUCMSCs would be promoted by the treatment with the synthetic peptides when combined with differentiation media, or it could even be directed exclusively by the synthetic peptides. Osteoinductivity was assessed by cell proliferation, bone morphogenetic protein-2 secretion, and gene expression of osteogenic markers after 1, 3, and 14 days of treatment. All peptides were safe with the dosages used, showing lower cell toxicity. P2, P4, and P6 reduced cell proliferation with growing media by 10%–15%. Higher expression of early osteoblast markers was found after 3 days of treatment with EMD in combination with osteogenic supplements, while after 14 days of treatment, cells treated by the different synthetic peptides in combination with osteogenic supplements showed higher osteocalcin mRNA levels. We can conclude that osteogenic differentiation of hUCMSCs is promoted by short-term EMD treatment in combination with osteogenic supplements and by long-term treatment by the synthetic peptides in combination with osteogenic supplements, showing similar results for all the peptide variants analyzed in this study.

Introduction

POLYPROLINE-RICH PROTEINS control the microstructure of vertebrate bones and teeth by serving as a scaffold to control the assembly of biological apatites.[1] To find new molecules for induction of bone formation and biomineralization, we have previously designed an artificial consensus peptide based on the common characteristics of the proline-rich regions in hard tissue extracellular matrix proteins.[2] The designed peptide contains a polyproline consensus sequence of 25AA length, further comprising a systematic variation of non-proline residues. In our previous study,[2] we have demonstrated that the peptide 2 variant of the consensus peptide has the capacity to stimulate osteo-blast differentiation *in vitro* either in mouse pre-osteoblastic cells (MC3T3-E1) or in human umbilical cord derived mesenchymal stem cells (hUCMSCs) cultured with osteogenic supplements.

In this study, two other variants of our designed consensus peptide (peptide 4 and peptide 5) and the analogous peptide to human amelogenin (peptide 6) were investigated for the osteoinductive potential of hUCMSCs, in a continuing effort to advance bone regeneration therapies and follow up our previous research findings.

The new variants of the consensus peptide have been designed with respect to different properties of composing amino acids other than prolines. Several serine residues have been integrated in the sequences of peptides 4 and 5.

[1]Group of Cell Therapy and Tissue Engineering, Research Institute on Health Sciences (IUNICS), University of the Balearic Islands, Palma de Mallorca, Spain.
[2]Institute of Biotechnology Czech Academy of Sciences, Videnska, Prague, Czech Republic.
[3]Institute of Organic Chemistry and Biochemistry, Czech Academy of Sciences, Prague, Czech Republic.
[4]Fundació Banc de Sang i Teixits de les Illes Balears, Palma de Mallorca, Spain.
[5]Department of Biomaterials, Institute for Clinical Dentistry, University of Oslo, Oslo, Norway.

Breakdown of bone and connective tissue matrix is mainly due to matrix metalloproteinases and serine proteases.[3] Therefore, a serine rich peptide with prolines would compete through substrate inhibition and slow down bone resorption. Moreover, apart from serines, replacement by cysteine residues has been studied in the peptide 5. Cysteines comprise sulfur atoms that may bind to metal surfaces by forming sulfur bridges;[4] therefore, this peptide would be optimized to functionalize implant surfaces to favor osteointegration and to promote osteoblastic differentiation.

We have used hUCMSCs to evaluate the effect of the synthetic peptides. hUCMSCs are undifferentiated cells that have the potential to differentiate into osteoblasts among a variety of cell lineages. To promote the osteogenic differentiation of hMSCs, dexamethasone, β-glycerolphosphate, and ascorbic acid (osteogenic supplements) are added to the culture media.[5] We hypothesized that the differentiation toward the osteogenic lineage of hUCMSCs could be synergistically enhanced by the treatment with the synthetic peptides when combined with differentiation media or it could even be directed exclusively by the synthetic peptides. To address this hypothesis, hUCMSCs were treated with the different synthetic peptides for 1, 3, and 14 days in both the presence and absence of osteogenic supplements. The osteoinductivity and potential synergistic effects were evaluated by cell proliferation, gene expression of osteogenic markers, and bone morphogenetic protein-2 (BMP-2) secretion to the culture media.

Materials and Methods

Peptide design

The precise selection of the proline-rich regions from amelogenin and ameloblastin was described in details in a previous study.[2] We designed our peptides with constraints on length (25 AA), conservation of proline positions, and with systematic variation of other composing amino acids (Table 1).

3D models of the designed peptides

The designed peptides (P2, P4, P5, and P6) should differ in their physical, chemical, and structural properties due to the different amino acid compositions, except the conserved proline positions in the sequence. We utilized a recently developed Web-based method of peptide design[6] to explore possible correlation between the structure and biological response to the particular peptide. The sequences of three designed peptides were modeled by MOBYLE server[7] and only the best energy conformer of each peptide was used for further analysis and optimization. The three resulted peptides and their structural and dynamical properties were explored by molecular dynamic simulations (MD) by means of AMBER 9.0 package[8] using ff99SB force field[9] in TIP3[10] explicit water environment. MD simulations were performed according to the following conditions: dielectric constant eps ~ r, 508 solvent molecules, equilibration–100ps (0–300K), production phase–500ps, and NPA Hamiltonian equations of motion.

Preparation of peptides and enamel matrix derivative

Enamel matrix derivative (EMD) was kindly supplied by Straumann GMbH (Basel, Switzerland). EMD was dissolved to 10 mg/mL in 0.1% acetic acid in phosphate-buffered saline (PBS). Aliquots were prepared and stored at −20°C until use. Four synthetic peptides (Table 1) were designed and purchased from Eurogentec (Seraing, Belgium). One vial containing 10–21 mg of the selected synthetic peptides was delivered in a freeze-dried pellet form and dissolved to 5 mg/mL in 0.1% acetic acid in PBS. Final concentrations of 50 μg/mL of EMD and peptides were used to assay their effect on cytotoxicity, proliferation, and differentiation of hUCMSCs cells in an *in vitro* system.

hUCMSCs isolation

hUCMSCs were isolated from umbilical cords obtained in the process of human umbilical cord blood donation under the Concordia Cord Blood Donation Program. The samples were obtained after informed consent and with the approval of the Ethical Committee of Balearic Islands (CEIC-IB). To isolate hUCMSCs, the cord was rinsed several times with sterile saline, the cord blood was drained, and clots flushed from the vessels. Next, the cord was cut into small pieces and incubated with 0.075% collagenase type IA (Sigma, St Louis, MO) for 2 h. Then, 0.125% trypsin was added for 30 min with gentle agitation at 37°C. The digested mixture was then passed through a 100 μm filter to obtain cell suspensions. Cell pellets were resuspended in NH4Cl-based erythrocyte lysis buffer, incubated for 10 min at room temperature, and washed in PBS. Finally, the cells were resuspended in Dubelcco's modified Eagle's medium with low glucose and Glutamax (DMEM-LG; Gibco, Grand Island, NY) and 20% FBS (HyClone, Thermo Scientific, Logan, UT) and plated in noncoated 25 cm^2 cell culture flask. Cultures were maintained in a humidified atmosphere with 5% CO_2 at 37°C. After 3 days of culture, the medium was replaced and nonadherent cells were removed. The medium was changed twice weekly thereafter. Once 80% confluence had been reached, adherent cells were replated at a density of 1×10^4 cells/cm^2.

Cell surface profile of the hUCMSCs used for the studies was confirmed by standard flow cytometry as previously

TABLE 1. AMINOACIDIC SEQUENCE OF SYNTHETIC PROLINE-RICH PEPTIDES

Peptide	Sequence (N-terminus to C-terminus)	Polar aminoacids	Hydrophobic aminoacids
P2	PLVPSQPLVPSQPLVPSQPQPPLPP	7 (S,Q)	18 (P,L,V)
P4	PLVPSSPLVPSSPLVPSSPSPPLPP	7 (S)	18 (P,L,V)
P5	PLVPSSPLVPCCPLVPCCPSPPLPP	3 (S)	22 (P,L,V,C)
P6	PHQPMQPQPPVHPMQPLPPQPPLPP	7(H,Q)	18 (P,M,V,L)

P2, Peptide 2; P4, Peptide 4; P5, Peptide 5; P6, Peptide 6; S, Ser; P, Pro; L, Leu; V, Val; Q, Gln; M, Met; H, His; C, Cys.

described[2]; cells did not express CD34, CD45, CD31, and HLA-DR, whereas were positive for CD105, CD90, and CD73, showing a typical profile of MSCs.[11]

Cell culture

hUCMSCs were seeded in 24-well plates and grown to confluence in a "growing media" consisting of DMEM/Glutamax/LG, supplemented with penicillin (50 IU/mL), streptomycin (50 μg streptomycin/mL), and 20% fetal bovine serum (HyClone). Cells were cultured at 37°C in a 95% air–5% CO_2 atmosphere.

At confluence (designated as day 0), cells were treated with 0.1% acetic acid-PBS (control), with synthetic peptides (50 μg/mL) or with EMD (50 μg/mL), either in "growing media" or in "differentiation media" consisting of growing media supplemented with hydrocortisone (200 nM), ascorbic acid (50 μg/mL), and β-glycerophosphate (10 mM). Media were replaced every Monday and Thursday. Treatments were added after changing the media to keep the concentration of peptides and EMD in solution throughout the whole experiment. Culture media were collected after 1 day of treatment to test cytotoxicity, and after 14 days to analyse BMP-2 release. Cells were harvested at days 1, 3, and 14 to analyze gene expression of several osteoblast differentiation markers using real-time reverse transcriptase–polymerase chain reaction (RT-PCR).

Determination of cell viability: lactate dehydrogenase activity

Lactate dehydrogenase (LDH) activity in the culture media was used as an index of cell death. LDH activity was determined spectrophotometrically after 30 min incubation at 25°C of 100 μL of culture and 100 μL of the reaction mixture by measuring the oxidation of nicotinamide adenine dinucleotide (NADH) at 490 nm in the presence of pyruvate, according to the manufacturer's kit instructions (Roche Diagnostics, Mannheim, Germany). Results were presented relative to the LDH activity in the medium of cells cultured in growing media and treated with 0.1% acetic acid-PBS (low control, 0% of cell death) and of cells treated with triton X-100 1% (high control, 100% of death), using the equation:

$$\text{Cytotoxicity } (\%) = (\text{exp.value} - \text{low control})/ (\text{high control} - \text{low control}) \times 100.$$

Cell proliferation

Proliferation rate was analyzed after the incorporation of bromodeoxyuridine (BrdU) as described by the manufacturer (Roche Diagnostics). To test the effect of the different synthetic peptides and EMD on cell proliferation, 2×10^3 cells were seeded in each well (96-well plates) for 24 h. After cell attachment, culture medium was changed and different treatments peptide/EMD (50 μg/mL) and BrdU were added to the wells. Cells were cultured for additional 4 days to allow the incorporation of BrdU to the proliferating cells. Media were replaced every Monday and Thursday. Treatments and BrdU were added after changing the media to keep the concentration of peptides and EMD in solution throughout the whole experiment. Values were expressed as a percentage of control cells, which were set to 100%.

RNA isolation and RT-PCR analysis

Total RNA was isolated using the NucleoSpin® TriPrep kit (Macherey-Nagel), following the instructions of the manufacturer. Total RNA was quantified at 260 nm using a Nanodrop spectrophotometer (NanoDrop Technologies, Wilmington, DE).

The same amount of total RNA (0.27 μg) from each sample was reverse transcribed to cDNA using High Capacity RNA-to-cDNA kit (Applied Biosystems, Foster City, CA) according to the protocol of the supplier. Each cDNA was diluted and aliquots were stored at −20°C until the PCR reactions were carried out.

Real-time PCR was performed using the LightCycler FastStart DNA Master PLUS SYBR Green I (Roche Diagnostics) following the manufacturer's instructions. Real-time PCR was done for two reference genes: glyceraldehyde-3-phosphate dehydrogenase (GAPDH) and β-actin, and five target genes: collagen type I (COLL-I), alkaline phosphatase (ALP), runt-related transcription factor 2, (RUNX2), decorin (DCN), and osteocalcin (OC). A negative control without cDNA template was run in each assay. Each reaction contained 500 nM of the corresponding oligonucleotide primers (h-β-actin-F: 5′-AAGGGACTTCCTGTAACAATGCA-3′; h-β-actin-R: 5′-CTGGAACGGTGAAGGTGACA-3′; h-GAPDH-F: 5′-TGCACCACC-AACTGCTTAGC-3′; h-GAPDH-R: 5′-GG CATGGACTGTGGTCATGAG-3′; h-COLL-I-F: 5-CCTGACG CACGGCCAAGAGG-3′; h-COLL-I-R: 5′- GGCAGGGCT CGGGTTTCCAC-3′; h-ALP-F: 5′-CCGCTATCCTGGCTCCG TGC-3′; h-ALP-R: 5′-GGTGGGCTGGCAGTGG-TCAG-3′; h-RUNX2-F: 5′- CTGTGCTCGGTGCTGCCCTC-3′; h-RUNX2-R: 5′- CGTTACCCGC-CATGACAGTA-3′; h-DCN-F: 5′- ATC TCAGCTTTGAGGG-CTCC-3′; h-DCN- R: 5′- GCCTCTCTG TTGAAACGGTC-3′; h-OC-F: 5′-GAAGCCCAGCGGTGCA-3′;h-OC-R: 5′- CACTACCTCGCTGCCCTCC-3′; hWNT7B-F: 5′- TCTGCTTTGGCGTCCTGTACGT-3′; hWNT7B-R: 5′-CCGACTCTGGCAGATGGCACG-3′), 5 μL of LightCycler FastStart DNA Master PLUS SYBR Green I (Roche Diagnostics), and 3 μL of cDNA in a final volume of 10 μL.

The amplification program consisted of a preincubation step for denaturation of the template cDNA (5 min, 95°C), followed by 45 cycles consisting of a denaturation step (10 s, 95°C), an annealing step (10 s, 60°C), and an extension step (10 s, 72°C) for β-actin, GAPDH, COLL-I, DCN, RUNX2, and WNT7B; or followed by 45 cycles consisting of a denaturation step (10 s, 95°C), an annealing step (5 s, 68°C), and an extension step (12 s, 72°C) for ALP and OC. After each cycle, fluorescence was measured at 72°C. A negative control without a cDNA template was run in each assay.

To allow relative quantification after PCR, standard curves were constructed from the standard reactions for each target and housekeeping genes by crossing points (Cp) values, that is, the cycle number at which the fluorescence signal exceeds background, versus log cDNA dilution. The Cp readings for each of the unknown samples were used to calculate the amount of either the target or the reference relative to a standard curve, using the Second Derivative Maximum Method with the LightCycler analysis software 4.0 (Roche Diagnostics). Relative mRNA levels were calculated as the

ratio of relative concentration for the target genes relative to that for the mean between the two reference genes (*GAPDH* and β-actin). Values were expressed as a percentage of control cells cultured in growing media, which were set to 100%.

Release of BMP-2 into the cell culture media

BMP-2 secreted to the culture media after 14 days of treatment was analyzed by enzyme-linked immunosorbent assay (ELISA). Aliquots from the culture media were centrifuged at 1800 rpm for 5 min at 4°C and supernatants were used for BMP-2 determination following instructions described by the manufacturer (Quantikine Immunoassay; R&D Systems, Minneapolis, MN). Total protein in the culture media for each sample was determined using a BCA protein assay kit (Pierce, Rockford, IL) and used for correction of BMP-2 secretion, expressed in pg BMP-2/mg protein.

Statistical analyses

The data were presented as mean values ± standard error of the mean. Differences between groups were assessed by student's *t*-test or by paired *t*-test and using a statistical software package (SPSS, Chicago, IL). Results were considered statistically significant at the *p*-values ≤ 0.05.

Results

Peptide structures

Models of all three new studied peptides showed signature of compact, well packed structures lacking secondary structure elements, as expected due to the rich content of prolines. We hypothesized in our previous paper that the effect of the peptides could be correlated with exposition of their C termini containing conserved proline-rich region (PPLPP). As one can see on the equilibrated structures of the three modeled peptides (Fig. 1), all of them show similar general properties (compactness and C-terminal exposition) and they also share general structural characteristic of their PPLPP region. Peptides 4 and 6 have similar overall topology—two distinct loops making the structures similarly compact. Regarding the compactness (could be measured as radius of gyration) the peptide 5 is not an exception; but it has different topology of loops and makes possible a contact between C an N terminus. All of them (and this is in agreement with previously reported P2 peptide property) expose their terminal PPLPP sequence stretch in a way

suitable for further interactions. They are not exactly in the same conformational state regarding their phi/psi torsions of PPLPP backbone, but it is quite visible that compactness of the molecules helps their C terminus to be conformational, similar, and interacting most probably by the same way. Having neither direct structural evidences about the isolated peptides conformations nor about their modus of interaction we cannot unambiguously state that the described structural features are directly responsible for the effect of the peptides in question, but they seem to be good candidates for explanation of their action.

Cell viability: LDH activity

The LDH activity in the culture media was used as an index of toxicity (Fig. 2). After 24 h of treatment, peptide 2 improved cell viability of hUCMSCs compared with control in both, growing and differentiation media. Although values did not reach statistical significance, all treatments (EMD and peptides) improved cell viability compared with control in both media.

Cell proliferation

The effect on cell proliferation of 4 days of treatment either with EMD or with synthetic peptides was assessed by analyzing the incorporation of BrdU into the cells cultured in growing media (Fig. 3). No differences were found when comparing EMD-treated cells to control cells. Treatment with P2, P4, and P6 reduced cell proliferation compared with control cells. Moreover, P6 showed significant lower proliferation compared with EMD.

mRNA levels of different osteogenic markers

The effect of synthetic peptides or EMD treatment (50 μg/mL) on mRNA levels of different osteogenic markers was analyzed by real-time RT-PCR after 1, 3, and 14 days in hUCMSC cell cultures. Five different osteogenic markers were analyzed (Figs. 4–6), including collagen-I, alkaline phosphatase, *RUNX2*, decorin, and osteocalcin. In addition to the osteogenic markers, *WNT7B* was also analyzed. After short cell treatment, EMD induced higher collagen-I mRNA expression levels than the synthetic peptides in cells cultured in growing media; when cells were cultured in differentiation media, this difference was only seen after 3 days of treatment. No significant differences in collagen-I mRNA levels were found at day 14, nonetheless, although values did not reach statistical significance, EMD treatment in
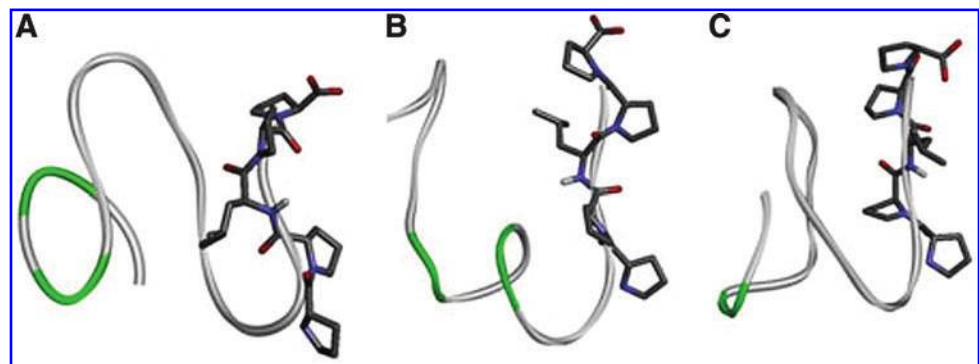

FIG. 1. PepFold predicted 3D structures of **(A)** peptide 4, **(B)** peptide 5, and **(C)** peptide 6. C-terminal sequence of peptides (PPLPP) is accented by using stick representation for corresponding amino acids. Color images available online at www.liebertonline.com/tea
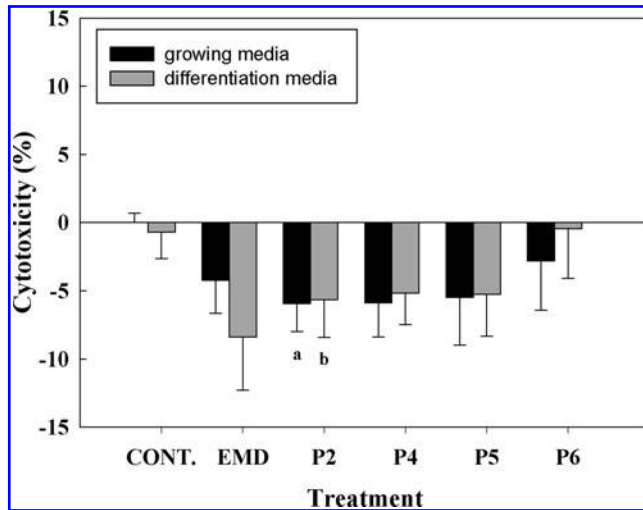
FIG. 2. Lactate dehydrogenase activity measured from culture media collected after treatments with the different peptides (50 μg/mL) or enamel matrix derivative (EMD; 50 μg/mL) for 24 h. Values represent the mean ± standard error of the mean (SEM) ($n = 6$ from three different donors). Paired t-test: (a) $p \leq 0.05$ versus control growing media, (b) $p \leq 0.05$ versus control differentiation media.

growing media induced higher levels of *COLL-I* mRNA expression compared with control and to peptide treatment.

ALP mRNA levels were increased in cells cultured in differentiation media for 3 days for all the treatments compared with growing media, and significantly higher levels were found in cells treated with EMD compared with the control and to P2 and P4. At day 14, EMD treatment induced a higher expression of *ALP* mRNA levels compared with the
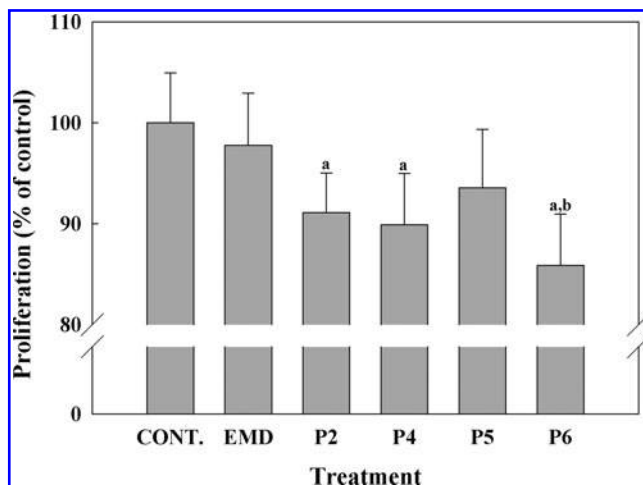
FIG. 3. Proliferation of human umbilical cord mesenchymal stem cells (hUCMSCs) cells incubated with the different peptides (50 μg/mL) or EMD (50 μg/mL) for 4 days. Cell proliferation was measured by bromodeoxyuridine incorporation into the cell for 4 days. Values were expressed as a percentage of control cells, which were set to 100%. Values represent the mean ± SEM ($n = 6$ from three different donors). Paired t-test: (a) $p \leq 0.05$ versus control growing media, (b) $p \leq 0.05$ versus EMD growing media.

control in growing media. No differences were found on *ALP* mRNA levels in cells treated with the different peptides after 14 days of treatment.

RUNX2 mRNA levels were higher in cells cultured with differentiation media for the different days analyzed. At day 3, EMD treatment induced significantly higher levels of *RUNX2* compared with the control and to peptide treatment. Moreover, in cells cultured in growing media EMD treatment for 1 and 3 days induced higher *RUNX2* levels compared with peptide treatment.

After 3 days of treatment, decorin expression showed the same profile as *RUNX2*, showing higher levels in cells cultured in differentiation media and a higher induction in cells treated with EMD compared with control and with peptide treatment. After 14 days of treatment, P5 treatment induced a higher expression of decorin mRNA levels compared with the control in differentiation media. No differences in mRNA levels were found with treatment with any other peptides or with EMD treatment at day 14.

WNT7B mRNA levels were found to be higher in cells cultured in growing media than in cells cultured in differentiation media, mainly after 1 and 3 days of culture. Moreover, after 1 day of treatment a significant reduction of *WNT7B* mRNA levels in cells treated with the peptides compared to cells treated with EMD was found. At day 3, cells cultured in differentiation media and treated with EMD showed higher levels of *WNT7B*, reaching significance when compared with the control and to P5. P6 showed significantly higher mRNA levels compared with the control in differentiation media at days 3 and 14 and lower *WNT7B* mRNA levels compared with EMD in growing media at day 14.

Osteocalcin mRNA was not detected after 1 and 3 days of culture. After 14 days of treatment, all peptides induced a higher expression of osteocalcin mRNA levels compared with the control in differentiation media. No differences were found on osteocalcin mRNA levels in cells treated with EMD compared to the control in any of the media.

Release of BMP-2 into the cell culture media

BMP-2 protein levels in culture media after 14 days of treatment were analyzed by ELISA (Fig. 7). The levels of BMP-2 in cells treated with the synthetic peptides were lower than in cells treated with EMD or control cells. However, statistical significance was only found in cells cultured in growing media for P2 and P5. No differences were found among culture media used with and without osteogenic supplements.

Discussion

In this study, synthetic peptides sharing a common polyproline sequence and the commercially available EMD were investigated for osteoinductive potential of hUCMSCs. hUCMSCs provides a multipotent cell source capable to differentiate into osteoblasts when cultured with osteogenic supplements.[5] In a previous study, we have shown that the peptide 2 variant enhanced the differentiation toward the osteogenic lineage of hUCMSCs. However, the individual effect of the synthetic peptide was not investigated. Thus, to provide a more comprehensive evaluation, the present study aimed to further investigate the ability of synthetic proline-
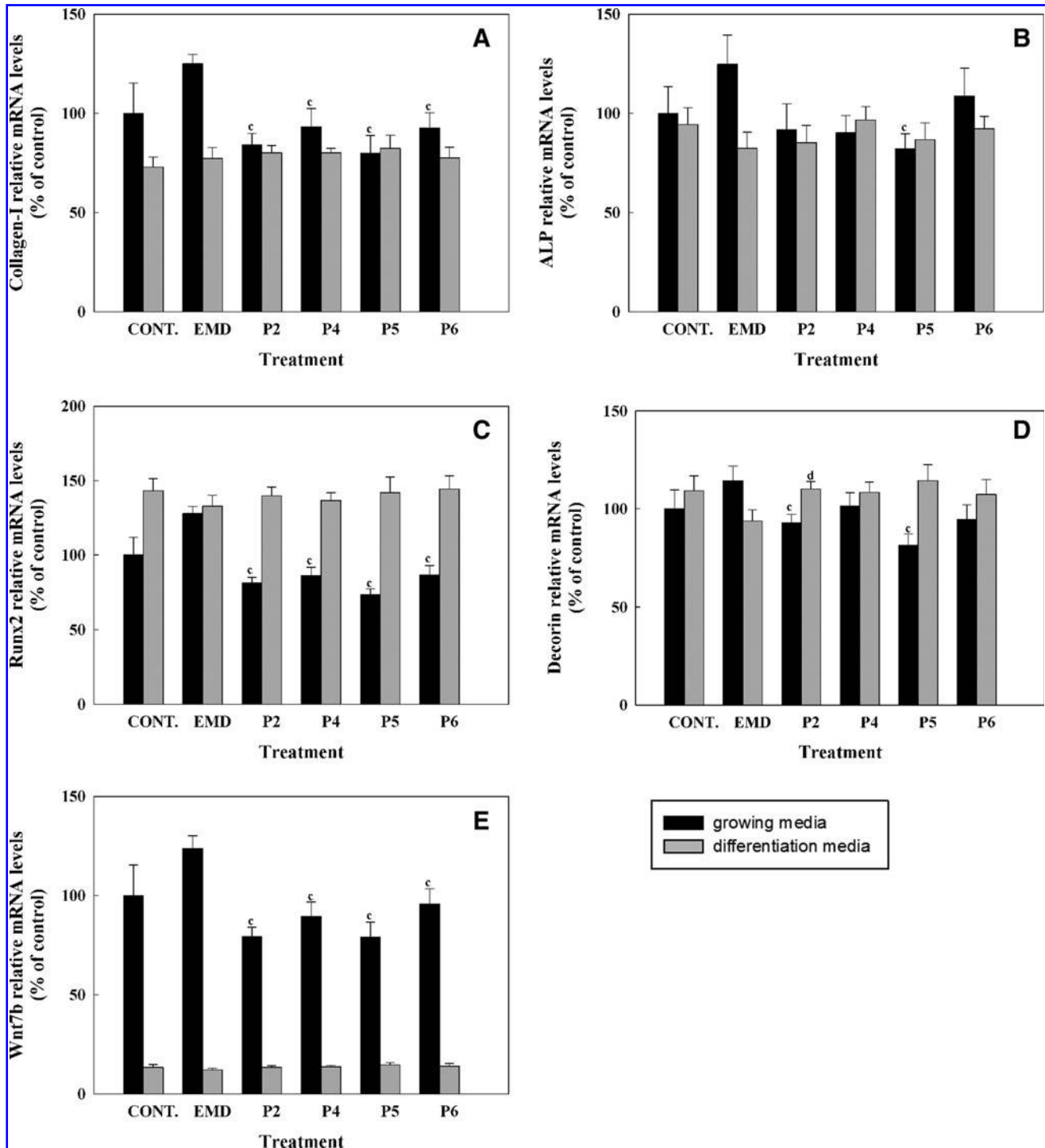
FIG. 4. Gene expression levels of collagen-I **(A)**, alkaline phosphatase **(B)**, runt-related transcription factor 2 (*RUNX2*) **(C)**, decorin **(D)**, and *WNT7B* **(E)** in hUCMSCs treated with the different peptides (50 μg/mL) or EMD (50 μg/mL) for 1 day. Data represent fold changes of target genes normalized with housekeeping genes (glyceraldehyde-3-phosphate dehydrogenase [GAPDH] and β-Actin), expressed as a percentage of control cells in growing media, which were set to 100%. Values represent the mean ± SEM ($n = 6$ from one donor). Student's *t*-test: (c) $p \leq 0.05$ versus EMD growing media, and (d) $p \leq 0.05$ versus EMD differentiation media.

rich peptides and of EMD to promote the osteogenic differentiation of hUCMSCs individually or in combination with osteogenic supplements.

Bone tissue formation, occurs throughout life, and is involved in bone remodeling in adults.[12] Mesenchymal stem cells are the main source of osteoprogenitor cells, being involved in normal skeletal homeostasis[13] and in reparative mechanisms of bone.[14] Since MSCs are directly involved in the bone regenerative process and are capable of propagating along the osteogenic lineage, primary cultures of
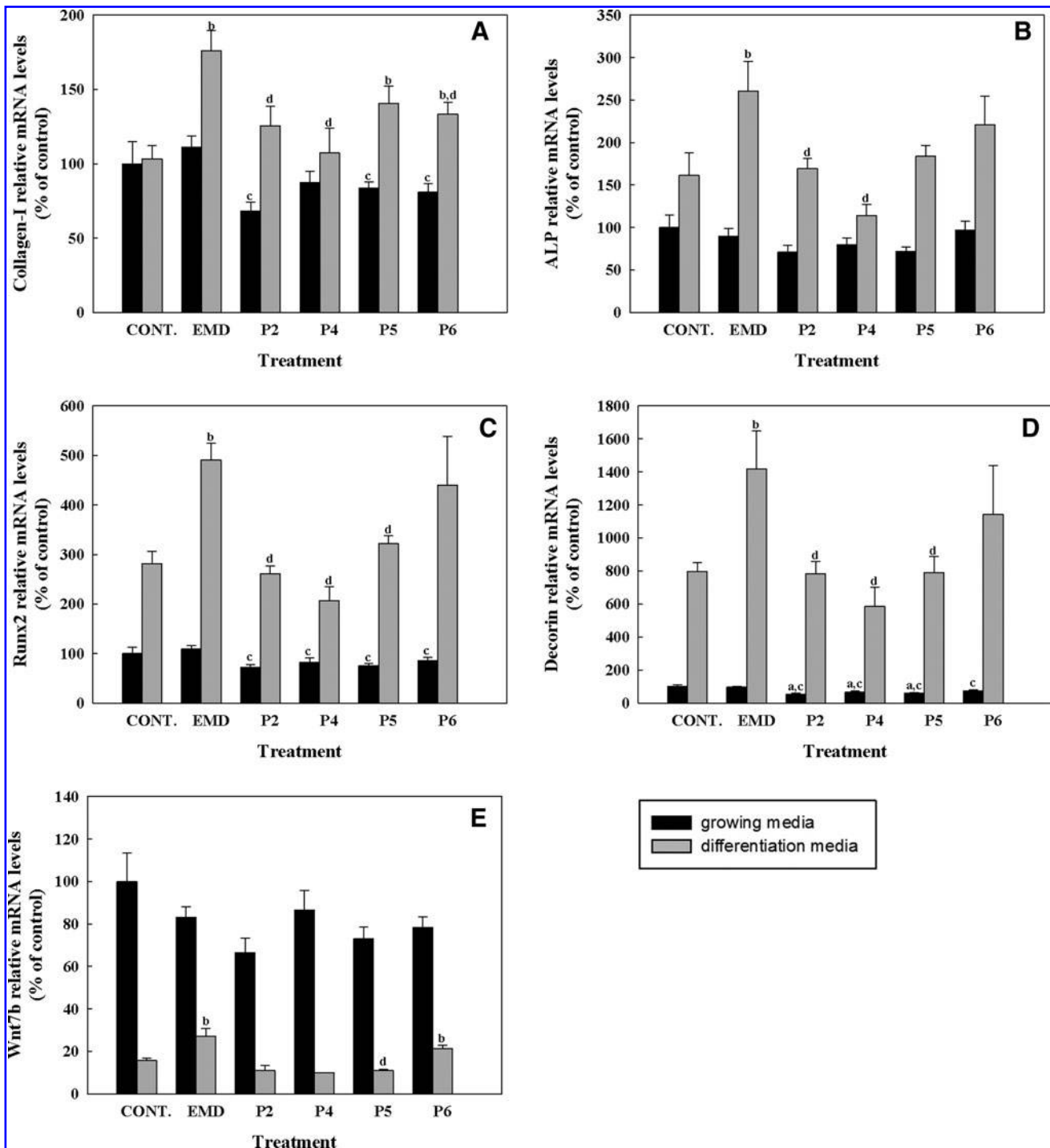
FIG. 5. Gene expression levels of collagen-I **(A)**, alkaline phosphatase **(B)**, *RUNX2* **(C)**, decorin **(D)**, and *WNT7B* **(E)** in hUCMSCs treated with the different peptides (50 μg/mL) or EMD (50 μg/mL) for 3 days. Data represent fold changes of target genes normalized with housekeeping genes (GAPDH and β-Actin), expressed as a percentage of control cells in growing media, which were set to 100%. Values represent the mean ± SEM ($n = 6$ from one donor). Student's *t*-test: (a) $p \leq 0.05$ versus control growing media, (b) $p \leq 0.05$ versus control differentiation media, (c) $p \leq 0.05$ versus EMD growing media, and (d) $p \leq 0.05$ versus EMD differentiation media.

hUCMSCs were chosen for our studies. However, variables among different donors must be taken into account when using primary cells; to overcome this problem and to improve validity of our data, we have used three different donors.

We have previously demonstrated the safety of peptide 2 after short- and long-time *in vitro* cell treatment.[2] Here, we confirmed that the new variants of our consensus peptide evaluated in the present study did not impair cell viability after a short period of treatment. Thus, we can conclude that
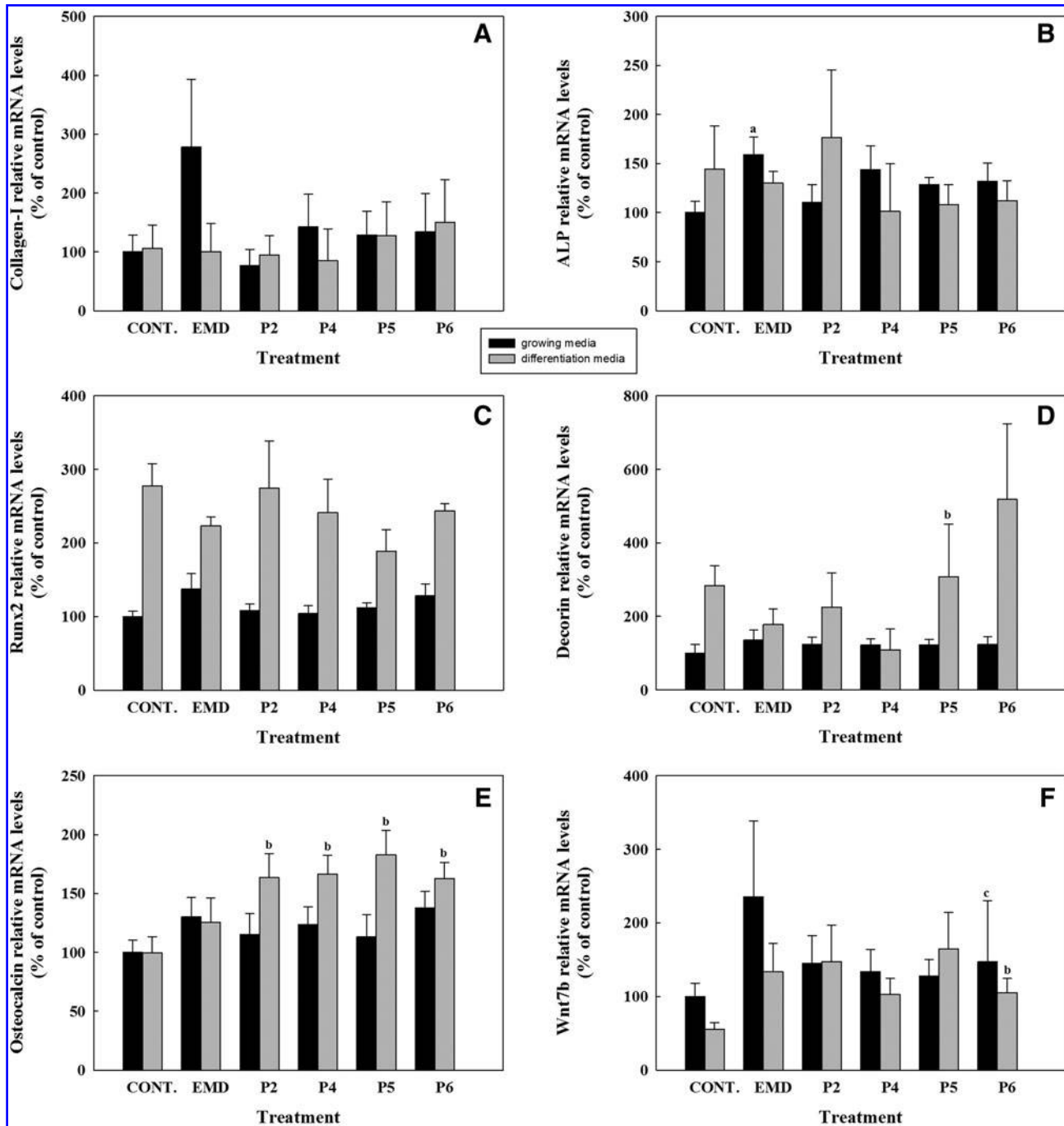
FIG. 6. Gene expression levels of collagen-I **(A)**, alkaline phosphatase **(B)**, runx2 **(C)**, decorin **(D)**, osteocalcin **(E)**, and Wnt7b **(F)** in hUCMSCs treated with the different peptides (50 μg/mL) or EMD (50 μg/mL) for 14 days. Data represent fold changes of target genes normalized with housekeeping genes (GAPDH and β-Actin), expressed as a percentage of control cells in growing media, which were set to 100%. Values represent the mean ± SEM ($n = 6$ from three different donors). Paired t-test: (a) $p \leq 0.05$ versus control growing media, (b) $p \leq 0.05$ versus control differentiation media, (c) $p \leq 0.05$ versus EMD growing media.

the synthetic consensus peptides at a dose of 50 μg/mL are safe regardless of the composition of the non-proline aminoacids.

In consistence with our previous study,[2] treatment with the synthetic peptides reduced cell proliferation compared with untreated cells, while no differences on cell proliferation on cells treated with EMD compared to control were found.

The lack of effect of EMD on cell proliferation might be due to an enhanced cell differentiation, in fact, previous studies have shown that EMD might exert a different effect depending on the maturation state of the cells.[15,16] The effect of EMD on MSCs proliferation has been evaluated in few studies with controversial results; different studies have proved that EMD enhanced proliferation,[17–19] while others
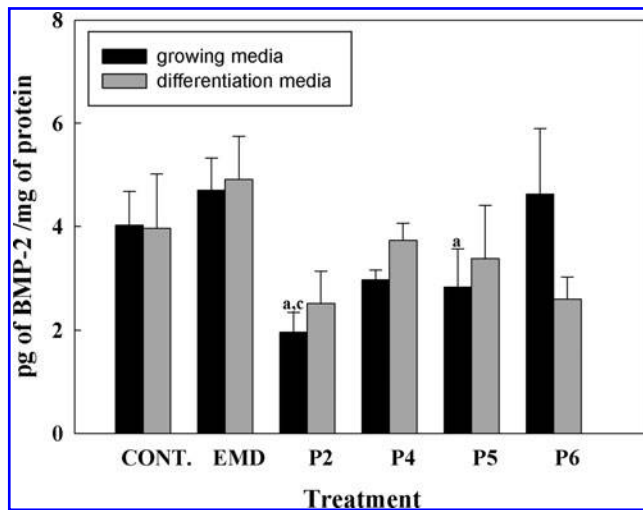
FIG. 7. Bone morphogenetic protein 2 (BMP-2) protein levels in culture media of hUCMSCs treated with the different peptides (50 μg/mL) or EMD (50 μg/mL) for 14 days. Data expressed as pg BMP-2/mg protein. Values represent the mean ± SEM ($n = 6$ from three different donors). Paired t-test: (a) $p \leq 0.05$ versus control growing media, (c) $p \leq 0.05$ versus EMD growing media.

have failed to find EMD-induced differences in terms of cell proliferation.[20] These inconsistencies in results might be due to differences in cell source and differences in experimental designs between different studies.

To investigate the osteoinductivity of the synthetic peptides and of EMD, we analyzed the expression of different osteoblast markers of hUCMSCs after 1, 3, and 14 days of treatment in the presence and absence of osteogenic supplements in the culture media. Five different marker genes were analyzed, including collagen-I, RUNX2, ALP, decorin, and osteocalcin. Higher osteopromotive effect was found for EMD after a short-term treatment of 3 days in cells cultured with osteogenic supplements, since we found higher expression levels of all the early osteoblast markers analyzed compared to both, control and peptide-treated cells.

However, after a long-term treatment of 14 days, this osteopromotive effect of EMD was not found any longer in the presence of osteogenic supplements, while some osteopromotive effect was observed in cells cultured in growing media. Type I collagen and alkaline phosphatase are considered early markers of differentiation,[21,22] and at day 14 we found that EMD-treated cells cultured without osteogenic supplements had higher expression levels of COLL-1 and ALP than control cells, while no differences were found in cells treated with the synthetic peptides. These results are in agreement with reports from other authors.[18,23–25] Similar response to treatments was found for RUNX2, an osteoblast specific transcription factor,[26] and for decorin, a small leucine rich proteoglycan highly expressed in extracellular bone matrix.[27] In all experimental groups, RUNX2 and decorin mRNA levels were higher when cells were cultured with the osteogenic supplements and no differences were found among treatments, except for P5, that induced decorin expression in cells cultured in differentiation media.

Among the osteoblast markers, osteocalcin—a major noncollagenous protein of bone highly expressed in mature osteoblasts—is currently considered the most specific and the latest of expressed markers, in fact, is the only gene that is only expressed by fully differentiated osteoblasts and regulates their function.[28–30] In fact, at days 1 and 3 osteocalcin mRNA levels were not detected by real-time RT-PCR in hUCMSCs, in the presence or absence of osteogenic supplements in the culture media. We found that treatment with any of the synthetic peptides increased osteocalcin mRNA levels but only when cells were stimulated with the osteogenic supplements after 14 days of treatment. No significant differences were found on osteocalcin expression levels in cells treated with EMD, in accordance to other reports.[17,18] The finding that the synthetic peptides induce an increase in osteocalcin mRNA levels indicates that cells are at a more mature stage of the differentiation process. Moreover, the relevance of this gene has been demonstrated in a recent *in vivo* study, in which osteocalcin was found to be the best predictive marker for osseointegration of titanium implants (Monjo *et al.* submitted).

Osteocalcin results indicate that although the synthetic peptides are not osteoinductive in hUCMSCs, they are osteopromotive in combination with osteogenic supplements after long-term treatment. These results, together with our previous observations[2] suggest a different mechanism of action for the synthetic peptides and EMD. Here, we have observed that EMD is osteopromotive after short-term treatment in cells cultured with osteogenic supplements, while after long-term treatment some osteopromotive effect is seen in cells cultured in growing media. It would be possible that longer EMD treatment than 14 days could induce the osteogenic differentiation of hUCMSCs in the absence of osteogenic supplements. On the other hand, synthetic peptides have shown an osteopromotive effect in combination with osteogenic supplements after long-term treatment.

Since it has recently been shown that platelet-released supernatant stimulates mesenchymal stem cell differentiation toward an osteoblastic phenotype, and that this effect could be mediated by BMP-2 through the Wnt-signaling pathway,[31] we analyzed BMP-2 secretion of hUCMSCs and WNT7B mRNA expression levels to test whether the synthetic peptides or EMD would exert their action through a similar mechanism. The obtained results are not conclusive, though we observe higher WNT7B mRNA expression levels in cells treated with EMD and cultured in growing media after 1 or 14 days of treatment and in cells cultured in osteogenic supplemented media after 3 days of treatment. Moreover, these data correlate with higher levels of BMP-2 secretion after 14 days of treatment. The finding that WNT7B mRNA expression levels were higher in cells cultured in the absence of the osteogenic supplements is in agreement with the reported observation that the canonical Wnt signaling maintains an undifferentiated proliferative state of MSCs.[32]

Consistent with the similar structural properties of the different synthetic peptides evaluated in this study, no differences have been found in the activity among them. In agreement with previously reported P2 peptide property,[2] all of the synthetic peptides exposed their PPLPP stretch in a way suitable for interactions. The short sequence of PPXPP in the C-terminal region of peptides has been shown to

participate in the transactivation activity of transcription factors and/or co-activators.[33,34] We have previously hypothesized that the mode of action of the synthetic peptides might involve interaction with a receptor capable of influencing intracellular signaling cascades, and that the accessibility and structural rigidity of this short consensus sequence (PPXPP) may be of importance in the signaling activity of our synthetic peptides. Actually, we are currently evaluating the significance of the PPLPP motif in the osteopromotive effect of the designed synthetic peptides and we expect to clarify its biological importance in future works.

Our findings that synthetic polyproline-rich peptides promote osteogenic differentiation of hUCMSCs after long-term treatment are relevant in the development of new treatments for tissue regeneration that could be more cost effective. The use of natural proteins like EMD in tissue engineering and regenerative medicine has some associated disadvantages including immunogenicity, relatively high cost, large molecular weight (100–200 amino acids), instability *in vivo*, and difficulty in sterilization. In contrast, synthetic peptides could be advantageous due to their ease of synthesis and handling, and their low immunogenic activity.

Conclusion

Osteogenic differentiation of hUCMSCs is promoted by EMD after short-term treatment. In contrast, synthetic polyproline-rich peptides promote osteogenic differentiation of hUCMSCs after long-term treatment regardless of the composition of the non-proline aminoacids spacing the proline motifs.

Acknowledgment

Disclosure Statement

No competing financial interests exist.

References

1. Jin, T., Ito, Y., Luan, X., Dangaria, S., Walker, C., Allen, M., *et al.* Elongated polyproline motifs facilitate enamel evolution through matrix subunit compaction. PLoS Biol **7**, e1000262, 2009.
2. Rubert, M., Ramis, J.M., Vondrasek, J., Gayà, A., Lyngstadaas, S.P., and Monjo, M. Synthetic peptides analogue to enamel proteins promote osteogenic differentiation of MC3T3-E1 and mesenchymal stem cells. J Biomater Tissue Eng **1**, 198, 2011.
3. Kokubo, T., Ishibashi, O., and Kumegawa, M. Role of proteases in osteoclastic resorption. In: Zaidi, M., Adebanjo, O.A., and Huang, C.L.H., eds. Advances in Organ Biology. Molecular and Cellular Biology of Bone. Stamford, CT: Elsevier, 1998, p. 359.
4. Vallee, A., Humblot, V., and Pradier CM. Peptide interactions with metal and oxide surfaces. Acc Chem Res **43**, 1297, 2010.
5. Jaiswal, N., Haynesworth, S.E., Caplan, A.I., and Bruder, S.P. Osteogenic differentiation of purified, culture-expanded human mesenchymal stem cells *in vitro*. J Cell Biochem **64**, 295, 1997.
6. Maupetit, J., Derreumaux, P., and Tuffery, P. A fast method for large-scale *de novo* peptide and miniprotein structure prediction. J Comput Chem **31**, 726, 2010.
7. Maupetit, J., Derreumaux, P., and Tuffery, P. PEP-FOLD: an online resource for *de novo* peptide structure prediction. Nucleic Acids Res **37**, W498, 2009.
8. Cornell, W.D., Cieplak, P., Bayly, C.I., Gould, I.R., Merz, K.M., Ferguson, D.M., *et al.* A second generation force field for the simulation of proteins, nucleic acids, and organic molecules. J Am Chem Soc **117**, 5179, 1995.
9. Hornak, V., Abel, R., Okur, A., Strockbine, B., Roitberg, A., and Simmerling, C. Comparison of multiple Amber force fields and development of improved protein backbone parameters. Proteins **65**, 712, 2006.
10. Jorgensen, W.L., Chandrasekhar, J., Madura, J.D., Impey, R.W., and Klein, M.L. Comparison of simple potential functions for simulating liquid water. J Chem Phys **79**, 926, 1983.
11. Dominici, M., Le Blanc, K., Mueller, I., Slaper-Cortenbach, I., Marini, F., Krause, D., *et al.* Minimal criteria for defining multipotent mesenchymal stromal cells. The International Society for Cellular Therapy position statement. Cytotherapy **8**, 315, 2006.
12. Duplomb, L., Dagouassat, M., Jourdon, P., and Heymann, D. Concise review: embryonic stem cells: a new tool to study osteoblast and osteoclast differentiation. Stem Cells **25**, 544, 2007.
13. Deschaseaux, F., Sensebe, L., and Heymann, D. Mechanisms of bone repair and regeneration. Trends Mol Med **15**, 417, 2009.
14. Bielby, R., Jones, E., and McGonagle, D. The role of mesenchymal stem cells in maintenance and repair of bone. Injury **38 Suppl 1,** S26, 2007.
15. Sculean, A., Schwarz, F., Becker, J., and Brecx, M. The application of an enamel matrix protein derivative (Emdogain) in regenerative periodontal therapy: a review. Med Princ Pract **16**, 167, 2007.
16. Bosshardt, D.D. Biological mediators and periodontal regeneration: a review of enamel matrix proteins at the cellular and molecular levels. J Clin Periodontol **35**, 87, 2008.
17. Guida, L., Annunziata, M., Carinci, F., Di Feo, A., Passaro, I., and Oliva, A. *In vitro* biologic response of human bone marrow stromal cells to enamel matrix derivative. J Periodontol **78**, 2190, 2007.
18. Jue, S.S., Lee, W.Y., Kwon, Y.D., Kim, Y.R., Pae, A., and Lee, B. The effects of enamel matrix derivative on the proliferation and differentiation of human mesenchymal stem cells. Clin Oral Implants Res **21**, 741, 2010.
19. Keila, S., Nemcovsky, C.E., Moses, O., Artzi, Z., and Weinreb, M. *In vitro* effects of enamel matrix proteins on rat bone marrow cells and gingival fibroblasts. J Dent Res **83**, 134, 2004.
20. van den Dolder, J., Vloon, A.P., and Jansen, J.A. The effect of Emdogain on the growth and differentiation of rat bone marrow cells. J Periodontal Res **41**, 471, 2006.

21. Aubin, J.E. Advances in the osteoblast lineage. Biochem Cell Biol **76,** 899, 1998.
22. Stein, G.S., Lian, J.B., Stein, J.L., Van Wijnen, A.J., and Montecino, M. Transcriptional control of osteoblast growth and differentiation. Physiol Rev **76,** 593, 1996.
23. He, J., Jiang, J., Safavi, K.E., Spangberg, L.S., and Zhu, Q. Emdogain promotes osteoblast proliferation and differentiation and stimulates osteoprotegerin expression. Oral Surg Oral Med Oral Pathol Oral Radiol Endod **97,** 239, 2004.
24. Jiang, J., Fouad, A.F., Safavi, K.E., Spangberg, L.S., and Zhu, Q. Effects of enamel matrix derivative on gene expression of primary osteoblasts. Oral Surg Oral Med Oral Pathol Oral Radiol Endod **91,** 95, 2001.
25. Reseland, J.E., Reppe, S., Larsen, A.M., Berner, H.S., Reinholt, F.P., Gautvik, K.M., *et al.* The effect of enamel matrix derivative on gene expression in osteoblasts. Eur J Oral Sci **114 Suppl 1,** 205, 2006.
26. Ducy, P. Cbfa1: a molecular switch in osteoblast biology. Dev Dyn **219,** 461, 2000.
27. Waddington, R.J., Roberts, H.C., Sugars, R.V., and Schonherr, E. Differential roles for small leucine-rich proteoglycans in bone formation. Eur Cell Mater **6,** 12, 2003.
28. Desbois, C., Hogue, D.A., and Karsenty, G. The mouse osteocalcin gene cluster contains three genes with two separate spatial and temporal patterns of expression. J Biol Chem **269,** 1183, 1994.
29. Ducy, P., Desbois, C., Boyce, B., Pinero, G., Story, B., Dunstan, C., *et al.* Increased bone formation in osteocalcin-deficient mice. Nature **382,** 448, 1996.
30. Hauschka, P.V., Lian, J.B., Cole, D.E., and Gundberg, C.M. Osteocalcin and matrix Gla protein: vitamin K-dependent proteins in bone. Physiol Rev **69,** 990, 1989.
31. Verrier, S., Meury, T.R., Kupcsik, L., Heini, P., Stoll, T., and Alini, M. Platelet-released supernatant induces osteoblastic differentiation of human mesenchymal stem cells: potential role of BMP-2. Eur Cell Mater **20,** 403, 2010.
32. Baksh, D., Boland, G.M., and Tuan, R.S. Cross-talk between Wnt signaling pathways in human mesenchymal stem cells leads to functional antagonism during osteogenic differentiation. J Cell Biochem **101,** 1109, 2007.
33. Boelaert, K., Yu, R., Tannahill, L.A., Stratford, A.L., Khanim, F.L., Eggo, M.C., *et al.* PTTG's C-terminal PXXP motifs modulate critical cellular processes *in vitro*. J Mol Endocrinol **33,** 663, 2004.
34. Wang, Z., and Melmed, S. Pituitary tumor transforming gene (PTTG) transforming and transactivation activity. J Biol Chem **275,** 7459, 2000.

Address correspondence to:
Staale Petter Lyngstadaas, B.Eng., D.D.S., Ph.D.
Department of Biomaterials
Institute for Clinical Dentistry
University of Oslo
P.O. Box 1109
Blindern
N-0317 Oslo
Norway

E-mail: spl@odont.uio.no

Paper 3

Evaluation of alginate and hyaluronic acid for their use in bone tissue engineering.

Rubert, M.; Alonso-Sande, M.; Monjo, M.; Ramis, J.M.

ARTICLE

Evaluation of Alginate and Hyaluronic Acid for Their Use in Bone Tissue Engineering

M. Rubert · M. Alonso-Sande · M. Monjo · J. M. Ramis

Abstract In this study, we compared the structural and physicochemical properties of different concentrations of alginate and high molecular weight hyaluronic acid (HA) hydrogels and their biocompatibility and bioactivity after long-term culture with MC3T3-E1 cells. Both hydrogels were biocompatible and supported long-term viability and cell proliferation. Alginate induced higher alkaline phosphatase (ALP) activity levels than HA. Calcium content was increased in concentration dependent manner in cells cultured with alginate compared to control. Culture with HA hydrogels reduced alkaline phosphatase (*Alp*), bone sialoprotein (*Bsp*) and osteocalcin (*Oc*), while alginate increased *Oc* mRNA levels. Unmodified alginate hydrogels supported osteoblast differentiation better than HA hydrogels, suggesting that alginates are more suitable for biomaterial applications in bone tissue engineering.

1 Introduction

Hydrogels have been used in a wide variety of tissue engineering applications [1]. Hydrogels show excellent biocompatibility, probably due to their structural similarity to the macromolecular-based components in the body [2]. Its high, tissue-like water content and porous structure allows the influx of low molecular weight solutes and nutrients crucial to cellular viability, as well as the transport of cellular waste out of the hydrogel [3]. As biomaterials, the use of injectable hydrogels also allows the administration of the material through minimally invasive techniques, to fill any area with a good physical integration into the defect, to incorporate cells or various therapeutic agents (e.g., growth factors) with a facile and homogenous distribution within any defect [4–7]. Therefore, hydrogels have been identified to be suitable as bone and cartilage repair materials because they can be carriers for growth and morphogenetic factors to exert host cell chemotaxis, proliferation, differentiation and new tissue formation at the site of injury or defect [8].

A variety of synthetic or natural polymers have been used in bone tissue engineering as delivery vehicles for cells or growth/morphogenetic factors [e.g., transforming growth factors, bone morphogenetic proteins (BMPs)] [8–10]. Among them, sodium alginate and hyaluronic acid (HA) have been widely used for tissue-engineering approaches, due to excellent biocompatibility and biodegradability [11–13].

Alginate is a linear unbranched polysaccharide composed of 1,4-linked β-D-mannuronic acid (M-block) and α-L-guluronic acid (G-block) [12], extensively studied in tissue engineering, including the regeneration of skin, cartilage, bone, liver and cardiac tissue [11]. It has previously been reported from in vitro studies that modified alginate hydrogels with RGD-sequences [14], with immobilization of osteogenic peptides [15], with BMP-2 [16] or in combination with other polymers [17] support cell attachment, cell proliferation, osteogenic differentiation and mineral deposition [14, 15, 17]. Further, in vivo studies have shown that chitosan–alginate gel alone or encapsulating MSCs and BMP-2 and that alginates with modified-peptides allow cell differentiation and an early calcification in vivo [15, 17, 18].

HA is a natural linear polysaccharide consisting of repeating D-glucuronic acid-β-1,3-*N*-acetyl-D-glucosamine-β-1,4 units

M. Rubert · M. Alonso-Sande · M. Monjo · J. M. Ramis (✉)
Group of Cell Therapy and Tissue Engineering, Research Institute on Health Sciences (IUNICS), University of Balearic Islands, PO Box 07122, Palma de Mallorca, Spain
e-mail: joana.ramis@uib.es

AVS 🍃 Springer

[13, 19]. HA is one of the main components of the extra-cellular matrix present in all connective tissues [20] and involved in a variety of biological functions [5, 21], including direct receptor-mediated effects on cell adhesion, growth and migration [22], as well as acting as a signaling molecule in cell mortality [23], inflammation [24] or wound healing [25]. HA hydrogels have been used as vehicle for delivery of BMP-2 in vitro [5, 8] and in vivo [21], as well for the delivery of biphosphonates [21]. In vitro studies using derivatized hyaluronic acid (Hyffa-11) have shown to support cell attachment and growth, and to induce ALP activity and osteocalcin expression in a murine fibroblast cell line when containing rhBMP-2 [8]. Moreover, when containing bFGF, HA hydrogels enhance calcium deposition, osteopontin and BSP expression and decrease alkaline phosphatase in rat bone marrow stromal cells [26]. In vivo, HA hydrogels containing BMP-2 showed increased bone formation [19, 27].

Although several modified sodium alginate and HA hydrogels have been used as osteogenic bone substitutes, a direct comparison of the effect on osteoblast differentiation of high molecular weight HA and alginate hydrogels has never been reported. The aim of this study was to compare the structural and chemical properties of two natural polymers at different concentrations and their biocompatibility and bioactivity in the pre-osteoblastic cell line MC3T3-E1. The present work demonstrates that alginate hydrogels support osteoblast differentiation better than high molecular weight hyaluronic acid hydrogels, pointing to alginates as a more suitable polymer for biomaterial applications in bone tissue engineering.

2 Materials and Methods

2.1 Preparation of the Hydrogels

Alginate (FMC Biopolymers, Protanal LF200M, Norway) and hyaluronic acid (HA) (Bioibérica, F002103, Mw 800–1,200 kDa, Spain) hydrogels were prepared overnight at 25 °C in Phosphate Buffer Saline (PBS) (240–320 mOsmol/kg) at 1, 2 and 3 % (w/v). Preliminary studies evaluating different media [water, saline solution 0.9 % (w/v) (308 mOsmol/kg), Phosphate Buffer Saline (PBS) (240–320 mOsmol/kg) and culture media] and several alginate concentrations [1, 2, 3, 6 % y 10 % (w/v)], showed that 1, 2 and 3 % alginate dissolved in PBS were the most promising formulations for their use in tissue engineering due to their pH (pH 7.0) and their viscosity values (0.3, 0.6 and 6.8 Pas at 1, 2 and 3 % of alginate concentration respectively) (data not presented).

To evaluate long term stability of the resulting hydrogels, freeze-drying studies were performed. More specifically, 1 mL of polymeric hydrogels (alginate or HA) were frozen at −80 °C, and then freeze-dried during at least 72 h. Final freeze-dried products were dissolved in water by simple agitation with vortex, and their macroscopic aspect evaluated.

2.2 Characterization of the Hydrogels

The effect of polymer concentration, pH and temperature on viscosity of the hydrogels was studied. Viscosities were determined using a R5 spindle and stirring at 200 rpm by using a Visco Star R viscosimeter (JP Selecta, Spain). The studies were performed three times and each sample analyzed in triplicate (n = 9).

The equilibrium swelling ratio (ESR) of the hydrogels was evaluated as follows: 1 mL of alginate or HA hydrogel at different concentrations was incubated in PBS at 37 °C. At prefixed time points (0.5, 1, 3 and 24 h) each sample was centrifuged at $16,000 \times g$ for 15 min. The supernatants were discarded, and the wet gels immediately weighted (Ws). Then, hydrogels were frozen at −80 °C and freeze-dried during at least 72 h. Lyophilized products were weighted again (Wd) in order to determine ESR values following the formula showed below. The experiment was performed in triplicate (n = 3). The swelling ratios of the resulting gels were determined using the following equation: $ESR = (Ws − Wd)/Wd$.

Qualitative determination of the hydrogel structure at each time point of incubation was carried out by scanning electron microscope (SEM, Hitachi S-3400N, Hitachi High-Technologies Europe GmbH, Krefeld, Germany) to evaluate the changes in the gel network and the effects of polymer concentration on the network structure (pore size and pore distribution). Briefly, after prefixed time points, the hydrogels were frozen at −80 °C and freeze-dried during at least 72 h. Samples were then frozen in liquid N_2 to allow an accurate transversal section using a sharp scalpel and observed at 15 kV, 40 Pa and $100\times$ of magnification. Pore size was measured along the largest axis of the pore by using Hitachi S-3400N software in at least two different gels, and two images per gel were scanned.

2.3 Cell Culture

The mouse osteoblastic cell line MC3T3-E1 (DSMZ, Braunschweig, Germany) was maintained in α-MEM (PAA Laboratories GmbH, Pasching, Austria), which contains ascorbic acid (45 μg/ml) and sodium dihydrogen phosphate (140 mg/l), and supplemented with 10 % fetal bovine serum (FBS) (PAA Laboratories GmbH, Pasching, Austria) and antibiotics (100 IU penicillin/ml and 100 μg streptomycin/ml) (PAA Laboratories GmbH, Pasching, Austria) under standard cell culture conditions (at 37 °C in a

humidified atmosphere of 5 % CO_2). Cells were subcultured 1:10 before reaching confluence using PBS and trypsin/EDTA.

Cells were seeded onto polyethylene terephthalate (PET) membrane inserts with a pore size of 1 μm (1×10^4 cells/membrane) (Millipore Corporation, Billerica, MA, USA) and were maintained in α-MEM supplemented with 10 % FBS and antibiotics (Fig. 1). After cells reached confluence, alginate or HA hydrogels at different concentrations were added on cells and culture media was added at the basolateral side. In the control group, PBS was added on cells growing on PET membrane inserts instead of hydrogel. Media was changed every 2–3 days in the basolateral side. After 24 h, culture media was collected to test cytotoxicity (LDH activity). Cells were harvested at day 21 and the number of cells, gene expression of osteoblast differentiation markers, calcium content and ALP activity were analysed.

2.4 Cell Morphology by Confocal Microscopy

To validate viability of cells growing in contact to alginate, cell morphology after 24 h of incubation with alginate hydrogel was observed by confocal microscopy (Leica TCS SPE Microsystems Wetzlar GmbH, Wetzlar, Germany). Briefly, 0.5 mL of cell suspension (20,000 cells/well) were seeded on 24 well plates, and cultured for 24 h before treatment. Then, culture media was replaced by a mixture (50:50) of culture media/1 % or 2 % (w/v) alginate hydrogel in PBS, and incubated for additional 24 h. Next, the monolayers were stained with FITC-phalloidin (P5282, Sigma Aldrich, St. Quentin Fallavier, Germany) and DAPI (F6057 St. Quentin Fallavier, Germany).

2.5 Cell Viability Determination

LDH activity in the culture media was used as an index of cell toxicity. The activity of the cytosolic enzyme was

estimated according to the manufacturer's kit instructions (Roche Diagnostics, Mannheim, Germany), by assessing the rate of oxidation of NADH at 490 nm in presence of pyruvate. Results from all the samples were presented relative to the LDH activity in the medium of cells treated with PBS (low control, 0 % of cell death) and of cells treated with PBS containing 1 % Triton X-100 (high control, 100 % cell death). The percentage of LDH activity was calculated using the following equation: Cytotoxicity (%) = (exp.value − low control)/ (high control − low control) × 100.

2.6 ALP Activity Determination

In order to compare the effect of different hydrogels on osteoblast differentiation, ALP activity was quantified from cell monolayers after 21 days of cell culture. Briefly, hydrogels were discarded and cells were washed twice in PBS and solubilised with 0.1 % Triton X-100. Then, samples were incubated with an assay mixture of p-Nitrophenyl Phosphate (pNPP). Cleavage of pNPP (Sigma, Saint Louis, Missouri, USA) in a soluble yellow end product which absorbs at 405 nm was used to assess ALP activity. In parallel to the samples, a standard curve with calf intestinal alkaline phosphatase (CIAP) (Promega, Madison, USA) was constructed; 1 μl from the stock CIAP was mixed with 5 ml of alkaline phosphatase buffer (1:5,000 dilution), and subsequently diluted 1:5.

2.7 Calcium Content Determination

Total calcium content was quantified after 21 days of cell culture. Cells were washed twice in PBS and solubilised with 0.1 % Triton X-100. Lysates were also treated with 0.5 N hydrochloric acid overnight, followed by centrifugation at $500 \times g$ for 2 min for the subsequent determination of Ca^{2+} content in the supernatant by inductively coupled plasma optical emission spectrometer (ICP-OES) Optima 5300 DV (PerkinElmer, Massachusetts, USA). Data were compared with $CaCl_2$ standards included in the assay.

2.8 Cell Number Determination

To assess the effect of the hydrogels on cell number, the DNA content after 21 days of cell culture was determined. DNA content was isolated using Tripure® (Roche Diagnostics, Mannheim, Germany), according to the manufacturer's protocol. DNA pellets were dissolved using TE buffer and quantified at 260 nm using a Nanodrop spectrophotometer (NanoDrop Technologies, Wilmington, DE, USA). The number of cells was calculated taking into account that 5.4 μg of DNA are equivalent to 1×10^6 murine cells.
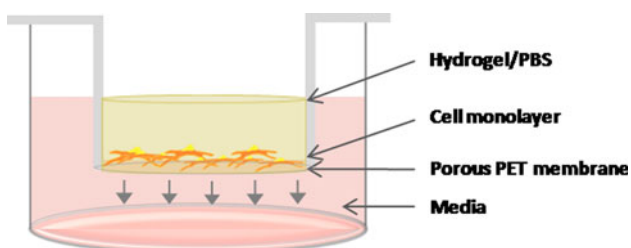

Fig. 1 Schematical drawing showing experimental setup with the MC3T3-E1 cells seeded onto polyethylene terephthalate (PET) membrane inserts and the addition of hydrogel or PBS to the different experimental groups analyzed in the study. Also indicated is the outer compartment with the cell culture media that was changed every 2–3 days in the basolateral side

2.9 RNA Isolation and RT-PCR Analysis

The effect of different types of hydrogels on gene expression was studied after 21 days of culture on pre-osteoblast MC3T3-E1 cells.

Briefly, hydrogels were discarded and total RNA was extracted using Tripure®, following the manufacturer's protocol. Total RNA was quantified at 260 nm using a nanodrop spectrophotometer and 350 ng of RNA were reverse transcribed to cDNA at 37 °C for 60 min using High Capacity RNA-to-cDNA kit (Applied Biosystems, Foster City, CA), according to the protocol of the supplier. Aliquots of each cDNA were frozen (-20 °C) until the PCR reactions were carried out.

Real-time PCR was performed in the Lightcycler 480® (Roche Diagnostics, Mannheim, Germany) using SYBR green detection. Real time PCR was done for two reference genes [18S and glyceraldehyde-3-phosphate dehydrogenase (Gapdh)] and three target genes [bone sialoprotein (Bsp), alkaline phosphatase (Alp) and osteocalcin (Oc)].

The primer sequences were as follows: 18 s rRNA-F: 5′-GTAACCCGTTGAACCCCATT-3′; 18 s rRNA-R: 5′-CCATCCAATCGGTAGTAGCG-3′; Gapdh-F: 5′-ACCCAGAAGACTGTGGATGG-3′; Gapdh-R: 5′-CACATTGGGGGTAGGAACAC-3′; Bsp-F: 5′-GAAAATGGAGACGGCGATAG-3′; Bsp-R: 5′-ACCCGAGAGTGTGGAAAGTG-3′; Alp-F: 5′-AACCCAGACACAAGCATTCC-3′; Alp-R: 5′-GAGAGCGAAGGGTCAGTCAG-3′; Oc-F: 5′-CCGGGAGCAGTGTGAGCTTA-3′; Oc-R: 5′-TAGATGC-GTTTGTAGGCGGTC-3′.

Each reaction contained 7 µl Lightcycler-FastStart DNA MasterPLUS SYBR Green I (containing Fast Start Taq polymerase, reaction buffer, dNTPs mix, SYBRGreen I dye and MgCl2), 0.5 µM of each, the forward and the reverse specific primers and 3 µl of the cDNA dilution in a final volume of 10 µl. The amplification program consisted of a preincubation step for denaturation of the template cDNA (10 min 95 °C), followed by 45 cycles consisting of a denaturation step (10 s 95 °C), an annealing step (8–10 s 60 °C, except for Alp that was 8 s 65 °C) and an extension step (10 s 72 °C). After each cycle, fluorescence was measured at 72 °C (λex 470 nm, λem 530 nm). A negative control without cDNA template was run in each assay.

Real-time efficiencies were calculated from the given slopes in the LightCycler 480 software using serial dilutions, showing all the investigated transcripts high real-time PCR efficiency rates, and high linearity when different concentrations are used. PCR products were subjected to a melting curve analysis on the LightCycler and subsequently 2 % agarose/TAE gel electrophoresis to confirm amplification specificity, Tm and amplicon size, respectively.

Relative quantification after PCR was calculated by dividing the concentration of the target gene in each sample by the mean of the concentration of the two reference genes in the same sample using the Advanced relative quantification method provided by the LightCycler 480 analysis software version 1.5 (Roche Diagnostics, Mannheim, Germany).

2.10 Statistical Analyses

Data are presented as mean values $\pm$ SEM or mean values $\pm$ SD. A Kolmogorov–Smirnov test was done to assume parametric or non-parametric distributions for the normality tests; differences between groups were assessed by Mann–Whitney-test or by Student t test depending on their normal distribution. SPSS® program for windows (Chicago, IL), version 17.0 was used. Results were considered statistically significant at p values ≤ 0.05.

3 Results

3.1 Characterization of the Hydrogels

Table 1 shows the effect of temperature and concentration of the alginate and HA hydrogels on viscosity values. Both polymers studied showed a significant increase on viscosity values in parallel to higher polymer concentrations. In addition, a significant reduction of the viscosity values was observed with higher temperatures, except for alginate 2 % where, although a decrease in viscosity was obtained at 37 °C compared to 25 °C, data did not reach statistical significance. Similar pH values were obtained in alginate hydrogels either at 1 and 2 % of polymer concentration; significant lower pH values were found for higher polymer concentrations for all the HA hydrogels tested in this study.

3.2 Swelling Studies of Alginate and HA Hydrogels

Quantitative ESR and pore size results of freeze-dried 1 and 2 % alginate and HA hydrogels are shown in Fig. 2a. Swelling happened immediately after dilution in PBS at 37 °C for any of the polymers and for any of the concentrations studied. The ESR capacity was higher in 1 % alginate compared to 1 % HA at any of the time points studied. However, when comparing differences on ESR capacity between both hydrogels at a concentration of 2 %, only after 3 h of incubation with PBS the ERS was significantly higher in 2 % alginate compared to 2 % HA. Further, whereas no differences in ERS were observed when comparing alginate polymer concentration at the different time points tested, an increase in HA polymer concentration was associated with significantly higher swelling capacity at any of the time points tested.

Table 1 Characterization of alginate and hyaluronic acid (HA) hydrogels

Polymer concentration	Alginate		HA	
	1 %	2 %	1 %	2 %
pH	7.10 ± 0.053	7.06 ± 0.049	7.30 ± 0.017	6.72 ± 0.032[a]
Viscosity at 25 °C (Pas)	0.324 ± 0.061	0.639 ± 0.080[a]	0.107 ± 0.020	0.966 ± 0.238[a]
Viscosity at 37 °C (Pas)	0.186 ± 0.040[b]	0.507 ± 0.099[a]	0.071 ± 0.019[b]	0.680 ± 0.152[a,b]

pH values of different hydrogels obtained in PBS at 25 °C (n = 3) and viscosimetric measures of alginate and HA hydrogels at 1 and 2 % (w/v) obtained in PBS, at 25 °C and at 37 °C (n = 9). Values represent the mean ± SD. Differences between groups were assessed by Mann–Whitney-test or by Student t test depending on their normal distribution. Results were considered statistically significant at p values ≤ 0.05 for each polymer

[a] 1 versus 2 %

[b] 25 versus 37 °C

a

|	Polymer							
	Alginate				Hyaluronic acid			
	1%		2%		1%		2%	
Time (h)	ESR	Pore Size (µm)	ESR	Pore Size (µm)	ESR	Pore Size (µm)	ESR	Pore Size (µm)
0,5	0,909 ± 0,112	74,5 ± 12,44	0,878 ± 0,091	74,4 ± 15,63	0,193 ± 0,108 [a]	45,8 ± 10,31 [a]	0,891 ± 0,053 [b]	31,2 ± 9,18 [ab]
1	0,896 ± 0,053	75,1 ± 13,50	0,875 ± 0,226	96,5 ± 7,79 [b]	0,084 ± 0,040 [a]	61,2 ± 18,48	0,864 ± 0,155 [b]	48,2 ± 7,33 [a]
3	0,894 ± 0,026	77,7 ± 27,31	0,862 ± 0,061	69,2 ± 17,58	0,157 ± 0,074 [a]	78,5 ± 23,20	0,556 ± 0,087 [ab]	48,1 ± 5,41 [ab]
24	0,857 ± 0,038	120,7 ± 30,00	0,846 ± 0,062	79,5 ± 11,28 [b]	0,149 ± 0,045 [a]	90,7 ± 22,73 [a]	0,726 ± 0,074 [b]	52,9 ± 15,67 [ab]
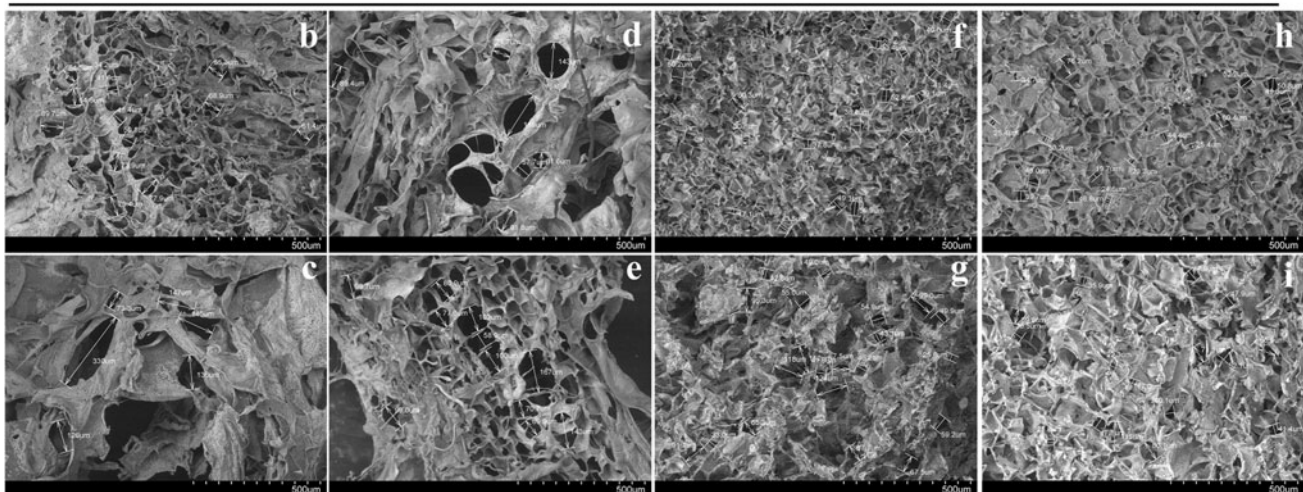
Fig. 2 Equilibrium of swelling ratio of 1 or 2 % of alginate and hyaluronic acid hydrogels obtained after incubation in PBS at 37 °C. **a** This table represents the evolution of ESR and pore size of 1 and 2 % (w/v) alginate and HA hydrogels after incubation in PBS at 37 °C for 0.5, 1, 3 and 24 h and freeze-dried during at least 72 h. Values represent the mean ± SD. Significant differences were assessed by Student t test; $p < 0.05$ **a** alginate versus HA, **b** 1 versus 2 %. **b–i** These images show the microscopic structure of alginate (**b–e**) and HA (**f–i**) hydrogels at different concentrations (1 and 2 %) after 0.5 h (**b**, **d**, **f**, **h**) and 24 h (**c**, **e**, **g**, **i**) of incubation in PBS. Observation by SEM was done at 15 kV, 40 Pa and ×100 of magnification

Lower pore diameters were observed for HA compared to alginate freeze-dried hydrogels (Fig. 2b–i), though statistical significance was only reached for 1 % concentrations after 0.5 and 24 h and for 2 %

concentrations at any of the time points of incubation studied. Further, an increase in the concentration of polymer was associated with a decrease in pore size for both hydrogels, although no differences were observed
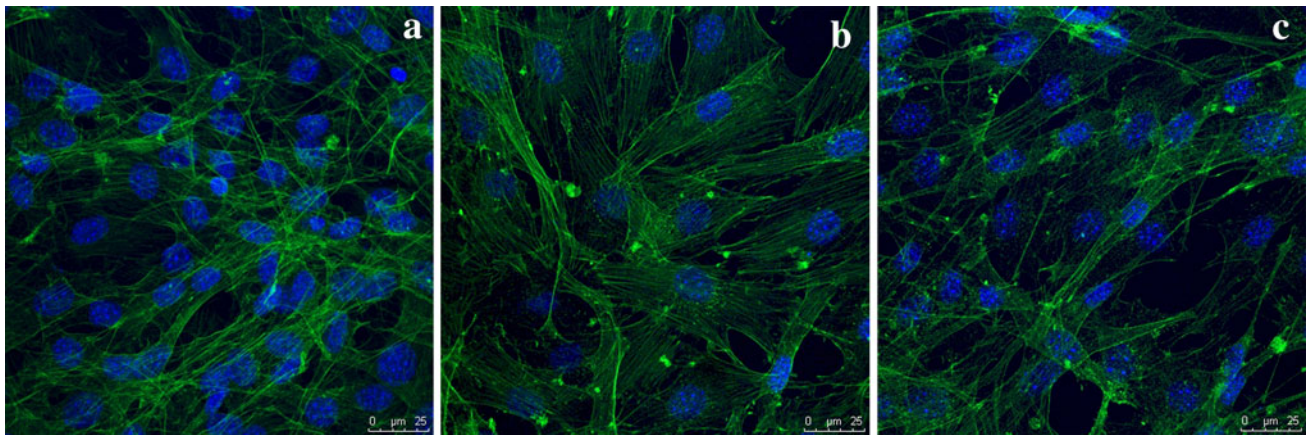
Fig. 3 Confocal images of MC3T3-E1 monolayers after 24 h of incubation with **a** culture media, **b** 1 % alginate hydrogel, and **c** 2 % alginate hydrogel

between alginate at 1 and 2 % after 0.5 and 3 h of incubation.

3.3 Cell Morphology by Confocal Microscope

The cytoskeleton organization of cells seeded with either 1 or 2 % alginate hydrogel and control cells was examined after 24 h of attachment. Representative confocal images of actin staining of osteoblasts cultured in different conditions are shown in Fig. 3. While control cells appeared elongated and with actin filaments haphazard orientated, cells cultured with alginate hydrogel presented the actin bundles aligned in the same direction and in osteoblasts cultured with alginate at 2 % more stretched actin filaments were observed. The formation of stretched and roughly parallel actin filaments may indicate the development of organized actin filaments in the form of stress fibers in cells cultured with alginate hydrogels.

3.4 Effect of the Hydrogels on Cell Viability

In order to determine the effect of the different hydrogels on cell viability, the LDH activity in the culture media was measured after 24 h of culture. As shown in Fig. 4, none of the hydrogels tested had a toxic effect on MC3T3-E1 cells. Further, a significant increase on cell viability was observed when comparing 1 % HA with 1 % alginate hydrogels.

3.5 Effect of the Hydrogels on ALP Activity

Cells cultured with HA hydrogels showed significantly lower ALP activity levels compared to control cells and to 2 and 3 % alginate hydrogels, respectively. In addition, a significant increase on ALP activity was found when comparing cells cultured on 2 % HA compared to 1 % HA (Fig. 5).
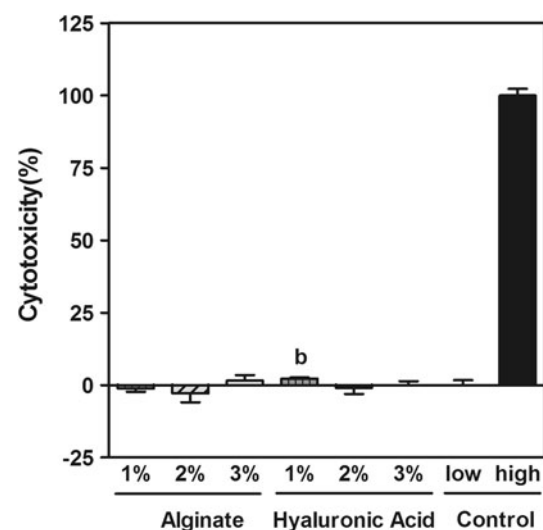

Fig. 4 LDH activity measured from culture media collected 24 h after exposure of MC3T3-E1 cells to alginate or hyaluronic acid hydrogels at different polymer concentrations (1 %, 2 % and 3 %). High control (100 % cytotoxicity) was cell culture media from cells seeded on polyethylene terephthalate (PET) membrane inserts and incubated with PBS containing 1 % Triton X-100. Low control (0 % cytotoxicity) was cell culture media from cells seeded on PET membrane insert and incubated with PBS. Values represent the mean $\pm$ SEM. Significant differences were assessed by Student t test: $p < 0.05$ *b* alginate versus HA

3.6 Effect of the Hydrogels on Calcium Content

Calcium content in the cell monolayer was quantified after 21 days of culture. As seen in Fig. 6, higher values of calcium content were found on cells cultured with alginate compared to control cells, and rising amount in calcium content were found as the polymer concentration increased. Unfortunately, calcium content in cells cultured in direct contact with HA could not be determined, since an interference of HA on the calcium determination method used could
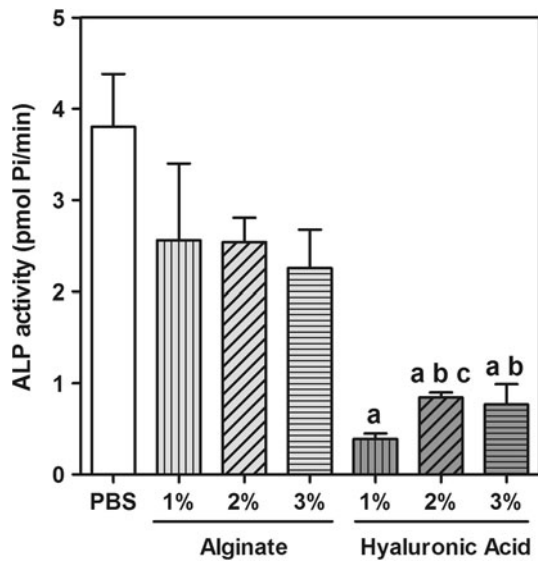
Fig. 5 Alkaline phosphatase (ALP) activity in MC3T3-E1 cells cultured for 21 days with alginate or hyaluronic acid at different polymer concentrations (1, 2 and 3 %). Values represent the mean ± SEM. Significant differences were assessed by Student t test: $p < 0.05$ **a** versus control PBS, **b** alginate versus HA, **c** between polymer concentrations
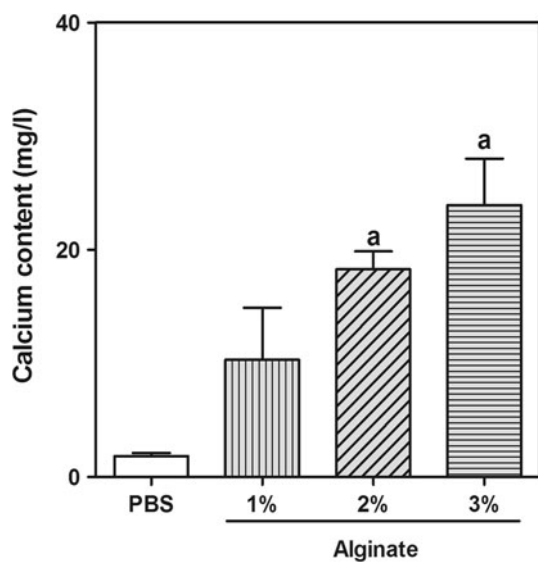

Fig. 6 Calcium content in MC3T3-E1 cells cultured for 21 days with alginate at different polymer concentrations (1, 2 and 3 %). Values represent the mean ± SEM. Significant differences were assessed by Student t test: $p < 0.05$ **a** versus control PBS

be confirmed by previous studies, where high molecular weight HA hydrogels alone incubated with cell culture media without cells gave high values of calcium content, and similar to HA hydrogels with cells (data not shown).

Based on ALP activity and calcium content results, 2 and 3 % polymer concentrations were selected for further experiments.
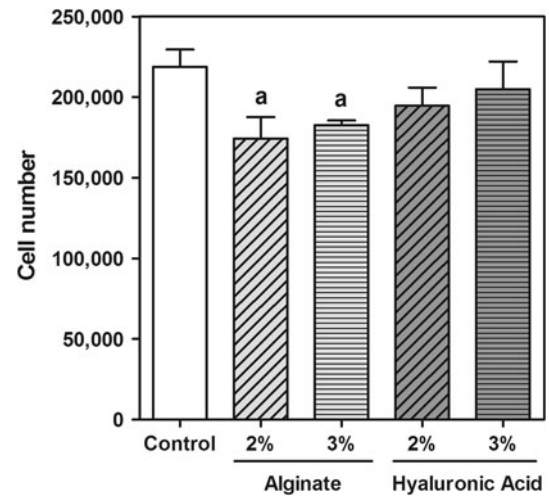

Fig. 7 Quantification of cell number in MC3T3-E1 cells cultured for 21 days with alginate or hyaluronic acid at different polymer concentrations (2 % and 3 %). Values represent the mean ± SEM. Significant differences between groups were assessed by Student t test: $p < 0.05$ *a* versus control PBS

3.7 Effect of the Hydrogels on Cell Number

As shown in Fig. 7, after 21 days of culture no differences in cell number were observed between control cells (PBS) or cells seeded with HA either at 2 or 3 %. However, when cells were cultured with 2 or 3 % alginate hydrogels a significant decrease on cell number was found compared to untreated cells. No differences on the cell number among polymers were found after 21 days of culture.

3.8 Effect of the Hydrogels on the Expression of Osteogenic Related Genes

The effect of the different polymers on osteoblast cell differentiation was also assessed at gene expression levels of several markers (Fig. 8). Higher mRNA expression levels of the different markers studied were found on cells cultured with alginate hydrogels compared to those cells cultured with the high molecular weight HA hydrogels used in this study.

Significantly higher expression levels of *Bsp* mRNA levels were found in cells cultured with 2 % alginate hydrogels compared to cells cultured with 2 % HA hydrogels. While no differences were observed in *Alp* mRNA levels between cells cultured with alginate hydrogels and control cells, a down-regulation of *Alp* mRNA levels was found in cells cultured with HA compared to control, and this down-regulation was also dependent on the concentration of HA. Osteocalcin mRNA expression levels were significantly higher in cells cultured with alginate hydrogels compared to control and to cells
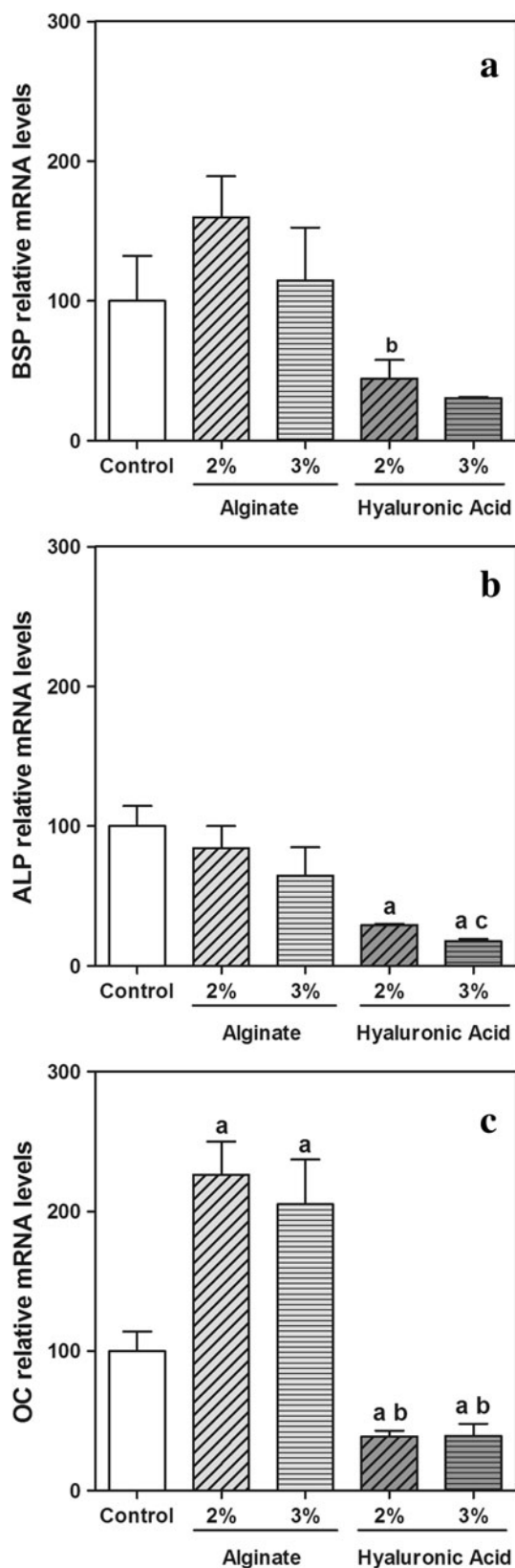
◀ **Fig. 8** Expression of osteoblast differentiation related genes in MC3T3-E1 cells cultured for 21 days with alginate or hyaluronic acid at different polymer concentrations (2 and 3 %). Data represent relative mRNA levels of target genes normalized with reference genes, expressed as a percentage of untreated cells (PBS), which were set to 100 %. Values represent the mean ± SEM. Differences between groups were assessed by Student t test: $p < 0.05$ **a** versus control PBS, **b** alginate versus HA, **c** between polymer concentrations

4 Discussion

The use of hydrogels for bone regeneration has recently been reviewed [28], suggesting that the use of hydrogels offers an option for bone-tissue engineering and that further research is needed to identify the biological and physical properties of hydrogels. Sodium alginate and hyaluronic acid are natural polymers that have widely been used for several applications in tissue engineering; however, to the best of our knowledge, the direct comparison of the effect on osteoblast differentiation of those two polymers has never been reported. Here, we report the structural and physicochemical properties of different concentrations of these two polymer hydrogels and their biocompatibility and bioactivity after long-term culture of MC3T3-E1 cells.

Hydrogels are used in tissue engineering as scaffolds that provide structural integrity to tissue constructs, as control drug and protein delivery to tissues and cultures, and as adhesives or barriers between tissue and material surfaces [29]. The pH of the environment, viscosity of the hydrogel matrix, the swelling behavior and the pore size of the microstructure will determine the suitability of the material for their different applications on tissue regeneration. Under the preparation conditions described in the present study for both polymers, alginate and high molecular weight HA formed reversible hydrogels with a weak structure, which could be related with the interactions between the polymer chains, as a consequence of their proximity and the polymer concentration used. In this context, we cannot discard the existence of some solvation processes, at least for the HA hydrogels used in this study. In fact, further modifications of the original polymer have been proposed in order to significantly increase hydrogels robustness and to improve their mechanical properties [30].

Viscosity is a decisive parameter for controlling the scaffold structure. The analysis of the different variables involving polymer solution viscosity, leads to the identification of the optimal conditions for polymer scaffold preparation [31]. The viscosity of the hydrogel is governed by the pH, the temperature, molecular weight and polymer concentration [32, 33]. Actually, it has been reported the role of temperature on the distribution of the ionic charges along the polyelectrolyte chain, which is related with the coiled or extended conformation of the polymer chain and

cultured with HA hydrogels. In addition, cells cultured with HA hydrogels showed a significant down-regulation of *Oc* mRNA expression levels compared to control cells.

its final viscosity solution [31]. Therefore, the viscosity of a solution can be modulated depending on the requirements of specific applications. For example, for the application of enamel matrix derivative (EMD) onto denuded root surfaces, an initial viscous formulation of polyethyleneglycol alginate (PGA) containing EMD at room temperature allowed easy application of the solution to the site of defect, which further, at physiological conditions (higher temperature and neutral pH), decreased its viscosity allowing the complete coating of the defect to be treated [33]. In the present study, both alginate and high molecular weight HA hydrogels were prepared in PBS (pH $\sim$ 7.0) to be used for tissue culture, and changes in viscosity were analyzed. Any of the polymer concentrations tested permitted its easy application and shape to the specific site due to a decrease in the viscosity associated to an increase of temperature when used in cell culture conditions. Additionally, this temperature dependency is an attractive approach in the drug delivery field. More specifically, high viscous hydrogels are interesting during drug loading; whereas a decrease of hydrogel viscosity allows drug release. Thus, previous studies performed in our laboratory showed the ability of those hydrogels to associate and deliver active molecules in vitro (unpublished results).

When a hydrophilic matrix is placed in an aqueous medium, the hydrophilic colloid components swell to form a gelatinous surface layer. This then controls the diffusion of water into the matrix [32]. In the present study, the water uptake happened in the first 30 min for both alginate and high molecular weight hyaluronic acid hydrogels at any of the polymer concentrations tested. The capacity of swelling obtained indicates the weakness for both polymer hydrogels in wet state as a result of their low cross linking grade and of the hydrophilic nature of these polymers. It is interesting to note that for HA an increase in polymer concentration was related to an increase in the water uptake. As regards to pore size, it should be expected that it differs in hydrated and dried hydrogels, in fact, while in wet state both hydrogels display an homogenous, uniform and continuous nonporous solution, due to weakness and hydrophilic properties of both polymers (data not shown), either alginate or HA yielded a porous three dimensional structure with a pore diameter in the range of 53–121 μm in a swollen freeze-dried state.

Once we confirmed the development of hydrogels with expected properties close to physiological pH and at adequate polymer concentration to achieve easy handling, we investigated the effect of those polymers on the biological response of osteoblasts. In agreement with previous reports [8, 34, 35], biocompatibility of alginate and hyaluronic acid hydrogels at any of concentrations evaluated on osteoblast cells was confirmed.

The ability of these natural polymers to achieve osteoblast proliferation and differentiation when they are placed in direct contact with pre-osteoblast cells was also studied. Previous studies have demonstrated that modified alginate and hyaluronic acid hydrogels induce bone formation in vitro [8, 14, 15, 17, 26, 36, 37] and in vivo [15, 17, 19, 27]. Here, we demonstrate that unmodified hydrogels also support osteoblast differentiation, though alginate hydrogels induced a higher degree of differentiation than the high molecular weight hyaluronic acid hydrogels used in the present study.

ALP activity is often used as a marker for increased osteoblastic metabolic activity and an indicator of osteoblastic differentiation [15]. Cells cultured in direct contact with alginate hydrogels showed higher ALP activity levels than those cultured in contact with hyaluronic hydrogels at 2 and 3 % of polymer concentrations. Previous studies have described upregulation of ALP activity by alginate microbeads [36, 38] or HA in a dose-dependent manner at different dosages [39]. Intracellular calcium content was also measured as an index of cell differentiation for alginate hydrogels. In contrast to the ALP activity profile, cells cultured with alginate showed increased calcium content compared to control cells, where raising amounts in calcium were related to higher polymer concentrations, suggesting that alginate induce matrix mineralization which is related with increasing polymer concentration. In agreement with previous reports that show an induction of mineral nodule formation by modified alginate hydrogels [40].

Taking all these into account, 2 and 3 % of polymer concentration were selected to further evaluate its effects on cell proliferation and on the mRNA expression levels of markers related to osteoblast differentiation. The effect of the hydrogels on cell number was investigated by DNA content quantification after 21 days of culture. Although a significant decrease in cell number was observed when cells were cultured with alginate compared to control cells, the DNA results indicate long-term viability and the support of the hydrogels for cell proliferation, as the number of cells at day 21 surpasses the initial seeding density. Supporting these data is the cytoskeleton organization of cells cultured with alginate hydrogels as seen by the confocal images. Actually, Hong and coworkers reported the relationship between the enhanced actin fiber density and an early stage of osteoblast differentiation [41].

Finally, expression of markers related to late stages of osteoblast cell differentiation was determined. The acquisition of an extracellular matrix competent for mineralization is governed by the expression of markers related with maturation and organization of the bone matrix. In the present study, on one hand, and consistent with the decrease of ALP activity induced by HA hydrogels, the

mRNA expression levels of *Alp* were also markedly decreased in MC3T3-E1 cells cultured with HA compared to both, control cells and cells cultured with alginate. Cells cultured with alginate showed increased mRNA levels of both, *Bsp* mRNA levels—a component of the extracellular matrix which has been described to bind to hydroxyapatite crystals [42]—and *Oc* mRNA levels—an extracellular matrix protein synthesized and secreted exclusively by osteoblastic cells in the late stage of maturation and considered an indicator of osteoblasts differentiation and mineralization [43]—indicating a higher degree of cell differentiation than cells cultured with HA. In agreement with these results, cells encapsulated into alginate microcapsules enhanced mRNA expression levels of osteocalcin when compared to monolayer cultures over the course of 21 days [38], while a decrease in OC secretion with HA has been reported in osteoarthritic osteoblast cells [44]. However, in vitro [8] and in vivo [5] studies using modified HA hydrogels with BMP-2 have reported high OC expression, thus, reinforcing the importance of the specific HA used.

On the other hand, it is interesting to note that even if cell number was lower when cells were cultured with alginate hydrogels compared to control cells, cytoskeleton organization, calcium content and gene expression levels indicate that cells cultured with alginate showed a significant increased osteogenic activity.

5 Conclusion

In conclusion, in this study we have compared for the first time the effect of different natural polymers that are widely used for tissue engineering in terms of osteoblast viability, proliferation and differentiation. The biocompatibility of hyaluronic acid and alginate hydrogels has been validated, and we have shown that alginate hydrogels might be more suitable for bone tissue engineering applications than high molecular weight hyaluronic acid hydrogels.

References

1. Mann BK (2003) Clin Plast Surg 30(4):601–609
2. Lee KY, Alsberg E, Mooney DJ (2001) J Biomed Mater Res A 56(2):228–233
3. Lum L, Elisseeff J (2003) In: Ferretti NAP (ed) Topics in tissue engineering. University of Oulu, Oulu p 25
4. Gutowska A, Jeong B, Jasionowski M (2001) Anat Rec 263(4):342–349
5. Martinez-Sanz E, Ossipov DA, Hilborn J, Larsson S, Jonsson KB, Varghese OP (2011) J Control Release 152(2):232–240
6. Tan H, Marra KG (2010) Materials 3(3):1746–1767
7. Tan H, Ramirez CM, Miljkovic N, Li H, Rubin JP, Marra KG (2009) Biomaterials 30(36):6844–6853
8. Kim HD, Valentini RF (2002) J Biomed Mater Res 59(3):573–584
9. George M, Abraham TE (2006) J Control Release 114(1):1–14
10. Wee S, Gombotz WR (1998) Adv Drug Deliv Rev 31(3):267–285
11. Barbetta A, Barigelli E, Dentini M (2009) Biomacromolecules 10(8):2328–2337
12. Chung TW, Yang J, Akaike T, Cho KY, Nah JW, Kim SI, Cho CS (2002) Biomaterials 23(14):2827–2834
13. Hahn SK, Park JK, Tomimatsu T, Shimoboji T (2007) Int I Biol Macromol 40(4):374–380
14. Alsberg E, Anderson KW, Albeiruti A, Franceschi RT, Mooney DJ (2001) J Dent Res 80(11):2025–2029
15. Lee JY, Choo JE, Park HJ, Park JB, Lee SC, Jo I, Lee SJ, Chung CP, Park YJ (2007) Biochem Biophys Res Commun 357(1):68–74
16. Kolambkar YM, Dupont KM, Boerckel JD, Huebsch N, Mooney DJ, Hutmacher DW, Guldberg RE (2011) Biomaterials 32(1):65–74
17. Li Z, Ramay HR, Hauch KD, Xiao D, Zhang M (2005) Biomaterials 26(18):3919–3928
18. Park D-J, Choi B-H, Zhu S-J, Huh J-Y, Kim B-Y, Lee S-H (2005) J Craniomaxillofac Surg 33(1):50–54
19. Bergman K, Engstrand T, Hilborn J, Ossipov D, Piskounova S, Bowden T (2009) J Biomed Mater Res 91A(4):1111–1118
20. Kim J, Kim IS, Cho TH, Lee KB, Hwang SJ, Tae G, Noh I, Lee SH, Park Y, Sun K (2007) Biomaterials 28(10):1830–1837
21. Varghese OP, Kisiel M, Martinez-Sanz E, Ossipov DA, Hilborn J (2010) Macromol Rapid Commun 31(13):1175–1180
22. Lee JY, Spicer AP (2000) Curr Opin Cell Biol 12(5):581–586
23. Hall CL, Turley EA (1995) J Neurooncol 26(3):221–229
24. Ialenti A, Di Rosa M (1994) Agents Actions 43(1):44–47
25. Weigel PH, Frost SJ, McGary CT, LeBoeuf RD (1988) Int J Tissue React 10(6):355–365
26. Lisignoli G, Zini N, Remiddi G, Piacentini A, Puggioli A, Trimarchi C, Fini M, Maraldi NM, Facchini A (2001) Biomaterials 22(15):2095–2105
27. Patterson J, Siew R, Herring SW, Lin AS, Guldberg R, Stayton PS (2010) Biomaterials 31(26):6772–6781
28. Park K (2011) J Control Release 152(2):207
29. Slaughter BV, Khurshid SS, Fisher OZ, Khademhosseini A, Peppas NA (2009) Adv Mater 21(32–33):3307–3329
30. Burdick JA, Prestwich GD (2011) Adv Mater 23(12):H41–H56
31. Florczyk SJ, Kim DJ, Wood DL, Zhang M (2011) J Biomed Mater Res 98(4):614–620
32. Liew CV, Chan LW, Ching AL, Heng PWS (2006) Int J Pharm 309(1–2):25–37
33. Gestrelius S, Andersson C, Johansson AC, Persson E, Brodin A, Rydhag L, Hammarstrom L (1997) J Clin Periodontol 24(9 Pt 2):678–684
34. Drury JL, Mooney DJ (2003) Biomaterials 24(24):4337–4351
35. Shapiro L, Cohen S (1997) Biomaterials 18(8):583–590

36. Abbah SA, Lu WW, Chan D, Cheung KM, Liu WG, Zhao F, Li ZY, Leong JC, Luk KD (2008) J Mater Sci Mater Med 19(5):2113–2119

37. Matsuno T, Hashimoto Y, Adachi S, Omata K, Yoshitaka Y, Ozeki Y, Umezu Y, Tabata Y, Nakamura M, Satoh T (2008) Dent Mater J 27(6):827–834

38. Abbah SA, Lu WW, Chan D, Cheung KM, Liu WG, Zhao F, Li ZY, Leong JC, Luk KD (2006) Biochem Biophys Res Commun 347(1):185–191

39. Huang L, Cheng YY, Koo PL, Lee KM, Qin L, Cheng JC, Kumta SM (2003) J Biomed Mater Res A 66(4):880–884

40. Matsuno T, Hashimoto Y, Adachi S, Omata K, Yoshitaka Y, Ozeki Y, Umezu Y, Tabata Y, Nakamura M, Satoh T (2008) Dent Mater J 27(6):827–834

41. Hong D, Chen HX, Yu HQ, Liang Y, Wang C, Lian QQ, Deng HT, Ge RS (2010) Exp Cell Res 316(14):2291–2300

42. Oldberg A, Franzen A, Heinegard D (1988) J Biol Chem 263(36):19430–19432

43. Sila-Asna M, Bunyaratvej A, Maeda S, Kitaguchi H, Bunyaratavej N (2007) Kobe J Med Sci 53(1–2):25–35

44. Lajeunesse D, Delalandre A, Martel-Pelletier J, Pelletier JP (2003) Bone 33(4):703–710

Paper 4

Effect of alginate hydrogel containing polyproline-rich peptides on osteoblast differentiation.

Rubert, M.; Monjo, M.; Lyngstadaas; S.P.; Ramis, J.M.

Effect of alginate hydrogel containing polyproline-rich peptides on osteoblast differentiation

M Rubert[1], M Monjo[1], S P Lyngstadaas[2] and J M Ramis[1,3]

[1] Group of Cell Therapy and Tissue Engineering, Research Institute on Health Sciences (IUNICS), University of Balearic Islands, Palma de Mallorca, Spain
[2] Department of Biomaterials, Institute for Clinical Dentistry, University of Oslo, Oslo, Norway

E-mail: joana.ramis@uib.es

Abstract

Polyproline-rich synthetic peptides have previously been shown to induce bone formation and mineralization *in vitro* and to decrease bone resorption *in vivo*. Alginate hydrogel formulations containing these synthetic peptides (P2, P5, P6) or Emdogain® (EMD) were tested for surface coating of bone implants. In an aqueous environment, the alginate hydrogels disclosed a highly compact structure suitable for cell adhesion and proliferation. Lack of cytotoxicity of the alginate-gel coating containing peptides was tested in MC3T3-E1 cell cultures. In the present study, relative mRNA expression levels of integrin alpha 8 were induced by P5 compared to untreated alginate gel, and osteopontin mRNA levels were increased after 21 days of culture by treatment with synthetic peptides or EMD compared to control. Further, in agreement with previous results when the synthetic peptides were administered in the culture media, osteocalcin mRNA was significantly upregulated after long-term treatment with the formulated synthetic peptides compared to untreated and EMD alginate gel. These results indicate that the alginate gel is a suitable carrier for the delivery of synthetic peptides, and that the formulation is promising as biodegradable and biocompatible coating for bone implants.

(Some figures may appear in colour only in the online journal)

1. Introduction

The deposition and growth of apatites into endoskeletal mineralized tissues is a process guided by polyproline-rich proteins [1]. Polyproline repeats are a common characteristic of hard tissue extracellular matrix proteins, playing a role in the compaction of protein matrix, conformational variability, the apatite crystal length and bond to protein domains frequently involved in signaling events [1, 2]. Due to the functional role of polyproline sequences on bone growth and formation, we have previously designed artificial synthetic peptides enriched in proline residues and studied their effect on the induction of bone formation and mineralization *in vitro,* demonstrating their capacity to stimulate osteoblast differentiation either in mouse pre-osteoblastic cells (MC3T3-E1) or in human umbilical cord derived mesenchymal stem cells (hUCMSCs) [3, 4]. *In vivo*, the capacity of osseointegration of peptide-coated titanium (Ti) implants was further evaluated, demonstrating their ability to promote osseointegration of Ti implants by reducing bone resorption [5].

To facilitate the use of the synthetic polyproline-rich peptides for bone tissue engineering, a suitable formulation allowing peptide delivery over time to the regeneration site is required. Hydrogels have been used for many different applications in tissue engineering such as space filling agents, as delivery vehicles for bioactive molecules, and as three-dimensional structures that organize cells and present stimuli to direct the formation of a desired tissue [6, 7]. Alginate is one of the main polymers chosen to form hydrogels for tissue engineering [8], having been used in a variety

---

[3] Author to whom any correspondence should be addressed.

Table 1. Aminoacidic sequence of synthetic proline-rich peptides.

Peptide	Sequence (N-terminus to C-terminus)	Polar AA	Hydrophobic AA
P2	PLVPSQPLVPSQPLVPSQPQPPLPP	7 (S,Q)	18 (P,L,V)
P5	PLVPSSPLVPCCPLVPCCPSPPLPP	3 (S)	22 (P,L,V,C)
P6	PHQPMQPQPPVHPMQPLPPQPPLPP	7 (H,Q)	18 (P,M,V,L)

Amino acid (AA); peptide 2 (P2); peptide 5 (P5); peptide 6 (P6); S = Ser; P = Pro; L = Leu; V = Val; Q = Gln; M = Met; H = His; C = Cys.

of medical applications including cell and/or growth factor encapsulation and drug stability and delivery [6, 9]. Alginate is a hydrophilic and linear polysaccharide copolymer of β-D-mannuronic acid (M) and α-L-glucuronic acid (G) monomers. Alginate gel is formed when divalent cations such as Ca^{2+}, Ba^{2+} or Sr^{2+} cooperatively interact with blocks of G monomers creating ionic bridges between different polymer chains [6, 9]. Due to favorable properties of biomaterials such as non-toxicity, biodegradability, and ease of processing into desired shape under normal physiological conditions [10–15] alginate has been extensively studied in tissue engineering, including the regeneration of skin, cartilage, bone, liver and cardiac tissue [15]. Thereby, alginate was selected as a carrier of synthetic proline-rich peptides to stimulate osteoblast cell differentiation and mineralization.

The aim of this study was to develop an alginate gel containing artificial peptides for their use in regenerative medicine. Pore size of the alginate was characterized by scanning microscopy. Peptide release profile over time was obtained by quantification of a FITC-labeled peptide using fluorescence spectroscopy. Osteoblast cell viability was evaluated by lactate dehydrogenase (LDH) activity and osteoblast adhesion and differentiation related markers were assessed by real-time reverse transcription polymerase chain reaction (RT-PCR).

2. Material and methods

2.1. Preparation of peptides and enamel matrix derivative

Enamel matrix derivative (EMD) was kindly supplied by Straumann GmbH (Basel, Switzerland). EMD was dissolved to 10 mg ml^{-1} in 0.1% acetic acid in phosphate-buffered saline (PBS) (PAA Laboratories GmbH, Pasching, Austria). Three synthetic peptides (table 1) were designed as described in detail in previous studies [4]. Peptides were purchased from Eurogentec (Seraing, Belgium). The synthetic peptides were dissolved to 5 or 10 mg ml^{-1} (in the case of peptide 2 FITC-labeled) in 0.1% acetic acid in PBS. Aliquots to avoid repeated freeze-thaw cycles were prepared and stored at −20 °C until use.

2.2. Preparation of alginate hydrogels

Sodium alginate (Pronova UP LVG®)—a low viscosity alginate where minimum 60% of monomers are guluronate—was purchased from NovaMatrix (FMC BioPolymer AS, Norway). The sodium alginate was used without further purification. Two percent (w v^{-1}) sodium alginate was prepared in PBS and stirred at 180 rpm at room temperature

overnight to get a homogenous hydrogel. The alginate solution was mixed with synthetic peptides or EMD at final concentration of 50 μg ml^{-1}. The solution of alginate containing synthetic peptides/EMD was then distributed into 24-well culture plate and sprayed with 300 mM $CaCl_2$ by means of an aerograph paint atomizer (Precisso®, Madrid, Spain). After 1–2 h of incubation at room temperature, alginate hydrogel was completely gelled.

2.3. Characterization of alginate hydrogel morphology by scanning electron microscopy

Morphology of control 2% alginate hydrogels and 2% alginate hydrogels containing synthetic peptide 2 (50 μg ml^{-1}) were observed using scanning electron microscope (SEM, Hitachi S-3400N, Hitachi High-Technologies Europe GmbH, Krefeld, Germany). The microstructure of alginate hydrogels (non-lyophilized and lyophilized) was observed. For the hydrogel lyophilization, samples were frozen at −80 °C followed by lyophilization at −35 °C. Samples were then frozen in N_2 to allow an accurated cut into cross sections using a sharp scalpel.

Structure of alginate hydrogels were observed at ×25 and ×100 magnification using 10 kV and 40 Pa. An environmental secondary electron detector (ESED) was used for images at ×25 magnification and a backscattered electron detector (BSED) was used for images at ×100 magnification. The diameter of each pore was measured using the software from the SEM.

2.4. Peptide release profile

To study the peptide release profile, P2 was labeled with FITC. The release of peptide contained into the 2% alginate hydrogel (50 μg ml^{-1}) was quantified by fluorescence spectroscopy. First, hydrogels were washed with culture media to remove the excess $CaCl_2$. Then, 750 μl of cell culture media were added onto peptide loaded alginate hydrogel. The samples were incubated at 37 °C and 5% CO_2 for 21 days and the cell culture media was changed twice a week. At prefixed time points (24 h, 4d, 7d, 11d, 14d, 18d and 21d), supernatants were collected and analyzed by fluorescence spectroscopy (λ ex 490 nm and λ em 525 nm) to determine the amount of peptide released to the media. The amount of peptide released during the washing step was also measured. The experiment was performed three times, and each sample analyzed in triplicate. Relative fluorescence units were correlated with the amount of peptide released using a linear standard curve for each time point.

2.5. Cell culture of MC3T3-E1

The mouse osteoblastic cell line MC3T3-E1 (DSMZ, Braunschweig, Germany) was maintained as previously described [16].

Before seeding, 24-well culture plates containing cross-linked hydrogels were washed with 750 μl of culture media to remove the excess $CaCl_2$. After evaluation of the efficiency of cell adhesion on 2% alginate gel using different cell densities, for the final experiments, cells were seeded at a density of 100 000 cells per well. The media was refreshed twice a week. Culture media was collected 24 h after seeding to study cell viability. Cells were harvested at days 14 and 21 to analyze gene expression of adhesion and osteogenic-related markers using real-time RT-PCR.

Cultures were routinely observed using light microscopy (Leica DMIRB, Leica Microsystems Wetzlar GmbH, Germany).

2.6. Cell adhesion to 2% alginate gel

Adhesion of cells onto the hydrogel after one and five days post-seeding was evaluated in order to determine the best seeding density for the experiments. Densities from 30×10^3 to 200×10^3 cells per well were tested. Cells that had adhered onto the hydrogel were lysed by a freeze–thaw method in deionized distilled water. Cell lysates were used for determination of DNA quantity using Hoechst 33 258 fluorescence assay. The samples were mixed with 20 μg ml^{-1} of Hoechst 33 258 fluorescence stain (Sigma, St. Quentin Fallavier, France) in TNE buffer (10 mM Tris; 2.0 M NaCl; 1 mM EDTA; pH 7.4), and the intensity of fluorescence was measured at excitation and emission wavelengths of 356/465 nm using a multifunction microplate reader (Cary Eclipse fluorescence spectrophotometer, Agilent Technologies, Santa Clara, USA). Relative fluorescence units were correlated with the cell number using a linear standard curve.

MC3T3-E1 cells adhered onto the hydrogels after one and five days of culture were visualized by confocal microscopy (Leica TCS SPE Microsystems Wetzlar GmbH, Wetlar, Germany). Briefly, cells seeded onto the hydrogels were fixed with 4% formaldehyde in PBS at 4 °C for 10 min. For staining, cells were permeabilized in 0.2% triton and material autofluorescence was blocked with 3% BSA in PBS. The cytoskeleton of the cells was stained using 5 μg ml^{-1} FITC phalloidin (Sigma, St. Quentin Fallavier, France) and the nuclei with DAPI (Sigma, Schnelldorf, Germany). Further, the cell adhesion and attachment of 100×10^3 cells initially seeded on 2% alginate hydrogels was observed after cell fixation with 4% formaldehyde in PBS at 4 °C for 10 min followed by visualization using the SEM and ESED at 10 kV, $\times 200$ and 40 Pa.

2.7. Cell viability

The LDH activity determined in the culture media after 24 h was taken as an indicator of membrane leakage or cell lysis. The activity of the cytosolic enzyme was estimated as previously described [4].

Table 2. Sequence of osteoblast markers related genes.

Gene	Primer sequence
18S	S 5′- GTAACCCGTTGAACCCCATT -3′
	A 5′- CCATCCAATCGGTAGTAGCG -3′
GAPDH	S 5′- ACCCAGAAGACTGTG-GATGG -3′
	A 5′- CACATTGGG-GGTAGGAACAC -3′
Itga8	S 5′- TCGCCTGGGGAGGAGGCGAAA -3′
	A 5′- TCTTAACCGCTGTGCTCCCCG -3′
Itgb1	S 5′- AGCAGGCGTGGTTGCTGGAA -3′
	A 5′- TTTCACCCGTGTCCCACTTGGC -3′
Itgb3	S 5′- AGGGGAGATGTGTTCCGGCCA -3′
	A 5′- ACACACAGCTGCCGCACTCG -3′
Fn1	S 5′- GCTGCCAGGAGACAGCCGTG -3′
	A 5′- GTCTTGCCGCCCTTCGGTGG -3′
Bmp2	S 5′- GCTCCACAAACGAGAAAAG-C -3′
	A 5′- AGCAAGGGGAAAAG-GACACT -3′
Coll-I	S 5′- AGAGC-ATGACCGATGGATTC -3′
	A 5′- CCTTCTTGAGGTTGCCAGTC -3′
Bsp	S 5′- GAAAATGGAGACGGCGATAG -3′
	A 5′- ACCCGAGAGTGTGGAAAGTG-3′
Alp	S 5′- AACCCAGACACAAGCATT-CC -3′
	A 5′- GAGAGCGAAGGGTC-AGTCAG -3′
Oc	S 5′- CCGGGAGCAG-TGTGAGCTTA -3′
	A 5′- TAGATGC-GTTTGTAGGCGGTC -3′
Opn	S 5′- TCTGCGGCAGGCATTCTCGG -3′
	A 5′- GTCACTTTCACCGGGAGGGAGGA -3′

2.8. Total RNA isolation and gene expression of osteoblast markers by real-time RT-PCR

The effect of synthetic peptides and EMD loaded into the hydrogels on gene expression was studied after 14 and 21 days of treatment on pre-osteoblast MC3T3-E1 cells. Total RNA was isolated using Tripure® (Roche Diagnostics, Mannheim, Germany), according to the manufacturer's protocol. Total RNA was quantified at 260 nm using a Nanodrop spectrophotometer (NanoDrop Technologies, Wilmington, DE, USA).

The same amount of RNA (350 ng) was reverse transcribed to cDNA using high capacity RNA-to-cDNA kit (Applied Biosystems, Foster City, CA), according to the protocol of the supplier. Aliquots of each cDNA were frozen (−20 °C) until the PCR reactions were carried out.

Real-time PCR was performed in the Lightcycler 480® (Roche Diagnostics, Mannheim, Germany) using SYBR green detection. Real-time PCR was done for two reference genes (18SrRNA and glyceraldehyde-3-phosphate dehydrogenase (GAPDH)) and ten target genes (integrin alpha 8 (*Itga8*), integrin beta1 (*Itgb1*), integrin beta 3 (*Itgb3*), fibronectin 1 (*Fn1*), bone morphogenetic protein 2 (*Bmp2*), collagen type I (*Coll-I*), bone sialoprotein (*Bsp*), alkaline phosphatase (*Alp*), osteocalcin (*Oc*) and osteopontin (*Opn*)). The primer sequences are detailed in table 2. Reaction conditions and relative quantification have been performed as previously described [16].

2.9. Statistical analyses

All data are presented as mean values $\pm$ SEM. Differences between groups were assessed by Mann–Whitney test or by Student *t*-test depending on their normal distribution. To
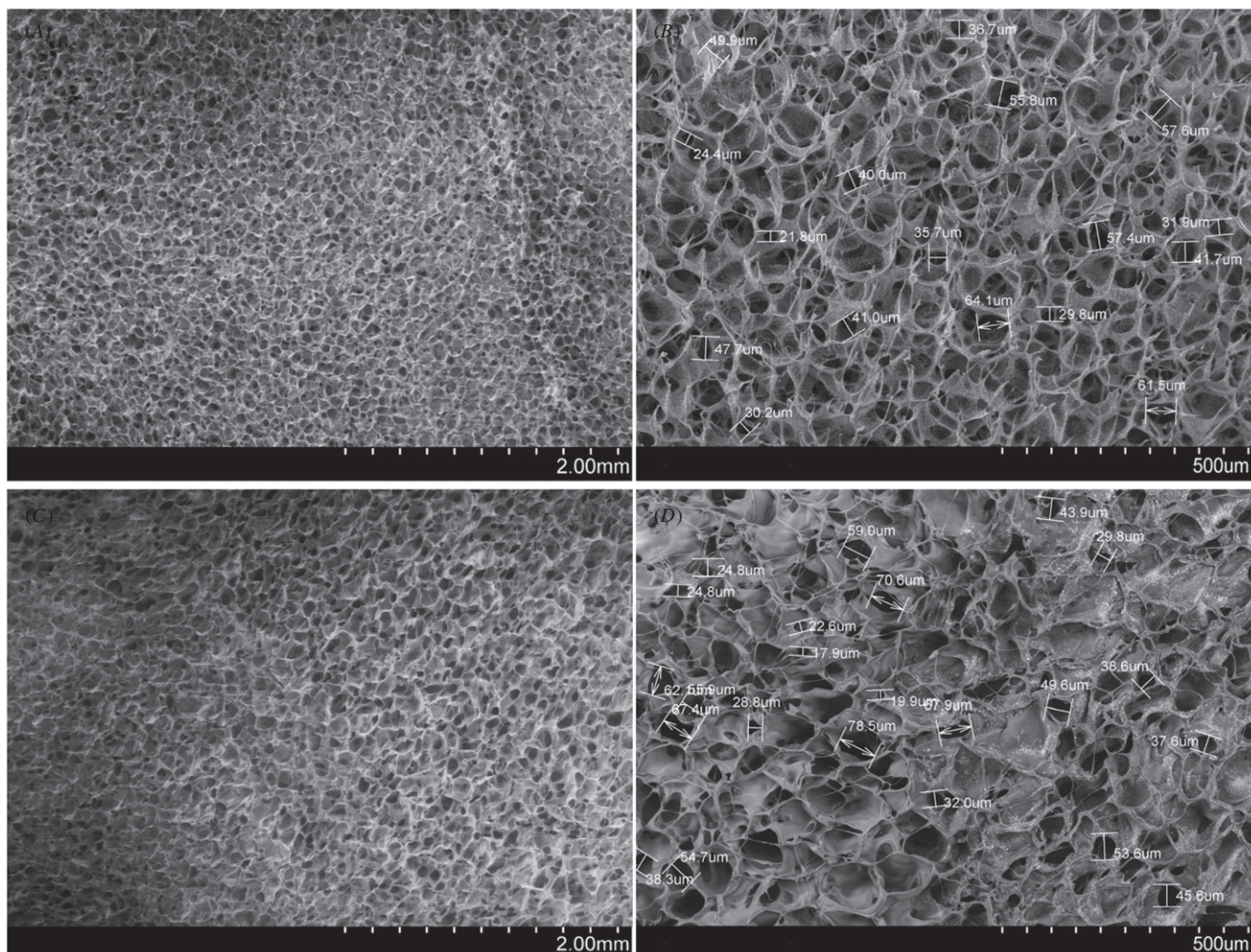
Figure 1. Microstructure of 2% of alginate (*A* and *B*) and 2% of alginate containing synthetic peptide (*C* and *D*) gelled by 300 mM of CaCl$_2$. Observation by SEM at ×25 (*A* and *C*) and ×100 of magnification (*B* and *D*).

measure the correlation among different variables, Pearson correlation analysis was used. The SPSS® program for Windows (Chicago, IL) version 17.0 was used. Results were considered statistically significant at the *p*-values ⩽ 0.05.

3. Results

3.1. Alginate microstructure

Figure 1 shows the microstructure of a cross section from a lyophilized 2% alginate hydrogel (figures 1(*A*) and (*B*)) and 2% alginate hydrogel containing synthetic peptide (figures 1(*C*) and (*D*)). As seen in the SEM images, although alginate hydrogel containing synthetic peptide showed a more irregular structure than 2% alginate hydrogel, a porous and interconnected structure was observed in all the gels analyzed. Both cross-linked hydrogels presented a porous and interconnected structure with a pore diameter of 42.9 ± 3.5 μm and 44.7 ± 4.1 μm, for 2% alginate hydrogel without or with synthetic peptide respectively.

3.2. Peptide delivery from 2% alginate hydrogel

Peptide release profile from 2% alginate hydrogels is depicted in figure 2. A burst release of the peptide during the first 24 h of incubation was observed (54.67%). Further, as seen in the cumulative release profile, a 25.8% of peptide was slowly released up to 11 days, followed by a sustained release over time up to 21 days. At the end of the experiment (after 21 days) a 5.6% of the total peptide theoretically contained into the hydrogel had not been released. It should be noted that a 12.7% of the loaded peptide was released during the washing step of the hydrogels with culture media to remove the excess CaCl$_2$.

3.3. Cell adhesion and proliferation

A low cell adhesion rate onto the alginate hydrogels was observed, since more than half of the seeded cells did not adhere to the gel one day after plating. Nevertheless, cells attached to the hydrogel and proliferated over the cell culture (figure 3). Further, cells were visualized by confocal microscopy in order to verify the ability of osteoblasts to attach
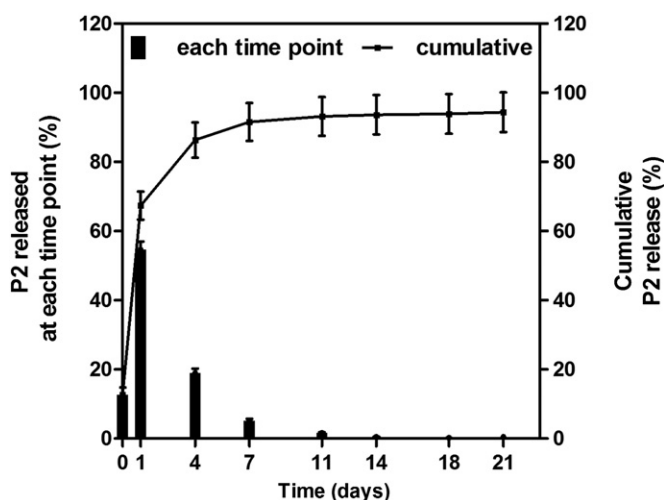
Figure 2. Release profile of peptide 2 labeled with FITC after 21 days of incubation at 37 °C. Bar graph show the amount of peptide released after each time point. Line graph represents cumulative amount of peptide released up to 21 days. Values represent mean $\pm$ SEM.

and spread on hydrogels surfaces. Confocal images show an increase in the number of nuclei accompanied by an increase in actin staining as much number of cells seeded and increasing from day one to day five (figures 3(*A*)–(*H*)). Moreover, the cell filopodia of osteoblasts cultured on the alginate hydrogel were appreciated by SEM (figure 3(*J*)).

The DNA content was used to determine the number of cells present onto alginate gels. As seen in figure 3(*I*), rising percentages of cell proliferation were found as the number of initial cells seeded on the gel increased. Thus, while no proliferation from days one to five was found when the seeding density was 30×10^3 cells per well, a 122.9%, 98.1% and 91.8% increase was found for seeding densities of 60×10^3, 100×10^3 and 200×10^3 cells per well, respectively. Among the different seeding densities tested, 100×10^3 cells per well was the one that exhibited jointly a reasonable initial cell attachment and an increase in cell proliferation, and therefore was chosen for further experiments.

3.4. Effect of alginate hydrogel loaded with synthetic peptides on cell viability

No toxic effects were found in cells cultured on alginate hydrogels containing synthetic peptides, either after 24 h (figure 4) or after a long-term period (data not shown). P2 increased significantly cell viability after 24 h compared to EMD, while P5 showed significantly lower toxic effects compared to EMD and to untreated alginate gel.

3.5. Effect of alginate hydrogel loaded with synthetic peptides on gene expression of cell adhesion markers

Expression of *Itga8* was increased in cells treated with P5 when compared to control after 21 days of culture (figure 5(*A*)). *Itgb1* mRNA levels significantly decreased after treatment with P2 and P6 for 14 days compared to control. After 21 days, cells treated with P6 reduced significantly *Itgb1*

mRNA levels compared to EMD (figure 5(*B*)). *Itgb3* and *Fn1* decreased significantly after 14 days of treatment with P2 and P6 compared to control (figures 5(*C*) and (*D*)), and no differences were observed after 21 days.

3.6. Effect of alginate hydrogel loaded with synthetic peptides on gene expression of osteoblast markers

Bmp2 relative mRNA levels increased significantly after 14 days of treatment with P6, while decreased after 21 days of treatment with P2 compared to EMD. Though EMD treatment induced a significant decrease on *Bmp2* mRNA levels after 14 days of cell culture compared to control, an increase on *Bmp2* mRNA levels was found after 21 days, although differences did not reach statistical significance (figure 6(*A*)). *Coll-I* gene expression decreased significantly after 14 days of treatment with any of the synthetic peptides compared to control (figure 6(*B*)). No differences in *Bsp* mRNA levels were found among the different treatments (figure 6(*C*)). ALP mRNA levels significantly decreased after treatment with P6 for 14 days and 21 days and with P2 after 21 days of treatment compared to control (figure 6(*D*)). After 14 days of cell culture, increased *Oc* mRNA levels were detected in cells cultured onto 2% alginate gel and containing synthetic peptides compared to cells treated with EMD. After 21 days, cells treated with P5 or P6 increased *Oc* mRNA levels when compared to control (figure 6(*E*)). Expression of *Opn* decreased significantly after 14 days of culture with P2 and P6 compared to control. After 21 days, *Opn* mRNA levels increased significantly with any of the synthetic peptides and EMD compared to control. EMD treatment markedly increased mRNA expression levels of *Opn* compared to P2 and P6 treatment (figure 6(*F*)).

4. Discussion

Polyproline-rich synthetic peptides have previously been shown to induce bone formation and mineralization *in vitro* [3, 4] and to decrease bone resorption *in vivo* [5]. The aim of this study was to develop a suitable formulation with a hydrogel for local treatment with these synthetic peptides to promote bone formation and mineralization, either alone or as a biodegradable coating for skeletal implants. In the present study, cells were exposed to alginate gel containing different synthetic peptides and cultured for a long-term period in order to evaluate the effect of those peptides on the biological response of osteoblasts.

The optimal formulation of the hydrogel has to allow the formation of a compact structure for a controlled, local and specific bioactive molecule delivery. Such features are governed by the physical property (e.g. mechanics, degradation, gel formation), the mass transport property (e.g. diffusion) and the biological interaction requirements (e.g. cell adhesion and signaling) of each specific application [6]. Previous studies carried out for our research group using alginate gel (Protanal LF200M, FMC polymers, Oslo, Norway) at different polymer concentrations (1%, 2%, 3%, 6% and 10%) have shown a decrease in pore size as the polymer concentration increases, resulting in the concentration
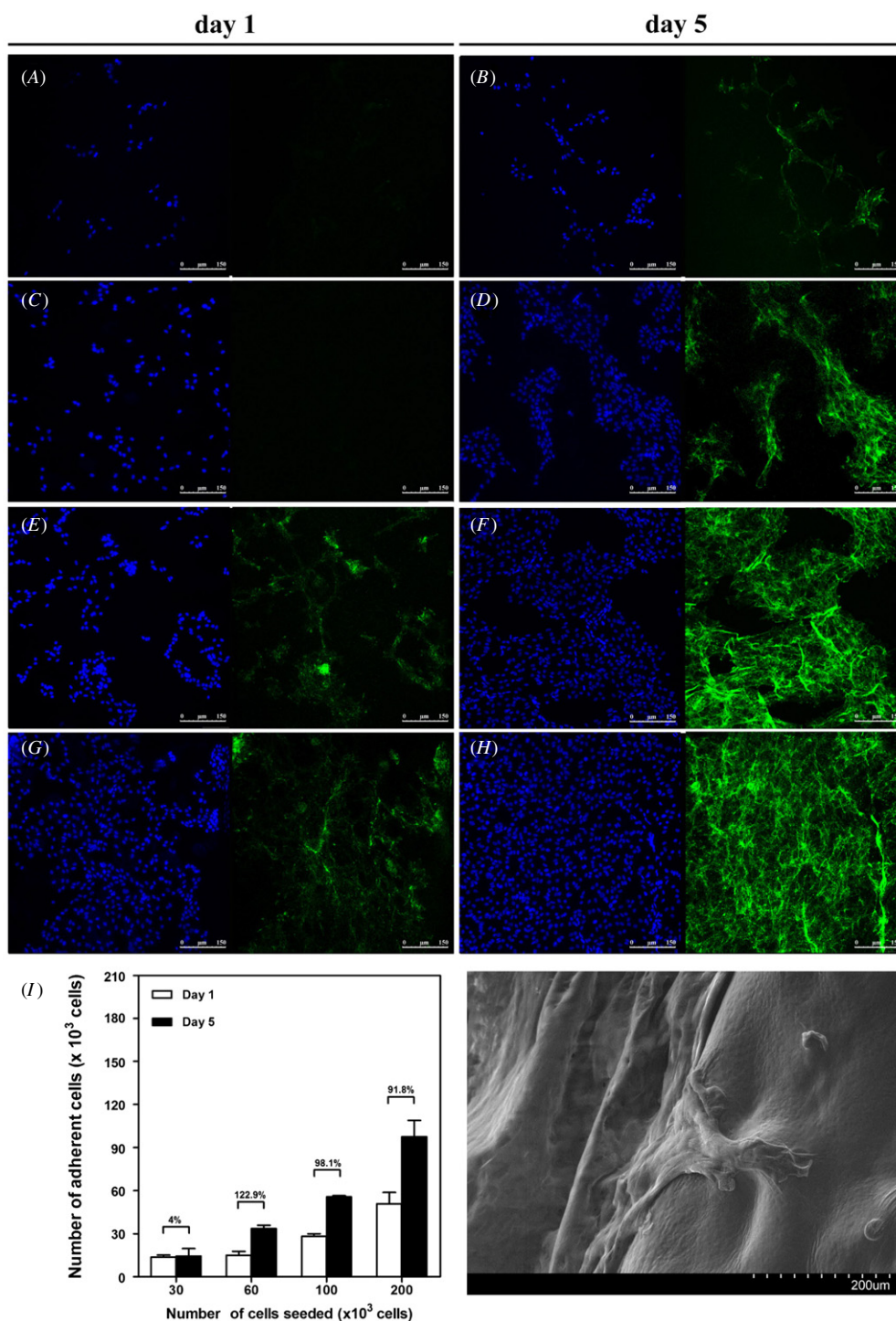
Figure 3. Osteoblast attachment on 2% alginate hydrogel. Representative pictures obtained by confocal microscopy of adherent cells when seeding 30×10^3 (*A* and *B*), 60×10^3 (*C* and *D*), 100×10^3 (*E* and *F*) and 200×10^3 (*G* and *H*) cells per well after 1 (*A*, *C*, *E*, *G*) and 5 (*B*, *D*, *F*, *H*) days of culture. Cell nuclei are presented in the right panel (DAPI staining) and actin filaments are presented in the left panel (phalloidin-FITC). Plot (*I*) shows the number of adherent cells when seeding different amounts of cells (30×10^3, 60×10^3, 100×10^3 and 200×10^3 cells per well) after one and five days of culture. Values represent the mean $\pm$ SEM. Plot (*J*) shows a representative picture of osteoblast cells adhered on 2% alginate hydrogels when seeding 100×10^3 cells per well obtained by SEM at $\times 200$ of magnification.

of 2% as the most promising formulation to act as a peptide vehicle (Rubert *et al* submitted). Keeping this in mind, 2% alginate hydrogel was ionically cross-linked with 300 mM of CaCl$_2$ and selected as the material of choice. SEM analysis of the microstructure of both alginate gels with and without synthetic peptides after a process of lyophilization revealed a porous and interconnected structure with a pore diameter of 42–44 μm; nevertheless, a compact structure with a pore size of approximately 1 μm diameter was observed after SEM analysis of non-lyophilized gels (data not shown). Diffusion
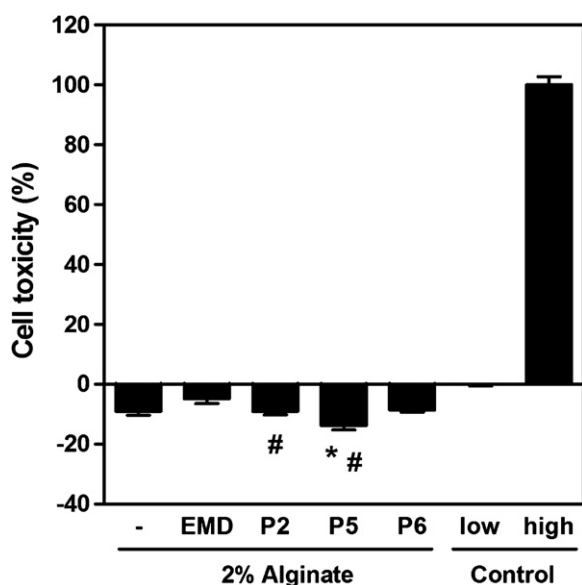
Figure 4. LDH activity measured from culture media collected 24 h after seeding MC3T3-E1 cells onto alginate gels without peptide (-) or alginate gels containing 50 μg ml^{-1} of either Emdogain (EMD) or synthetic peptides (P2, P5 and P6). High control (100%) was cell culture media from cells seeded on tissue culture plastic and incubated with 1% Triton X-100. Low control (0%) was cell culture media from cells seeded on tissue culture plastic and incubated with 0.1% acetic acid-PBS. The percentage of LDH activity was calculated using the following equation: cytotoxicity (%) = (exp.value – low control)/(high control – low control) * 100. Values represent the mean ± SEM. Differences between groups were assessed by Mann–Withney test *$p < 0.05$ versus control alginate gel (-), #$p < 0.05$ versus alginate gel containing EMD.

rate of proteins is affected by the molecular weight and size of the diffusion species (defined by Stokes radii) compared to these pores and depends on the chemical nature of the protein (interactions molecule-alginate, polarization, i.e. hydrophilic drugs may diffuse very quickly while hydrophobic drugs diffuse slowly through the gel pores) [6, 17]. Due to the fact that the synthetic peptides used in the present study are small peptides with 25 amino acids length (molecular weight into the range of 2509.17–2782.34 Da), an easy diffusion rate through the gel should be expected. Accordingly in this study, peptide loaded into 2% alginate hydrogels exhibited a burst release during the first 24 h of incubation followed by progressive and sustained release during the 21 day period.

We further examined the efficiency of alginate gel for cell adhesion and proliferation since alginate has been described as an inert substrate with insufficient protein interaction for cell attachment [18, 19], and it has been suggested that mammalian cells cannot interact with unmodified alginate gels [8]. In fact, to get a highly specific adhesive surface, most of the studies with alginate hydrogel covalently couple to the polymer an entire ECM protein or a peptide sequence capable of binding to cellular receptors [6]. Indeed, some studies have reported that modification of alginate with an RGD (arginine–glycine–aspartic acid)-containing peptide promoted cell adhesion and spreading, whereas minimal cell adhesion was observed on unmodified alginate hydrogels [8, 18]. However, the present study shows that unmodified

alginate hydrogel (Pronova UP LVG®) allow cell attachment and spreading. The differences among the reported studies seem to be due to the described relationship between the composition and purity of the alginate gels used and the ability of cells to proliferate on their surfaces; it has been suggested that M-block fractions are anti-adhesive preventing proliferation and colonization whilst G-fractions promote adhesion and subsequent colonization [19]. In the present study the alginate used contained a minimum of 60% G-fractions, therefore allowing cell attachment and spreading.

The optimal seeding density for the *in vitro* studies was evaluated by DNA quantification. Our results showed that 100×10^3 cells per well was the density with higher efficiency in both, cell adhesion and cell proliferation and, therefore, was chosen for further studies. In agreement with previous reports [6, 10, 15], alginate hydrogel showed to be non-toxic for the MC3T3-E1 cells, displaying some kind of protective effect on cell viability compared to cells cultured on tissue culture plastic. Moreover, we have validated that the synthetic peptides administered as a hydrogel formulation are non-cytotoxic, in agreement with the results obtained in previous studies after short- and long-time cell treatment [3, 4].

Stable osteoblastic cell adhesion is largely mediated by integrins, heterodimeric receptors composed of α and β subunits that dimerize in specific combinations and interact with extracellular matrix proteins [20, 21]. It has been shown that osteoblasts express different integrin receptors depending on the material where they are grown [22–26]. In addition to their role in cell adhesion, integrins regulate cytoskeleton organization and mediate signal transduction, and therefore regulate the expression of genes controlling proliferation, differentiation and matrix remodeling [27, 28]. In order to investigate if the synthetic peptides may affect integrin expression and cell adhesion on the alginate hydrogels, the mRNA expression levels of *Itga8*, *Itgb1*, *Itgb3* and the extracellular matrix protein *Fn1* were studied.

The expression of *Itgb1*, *Itgb3* and *Fn1* was significantly decreased after 14 days of treatment with synthetic peptides, especially for P2 and P6. The β1integrin subunit is found in the bone receptors for collagen, fibronectin and laminin [23, 29–32] mediating adhesion of osteoblasts to ECM whereas $\alpha v \beta$3-integrin would mediate the adhesion to *Opn* [33] and vitronectin [30, 34]. It is interesting to find that expression of $\alpha v \beta$3-integrin stimulates cell proliferation, and inhibits matrix mineralization in osteoblast cells [30]; also that FN—an abundant ECM protein that binds to a large number of integrins, including β1- and β3-integrin subunits [35]—is as well highly expressed in the early stages of osteogenesis while during cell maturation its accumulation in the matrix is reduced [28]. Moreover, treatment with the synthetic peptides increased significantly *Itga8* expression after 21 days of treatment, and markedly when cells were treated with P5. *Itga8* has been shown to interact with osteopontin (*Opn*) [36], a protein secreted by osteoblasts involved in cell adhesion and proliferation [37], whose expression is increased after mineralization has been initiated [38, 39]. Here, bilateral correlation analysis of the *Itga8* and the *Opn* mRNA expression levels showed a Pearson correlation of 0.678 ($p < 0.01$). These
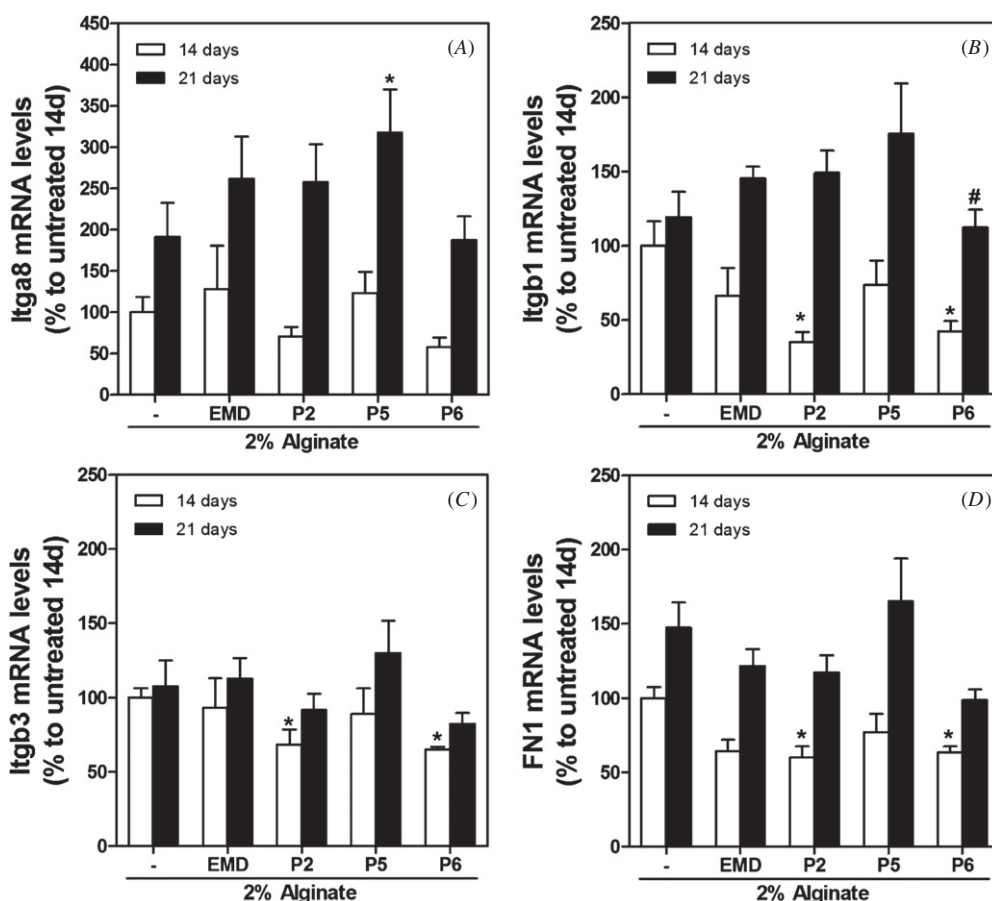
Figure 5. Expression of cell adhesion related genes after culture of MC3T3-E1 cells onto 2% of alginate gels without peptide (-, control group), containing synthetic peptides or EMD (50 μg ml^{-1}) for 14 and 21 days. Data represent relative mRNA levels of target genes normalized with reference genes, expressed as a percentage of control alginate gel at 14 days of culture, which was set to 100%. Values represent the mean $\pm$ SEM. Differences between groups were assessed by Student *t*-test; (*) $p \leqslant 0.05$ versus control alginate gel (-), (#) $p \leqslant 0.05$ versus EMD.

results might indicate that cells treated with the synthetic peptides are in a later stage of cell maturation compared to the control group, and are in line with the expression results of the osteoblast markers analyzed.

It has been described that the short sequence of PPXPP in the C-terminal region of peptides participates in the transactivation activity of transcription factors and/or co-activators [40]. We have previously hypothesized that the mode of action of the synthetic peptides might involve interaction with a receptor capable of influencing intracellular signaling cascades, and that the exposition of their C termini containing conserved proline-rich region (PPLPP) may be of importance in the signaling activity of our synthetic peptides [3]. We have previously shown that all of the studied synthetic peptides showed signature of compact, well-packed structures lacking secondary structure elements, as expected due to the rich content of prolines and expose their PPLPP stretch in a way suitable for interactions, they present different topology of loops. While peptide 2 and peptide 6 present two distinct loops, peptide 5 has different topology of loops that makes possible a contact between C an N terminus. Therefore, the fact these structural differences in the accessibility of the C terminus and structural rigidity of these short consensus sequences (PPXPP) between different peptides could affect the interaction with a

receptor may explain the differential expression of adhesion genes.

On one hand we found that osteocalcin, the most specific and the latest of expressed osteoblast markers with a role in mineralization [41–43], was significantly induced after 14 and 21 days of treatment with the formulated synthetic peptides compared to untreated and EMD alginate gel, i.e. in agreement with the results obtained when administered in the culture media [3, 4]. Accordingly, *Opn*, a sialoprotein produced at various stages of differentiation [44] with higher levels expressed after mineralization has been initiated [38, 39], was significantly up-regulated after 21 days of treatment with both EMD and synthetic peptides compared to control. On the other hand, at the time points studied, no differences were observed in the expression of genes related to osteogenesis (*Coll-I, Bmp-2, Bsp* and *Alp*), as these genes are regulated at earlier stages than osteocalcin during osteoblast differentiation, mainly in the proliferation and matrix maturation phase. It is interesting to note that all the studies that have been performed so far with synthetic peptides that have repetitively shown an increase in osteocalcin mRNA levels, both *in vitro* [3, 4] and in a recent *in vivo* study where Ti implants were coated with the peptides [5]. The relevance of this marker has been demonstrated in a recent *in vivo* study [45], where the best
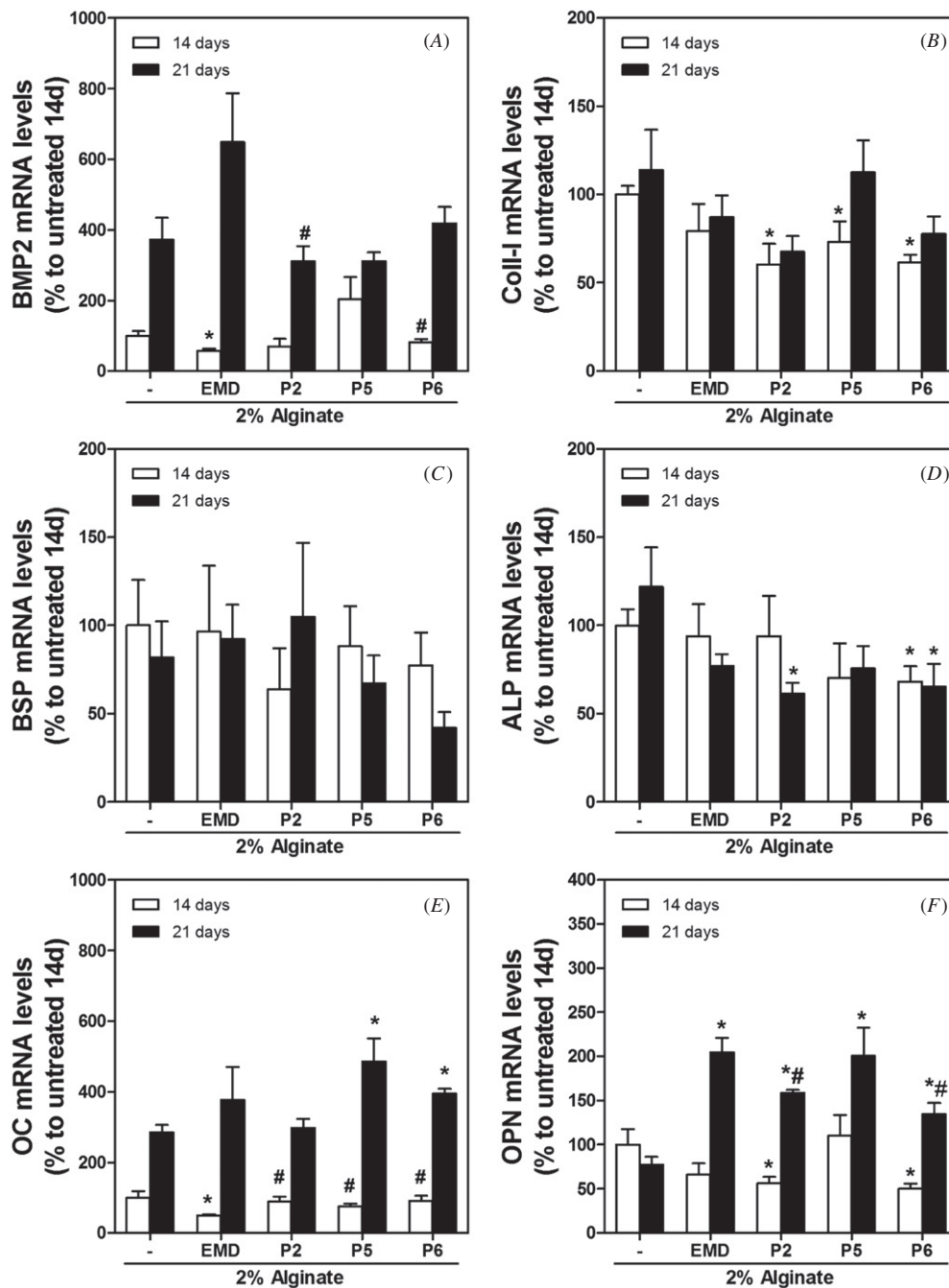
Figure 6. Expression of osteoblast differentiation related genes after culture of MC3T3-E1 cells onto 2% of alginate gels without peptide (-, control group), containing synthetic peptides or EMD (50 μg ml^{-1}) for 14 and 21 days. Data represent relative mRNA levels of target genes normalized with reference genes, expressed as a percentage of control alginate gel at 14 days of culture, which was set to 100%. Values represent the mean $\pm$ SEM. Differences between groups were assessed by Student *t*-test; (*) $p \leqslant 0.05$ versus control alginate gel (-), (#) $p \leqslant 0.05$ versus EMD.

predictive marker for osseointegration of Ti implants among all was osteocalcin. The results from this study suggest that the synthetic peptides improve the alginate gel properties for cell attachment and that the cells cultured on the hydrogel formulated with synthetic peptides were at a more mature stage of the differentiation process over the cells cultured on control hydrogel and hydrogel formulated with EMD.

We have previously hypothesized that the mode of action of the synthetic peptides might involve interaction with a receptor capable of influencing intracellular signaling cascades at the initial states of cell differentiation to finally stimulate osteoblast-differentiation and that the accessibility and structural rigidity of this short consensus sequence (PPXPP) may be of importance in the signaling activity of the synthetic peptides [4]. Further, from the present results we could hypothesize that the peptides could bind to the integrins expressed on cell surface, which first could increase the osteoblast attachment on the alginate hydrogel surface and secondly modulate the expression of genes related with mature osteoblast phenotype.

5. Conclusion

In conclusion, our results demonstrate that 2% of alginate gel is a suitable formulation for the local delivery of synthetic polyproline-rich peptides, inducing integrin alpha 8, osteopontin and osteocalcin expression in MC3T3-E1 cells. These peptide-modified alginate hydrogels may represent a new generation of injectable carriers with bioactive molecules for bone tissue engineering applications and are promising for use as biodegradable coatings for skeletal implants.

Acknowledgments

References

[1] Jin T *et al* 2009 Elongated polyproline motifs facilitate enamel evolution through matrix subunit compaction *PLoS Biol.* **7** 1000262

[2] Ball L J, Kuhne R, Schneider-Mergener J and Oschkinat H 2005 Recognition of proline-rich motifs by protein–protein–interaction domains *Angew. Chem. Int. Ed. Engl.* **44** 2852–69

[3] Ramis J M, Rubert M, Vondrasek J, Gayà A, Lyngstadaas S P and Monjo M 2012 Effect of enamel matrix derivative and of proline-rich synthetic peptides on the differentiation of human mesenchymal stem cells towards the osteogenic lineage *Tissue Eng.* A **18** 1–11

[4] Rubert M, Ramis J M, Vondrasek J, Gayà A, Lyngstadaas SP and Monjo M 2011 Synthetic peptides analogue to enamel proteins promote osteogenic differentiation of MC3T3-E1 and mesenchymal stem cells *J. Biomater. Tissue Eng.* **1** 198–209

[5] Petzold C, Monjo M, Rubert M, Reinholt F P, Gomez-Florit M, Ramis J M, Ellingsen J E and Lyngstadaas S P 2012 Effect of coated titanium implants with a proline-rich synthetic peptide on bone healing *Oral Craniofac. Tissue Eng.* **2** 35–43

[6] Drury J L and Mooney D J 2003 Hydrogels for tissue engineering: scaffold design variables and applications *Biomaterials* **24** 4337–51

[7] Tan H, Li H, Rubin J P and Marra K G 2011 Controlled gelation and degradation rates of injectable hyaluronic acid-based hydrogels through a double crosslinking strategy *J. Tissue Eng. Regen. Med.* **5** 790–97

[8] Rowley J A, Madlambayan G and Mooney D J 1999 Alginate hydrogels as synthetic extracellular matrix materials *Biomaterials* **20** 45–53

[9] Lopiz-Morales Y, Abarrategi A, Ramos V, Moreno-Vicente C, Lopez-Duran L, Lopez-Lacomba J and Marco F 2010 *In vivo* comparison of the effects of rhBMP-2 and rhBMP-4 in

osteochondral tissue regeneration *Eur. Cell. Mater.* **20** 367–78

[10] Lee J Y, Choo J E, Park H J, Park J B, Lee S C, Jo I, Lee S J, Chung C P and Park Y J 2007 Injectable gel with synthetic collagen-binding peptide for enhanced osteogenesis *in vitro* and *in vivo Biochem. Biophys. Res. Commun.* **357** 68–74

[11] Lin C-C and Metters A T 2006 Hydrogels in controlled release formulations: network design and mathematical modeling *Adv. Drug Deliv. Rev.* **58** 1379–408

[12] Tan H, Ramirez C M, Miljkovic N, Li H, Rubin J P and Marra K G 2009 Thermosensitive injectable hyaluronic acid hydrogel for adipose tissue engineering *Biomaterials* **30** 6844–53

[13] Lin N, Lin J, Bo L, Weidong P, Chen S and Xu R 2010 Differentiation of bone marrow-derived mesenchymal stem cells into hepatocyte-like cells in an alginate scaffold *Cell Prolif.* **43** 427–34

[14] Tan H, Chu C R, Payne K A and Marra K G 2009 Injectable *in situ* forming biodegradable chitosan-hyaluronic acid based hydrogels for cartilage tissue engineering *Biomaterials* **30** 2499–506

[15] Barbetta A, Barigelli E and Dentini M 2009 Porous alginate hydrogels: synthetic methods for tailoring the porous texture *Biomacromolecules* **10** 2328–37

[16] Tiainen H, Monjo M, Knychala J, Nilsen O, Lyngstadaas S P, Ellingsen J E and Haugen H J 2011 The effect of fluoride surface modification of ceramic TiO_2 on the surface properties and biological response of osteoblastic cells *in vitro Biomed. Mater.* **6** 045006

[17] Augst A D, Kong H J and Mooney D J 2006 Alginate hydrogels as biomaterials *Macromol. Biosci.* **6** 623–33

[18] Alsberg E, Anderson K W, Albeiruti A, Franceschi R T and Mooney D J 2001 Cell-interactive alginate hydrogels for bone tissue engineering *J. Dent. Res.* **80** 2025–9

[19] Wang L, Shelton R M, Cooper P R, Lawson M, Triffitt J T and Barralet J E 2003 Evaluation of sodium alginate for bone marrow cell tissue engineering *Biomaterials* **24** 3475–81

[20] Adams J C and Watt F M 1993 Regulation of development and differentiation by the extracellular matrix *Development* **117** 1183–98

[21] Danen E H and Yamada K M 2001 Fibronectin, integrins, and growth control *J. Cell. Physiol.* **189** 1–13

[22] El-Amin S F, Attawia M, Lu H H, Shah A K, Chang R, Hickok N J, Tuan R S and Laurencin C T 2002 Integrin expression by human osteoblasts cultured on degradable polymeric materials applicable for tissue engineered bone *J. Orthop. Res.* **20** 20–8

[23] Gronowicz G and McCarthy M B 1996 Response of human osteoblasts to implant materials: integrin-mediated adhesion *J. Orthop. Res.* **14** 878–87

[24] Lynch M P, Stein J L, Stein G S and Lian J B 1995 The influence of type I collagen on the development and maintenance of the osteoblast phenotype in primary and passaged rat calvarial osteoblasts: modification of expression of genes supporting cell growth, adhesion, and extracellular matrix mineralization *Exp. Cell Res.* **216** 35–45

[25] Siebers M C, ter Brugge P J, Walboomers X F and Jansen J A 2005 Integrins as linker proteins between osteoblasts and bone replacing materials. A critical review *Biomaterials* **26** 137–46

[26] Steele J G, Dalton B A, Johnson G and Underwood P A 1993 Polystyrene chemistry affects vitronectin activity: an explanation for cell attachment to tissue culture polystyrene but not to unmodified polystyrene *J. Biomed. Mater. Res.* A **27** 927–40

[27] Hynes R O 1992 Integrins: versatility, modulation, and signaling in cell adhesion *Cell* **69** 11–25

[28] Moursi A M, Globus R K and Damsky C H 1997 Interactions between integrin receptors and fibronectin are required for calvarial osteoblast differentiation *in vitro J. Cell. Sci.* **110** 2187–96

[29] Carvalho R S, Kostenuik P J, Salih E, Bumann A and Gerstenfeld L C 2003 Selective adhesion of osteoblastic cells to different integrin ligands induces osteopontin gene expression *Matrix Biol.* **22** 241–9

[30] Cheng S-L, Lai C-F, Blystone S D and Avioli L V 2001 Bone mineralization and osteoblast differentiation are negatively modulated by integrin $\alpha v \beta 3$ *J. Bone Miner. Res.* **16** 277–88

[31] Grzesik W J and Robey PG 1994 Bone matrix RGD glycoproteins: immunolocalization and interaction with human primary osteoblastic bone cells *in vitro J. Bone Miner. Res.* **9** 487–96

[32] Johansson S, Svineng G, Wennerberg K, Armulik A and Lohikangas L 1997 Fibronectin-integrin interactions *Front. Biosci.* **2** d126–46

[33] Chellaiah M A and Hruska K A 2003 The integrin alpha(v)beta(3) and CD44 regulate the actions of osteopontin on osteoclast motility *Calcif. Tissue Int.* **72** 197–205

[34] Helfrich M H, Nesbitt S A, Dorey E L and Horton M A 1992 Rat osteoclasts adhere to a wide range of RGD (Arg-Gly-Asp) peptide-containing proteins, including the bone sialoproteins and fibronectin, via a beta 3 integrin *J. Bone Miner. Res.* **7** 335–43

[35] Li J, Wang L, He G, Luo M, Qian A and Shang P 2011 Fibronectin is involved in gravity-sensing of osteoblast like cell *J. Japan Soc. Microgravity Appl.* **28** S36–40

[36] Denda S, Reichardt L F and Müller U 1998 Identification of osteopontin as a novel ligand for the integrin $\alpha 8 \beta 1$ and potential roles for this integrin–ligand interaction in kidney morphogenesis *Mol. Biol. Cell.* **9** 1425–35

[37] Bueno Rde B, Adachi P, Castro-Raucci L M, Rosa A L, Nanci A and Oliveira P T 2011 Oxidative nanopatterning of titanium surfaces promotes production and extracellular accumulation of osteopontin *Braz. Dent. J.* **22** 179–84

[38] McKee M D and Nanci A 1995 Osteopontin and the bone remodeling sequence *Ann. NY Acad. Sci.* **760** 177–89

[39] Sodek J, Chen J, Nagata T, Kasugai S, Todescan R Jr, Li I W and Kim R H 1995 Regulation of osteopontin expression in osteoblasts *Ann. NY Acad. Sci.* **760** 223–41

[40] Wang Z and Melmed S 2000 Pituitary tumor transforming gene (PTTG) transforming and transactivation activity *J. Biol. Chem.* **275** 7459–61

[41] Desbois C, Hogue D A and Karsenty G 1994 The mouse osteocalcin gene cluster contains three genes with two separate spatial and temporal patterns of expression *J. Biol. Chem.* **269** 1183–90

[42] Ducy P *et al* 1996 Increased bone formation in osteocalcin-deficient mice *Nature* **382** 448–52

[43] Hauschka P V, Lian J B, Cole D E and Gundberg C M 1989 Osteocalcin and matrix Gla protein: vitamin K-dependent proteins in bone *Physiol. Rev.* **69** 990–1047

[44] Sodek J, Ganss B and McKee M D 2000 Osteopontin *Crit. Rev. Oral Biol. Med.* **11** 279–303

[45] Monjo M, Ramis J M, Ronold H J, Taxt-Lamolle S F, Ellingsen J E and Lyngstadaas S P 2012 Correlation between molecular signals and bone bonding to titanium implants *Clin. Oral Implants Res.* doi: 10.1111/j.1600-0501.2012.02496.x

Paper 5

TiO$_2$ scaffolds sustain differentiation of MC3T3-E1 cells.

Gómez-Florit, M.; Rubert, M.; Ramis, J.M.; Haugen, H.J.; Tiainen, H.; Lyngstadaas, S.P;

Monjo, M.

TiO$_2$ Scaffolds Sustain Differentiation of MC3T3-E1 Cells

Manuel Gómez-Florit[1], Marina Rubert[1], Joana M. Ramis[1], Håvard J. Haugen[2],
Hanna Tiainen[2], Staale Petter Lyngstadaas[2], and Marta Monjo[1, *]

[1] *Department of Fundamental Biology and Health Sciences, Research Institute on Health Sciences (IUNICS),
University of Balearic Islands, Palma de Mallorca, E-07122, Spain*
[2] *Department of Biomaterials, University of Oslo, Oslo, N-0317, Norway*

The aim of the present study was to investigate distribution, growth and differentiation of MC3T3-E1 osteoblasts over time using an agitated seeding method into highly porous TiO$_2$ scaffolds. Cells penetrated into the core of the 3D scaffold structure as confirmed with confocal microscopy analysis. DNA quantification and scanning electron microscopy confirmed a good proliferation of cells on the TiO$_2$ scaffolds. Moreover, time course of gene expression profile of cell adhesion (fibronectin and integrins) and osteoblast phenotypic markers (collagen type 1, bone morphogenetic protein 2, bone sialoprotein, osteopontin and osteocalcin) showed a good progression in the sequential stages of osteoblast differentiation, i.e., initial adhesion and proliferation, extracellular matrix maturation and mineralization. This was followed by an increase in ALP activity and calcium content after 21 days, the hallmark of osteoblast function. Taking all these results together, TiO$_2$ scaffolds have shown to sustain MC3T3-E1 growth towards a mature and differentiated state.

Keywords: Titanium Dioxide, Three-Dimensional Scaffold, Osteoblast, Seeding, Differentiation, Gene Expression.

1. INTRODUCTION

Scaffold-based bone tissue engineering aims at restoring damaged, diseased and resorbed bone tissue as an alternative to bone autografts, which add another surgical site, often resulting in additional pain and complications, or to allogenic bone grafts, which have a minimal but real risk of immunological rejection or disease transmission.[1–4] Scaffolds are expected to guide the development of new bone tissue by supporting cell colonization, migration, growth and differentiation of bone-forming cells. Optimal scaffolds are designed to provide mechanical stability while supporting osteoconduction, osteoinduction and osteogenesis. The structure of a scaffold determines cell migration and differentiation, bone ingrowth, vascularization, and mass transfer between the cells and the environment. All of these processes benefit from increased scaffold porosity, interconnected pore networks, large surface-area-to-volume ratio and increased surface roughness.[5]

Over the last decades, different polymers and bioceramics have been tested for use in bone tissue engineering. Mechanical properties of polymers are insufficient to support bone growth under loading conditions or they have concerns about biocompatibility and immunogenicity.[5] Ceramics like bioactive glass, calcium sulfate or calcium phosphate, despite their high compressive strength, are too brittle[4] and do not, on their own, have sufficient osteogenic properties to allow the bone to reconstruct over large defects;[6] their use, therefore, is limited to non-load-bearing sites.[4]

Titanium dioxide (TiO$_2$) is a biocompatible material, which has also been reported to have bioactive properties[7, 8] and a certain degree of bacteriostatic effect.[9] In previous studies, TiO$_2$ scaffolds have shown to promote good cell adhesion and growth of mouse osteoblasts into the TiO$_2$ structure.[10, 11] It has also been reported that TiO$_2$ scaffolds provide a better substrate for the proliferation and viability of human mesenchymal stem cells rather than different commercially available bone graft substitutes.[12] However, these scaffolds had limited mechanical properties for load-bearing applications (maximum compressive strength of 1.2 MPa).[10] Highly porous and well interconnected TiO$_2$ scaffolds with high compressive strength (above 2.5 MPa) have been developed,[13] optimizing the parameters described by Tiainen et al. and Fostad et al.[10, 13] No other studies with scaffolds made from bioactive ceramics have been reported with equally high compressive strength and an average porosity between 80–90%.[13] *In vivo*, these scaffolds have shown to permit newly bone

tissue formation throughout the entire scaffold volume, showing the generated bone a mineral density comparable to that of the native cortical bone.[14]

The initial cell number and the spatial distribution in three dimensional (3D) structures are determined by the seeding method used. Therefore, proliferation, cell–cell interactions and differentiation of cells will be affected by the seeding method.[15, 16] Static cell seeding has been widely used in 3D structures; however, low seeding efficiencies and no uniform cell distributions are obtained with this method.[15, 17] Many studies have demonstrated the beneficial effects of non-static seeding methods as regards to cell attachment, cell distribution, and long-term survival and function in different cell types;[18] hence, it is important to achieve a homogeneous distribution of cells inside 3D structures.[19] Agitated seeding methods have enabled a better attachment[18, 20] and better distribution of cells[21] to 3D scaffolds compared to conventional static methods. As the structure of a scaffold affects cell adhesion, growth and differentiation, and MC3T3-E1 cells represent a commonly used model for testing biomaterials, it was of interest to investigate the behavior over time of MC3T3-E1 osteoblasts on highly porous TiO₂ scaffolds, since this has never been reported before.

Therefore, the aims of the present investigation were: (1) To study the distribution and growth of cells on highly porous scaffolds using an agitated seeding method; (2) to test the *in vitro* adhesion and differentiation process of MC3T3-E1 osteoblasts analyzing osteogenic biomarkers profiles over time; and (3) to study the formation of a mineralized ECM within the 3D highly porous structure of TiO₂ scaffolds.

2. MATERIALS AND METHODS

2.1. Production of TiO₂ Scaffolds

Ceramic TiO₂ scaffolds were fabricated by replication process as previously described.[13] Briefly, TiO₂ slurry was prepared by dispersing 65 g of TiO₂ powder (Kronos 1171, Kronos Titan GmbH, Leverkusen, Germany) in 25 ml of sterilized H₂O and the pH of the dispersion was kept at 1.5 for the entire duration of the stirring with small additions of 1 M HCl. The stirring was continued for 2.5 h at 5000 rpm. Cylindrical polyurethane foam templates (60 ppi, Bulbren S, Eurofoam GmbH, Wiesbaden, Germany) were coated with the prepared slurry. Prior to sintering at 1500 °C for 40 h, the polymer sponge was carefully burnt out of the green body at a lower temperature. After sintering, the scaffolds were recoated with slurry that was prepared using the previously described procedure, but this time mixing 40 g of TiO₂ powder with 25 ml of H₂O. The recoated scaffolds were then sintered in 1500 °C for 24 h. The final dimensions of the scaffolds were 8 mm in diameter and 7 mm height. The scaffolds were steam sterilized in 121 °C for 20 minutes.

2.2. Homogeneous MC3T3-E1 Cell Seeding on TiO₂ Scaffolds

The mouse osteoblastic cell line MC3T3-E1 (DSMZ, Braunschweig, Germany) was chosen as an *in vitro* model. Cells were regularly cultured at 37 °C in a humidified atmosphere of 5% CO₂, and maintained in α-MEM (PAA Laboratories GmbH, Pasching, Austria) supplemented with 10% fetal calf serum (FCS, PAA Laboratories GmbH, Pasching, Austria), 100 U penicillin/ml and 100 μg streptomycin/ml (PAA Laboratories GmbH, Pasching, Austria). Culture media was changed every other day. Cells were subcultured 1:5 before reaching confluence using PBS and trypsin/EDTA. All experiments were carried out after 12 passages of the MC3T3-E1 cells.

The scaffold samples were placed into 48-well cell culture plates ($\varnothing$9.75 mm) in sterile conditions. Different cell seeding densities (6.0×10^4, 1.2×10^5 or 2.0×10^5 cells/scaffold in 800 μl) were seeded on the TiO₂ scaffolds. Special attention was taken to pipette the cell suspension on the well wall to avoid that the cells remained on the scaffold surface by surface tension. After adding the cell suspension to the scaffolds, plates were agitated on an orbital shaker (Unitron, Infors HT, Basel, Switzerland) for 6 hours at 180 rpm at 37 °C. Then, the scaffolds were placed in new 48-well cell culture plates and 500 μl of culture media were added. MC3T3-E1 cells were maintained in culture media for different times. At the day of analysis, samples for scanning electron microscopy (SEM) and confocal microcopy visualization and for ALP and Ca²⁺ determination were placed in a new plate and washed with 700 μl of PBS. Samples for DNA quantification and real time RT-PCR analysis were frozen at −80 °C for later analysis.

2.3. Cell Number Determination

For cell number determination, cells growing on the scaffolds and cells that remained on TCP after 1, 7, 14 and 21 days were lysed by a freeze-thaw method in 700 μl of deionized distilled water.[22] 100 μl of the cell lysates were used for determination of DNA quantity using Hoechst 33258 fluorescence assay. Samples were mixed with 20 μg/ml of Hoechst 33258 fluorescence stain (Sigma, St. Quentin Fallavier, France) in TNE buffer, and the intensity of fluorescence was measured at excitation and emission wavelengths of 356/465 nm using a multifunction microplate reader (Cary Eclipse fluorescence spectrophotometer, Agilent Technologies, Santa Clara, USA). Relative fluorescence units were correlated with the cell number using a linear standard curve.

2.4. Confocal Laser Scanning Microscopy

MC3T3-E1 cells growing for 1, 7, 14 and 21 days on TiO₂ scaffolds were washed twice with cold PBS, followed by fixation for 15 minutes with 4% formaldehyde

in PBS. Cells were washed twice with PBS before cutting the scaffolds in three slices with a razor-blade. Cells were permeabilized with Triton X-100 1% in PBS for 4 minutes. Again, cells were washed with PBS and were stained with 5 μg/ml of Phalloidin-FITC (Sigma, St. Quentin Fallavier, France) in PBS for 30 minutes in the dark. Cells were washed with PBS and the scaffold slices were placed on slides. Finally, a drop of Fluoroshield™ with DAPI (Sigma, Schnelldorf, Germany) was added and cover glasses were mounted on the scaffolds.

Each scaffold slice (top, centre and bottom) was examined with a confocal microscope (Leica TCS SPE) and 400 μm depth projection micrographs were constructed from 40 horizontal image sections through the scaffold. Excitation wavelengths of DAPI and Phalloidin-FITC were set at 405 and 488 nm, respectively; fluorescence was captured between 430–480 nm for DAPI and between 500–525 nm for Phalloidin-FITC. Images presented are from a representative area of a central slice.

2.5. Scanning Electron Microscopy

Morphology of cells growing on TiO$_2$ scaffolds after 1, 7, 14 and 21 days of cell culture was observed using a scanning electron microscope (Hitachi S-3400N, Hitachi High-Technologies Europe GmbH, Krefeld, Germany). Briefly, cells were washed twice with PBS and fixed with glutaraldehyde 4% in PBS for 2 hours. Then, the fixative solution was removed and the cells were washed with distilled water twice. At 30 minute intervals, the cells were dehydrated by the addition of 50%, 70%, 90% and 100% ethanol solutions. Ethanol was removed and the cells were left at room temperature to evaporate the remaining ethanol. Scaffolds were observed at 10 kV and 40 Pa using back scattered and secondary electrons. Images presented are from a representative superficial area.

2.6. RNA Isolation and RT-PCR Analysis

Total RNA was isolated using Tripure® (Roche Diagnostics, Mannheim, Germany), according to the manufacturer's protocol. Total RNA was quantified at 260 nm using a Nanodrop spectrophotometer (NanoDrop Technologies, Wilmington, DE, USA). The same amount of RNA (600 ng) was reverse transcribed to cDNA at 42 °C for 60 min using High Capacity RNA-to-cDNA kit (Applied Biosystems, Foster City, CA), according to the protocol of the supplier. Aliquots of each cDNA were frozen (-20 °C) until the PCR reactions were carried out.

Real-time PCR was performed in the Lightcycler 480® (Roche Diagnostics, Mannheim, Germany) using SYBR green detection. Real time PCR was done for two reference genes (18 S rRNA and glyceraldehyde-3-phosphate dehydrogenase (*Gapdh*)) and target genes (collagen type I (*Col1a1*), bone morphogenetic protein 2 (*Bmp2*), bone sialoprotein (*Bsp*), osteocalcin (*Oc*), osteopontin (*Opn*)

Table I. Primer sequences used for real-time RT-PCR analysis.

Gene	Primer sequence
18 S rRNA	S 5′-GTAACCCGTTGAACCCCATT-3′
	A 5′-CCATCCAATCGGTAGTAGCG-3′
Gapdh	S 5′-ACCCAGAAGACTGTGGATGG-3′
	A 5′-CACATTGGGGGTAGGAACAC-3′
*Bmp*2	S 5′-GCTCCACAAACGAGAAAAGC-3′
	A 5′-AGCAAGGGGAAAAGGACACT-3′
Bsp	S 5′-GAAAATGGAGACGGCGATAG-3′
	A 5′-ACCCGAGAGTGTGGAAAGTG-3′
*Col*1*a*1	S 5′- AGAGCATGACCGATGGATTC -3′
	A 5′- CCTTCTTGAGGTTGCCAGTC-3′
*Fn*1	S 5′- GCTGCCAGGAGACAGCCGTG-3′
	A 5′- GTCTTGCCGCCCTTCGGTGG-3′
*Itga*8	S 5′- TCGCCTGGGAGGAGGCGAAA-3′
	A 5′- TCTTAACCGCTGTGCTCCCCG-3′
*Itgb*1	S 5′-AGCAGGCGTGGTTGCTGGAA-3′
	A 5′- TTTCACCCGTGTCCCACTTGGC-3′
*Itgb*3	S 5′- AGGGGAGATGTGTTCCGGCCA-3′
	A 5′-ACACACAGCTGCCGCACTCG-3′
Oc	S 5′- CCGGGAGCAGTGTGAGCTTA-3′
	A 5′-TAGATGCGTTTGTAGGCGGTC -3′
Opn	S 5′-TCTGCGGCAGGCATTCTCGG-3′
	A 5′-GTCACTTTCACCGGGAGGGAGGA-3′

fibronectin-1 (*Fn*1) and integrins α8, β1 and β3 (*Itga*8, *Itgb*1 and *Itgb*3)). The primer sequences were designed using the NCBI primer designing tool and are detailed in Table I.

Each reaction contained 7 μl Lightcycler-FastStart DNA MasterPLUS SYBR Green I (containing Fast Start Taq polymerase, reaction buffer, dNTPs mix, SYBR Green I dye and MgCl$_2$), 0.5 μM of each, the sense and the antisense specific primers and 3 μl of the cDNA dilution in a final volume of 10 μl. The amplification program consisted of a preincubation step for denaturation of the template cDNA (10 min 95 °C), followed by 45 cycles consisting of a denaturation step (10 s 95 °C), an annealing step (10 s 60 °C) and an extension step (10 s 72 °C). After each cycle, fluorescence was measured at 72 °C (λ_{ex} 470 nm, λ_{em} 530 nm). A negative control without cDNA template was run in each assay.

Real-time efficiencies (E) were calculated from the given slopes in the LightCycler 480 software using serial dilutions, showing all the investigated transcripts high real-time PCR efficiency rates, and high linearity when different concentrations were used. PCR products were subjected to a melting curve analysis on the LightCycler and subsequently 2% agarose/TAE gel electrophoresis to confirm amplification specificity, T_m and amplicon size, respectively.

All samples were normalized by the geometric mean of the expression levels of 18 S rRNA and *Gapdh* and fold changes were related to day 1 of culture using the mathematical model described by Pfaffl:[23] Ratio = $E_{target}^{\Delta Cp\,target\,(mean\,day\,1-sample)}/E_{reference}^{\Delta Cp\,target\,(mean\,day\,1-sample)}$, where Cp is the is the crossing point of the reaction amplification curve as determined by the LightCycler 480 software.

RESEARCH ARTICLE

Stability of reference genes was calculated using the BestKeeper tool.[24]

2.7. ALP Activity

ALP activity was determined from cells after 1, 7, 14 and 21 days of cell culture, as described previously by Hinoi et al.[25] Briefly, cells were washed twice in PBS, solubilized with 0.1% Triton X-100. Then, samples were incubated with an assay mixture of *p*-Nitrophenyl Phosphate (*p*NPP). Cleavage of *p*NPP (Sigma, Saint Louis, Missouri, USA) in a soluble yellow end product which absorb at 405 nm was used to assess ALP activity. In parallel to the samples, a standard curve with calf intestinal alkaline phosphatase (CIAP) (Promega, Madison, USA) was constructed; 1 μl from the stock CIAP was mixed with 5 ml of alkaline phosphatase buffer (1:5000 dilution), and subsequently diluted 1:5.

2.8. Determination of Calcium Content

Total calcium content was quantified after 1, 7, 14 and 21 days of culture. Cells were washed twice in PBS and solubilized with 0.1% Triton X-100. Lysates were also treated with 0.5 N hydrochloric acid overnight, followed by centrifugation at 500$\times$ g for 2 minutes for the subsequent determination of Ca^{2+} content in the supernatant by inductively coupled plasma atomic emission spectrometer (ICP-AES) Optima 5300 DV (PerkinElmer, Massachusetts, USA). Data were compared with CaCl$_2$ standards included in the assay.

2.9. Statistics

All data are presented as mean values $\pm$ SEM (standard error of the mean). The Kolmogorov-Smirnov test was done to assume parametric or non-parametric distributions for the normality tests. Differences between groups were assessed by Mann-Whitney-test or by Student *t*-test depending on their normal distribution. SPSS® program for Windows, version 17.0 was used. Results were considered statistically significant at *p*-values ≤ 0.05.

3. RESULTS

3.1. Cell Number

The number of MC3T3-E1 cells attached to the scaffolds and the number of cells that remained on the plastic wells was measured through cellular DNA quantification at different time points. In a preliminary experiment, the seeding efficiency was evaluated (Fig. 1(A)). Results showed that after an overnight incubation, approximately half of the cells that had been added were attached to the scaffold surface and the other half were attached to the TCP surface. From these results, a seeding density of 2.0×10^5 cells/scaffold was selected for further experiments. Then, the number of cells attached to the scaffolds over time was determined (Fig. 1(B)). After 24 hours of cell culture, half of the cells initially seeded were attached to the scaffolds, in agreement to the preliminary experiment. Compared to day 1, cell number was significantly increased at further time points. The number of cells after 7 days of culture was about three times higher than after day one. However, from day 14, cell number decreased to $\sim 2.0 \times 10^5$ cells.

3.2. Confocal Laser Scanning Microscopy Analysis

Confocal images were used to qualitatively evaluate the initial cell distribution and long-term infiltration throughout the scaffolds. As seen in Figure 2 (pictures from the
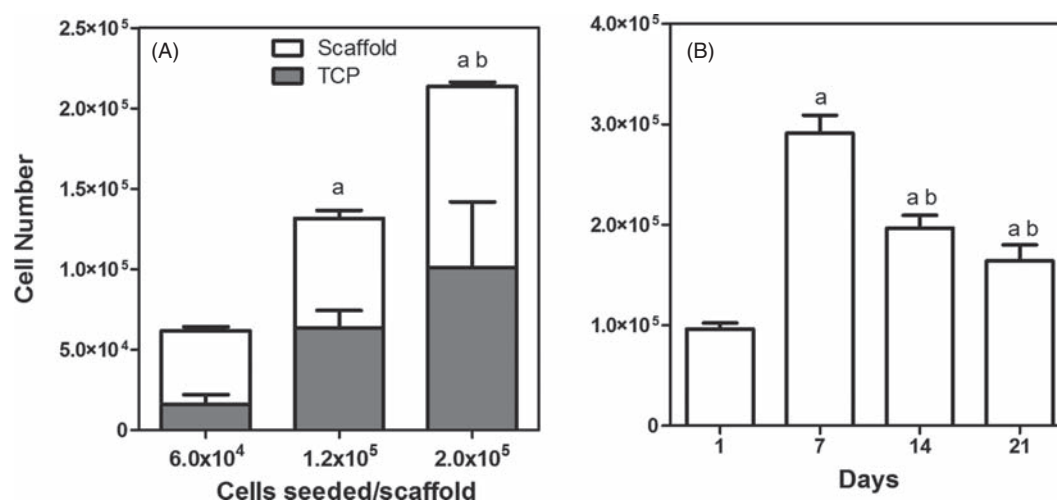

Fig. 1. Number of cells attached to the scaffolds after 1 day (A) and after 1, 7, 14 and 21 days (B) of culture. DNA content was analyzed by Hoechst fluorescence staining and correlated to a linear standard curve. Data shown represent the mean $\pm$ SEM ($n = 6$). Student *t*-test, $p \leq 0.05$: (a) versus day 1, (b) versus day 7, (c) versus day 14.
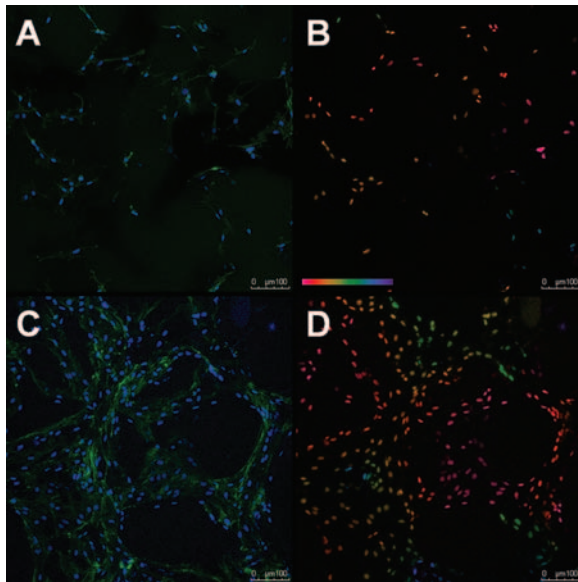
Fig. 2. Confocal depth projection micrographs of MC3T3-E1 cells cultured for 1 (A), (B) and 14 (C), (D) days on TiO₂ scaffolds. Cells were stained with Phalloidin-FITC (stains actin filaments; green) and DAPI (stains nucleus; blue). Images were 2D reconstructions of sections acquired repeatedly in sequential steps along the *z*-axis. In (B) and (D), the color scale bar corresponds to the *z*-axis depth of DAPI-stained nucleus, coded from pink at 0 μm and blue at 400 μm depth.

central slice of the scaffold), a homogeneous cell presence throughout the scaffold structure was observed after 1 day of culture, confirming the penetration of cells into the scaffold core using the agitated seeding method. After 14 days, cell number was higher, confirming the long-term growth inside the scaffolds. It was also observed that cells had already covered the most of the scaffold surface and a dense network of actin filaments had been synthesized that stretched along the scaffold. The same behaviour was found on the top and bottom slices of the scaffolds after 1 and 14 days (data not shown).

3.3. Scanning Electron Microscopy Analysis

Morphological changes of seeded cells on the scaffolds were observed after 1, 7, 14 and 21 days of culture by SEM. After one day of culture (Figs. 3(A)–(B)), cells appeared polygonal, spindle-shaped, and attached and spread on the TiO₂ scaffolds. Individual cells could be seen deeper into the scaffold structures. Many cells spreaded and colonized the material surface within 7 days of culture (Figs. 3(C)–(D)), in addition, some cells bridging the scaffold pores were observed. After 14 days of culture (Figs. 3(E)–(F)), the spreading cells maintained physical contact with each other through filopodia or lamellopodia. At the day 21 of culture (Figs. 3(G)–(H)), dense layers of cells covered patches of the TiO₂ surface. Cell growth within the larger pores was limited by the ability of the cells to bridge the pore. The morphological behaviour of
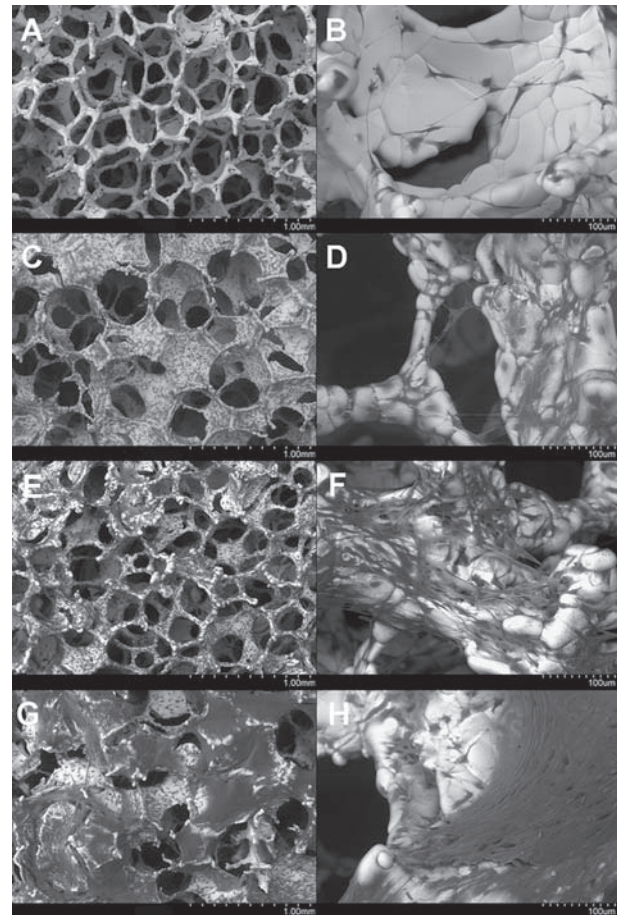

Fig. 3. SEM visualization of MC3T3-E1 cells growing on the scaffolds for 1 (A), (B), 7 (C), (D), 14 (E), (F) or 21 (G), (H) days. Scaffolds were observed by SEM at 10 kV, 40 Pa and at a magnification of ×50 (A), (C), (E), (G) or ×300 (B), (D), (F), (H).

the cells on the TiO₂ scaffolds was similar to that in the material-free culture (not shown).

3.4. RT-PCR Analysis

Stability of the reference genes was assessed with the BestKeeper tool. The crossing point variation of the reference genes among samples was lower than 0.64. Moreover, a good consistence of the bestkeeper index was proved as its contributing reference genes were tightly correlated with it ($0.848 < r < 0.922$), with a significance level of $p = 0.001$ for all reference genes.

Regarding the gene expression of the cell adhesion markers analysed (Fig. 4(A)), an up-regulation over time of the mRNA levels of fibronectin was observed, though significant differences were only found after 14 and 21 days of culture compared to day 1. About the integrin receptors, the mRNA levels of *Itga*8 remained unchanged over time, while mRNA levels of *Itgb*1 and *Itgb*3 were downregulated after 7 days of culture and then remained stable for *Itgb*3 and were further downregulated at day 21 for *Itgb*1.
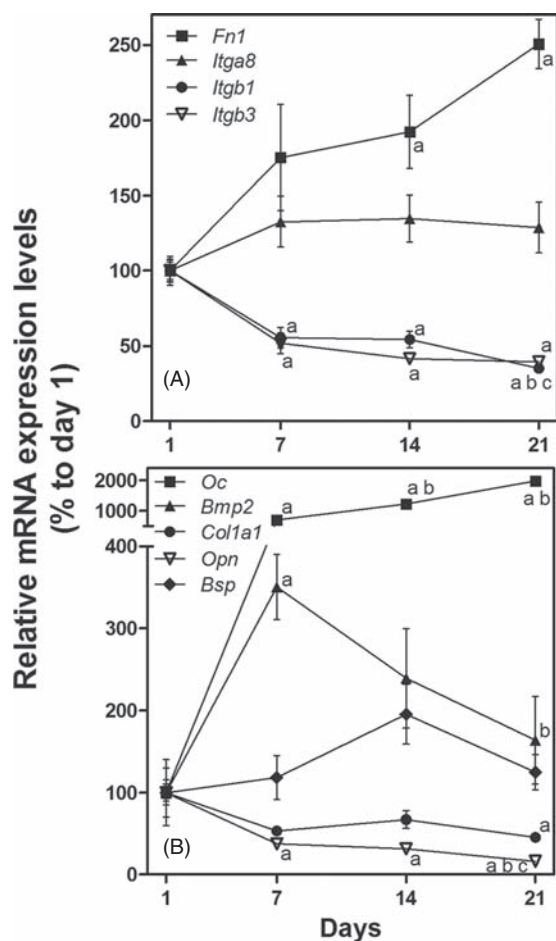
Fig. 4. Relative mRNA levels of *Fn*1, *Itga*8, *Itgb*1 and *Itgb*3 (A) and *Oc*, *Col*1*a*1, *Bmp*2, *Bsp* and *Opn* (B) in MC3T3-E1 cells cultured on TiO$_2$ scaffolds for 1, 7, 14 and 21 days. Data represent fold changes of target genes normalized with reference genes (rRNA 18 S and *Gapdh*), expressed as a percentage of cells seeded on scaffolds at 1 day, which were set to 100%. Data shown represent the mean ± SEM ($n = 6$). Student t-test, $p \leq 0.05$: (a) versus day 1, (b) versus day 7, (c) versus day 14.

Regarding the gene expression of selected osteoblast differentiation markers (Fig. 4(B)), an increase on the mRNA expression levels of *Bmp*2 was observed after 7 days of cell culture, followed by a decrease that was statistically significant compared to day 7 at day 21. No significant differences over the first 14 days of culture were observed for *Col*1*a*1 mRNA levels, although a significant decrease was observed at day 21 compared to day 1. As regards to *Bsp* mRNA levels, no significant differences over time were found. While *Oc* gene expression was highly upregulated, *Opn* expression was downregulated over time.

3.5. ALP Activity and Calcium Content

To examine osteoblasts differentiation on the scaffolds over time, ALP activity and calcium content was measured. ALP activity showed a significant increase at
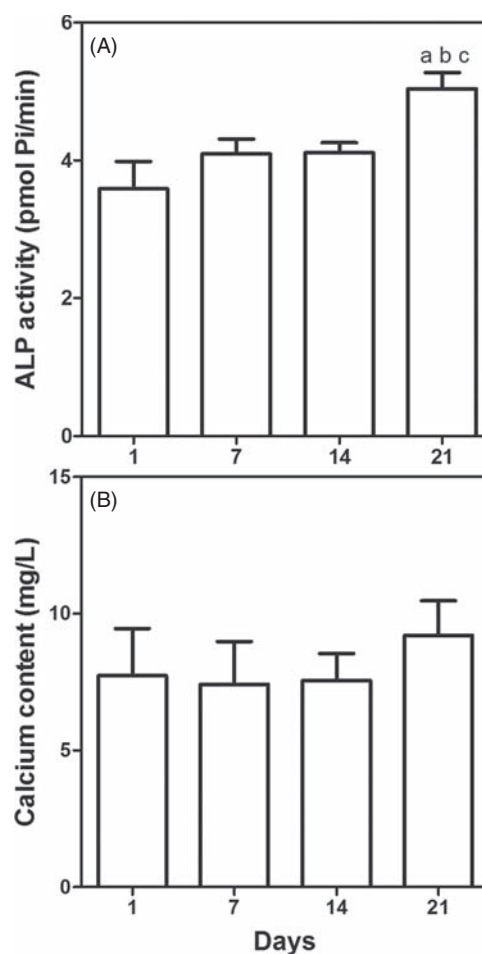
Fig. 5. ALP activity (A) and calcium content (B) after 1, 7, 14 and 21 days of cell culture. Data shown represent the mean ± SEM ($n = 6$). Student t-test, $p \leq 0.05$: (a) versus day 1, (b) versus day 7, (c) versus day 14.

day 21 compared to the previous days (Fig. 5(A)), giving an indication of progressing maturation of the extracellular matrix. Calcium content was increased after 21 days of culture, although yet no significant differences were found.

4. DISCUSSION

In the present study, the distribution, adhesion, proliferation and differentiation of MC3T3-E1 cells on highly porous TiO$_2$ scaffolds were evaluated using an agitated seeding method. MC3T3-E1 mouse pre-osteoblasts were selected for their ability to form a bone-like ECM and express osteoblast markers.[26, 27]

An agitated seeding method was used to achieve a better attachment and distribution of cells throughout the 3D scaffold structure compared to conventional static methods as previously reported.[18, 20, 21] Different densities of MC3T3-E1 cells were seeded and cultured on TiO$_2$ scaffolds in order to determine the initial number of cells attached to the scaffold. After seeding, approximately half

6

of the cells initially seeded were attached to the scaffold and the other half were attached to the wells. In addition, the homogeneous cell distribution inside the scaffold was confirmed by confocal microscopy. Thus, the agitated seeding avoided the limitation of growth to a few hundred microns from the scaffold surface that is observed when conventional seeding methods are used.[28]

The cell growth profile, as measured by cellular DNA quantification, presented a peak after 7 days of culture. Afterwards, cell number decreased and remained constant up to 21 days. Nevertheless, this decrease could be due to an uncompleted cell lysis, because of the dense ECM produced by the cells, resulting in an underestimation of the DNA content. Decreases in DNA quantification of osteoblasts grown on materials have previously been documented.[29, 30] The analysis of qualitative SEM micrographs sustains this hypothesis, since the cell layer after 14 and 21 days was denser than after 7 days. Therefore, our results point that the proliferative phase of the cells lasted for a longer period, due to the high surface area of the TiO$_2$ scaffolds.

Integrins are not only involved in the initial attachment of the osteoblasts to materials, but also in matrix mineralization and bone formation.[31] While $\alpha\beta1$ integrins interact with collagen and fibronectin, playing a major role in cell integrin-mediated adhesion,[32–34] integrin $\alpha\beta3$ overexpression has been found to retard osteoblast differentiation.[35] In this study, osteoblasts growing on TiO$_2$ scaffolds have shown a decrease in mRNA expression of the $\beta1$ and $\beta3$ subunits while the expression of the $\alpha8$ subunit, component of a fibronectin (FN) receptor,[36] was maintained over time. While the down-regulation of the $\beta1$ subunit could be due to its key role in initial adhesion after 24 hours, the down-regulation of the $\beta3$ subunit could result in a benefit for osteoblast differentiation. These results are in concordance with previous *in vivo* studies with implanted oxidized surfaces.[37] Is has been shown that osteoblast differentiation was impaired in the presence of anti-$\alpha8$ integrins antibodies suggesting that this receptor is involved in the transduction of signals generated by FN.[38] Fibronectin is a component of the ECM that has been shown to regulate osteoblast differentiation, ECM assembly and mineralization.[38, 39] through BMP2[31] and whose interaction with integrin receptors is required for osteoblast differentiation.[36] Our results show that along with the sustained mRNA levels of $\alpha8$ integrin, there was a strong up-regulation of *Fn1* and *Bmp*2 mRNA levels during differentiation. It is possible that fibronectin may play a messenger role between surface integrins and BMP2, to promote differentiation.

Bone morphogenic proteins (BMPs) are secreted by osteoblasts and are incorporated into the ECM, stimulating the differentiation of MC3T3-E1 cells.[40, 41] In the present study, *Bmp*2 mRNA levels showed an expression peak after 7 days of cell culture, suggesting a differentiation

promotion of MC3T3-E1 cells on TiO$_2$. It has been shown that the addition of BMPs to cells that are actively producing ECM enhances the expression of OC and BSP.[40] Other studies have demonstrated that BMP2 can accelerate osteoblast differentiation and stimulate the expression of bone ECM proteins such as collagen type I, BSP and fibronectin.[42, 43] BSP is a potent nucleator of hydroxyapatite crystal formation under conditions where OPN is inactive and presents a pattern of expression closely parallel to early mineral formation.[44] In the present study, the relation *Bsp/Opn* mRNA clearly stimulates the mineralization of the ECM.

Temporal expression of cell growth and osteoblast phenotype markers during *in vitro* differentiation is characterized by a decrease of collagen type I in the proliferative phase, an increase of alkaline phosphatase during the maturation phase and an increase of bone sialoprotein and osteocalcin during mineralization, leading to an increase in calcium content.[45, 46] We analyzed the time course of gene expression during the differentiation of MC3T3-E1 cells seeded on TiO$_2$ scaffolds. In addition to the decreased *Col1a*1 mRNA expression, osteoblast differentiation was confirmed by high *Oc* mRNA expression up to 21 days and an increased ALP activity after 21 days of culture. In addition, a moderate increase in calcium levels over time was observed.

Our results suggest that cells are still at the beginning of the mineralization phase and that longer culture periods would lead to higher mineralization rates. This is probably due to the high surface area-to-volume ratio and the pore size of the TiO$_2$ scaffolds. Moreover, higher concentration of cells might have resulted in faster cell-to-cell interaction and enhanced osteogenic responses as has been shown with TiO$_2$ coated Ti fiber meshes.[47] Previous *in vitro* studies have shown that while high scaffold porosities increase cell proliferation due to a better transport of oxygen and nutrients, lower porosities stimulate osteogenesis by suppressing cell proliferation and forcing cell aggregation.[48] *In vivo*, increased porosity and pore size enhance bone ingrowth and osseointegration after surgery. Based on early studies, bigger pore sizes and increased porosities reduced the mechanical properties of the scaffold.[49] Anyway, pore sizes greater than 300 μm and porosity higher than 70% are required to stimulate vascularisation and bone formation.[49] Here, TiO$_2$ scaffolds pore sizes were about 392 μm, achieving compressive strength values of 1.63–2.67 MPa at 85%–90% porosities.[13] The combination of these physical properties of the TiO$_2$ scaffolds together with the high porosity has allowed an increase of the proliferation rates *in vitro*.

Taking all the results together, we can conclude that although several osteoblast differentiation markers were increased after 21 days of culture, cells at this time point were at the beginning of the mineralization phase. Accordingly, longer cultivation times or higher seeding

RESEARCH ARTICLE

densities would allow a higher differentiation degree of MC3T3-E1 cells on TiO₂ scaffolds. All in all, we show that TiO₂ scaffolds sustain MC3T3-E1 growth towards a mature and differentiated state.

References and Notes

1. C. f. D. C. a. P. (CDC), *MMWR. Morb. Mortal. Wkly. Rep.* 51, 207 (**2002**).
2. V. M. Goldberg and S. Akhavan, Biology of Bone Grafts Bone Regeneration and Repair, edited by J. R. Lieberman and G. E. Friedlaender, Humana Press (**2005**), pp. 57–65.
3. S. N. Khan, F. P. Cammisa, H. S. Sandhu, A. D. Diwan, F. P. Girardi, and J. M. Lane, *J. Am. Acad. Orthop. Surg.* 13, 77 (**2005**).
4. Y. Khan, M. J. Yaszemski, A. G. Mikos, and C. T. Laurencin, *J. Bone Joint Surg. Am.* 90 Suppl. 1, 36 (**2008**).
5. E. M. Bueno and J. Glowacki, *Nat. Rev. Rheumatol.* 5, 685 (**2009**).
6. T. Cordonnier, J. Sohier, P. Rosset, and P. Layrolle, *Adv. Eng. Mater.* 13, B135 (**2011**).
7. H. Nygren, P. Tengvall, and I. Lundstrom, *J. Biomed. Mater. Res.* 34, 487 (**1997**).
8. M. Jokinen, M. Pätsi, H. Rahiala, T. Peltola, M. Ritala, and J. B. Rosenholm, *J. Biomed. Mater. Res.* 42, 295 (**1998**).
9. L. Liu, J. Barford, and K. L. Yeung, *J. Environ. Sci. (China)* 21, 700 (**2009**).
10. G. Fostad, B. Hafell, A. Førde, R. Dittmann, R. Sabetrasekh, J. Will, J. E. Ellingsen, S. P. Lyngstadaas, and H. J. Haugen, *J. Eur. Ceram. Soc.* 29, 2773 (**2009**).
11. R. Sabetrasekh, H. Tiainen, J. E. Reseland, J. Will, J. E. Ellingsen, S. P. Lyngstadaas, and H. J. Haugen, *Biomed. Mater.* 5, 15003 (**2010**).
12. R. Sabetrasekh, H. Tiainen, S. P. Lyngstadaas, J. Reseland, and H. Haugen, *J. Biomater. Appl.* 25, 559 (**2011**).
13. H. Tiainen, S. P. Lyngstadaas, J. E. Ellingsen, and H. J. Haugen, *J. Mater. Sci. Mater. Med.* 21, 2783 (**2010**).
14. H. Tiainen, J. C. Wohlfahrt, A. Verket, S. P. Lyngstadaas, and H. J. Haugen, *Acta Biomater.* 8, 2384 (**2012**).
15. K. J. Burg, W. D. Holder, Jr, C. R. Culberson, R. J. Beiler, K. G. Greene, A. B. Loebsack, W. D. Roland, P. Eiselt, D. J. Mooney, and C. R. Halberstadt, *J. Biomed. Mater. Res.* 52, 576 (**2000**).
16. Y. Li, T. Ma, D. A. Kniss, L. C. Lasky, and S. T. Yang, *Biotechnol. Prog.* 17, 935 (**2001**).
17. C. E. Holy, M. S. Shoichet, and J. E. Davies, *J. Biomed. Mater. Res.* 51, 376 (**2000**).
18. S. S. Kim, C. A. Sundback, S. Kaihara, M. S. Benvenuto, B. S. Kim, D. J. Mooney, and J. P. Vacanti, *Tissue Eng.* 6, 39 (**2000**).
19. I. Martin, D. Wendt, and M. Heberer, *Trends Biotechnol.* 22, 80 (**2004**).
20. B.-S. Kim, A. J. Putnam, T. J. Kulik, and D. J. Mooney, *Biotechnol. Bioeng.* 57, 46 (**1998**).
21. Y. Takahashi and Y. Tabata, *Tissue Eng.* 9, 931 (**2003**).
22. R. Rago, J. Mitchen, and G. Wilding, *Anal. Biochem.* 191, 31 (**1990**).
23. M. W. Pfaffl, *Nucleic Acids Res.* 29, e45 (**2001**).
24. M. W. Pfaffl, A. Tichopad, C. Prgomet, and T. P. Neuvians, *Biotechnol. Lett.* 26, 509 (**2004**).
25. E. Hinoi, S. Fujimori, and Y. Yoneda, *FASEB J.* (**2003**).
26. D. Wang, K. Christensen, K. Chawla, G. Xiao, P. H. Krebsbach, and R. T. Franceschi, *J. Bone Miner. Res.* 14, 893 (**1999**).
27. H. Sudo, H. A. Kodama, Y. Amagai, S. Yamamoto, and S. Kasai, *J. Cell Biol.* 96, 191 (**1983**).
28. P. Thevenot, A. Nair, J. Dey, J. Yang, and L. Tang, *Tissue Eng. Part C Methods* 14, 319 (**2008**).
29. G. N. Bancroft, V. I. Sikavitsas, J. van den Dolder, T. L. Sheffield, C. G. Ambrose, J. A. Jansen, and A. G. Mikos, *Proc. Natl. Acad. Sci. USA* 99, 12600 (**2002**).
30. J.-P. St-Pierre, M. Gauthier, L.-P. Lefebvre, and M. Tabrizian, *Biomaterials* 26, 7319 (**2005**).
31. C.-F. Lai and S.-L. Cheng, *J. Bone Miner. Res.* 20, 330 (**2005**).
32. S. Gronthos, K. Stewart, S. E. Graves, S. Hay, and P. J. Simmons, *J. Bone Miner. Res.* 12, 1189 (**1997**).
33. G. Gronowicz and M. B. McCarthy, *J. Orthop. Res.* 14, 878 (**1996**).
34. K. Anselme, *Biomaterials* 21, 667 (**2000**).
35. S.-L. Cheng, C.-F. Lai, S. D. Blystone, and L. V. Avioli, *J. Bone Miner. Res.* 16, 277 (**2001**).
36. A. M. Moursi, R. K. Globus, and C. H. Damsky, *J. Cell. Sci.* 110, 2187 (**1997**).
37. O. Omar, M. Lennerås, S. Svensson, F. Suska, L. Emanuelsson, J. Hall, U. Nannmark, and P. Thomsen, *J. Mater. Sci. Mater. Med.* 21, 969 (**2010**).
38. A. M. Moursi, C. H. Damsky, J. Lull, D. Zimmerman, S. B. Doty, S. Aota, and R. K. Globus, *J. Cell. Sci.* 109, 1369 (**1996**).
39. G. Daculsi, P. Pilet, M. Cottrel, and G. Guicheux, *J. Biomed. Mater. Res.* 47, 228 (**1999**).
40. G. Xiao, R. Gopalakrishnan, D. Jiang, E. Reith, M. D. Benson, and R. T. Franceschi, *J. Bone Miner. Res.* 17, 101 (**2002**).
41. H. Siggelkow, E. Schmidt, B. Hennies, and M. Hüfner, *Bone* 35, 570 (**2004**).
42. A. K. Shah, J. Lazatin, R. K. Sinha, T. Lennox, N. J. Hickok, and R. S. Tuan, *Biol. Cell.* 91, 131 (**1999**).
43. F. Lecanda, L. V. Avioli, and S. L. Cheng, *J. Cell. Biochem.* 67, 386 (**1997**).
44. G. K. Hunter, P. V. Hauschka, A. R. Poole, L. C. Rosenberg, and H. A. Goldberg, *Biochem. J.* 317, 59 (**1996**).
45. J. B. Lian and G. S. Stein, *Crit. Rev. Oral Biol. Medicine* 3, 269 (**1992**).
46. T. A. Owen, M. Aronow, V. Shalhoub, L. M. Barone, L. Wilming, M. S. Tassinari, M. B. Kennedy, S. Pockwinse, J. B. Lian, and G. S. Stein, *J. Cell. Physiol.* 143, 420 (**1990**).
47. V. V. Meretoja, A. E. De Ruijter, T. O. Peltola, J. A. Jansen, and T. O. Narhi, *Tissue Eng.* 11, 1489 (**2005**).
48. Y. Takahashi and Y. Tabata, *J. Biomater. Sci. Polym. Ed.* 15, 41 (**2004**).
49. V. Karageorgiou and D. Kaplan, *Biomaterials* 26, 5474 (**2005**).

8

J. Biomater. Tissue Eng. 2, 1–8, **2012**

Paper 6

Effect of TiO$_2$ scaffolds coated with alginate hydrogel containing a proline-rich peptide on osteoblast growth and differentiation in vitro.

Rubert, M.; Pullisaar, H.; Gómez-Florit, M.; Ramis, J.M.; Tiainen, H.;

Haugen, H.J.; Lyngstadaas S.P.; Monjo, M.

Effect of TiO$_2$ scaffolds coated with alginate hydrogel containing a proline-rich peptide on osteoblast growth and differentiation in vitro

Rubert M[1], Pullisaar H[2], Gómez-Florit M[1], Ramis JM[1], Tiainen H[2], Haugen HJ[2], Lyngstadaas SP[2] and Monjo M[1]

[1]Group of Cell Therapy and Tissue Engineering, Research Institute on Health Sciences (IUNICS). University of Balearic Islands, Palma de Mallorca, Spain.

[2]Department of Biomaterials, Institute for Clinical Dentistry. University of Oslo, Oslo, Norway.

Corresponding author:

Marta Monjo, PhD

Research Institute on Health Sciences (IUNICS).

University of Balearic Islands, Crta. Valldemossa km 7.5, E-07122, Palma de Mallorca, Spain.

Phone: +34971259960

Fax: +34971173184

E-mail: marta.monjo@uib.es

Running title: Osteoblast response to alginate-coated TiO$_2$ scaffolds with polyproline peptide

ABSTRACT

The aim of this study was to investigate the effect of TiO_2 scaffold (SC) coated with an alginate hydrogel containing a proline-rich peptide (P2) on osteoblast proliferation and differentiation in vitro. Peptide release from alginate-coated TiO_2 SC was evaluated and a burst release was observed during the first hours of incubation, and then progressively released overtime. When seeding MC3T3-E1 cells on the coated and uncoated TiO_2 SC, no changes were observed in the cytotoxicity after 48h. SEM images revealed that cells were able to penetrate and adhere on alginate-coated TiO_2 SC either with or without P2, although the amount of cells were higher on uncoated TiO_2 SC, which was also in accordance to the DNA content results after 7 days of culture. A lower expression of integrin beta1 was detected for alginate-coated TiO_2 SC at this time point, but similar gene expression was observed for other integrins, fibronectin-1, and several osteoblast differentiation markers after 21 days. At this time, gene expression of integrin beta3, fibronectin-1, osterix and collagen-I was increased in alginate-coated compared to TiO_2 SC. P2 alginate-coated TiO_2 SC showed increased gene expression of bone morphogenetic protein 2 and collagen-I compared to alginate-coated and uncoated TiO_2 SC. In conclusion, our results indicate that alginate-coated TiO_2 SC can act as a matrix for delivery of proline-rich peptides increasing osteoblast differentiation. Thus, the combination of the osteoconductive properties of TiO_2 SC with the osteogenic effects of proline-rich peptides may represent a new strategy for bone tissue regeneration in load-bearing applications.

Keywords: TiO_2 scaffolds, alginate, proline-rich peptide, cell attachment, osteoblast differentiation.

INTRODUCTION

Natural bone tissue formation from osteogenic cells with the aid of a three-dimensional scaffold offers an alternative to autografts and allografts to repair and regenerate lost bone. A well-constructed scaffold provides a suitable surface for cells to attach and adhere with a porous and well interconnected network guiding the development of new bone, supporting migration, proliferation and differentiation of bone-forming cells and vascularization of the ingrowth tissue [1-3]. Although several polymers and bioceramics have been developed for their use in bone tissue engineering, their low mechanical properties have limited their use for load-bearing applications [4, 5].

Titanium dioxide (TiO_2) is a biocompatible material, which has also been reported to have bioactive properties and a certain degree of bacteriostatic effect [6-8]. Therefore, ceramic TiO_2 has been studied as a material for bone tissue engineering purposes [6, 9, 10]. High porous and well-interconnected TiO_2 scaffolds with high mechanical strength achieving values of 90% of porosity and of 1.63-2.67MPa of compressive strength have been recently developed [10] and their biocompatibility and osteoconductive properties have been demonstrated in *in vitro* [11] and *in vivo* [12] studies. *In vitro*, TiO_2 scaffolds provided a suitable surface for osteoblast cell attachment and cell differentiation and cells were well-distributed through the entire 3D structure over time [11]. Further, the formation of new mineralized bone tissue and vascularization of the ingrowth tissue has been observed *in vivo* [12].

Proline-rich proteins guide the deposition and growth of hydroxyapatite (Hap) into endoskeletal mineralized tissues by serving as a scaffold to control Hap crystal assembly and bind to protein domains frequently involved in signalling events [13, 14]. We have previously designed synthetic proline-rich peptides of 25 aminoacid length based on polyproline consensus sequences of hard tissue extracellular matrix proteins and have demonstrated their ability to stimulate osteoblast differentiation *in vitro* either in mouse pre-osteoblast like cells (MC3T3-E1) [15] or in human umbilical cord derived mesenchymal stem cells (hUCMSCs) [16] and to

3

promote osseointegration *in vivo* [17]. Further, we have shown that 2% alginate hydrogels are a suitable formulation for local delivery of synthetic proline-rich peptides [18].

In the present study, the best variant of our designed proline-rich peptides tested earlier *in vitro* was selected to coat TiO_2 scaffolds with an alginate hydrogel containing these peptides, and their effect investigated *in vitro* with MC3T3-E1 osteoblasts. Osteoblast cell viability was evaluated by determination of lactate dehydrogenase (LDH) activity and cell proliferation by quantification of DNA content. Relative mRNA levels of cell adhesion and of osteoblasts markers were also investigated by using real-time RT-PCR. The behaviour of cells into this 3D structure was visualized by scanning electron microscope (SEM). The release profile of the peptide to the medium was as well monitored by UV spectroscopy.

2. MATERIAL AND METHODS

2.1. *Preparation of synthetic peptide 2* (P2).

Synthetic proline-rich peptide 2 (2HN- PLVPSQPLVPSQPLVPSQPQPPLPP-COOH) was purchased from Eurogentec (Seraing, Belgium). One vial containing 7.2 mg of the selected synthetic peptide was delivered in a freeze-dried pellet form and dissolved to 10 mg/ml in 0,1% acetic acid in phosphate-buffered saline (PBS) (PAA Laboratories GmbH, Pasching, Austria). Aliquots to avoid repeated freeze-thaw cycles were prepared and stored at -20 °C until use.

2.2. *Preparation of 2% alginate gel containing peptide 2.*

Sodium alginate (Pronova UP LVG®) -a low viscosity alginate where minimum 60% of monomers are guluronate- was purchased from NovaMatrix (FMC BioPolymer AS, Norway). The sodium alginate was used without further purification. Quantity (2%, w/v) of sodium alginate was dissolved in distilled water by stirring for 3 h at room temperature to get a homogenous alginate solution. A fixed concentration (50µg/ml) of P2 was added to the solution and stirred for 1 h.

2.3. Fabrication of TiO$_2$ scaffolds coated with 2% alginate gel containing P2.

The porous TiO$_2$ scaffolds were produced by polymer sponge replication as previously described by [10], with a size of 9 mm of diameter and 8 mm high. Then, scaffolds were coated with one layer of 2% alginate gel with or without P2. Briefly, TiO$_2$ scaffolds were submerged into 2% alginate solution with or without P2 under agitation at 100rpm on an orbital shaker (IKA Vibrax VXR basic, Staufen, Germany) for 1 h at room temperature. Scaffolds were then centrifuged at 252xg for 1 min. Samples were immersed into 50mM CaCl$_2$ for 1h to allow gelation. Scaffolds were then rinsed with dH$_2$O to remove the excess of CaCl$_2$. Finally, samples were let to dry overnight at room temperature. Scaffolds coated with one layer of 2% alginate gel (control alginate scaffold), were used as control group, whereas uncoated TiO$_2$ scaffolds (without alginate, SC) were also used as control group.

2.4. Peptide 2 release profile from TiO$_2$ scaffolds coated with 2% alginate gel.

TiO$_2$ scaffolds coated with 2% alginate containing peptide 2 (P2-alginate-coated scaffold) were placed into 48-well plates (Nunc GmBh & Co. Kg, Langenselbold, Germany) containing 1 ml distilled water (pH 7.4). In order to mimic cell culture conditions, the samples were agitated on an orbital shaker at 200 rpm (IKA® Schüttler MTS 2, Germany) for 6 h at 37ºC and in humidity conditions (using a distilled water container). Then, samples were maintained at 37°C in a humidified atmosphere for up to 21 days. At prefixed time points (2d, 5d, 7d, 9d, 12d, 14d, 16d, 19d and 21d), distilled water was collected and fresh distilled water was added into each well. Sample absorbances were analyzed by UV-Vis spectrophotometer (PerkinElmer® Lambda 25 UV/Vis Systems, USA) at a wavelength of 206nm to determine the amount of peptide released. In parallel, scaffolds coated with one layer of 2% alginate gel were used as control to subtract absorbance values obtained from degradation products from alginate. Relative absorbance units were correlated with the amount of peptide released using a linear standard curve for each time point and the cumulative P2 released was then calculated. The experiment was performed in triplicate.

2.5. Cell culture of MC3T3-E1 on coated and uncoated TiO$_2$ scaffolds.

TiO$_2$ scaffolds (SC) uncoated and coated with 2% alginate with or without peptide (P2 and control (-)) were placed into 48-well plates (Nunc GmbH & CO. KG, Langenselbold, Germany) in sterile conditions. Cells were seeded at a density of 200,000 cells/scaffold and maintained in α-MEM (PAA Laboratories, Pasching, Austria) supplemented with 10% FBS (PAA Laboratories, Pasching, Austria) and 100 U penicillin/ml and 100 μg streptomycin/ml antibiotics (PAA Laboratories, Pasching, Austria). In order to guarantee a homogenous cell distribution inside the scaffold, an agitated seeding method was used [19]. Briefly, after adding 1ml of cell suspension to the scaffolds, plates were agitated on an orbital shaker (Unitron, Infors HT, Basel, Switzerland) for 6 h at 180rpm at 37ºC and in humidity conditions. Then, cells were maintained at 37°C in a humidified atmosphere of 5% CO$_2$ for up to 21 days. Culture media (1 ml) was refreshed every other day.

Culture media was collected after 48 h of treatment to test cytotoxicity (LDH activity). To assess the ability of cell proliferation into this 3D system, the number of cells after 7 days was also studied by DNA quantification using Hoechst staining. In parallel, the cell attachment of MC3T3-E1 into the scaffold was also visualized by SEM after 7 and 21 days of culture. Expression of markers related to osteoblast cell maturation and differentiation after 7 and 21 days of cell culture was assessed by real-time RT-PCR.

2.6. SEM visualization of 2% alginate-coated TiO$_2$ scaffolds.

Morphology of alginate-coated TiO$_2$ scaffolds was observed using a scanning electron microscope (SEM, Hitachi S-3400N, Hitachi High-Technologies Europe GmbH, Krefeld, Germany). SEM was further used to visualize the cell adhesion into the TiO$_2$ scaffold structure after 7 and 21 days of culture. Briefly, cells were washed twice with PBS and fixed with glutaraldehyde 4% in PBS for 2 h. Then the fixative solution was removed and the cells were washed with distilled water twice. At 30 minute intervals, the cells were dehydrated by the addition of 50%, 70%, 90% and 100% ethanol solutions. Ethanol was removed and the cells were left at room temperature to evaporate the remaining ethanol. Scaffolds were observed at

10kV and 40Pa using back scattered and secondary electrons detector. Images presented are from a representative area.

2.7. Cell viability.

The lactate dehydrogenase (LDH) activity determined in the culture media after 48 h was taken as an indicator of cell survival. The activity of the cytosolic enzyme was determined according to the manufacturer's kit instructions (Roche Diagnostics, Mannheim, Germany). Results were presented relative to the LDH activity in the medium of cells cultured in uncoated scaffolds, which were set to 100%.

2.8. Cell number determination.

Cells growing on the 3D scaffolds were lysed by a freeze-thaw method in deionised distilled water [20]. Cell lysates were used for determination of DNA quantity using Hoechst 33258 fluorescence assay. Samples were mixed with 20µg/ml of Hoechst 33258 fluorescence stain (Sigma, St. Quentin Fallavier, France) in TNE buffer, and the intensity of fluorescence was measured at excitation and emission wavelengths of 356/465nm using a multifunction microplate reader (Cary Eclipse fluorescence spectrophotometer, Agilent Technologies, Santa Clara, United States). Relative fluorescence units were correlated with the cell number using a linear standard curve.

2.9. RNA isolation and real-time RT-PCR analysis.

Total RNA was isolated using Tripure® (Roche Diagnostics, Mannheim, Germany), according to the manufacturer's protocol. Total RNA was quantified at 260 nm using a Nanodrop spectrophotometer (NanoDrop Technologies, Wilmington, DE, USA). The same amount of total RNA (850ng) was reverse transcribed to cDNA at 42°C for 60 min using High Capacity RNA-to-cDNA kit (Applied Biosystems, Foster City, CA), according to the protocol of the supplier. Aliquots of each cDNA were frozen (-20 °C) until the PCR reactions were carried out.

Real-time PCR was performed in the Lightcycler 480® (Roche Diagnostics, Mannheim, Germany) using SYBR green detection. Real-time PCR was done for two reference genes

(18SrRNA and glyceraldehyde-3-phosphate dehydrogenase (*Gapdh*)) and 12 target genes (integrin alpha8 (*Itga8*), integrin beta1 (*Itgb1*), integrin beta3 (*Itgb3*), fibronectin 1 (*Fn1*), , osterix (*Osx*), bone morphogenetic protein 2 (*Bmp2*), collagen-I (*Coll-I*), interleukin-6 (*Il-6*), bone sialoprotein (*Bsp*), alkaline phosphatase (*Alp*), osteocalcin (*Oc*) and osteopontin (*Opn*)). The primer sequences are detailed in table 1.

Each reaction contained 7 μl Lightcycler-FastStart DNA MasterPLUS SYBR Green I (containing Fast Start Taq polymerase, reaction buffer, dNTPs mix, SYBRGreen I dye and MgCl$_2$), 0.5 μM of each, the sense and the antisense specific primers and 3μl of the cDNA dilution in a final volume of 10 μl. The amplification program consisted of a preincubation step for denaturation of the template cDNA (10 min 95 °C), followed by 45 cycles consisting of a denaturation step (10 s 95 °C), an annealing step (8-10 s 60 °C, except for *Osx* that was 5 s 68ºC and *Alp* that was 8s 65 ºC) and an extension step (10 s 72 °C). After each cycle, fluorescence was measured at 72 °C (λex 470 nm, λem 530 nm). A negative control without cDNA template was run in each assay.

Real-time efficiencies were calculated from the given slopes in the LightCycler 480 software using serial dilutions, showing all the investigated transcripts high real-time PCR efficiency rates, and high linearity when different concentrations are used. PCR products were subjected to a melting curve analysis on the LightCycler and subsequently 2% agarose/TAE gel electrophoresis to confirm amplification specificity, Tm and amplicon size, respectively.

Relative quantification after PCR was calculated by dividing the concentration of the target gene in each sample by the mean of the concentration of the two reference genes in the same sample using the Advanced relative quantification method provided by the LightCycler 480 analysis software version 1.5 (Roche Diagnostics, Mannheim, Germany).

2.10. *Statistics*

All data are presented as mean values ± SEM. A Kolmogorov-Smirnov test was done to assume parametric or non-parametric distributions for the normality tests, differences between groups were assessed by Mann-Whitney-test or by Student t-test depending on their normal

distribution. SPSS® program for Windows (Chicago, IL, US), version 17.0 was used. Results were considered statistically significant at p-values ≤ 0.05.

3. RESULTS

3.1 Peptide release.

Peptide release profile from P2-alginate-coated scaffolds is depicted in Figure 1. A burst release of the peptide during the first 2 days of incubation was observed (42.8% of the cumulative amount of P2 released after 21 days). After 5 days, the amount of peptide released decreased to a 9.4% (of the cumulative amount released up to 21 days) followed by a slower but sustained peptide release over time up to 21 days of incubation. Further, the cumulative release suggests that, after 21 days of incubation, there were still P2 entrapped into the 2% alginate gel.

3.2 LDH activity.

As shown in Figure 2, no toxic effects were observed for any of the experimental groups studied. Similar percentage of cell viability was determined in all the groups tested, indicating that either control alginate scaffolds (-) and P2-alginate-coated scaffolds (P2) did not show any toxic effects on cells after 48h of cell culture.

3.3 SEM visualization of TiO_2 scaffolds coated with 2% alginate gel.

Alginate-coated TiO_2 scaffolds were observed by SEM. As shown in figures 3A and 3B, some pores of the TiO_2 scaffolds were blocked after the coating process with alginate, though, after cell seeding and 7 days of incubation in standard cell culture conditions (37ºC and in a humidified atmosphere), almost all pores were unblocked (Figure 3C and 3D). Thus, certain degradation of the blocking alginate gel was seen in those pores that remained blocked right after the coating process.

Although the amount of cells growing on uncoated TiO_2 scaffolds (SC) was higher (Figure 4A and 4B) than on alginate-coated TiO_2 scaffolds (Figure 4C-4F), cells were able to penetrate and to adhere into the coated scaffolds with 2% alginate gel either with or without P2.

An increase from day 7 to day 21 in the number of cells growing on the scaffolds was seen for all the experimental groups.

3.4   Cell number.

DNA quantification was used to determine the number of cells growing on the TiO$_2$ scaffolds after 7 days of culture (Figure 5). In accordance to SEM images, after 7 days of culture the number of cells was significantly lower in any of the alginate-coated TiO$_2$ scaffolds compared to TiO$_2$ scaffolds (SC). Thus, compared to SC, a 61% and a 49% reduction in cell number was found on alginate-coated scaffolds without and with P2, respectively. Although data did not reach statistical significance, scaffolds coated with P2 showed 32% more cells than the alginate control scaffolds (-).

3.5   Gene expression of cell adhesion-related markers.

As shown in Figure 6, relative mRNA levels of *Itb1* were significantly decreased in cells growing onto alginate-coated scaffolds (either with or without P2) compared to TiO$_2$ scaffolds (SC) after 7 days of culture. Nevertheless, after 21 days of cell culture no differences were observed among groups. After 21 days, *Itgb3* mRNA levels were increased in cells growing on alginate-coated scaffolds (either with or without P2) compared to TiO$_2$ scaffolds (SC). Higher mRNA levels of *Fn1* were found in cells growing on 2% alginate-coated scaffolds after 21 days, and in cells growing on P2-alginate-coated scaffolds compared to uncoated scaffolds, although for the last group data did not reach statistical significance. *Itga8* mRNA was significantly increased in cells growing on P2-alginate-coated scaffolds compared to control alginate scaffolds after 21 days of culture.

3.6   Gene expression of several osteoblast differentiation markers.

Figure 7 shows relative mRNA levels for several osteoblast differentiation marker genes. After 21 days of culture, osterix mRNA levels were increased in cells growing on alginate-coated scaffolds (either with or without P2) compared to uncoated scaffolds. *Bmp-2* and *Il-6* mRNA levels were significantly increased in cells cultured on P2-alginate-coated scaffolds compared to both uncoated scaffolds and alginate-coated scaffolds after 21days of cell

culture. *Coll-I* mRNA levels, a marker related with cell proliferation [21], were significantly increased in cells cultured on P2-alginate-coated scaffolds compared to alginate-coated scaffolds after 7 days of cell culture. After 21 days of culture *Coll-I* was significantly increased in both alginate-coated scaffolds and P2-alginate-coated scaffolds compared to uncoated scaffolds. No significant differences were observed in *Opn, Bsp, Alp* and *Oc* mRNA expression levels among experimental groups at any of the time points studied.

3. DISCUSSION

In the present study, we have combined the improved reported biocompability and osteoconductivity of TiO_2 scaffolds with the suitability of alginate gel as a carrier for the delivery of a proline-rich peptide, for their use in load-bearing bone tissue applications to promote bone formation and mineralization. TiO_2 scaffolds have been reported to have strength up to 2.6 MPa in compressive strength [10] and showed excellent mechanical resistance in a pig *in vivo* study [12].

In bone tissue engineering, the structure of the scaffold must provide an optimal microenvironment for osteogenesis [10]. The scaffold porosity, pore network interconnectivity, the surface-area-to-volume ratio and the physico-chemical properties of the surface determines cell migration and differentiation, bone ingrowth, vascularization, and mass transfer between the cells and the environment [22]. The use of highly porous TiO_2 scaffolds using an agitated cell seeding method has proved to achieve a good attachment and distribution of mouse pre-osteoblastic cells [11]. In the present study, TiO_2 scaffolds coated with one layer of 2% alginate displayed a microstructure suitable for their use as scaffold for three-dimensional cell growth. Although a few pores remained blocked right after the coating process, almost all pores were unblocked after 7 days of incubation at 37ºC due to biodegradability properties of alginate [23], thus providing opening windows for cells to penetrate and migrate into the structure. In this study, no differences on cell viability were observed between coated and uncoated TiO_2 scaffolds, in agreement with previous reports showing cell safety and biocompatibility of TiO_2

scaffolds [7] and of alginate gels [18, 24-26]. Alginate has been widely used for delivery of bioactive molecules [25, 27] and constitute a suitable carrier for delivery of synthetic peptides at the local site [18]. We found a burst release of P2 during the first hours of incubation followed by progressive and sustained release during the 21-days period, following the same pattern as in alginate hydrogels alone (Rubert et al, submitted).

Consistent with previous studies [6, 9, 11], TiO_2 scaffolds provided an appropriate surface for osteoblasts to adhere, migrate and proliferate. Although the amount of cells into alginate-coated TiO_2 scaffolds was lower than in uncoated TiO_2 scaffolds, scaffolds coated with alginate supported cell progression and differentiation. These results are in accordance with previous studies reporting that the alginate is an innert substrate for cell attachment [28] and that synthetic peptides rich in proline sequences increase properties for cell attachment of the alginate hydrogel [18]. Thus, although not significantly, TiO_2 scaffolds coated with 2% alginate containing synthetic peptide 2 showed a trend to improve cell attachment (+32 %) after 7 days compared to alginate-coated TiO_2 scaffolds.

It has been reported that biomaterial composition regulates cell attachment and cytoskeletal organization with long-term effects on osteoblast cell maturation and mineralization [29]. In accordance to the efficiency in cell attachment observed by SEM and DNA quantification onto the different groups, *Itgb1* mRNA levels were decreased in cells growing on alginate-coated TiO_2 scaffolds compared to those growing on uncoated scaffolds. Further, *Itgb3* and *Fn1* mRNA levels (which are highly expressed at early stages of osteogenesis and reduced through the cellular maturation process [11, 30, 31]) were significantly increased in cells growing into alginate-coated TiO_2 scaffolds compared to the uncoated scaffolds after 21 days of culture. Moreover, expression of *Itga8*, an integrin that plays a role during the mineralization stage through the binding to osteopontin, was induced by P2-alginate-coated scaffolds compared to alginate-coated scaffolds, suggesting that P2 might influence mineralization processes, as previously reported with the increased mineralization in MC3T3-E1 and hUCMSCs after P2 treatment [15]. Integrins are not only involved in the attachment of cells to

12

the material surface [32-36] but also mediate signal transduction pathways inducing bone formation and mineralization [31, 37]. Interestingly, expression of genes like *Itgb3, Fn1, Coll-I* and *Osx* that are related to early stages of osteoblast differentiation, and which are normally upregulated at short term and downregulated thereafter, were increased in the later time point studied (21 days) in cells grown into alginate-coated TiO_2 scaffolds compared to cells growing on uncoated scaffolds. It is possible that the temporal sequence of early markers related to osteoblast differentiation varies when MC3T3-E1 cells are growing on uncoated scaffolds or on alginate-coated scaffolds, so that cells growing onto alginate-coated surfaces showed an improved cell differentiation over proliferation compared to uncoated TiO_2 scaffolds, probably due to the initial difficulties of cell adhesion onto the alginate. Although alginate coating seems to impair cell adhesion and proliferation on the scaffolds, the acquisition of a mature and organized matrix (ECM) competent for mineralization was confirmed by a marked increase in *Alp* and *Bsp* mRNA levels from day 7 to 21 days for any of the groups. Once the synthesis, organization and maturation of the ECM has finalized, *Oc* expression is upregulated leading to mineralization [38, 39]. Our results showed a slight increase in *Oc* mRNA levels after 21 days of culture, therefore, we can conclude that cells were just at the beginning of the mineralization process. Moreover, in accordance to our results with gene expression levels of *Opn* and *Bsp*, the increased relation Bsp/Opn mRNA in osteoblastic cells could be indicative for the stimulation of ECM mineralization, as previously reported with MC3T3-E1 cells seeded on uncoated TiO_2 scaffolds [11].

It is important to highlight that the addition of P2 to alginate improved the properties for cell proliferation and differentiation compared to alginate-coated scaffolds, as it can be appreciated by the amount of cells measured by DNA content and the higher expression levels of *Bmp2, Coll-I* and *Il-6*. So far the synthetic peptides rich in polyproline sequences have repetitively shown an increase in osteocalcin mRNA levels, both *in vitro* [15, 16] and in *in vivo* studies where titanium implants were coated with the peptide [17], and further when loaded into an alginate hydrogel for their use as a carrier for local delivery [18]. Thus, taken together our

previous studies and the results from the present study, this allows us to suggest that P2-alginate-coated scaffolds would promote higher cell differentiation and mineralization in an *in vivo* environment.

4. CONCLUSION

In conclusion, our results demonstrate that alginate-coated TiO$_2$ scaffolds can act as a matrix for delivery of synthetic peptide rich in proline sequences inducing osteoblast cell differentiation. The combination of the physical and osteoconductive properties of TiO$_2$ scaffolds with the osteogenic effects of synthetic proline-rich peptides on bone formation and mineralization may represent a new strategy for bone tissue regeneration in load-bearing applications.

5. ACKNOWLEDGMENTS

6. REFERENCES

[1] Jokinen M, Patsi M, Rahiala H, Peltola T, Ritala M, Rosenholm JB. Influence of sol and surface properties on in vitro bioactivity of sol-gel-derived TiO2 and TiO2-SiO2 films deposited by dip-coating method. Journal of biomedical materials research 1998;42:295-302.

[2] Lee N, Oh H, Hong C, Suh H, Hong S. Comparison of the synthetic biodegradable polymers, polylactide (PLA), and polylactic-co-glycolic acid (PLGA) as scaffolds for artificial cartilage. Biotechnology and Bioprocess Engineering 2009;14:180-6.

[3] Thonmson RC, Shung AK, Yaszemski MJ, Mikos AG. Scaffolds processing. In: R. Lanza R-LaJV, editor. Principles of tissue engineering. San Diego: Academic Press; 2000. p. 252-9.

[4] Bueno Rde B, Adachi P, Castro-Raucci LM, Rosa AL, Nanci A, Oliveira PT. Oxidative nanopatterning of titanium surfaces promotes production and extracellular accumulation of osteopontin. Braz Dent J 2011;22:179-84.

[5] Khan Y, Yaszemski MJ, Mikos AG, Laurencin CT. Tissue Engineering of Bone: Material and Matrix Considerations. J Bone Joint Surg Am 2008;90 Sippl 1:36-42.

[6] Fostad G, Hafell B, FÃ¸rde A, Dittmann R, Sabetrasekh R, Will J, et al. Loadable TiO2 scaffolds-A correlation study between processing parameters, micro CT analysis and mechanical strength. Journal of the European Ceramic Society 2009;29:2773-81.

[7] Nygren H, Tengvall P, Lundstrom I. The initial reactions of TiO2 with blood. Journal of biomedical materials research 1997;34:487-92.

[8] Rincon JC, Xiao Y, Young WG, Bartold PM. Enhanced proliferation, attachment and osteopontin expression by porcine periodontal cells exposed to Emdogain. Archives of oral biology 2005;50:1047-54.

[9] Sabetrasekh R, Tiainen H, Reseland JE, Will J, Ellingsen JE, Lyngstadaas SP, et al. Impact of trace elements on biocompatibility of titanium scaffolds. Biomed Mater 2010;5:15003.

[10] Tiainen H, Lyngstadaas SP, Ellingsen JE, Haugen HJ. Ultra-porous titanium oxide scaffold with high compressive strength. J Mater Sci Mater Med 2010;21:2783-92.

[11] Gómez-Florit M, Rubert M, Ramis JM, Haugen HJ, Lyngstadaas SP, Monjo M. Homogeneous seeding and differentiation of MC3T3-E1 cells on TiO$_2$ scaffolds. Submitted.

[12] Tiainen H, Wohlfahrt JC, Verket A, Lyngstadaas SP, Haugen HJ. Bone formation in TiO2 bone scaffolds in extraction sockets of minipigs. Acta Biomater 2012;8:2384-91.

[13] Ball LJ, Kuhne R, Schneider-Mergener J, Oschkinat H. Recognition of proline-rich motifs by protein-protein-interaction domains. Angew Chem Int Ed Engl 2005;44:2852-69.

[14] Jin T, Ito Y, Luan X, Dangaria S, Walker C, Allen M, et al. Elongated polyproline motifs facilitate enamel evolution through matrix subunit compaction. PLoS Biol 2009;7:e1000262.

[15] Rubert M, Ramis JM, Vondrasek J, Gayà A, Lyngstadaas SP, Monjo M. Synthetic peptides analogue to enamel proteins promote osteogenic differentiation of MC3T3-E1 and mesenchymal stem cells. J Biomater Tissue Eng 2011;1:198-209.

[16] Ramis JM, Rubert M, Vondrasek J, Gayà A, Lyngstadaas SP, Monjo M. Effect of enamel matrix derivative and of proline-rich synthetic peptides on the differentiation of human mesenchymal stem cells towards the osteogenic lineage. Tissue Eng Part A 2012;18:1-11.

[17] Petzold C, Monjo M, Rubert M, Reinholt FP, Gomez-Florit M, Ramis JM, et al. Effect of coated titanium implants with a proline-rich synthetic peptide on bone healing. Oral Craniofac Tissue Eng 2012;2:35-43.

[18] Rubert M, Monjo M, Lyngstadaas SP, Ramis JM. Effect of alginate hydrogel containing polyproline-rich peptides on osteoblast differentiation. Submitted.

[19] Takahashi Y, Tabata Y. Homogeneous seeding of mesenchymal stem cells into nonwoven fabric for tissue engineering. Tissue Eng 2003;9:931-8.

[20] Rage R, Mitchen J, Wilding G. DNA fluorometric assay in 96-well tissue culture plates using Hoechst 33258 after cell lysis by freezing in distilled water. Anal Biochem 1990;191:31-4.

[21] Stein GS, Lian JB, Stein JL, Van Wijnen AJ, Montecino M. Transcriptional control of osteoblast growth and differentiation. Physiological reviews 1996;76:593-629.

[22] Hutmacher DW. Scaffolds in tissue engineering bone and cartilage. Biomaterials 2000;21:2529-43.

[23] Rowley JA, Madlambayan G, Mooney DJ. Alginate hydrogels as synthetic extracellular matrix materials. Biomaterials 1999;20:45-53.

[24] Barbetta A, Barigelli E, Dentini M. Porous alginate hydrogels: synthetic methods for tailoring the porous texture. Biomacromolecules 2009;10:2328-37.

[25] Lee JY, Choo JE, Park HJ, Park JB, Lee SC, Jo I, et al. Injectable gel with synthetic collagen-binding peptide for enhanced osteogenesis in vitro and in vivo. Biochemical and biophysical research communications 2007;357:68-74.

[26] Rubert M, Alonso-Sande M, Monjo M, Ramis JM. Evaluation of alginate and hyaluronic acid for their use in bone tissue engineering. Submitted.

[27] Kolambkar YM, Dupont KM, Boerckel JD, Huebsch N, Mooney DJ, Hutmacher DW, et al. An alginate-based hybrid system for growth factor delivery in the functional repair of large bone defects. Biomaterials 2011;32:65-74.

[28] Alsberg E, Anderson KW, Albeiruti A, Franceschi RT, Mooney DJ. Cell-interactive alginate hydrogels for bone tissue engineering. Journal of dental research 2001;80:2025-9.

[29] Shah AK, Lazatin J, Sinha RK, Lennox T, Hickok NJ, Tuan RS. Mechanism of BMP-2 stimulated adhesion of osteoblastic cells to titanium alloy. Biol Cell 1999;91:131-42.

[30] Cheng S-L, Lai C-F, Blystone SD, Avioli LV. Bone Mineralization and Osteoblast Differentiation Are Negatively Modulated by Integrin $\alpha v \beta 3$. J Bone Miner Res 2001;16:277-88.

[31] Moursi AM, Globus RK, Damsky CH. Interactions between integrin receptors and fibronectin are required for calvarial osteoblast differentiation in vitro. J Cell Sci 1997;110:2187-96.

[32] El-Amin SF, Attawia M, Lu HH, Shah AK, Chang R, Hickok NJ, et al. Integrin expression by human osteoblasts cultured on degradable polymeric materials applicable for tissue engineered bone. J Orthop Res 2002;20:20-8.

[33] Gronowicz G, McCarthy MB. Response of human osteoblasts to implant materials: Integrin-mediated adhesion. J Orthop Res 1996;14:878-87.

[34] Lynch MP, Stein JL, Stein GS, Lian JB. The influence of type I collagen on the development and maintenance of the osteoblast phenotype in primary and passaged rat calvarial

osteoblasts: modification of expression of genes supporting cell growth, adhesion, and extracellular matrix mineralization. Exp Cell Res 1995;216:35-45.

[35] Siebers MC, ter Brugge PJ, Walboomers XF, Jansen JA. Integrins as linker proteins between osteoblasts and bone replacing materials. A critical review. Biomaterials 2005;26:137-46.

[36] Steele JG, Dalton BA, Johnson G, Underwood PA. Polystyrene chemistry affects vitronectin activity: an explanation for cell attachment to tissue culture polystyrene but not to unmodified polystyrene. Journal of biomedical materials research 1993;27:927-40.

[37] Hynes RO. Integrins: Versatility, modulation, and signaling in cell adhesion. Cell 1992;69:11-25.

[38] Sodek J, Chen J, Nagata T, Kasugai S, Todescan R, Jr., Li IW, et al. Regulation of osteopontin expression in osteoblasts. Ann N Y Acad Sci 1995;760:223-41.

[39] McKee MD, Nanci A. Osteopontin and the Bone Remodeling Sequence. Ann N Y Acad Sci 1995;760:177-89.

7. TABLES

Table 1. *Primer sequences of osteoblast markers related genes used in the real-time PCR.*

Gene	Primer sequence
18S	S 5'-GTAACCCGTTGAACCCCATT-3'
	A 5'- CCATCCAATCGGTAGTAGCG-3'
Gapdh	S 5'-ACCCAGAAGACTGTG-GATGG-3'
	A 5'-CACATTGGG-GGTAGGAACAC-3'
Itgb1	S 5'- AGCAGGCGTGGTTGCTGGAA -3'
	A 5'- TTTCACCCGTGTCCCACTTGGC -3'
Itgb3	S 5'- AGGGGAGATGTGTTCCGGCCA -3'
	A 5'- ACACACAGCTGCCGCACTCG -3'
Fn1	S 5'- GCTGCCAGGAGACAGCCGTG -3'
	A 5'- GTCTTGCCGCCCTTCGGTGG -3'
Itga8	S 5'- TCGCCTGGGAGGAGGCGAAA -3'
	A 5'- TCTTAACCGCTGTGCTCCCCG -3'
Osx	S 5' - ACTGGCTAG GTGGTGGTCAG- 3'
	A 5' - GGTAGGGAGCTGGGTTAAGG- 3'
Bmp2	S 5'- GCTCCACAAACGAGAAAAG-C-3'
	A 5'- AGCAAGGGGAAAAG-GACACT-3'
Coll-I	S 5'- AGAGC-ATGACCGATGGATTC -3'
	A 5'- CCTTCTTGAGGTTGCCAGTC -3'
Il-6	S 5'- ACTTCCATCCAGTTGCCTTC- 3'
	A 5' -TTTCCACGATTT CCCAGAGA- 3'
Bsp	S 5'-GAAAATGGAGACGGCGATAG-3'
	A 5'-ACCCGAGAGTGTGGAAAGTG-3'
Alp	S 5'-AACCCAGACACAAGCATT-CC-3'
	A 5'- GAGAGCGAAGGGTC-AGTCAG-3'
Oc	S 5'- CCGGGAGCAG-TGTGAGCTTA-3'
	A 5'-TAGATGC-GTTTGTAGGCGGTC -3'
Opn	S 5'-TCTGCGGCAGGCATTCTCGG-3'
	A 5'-GTCACTTTCACCGGGAGGGAGGA-3'

8.

8. FIGURE LEGENDS

Figure 1.   Release profile of peptide 2 from P2-alginate-coated scaffolds after 21 days of incubation at 37ºC. Bar graph show the amount of peptide released after each time point. Line graph represents cumulative amount of peptide released up to 21 days. Values represent mean ± SD.

Figure 2. LDH activity measured from culture media collected after 48 h of culture. Values represent the mean ± SEM. Mann-Whitney test ($p \leq 0.05$): (a) versus regular scaffold (SC) and (b) versus control alginate scaffold (-).

Figure 3. SEM visualization of 2% alginate-coated TiO_2 scaffolds (control alginate scaffold) at 10kV and 40Pa. Figures A and B show the microstructure of TiO_2 scaffolds right after the coating process with one layer of 2% alginate gel at 50x (A) and 300x (B) of magnification. Figures C and D show cells cultured on control alginate scaffolds after 7 days of culture at 50x (C) and 300x (D) of magnification.

Figure 4. SEM visualization of MC3T3-E1 cells growing on regular scaffolds (A and B), control alginate scaffolds (C and D) and P2-alginate-coated scaffolds (E and F) after 7 (A, C and E) and 21 (B, D and F) days of culture. Scaffolds were observed by SEM at 10kV, 40Pa and x50 of magnification.

Figure 5. Number of cells growing on the scaffolds after 7 days of culture. DNA content was analyzed by Hoechst fluorescence staining and correlated to a linear standard curve. Values represent the mean ± SEM. Values represent the mean ± SEM. Mann-Whitney test: (a) $p \leq 0.05$ versus regular scaffold (SC) and (b) versus control alginate scaffold (-).

Figure 6. Relative mRNA expression levels of *Itgb1*(A), *Itgb3* (B), *Fn1*(C) and *Itga8* (D) in MC3T3-E1 cells cultured on TiO_2 scaffolds for 7 (□) and 21 days (■). Regular scaffolds (SC) were used as reference group. Data represent fold changes of target genes normalized with reference genes (*Gapdh* and *18S*), expressed as a percentage of cells cultured on regular

scaffolds (SC) at day 7, which were set to 100%. Values represent the mean ± SEM. Student t-test: (a) p≤ 0.05 versus regular scaffold (SC) and (b) versus control alginate scaffold (-).

Figure 7. Relative mRNA expression levels of (A) osterix (*Osx*), (B) bone morphogenetic protein 2 (*Bmp2*), (C) collagen-I (*Coll-I*), (D) interleukin 6 (*Il-6*), (E) osteopontin (*Opn*), (F) bone sialoprotein *(Bsp)*, (G) alkaline phosphatase (*Alp*) and (H) osteocalcin (*Oc*) in MC3T3-E1 cells cultured on TiO2 scaffolds for 7 (□) and 21 days (▣). Regular scaffolds (SC) were used as reference group. Data represent fold changes of target genes normalized with reference genes (*Gapdh* and *18S*), expressed as a percentage of cells cultured on regular scaffolds (SC) at day 7, which were set to 100%. Values represent the mean ± SEM. Student t- test: (a) p≤ 0.05 versus regular scaffold (SC) and (b) versus control alginate scaffold (-).

Effect of TiO$_2$ scaffolds coated with alginate hydrogel containing a proline-rich peptide on osteoblast growth and differentiation in vitro

Rubert M[1], Pullisaar H[2], Gómez-Florit M[1], Ramis JM[1], Tiainen H[2], Haugen HJ[2], Lyngstadaas SP[2] and Monjo M[1]

[1]Group of Cell Therapy and Tissue Engineering, Research Institute on Health Sciences (IUNICS). University of Balearic Islands, Palma de Mallorca, Spain.

[2]Department of Biomaterials, Institute for Clinical Dentistry. University of Oslo, Oslo, Norway.

Corresponding author:

Marta Monjo, PhD

Research Institute on Health Sciences (IUNICS).

University of Balearic Islands, Crta. Valldemossa km 7.5, E-07122, Palma de Mallorca, Spain.

Phone: +34971259960

Fax: +34971173184

E-mail: marta.monjo@uib.es

Running title: Osteoblast response to alginate-coated TiO$_2$ scaffolds with polyproline peptide

ABSTRACT

The aim of this study was to investigate the effect of TiO_2 scaffold (SC) coated with an alginate hydrogel containing a proline-rich peptide (P2) on osteoblast proliferation and differentiation in vitro. Peptide release from alginate-coated TiO_2 SC was evaluated and a burst release was observed during the first hours of incubation, and then progressively released overtime. When seeding MC3T3-E1 cells on the coated and uncoated TiO_2 SC, no changes were observed in the cytotoxicity after 48h. SEM images revealed that cells were able to penetrate and adhere on alginate-coated TiO_2 SC either with or without P2, although the amount of cells were higher on uncoated TiO_2 SC, which was also in accordance to the DNA content results after 7 days of culture. A lower expression of integrin beta1 was detected for alginate-coated TiO_2 SC at this time point, but similar gene expression was observed for other integrins, fibronectin-1, and several osteoblast differentiation markers after 21 days. At this time, gene expression of integrin beta3, fibronectin-1, osterix and collagen-I was increased in alginate-coated compared to TiO_2 SC. P2 alginate-coated TiO_2 SC showed increased gene expression of bone morphogenetic protein 2 and collagen-I compared to alginate-coated and uncoated TiO_2 SC. In conclusion, our results indicate that alginate-coated TiO_2 SC can act as a matrix for delivery of proline-rich peptides increasing osteoblast differentiation. Thus, the combination of the osteoconductive properties of TiO_2 SC with the osteogenic effects of proline-rich peptides may represent a new strategy for bone tissue regeneration in load-bearing applications.

Keywords: TiO_2 scaffolds, alginate, proline-rich peptide, cell attachment, osteoblast differentiation.

INTRODUCTION

Natural bone tissue formation from osteogenic cells with the aid of a three-dimensional scaffold offers an alternative to autografts and allografts to repair and regenerate lost bone. A well-constructed scaffold provides a suitable surface for cells to attach and adhere with a porous and well interconnected network guiding the development of new bone, supporting migration, proliferation and differentiation of bone-forming cells and vascularization of the ingrowth tissue [1-3]. Although several polymers and bioceramics have been developed for their use in bone tissue engineering, their low mechanical properties have limited their use for load-bearing applications [4, 5].

Titanium dioxide (TiO_2) is a biocompatible material, which has also been reported to have bioactive properties and a certain degree of bacteriostatic effect [6-8]. Therefore, ceramic TiO_2 has been studied as a material for bone tissue engineering purposes [6, 9, 10]. High porous and well-interconnected TiO_2 scaffolds with high mechanical strength achieving values of 90% of porosity and of 1.63-2.67MPa of compressive strength have been recently developed [10] and their biocompatibility and osteoconductive properties have been demonstrated in *in vitro* [11] and *in vivo* [12] studies. *In vitro*, TiO_2 scaffolds provided a suitable surface for osteoblast cell attachment and cell differentiation and cells were well-distributed through the entire 3D structure over time [11]. Further, the formation of new mineralized bone tissue and vascularization of the ingrowth tissue has been observed *in vivo* [12].

Proline-rich proteins guide the deposition and growth of hydroxyapatite (Hap) into endoskeletal mineralized tissues by serving as a scaffold to control Hap crystal assembly and bind to protein domains frequently involved in signalling events [13, 14]. We have previously designed synthetic proline-rich peptides of 25 aminoacid length based on polyproline consensus sequences of hard tissue extracellular matrix proteins and have demonstrated their ability to stimulate osteoblast differentiation *in vitro* either in mouse pre-osteoblast like cells (MC3T3-E1) [15] or in human umbilical cord derived mesenchymal stem cells (hUCMSCs) [16] and to

3

promote osseointegration *in vivo* [17]. Further, we have shown that 2% alginate hydrogels are a suitable formulation for local delivery of synthetic proline-rich peptides [18].

In the present study, the best variant of our designed proline-rich peptides tested earlier *in vitro* was selected to coat TiO$_2$ scaffolds with an alginate hydrogel containing these peptides, and their effect investigated *in vitro* with MC3T3-E1 osteoblasts. Osteoblast cell viability was evaluated by determination of lactate dehydrogenase (LDH) activity and cell proliferation by quantification of DNA content. Relative mRNA levels of cell adhesion and of osteoblasts markers were also investigated by using real-time RT-PCR. The behaviour of cells into this 3D structure was visualized by scanning electron microscope (SEM). The release profile of the peptide to the medium was as well monitored by UV spectroscopy.

2. MATERIAL AND METHODS

2.1. *Preparation of synthetic peptide 2* (P2).

Synthetic proline-rich peptide 2 (2HN- PLVPSQPLVPSQPLVPSQPQPPLPP-COOH) was purchased from Eurogentec (Seraing, Belgium). One vial containing 7.2 mg of the selected synthetic peptide was delivered in a freeze-dried pellet form and dissolved to 10 mg/ml in 0,1% acetic acid in phosphate-buffered saline (PBS) (PAA Laboratories GmbH, Pasching, Austria). Aliquots to avoid repeated freeze-thaw cycles were prepared and stored at -20 °C until use.

2.2. *Preparation of 2% alginate gel containing peptide 2.*

Sodium alginate (Pronova UP LVG®) -a low viscosity alginate where minimum 60% of monomers are guluronate- was purchased from NovaMatrix (FMC BioPolymer AS, Norway). The sodium alginate was used without further purification. Quantity (2%, w/v) of sodium alginate was dissolved in distilled water by stirring for 3 h at room temperature to get a homogenous alginate solution. A fixed concentration (50µg/ml) of P2 was added to the solution and stirred for 1 h.

2.3. Fabrication of TiO₂ scaffolds coated with 2% alginate gel containing P2.

The porous TiO**₂** scaffolds were produced by polymer sponge replication as previously described by [10], with a size of 9 mm of diameter and 8 mm high. Then, scaffolds were coated with one layer of 2% alginate gel with or without P2. Briefly, TiO₂ scaffolds were submerged into 2% alginate solution with or without P2 under agitation at 100rpm on an orbital shaker (IKA Vibrax VXR basic, Staufen, Germany) for 1 h at room temperature. Scaffolds were then centrifuged at 252xg for 1 min. Samples were immersed into 50mM CaCl₂ for 1h to allow gelation. Scaffolds were then rinsed with dH₂O to remove the excess of CaCl₂. Finally, samples were let to dry overnight at room temperature. Scaffolds coated with one layer of 2% alginate gel (control alginate scaffold), were used as control group, whereas uncoated TiO₂ scaffolds (without alginate, SC) were also used as control group.

2.4. Peptide 2 release profile from TiO₂ scaffolds coated with 2% alginate gel.

TiO₂ scaffolds coated with 2% alginate containing peptide 2 (P2-alginate-coated scaffold) were placed into 48-well plates (Nunc GmBh & Co. Kg, Langenselbold, Germany) containing 1 ml distilled water (pH 7.4). In order to mimic cell culture conditions, the samples were agitated on an orbital shaker at 200 rpm (IKA® Schüttler MTS 2, Germany) for 6 h at 37ºC and in humidity conditions (using a distilled water container). Then, samples were maintained at 37°C in a humidified atmosphere for up to 21 days. At prefixed time points (2d, 5d, 7d, 9d, 12d, 14d, 16d, 19d and 21d), distilled water was collected and fresh distilled water was added into each well. Sample absorbances were analyzed by UV-Vis spectrophotometer (PerkinElmer® Lambda 25 UV/Vis Systems, USA) at a wavelength of 206nm to determine the amount of peptide released. In parallel, scaffolds coated with one layer of 2% alginate gel were used as control to subtract absorbance values obtained from degradation products from alginate. Relative absorbance units were correlated with the amount of peptide released using a linear standard curve for each time point and the cumulative P2 released was then calculated. The experiment was performed in triplicate.

2.5. Cell culture of MC3T3-E1 on coated and uncoated TiO₂ scaffolds.

TiO$_2$ scaffolds (SC) uncoated and coated with 2% alginate with or without peptide (P2 and control (-)) were placed into 48-well plates (Nunc GmbH & CO. KG, Langenselbold, Germany) in sterile conditions. Cells were seeded at a density of 200,000 cells/scaffold and maintained in α-MEM (PAA Laboratories, Pasching, Austria) supplemented with 10% FBS (PAA Laboratories, Pasching, Austria) and 100 U penicillin/ml and 100 µg streptomycin/ml antibiotics (PAA Laboratories, Pasching, Austria). In order to guarantee a homogenous cell distribution inside the scaffold, an agitated seeding method was used [19]. Briefly, after adding 1ml of cell suspension to the scaffolds, plates were agitated on an orbital shaker (Unitron, Infors HT, Basel, Switzerland) for 6 h at 180rpm at 37ºC and in humidity conditions. Then, cells were maintained at 37°C in a humidified atmosphere of 5% CO$_2$ for up to 21 days. Culture media (1 ml) was refreshed every other day.

Culture media was collected after 48 h of treatment to test cytotoxicity (LDH activity). To assess the ability of cell proliferation into this 3D system, the number of cells after 7 days was also studied by DNA quantification using Hoechst staining. In parallel, the cell attachment of MC3T3-E1 into the scaffold was also visualized by SEM after 7 and 21 days of culture. Expression of markers related to osteoblast cell maturation and differentiation after 7 and 21 days of cell culture was assessed by real-time RT-PCR.

2.6. SEM visualization of 2% alginate-coated TiO₂ scaffolds.

Morphology of alginate-coated TiO$_2$ scaffolds was observed using a scanning electron microscope (SEM, Hitachi S-3400N, Hitachi High-Technologies Europe GmbH, Krefeld, Germany). SEM was further used to visualize the cell adhesion into the TiO$_2$ scaffold structure after 7 and 21 days of culture. Briefly, cells were washed twice with PBS and fixed with glutaraldehyde 4% in PBS for 2 h. Then the fixative solution was removed and the cells were washed with distilled water twice. At 30 minute intervals, the cells were dehydrated by the addition of 50%, 70%, 90% and 100% ethanol solutions. Ethanol was removed and the cells were left at room temperature to evaporate the remaining ethanol. Scaffolds were observed at

10kV and 40Pa using back scattered and secondary electrons detector. Images presented are from a representative area.

2.7. Cell viability.

The lactate dehydrogenase (LDH) activity determined in the culture media after 48 h was taken as an indicator of cell survival. The activity of the cytosolic enzyme was determined according to the manufacturer's kit instructions (Roche Diagnostics, Mannheim, Germany). Results were presented relative to the LDH activity in the medium of cells cultured in uncoated scaffolds, which were set to 100%.

2.8. Cell number determination.

Cells growing on the 3D scaffolds were lysed by a freeze-thaw method in deionised distilled water [20]. Cell lysates were used for determination of DNA quantity using Hoechst 33258 fluorescence assay. Samples were mixed with 20μg/ml of Hoechst 33258 fluorescence stain (Sigma, St. Quentin Fallavier, France) in TNE buffer, and the intensity of fluorescence was measured at excitation and emission wavelengths of 356/465nm using a multifunction microplate reader (Cary Eclipse fluorescence spectrophotometer, Agilent Technologies, Santa Clara, United States). Relative fluorescence units were correlated with the cell number using a linear standard curve.

2.9. RNA isolation and real-time RT-PCR analysis.

Total RNA was isolated using Tripure® (Roche Diagnostics, Mannheim, Germany), according to the manufacturer's protocol. Total RNA was quantified at 260 nm using a Nanodrop spectrophotometer (NanoDrop Technologies, Wilmington, DE, USA). The same amount of total RNA (850ng) was reverse transcribed to cDNA at 42°C for 60 min using High Capacity RNA-to-cDNA kit (Applied Biosystems, Foster City, CA), according to the protocol of the supplier. Aliquots of each cDNA were frozen (-20 °C) until the PCR reactions were carried out.

Real-time PCR was performed in the Lightcycler 480® (Roche Diagnostics, Mannheim, Germany) using SYBR green detection. Real-time PCR was done for two reference genes

(18SrRNA and glyceraldehyde-3-phosphate dehydrogenase (*Gapdh*)) and 12 target genes (integrin alpha8 (*Itga8*), integrin beta1 (*Itgb1*), integrin beta3 (*Itgb3*), fibronectin 1 (*Fn1*), , osterix (*Osx*), bone morphogenetic protein 2 (*Bmp2*), collagen-I (*Coll-I*), interleukin-6 (*Il-6*), bone sialoprotein (*Bsp*), alkaline phosphatase (*Alp*), osteocalcin (*Oc*) and osteopontin (*Opn*)). The primer sequences are detailed in table 1.

Each reaction contained 7 μl Lightcycler-FastStart DNA MasterPLUS SYBR Green I (containing Fast Start Taq polymerase, reaction buffer, dNTPs mix, SYBRGreen I dye and MgCl$_2$), 0.5 μM of each, the sense and the antisense specific primers and 3μl of the cDNA dilution in a final volume of 10 μl. The amplification program consisted of a preincubation step for denaturation of the template cDNA (10 min 95 °C), followed by 45 cycles consisting of a denaturation step (10 s 95 °C), an annealing step (8-10 s 60 °C, except for *Osx* that was 5 s 68ºC and *Alp* that was 8s 65 ºC) and an extension step (10 s 72 °C). After each cycle, fluorescence was measured at 72 °C (λex 470 nm, λem 530 nm). A negative control without cDNA template was run in each assay.

Real-time efficiencies were calculated from the given slopes in the LightCycler 480 software using serial dilutions, showing all the investigated transcripts high real-time PCR efficiency rates, and high linearity when different concentrations are used. PCR products were subjected to a melting curve analysis on the LightCycler and subsequently 2% agarose/TAE gel electrophoresis to confirm amplification specificity, Tm and amplicon size, respectively.

Relative quantification after PCR was calculated by dividing the concentration of the target gene in each sample by the mean of the concentration of the two reference genes in the same sample using the Advanced relative quantification method provided by the LightCycler 480 analysis software version 1.5 (Roche Diagnostics, Mannheim, Germany).

2.10. *Statistics*

All data are presented as mean values ± SEM. A Kolmogorov-Smirnov test was done to assume parametric or non-parametric distributions for the normality tests, differences between groups were assessed by Mann-Whitney-test or by Student t-test depending on their normal

distribution. SPSS® program for Windows (Chicago, IL, US), version 17.0 was used. Results were considered statistically significant at p-values ≤ 0.05.

3. **RESULTS**

3.1   Peptide release.

Peptide release profile from P2-alginate-coated scaffolds is depicted in Figure 1. A burst release of the peptide during the first 2 days of incubation was observed (42.8% of the cumulative amount of P2 released after 21 days). After 5 days, the amount of peptide released decreased to a 9.4% (of the cumulative amount released up to 21 days) followed by a slower but sustained peptide release over time up to 21 days of incubation. Further, the cumulative release suggests that, after 21 days of incubation, there were still P2 entrapped into the 2% alginate gel.

3.2   LDH activity.

As shown in Figure 2, no toxic effects were observed for any of the experimental groups studied. Similar percentage of cell viability was determined in all the groups tested, indicating that either control alginate scaffolds (-) and P2-alginate-coated scaffolds (P2) did not show any toxic effects on cells after 48h of cell culture.

3.3   SEM visualization of TiO_2 scaffolds coated with 2% alginate gel.

Alginate-coated TiO_2 scaffolds were observed by SEM. As shown in figures 3A and 3B, some pores of the TiO_2 scaffolds were blocked after the coating process with alginate, though, after cell seeding and 7 days of incubation in standard cell culture conditions (37ºC and in a humidified atmosphere), almost all pores were unblocked (Figure 3C and 3D). Thus, certain degradation of the blocking alginate gel was seen in those pores that remained blocked right after the coating process.

Although the amount of cells growing on uncoated TiO_2 scaffolds (SC) was higher (Figure 4A and 4B) than on alginate-coated TiO_2 scaffolds (Figure 4C-4F), cells were able to penetrate and to adhere into the coated scaffolds with 2% alginate gel either with or without P2.

9

An increase from day 7 to day 21 in the number of cells growing on the scaffolds was seen for all the experimental groups.

3.4   Cell number.

DNA quantification was used to determine the number of cells growing on the TiO_2 scaffolds after 7 days of culture (Figure 5). In accordance to SEM images, after 7 days of culture the number of cells was significantly lower in any of the alginate-coated TiO_2 scaffolds compared to TiO_2 scaffolds (SC). Thus, compared to SC, a 61% and a 49% reduction in cell number was found on alginate-coated scaffolds without and with P2, respectively. Although data did not reach statistical significance, scaffolds coated with P2 showed 32% more cells than the alginate control scaffolds (-).

3.5   Gene expression of cell adhesion-related markers.

As shown in Figure 6, relative mRNA levels of *Itb1* were significantly decreased in cells growing onto alginate-coated scaffolds (either with or without P2) compared to TiO_2 scaffolds (SC) after 7 days of culture. Nevertheless, after 21 days of cell culture no differences were observed among groups. After 21 days, *Itgb3* mRNA levels were increased in cells growing on alginate-coated scaffolds (either with or without P2) compared to TiO_2 scaffolds (SC). Higher mRNA levels of *Fn1* were found in cells growing on 2% alginate-coated scaffolds after 21 days, and in cells growing on P2-alginate-coated scaffolds compared to uncoated scaffolds, although for the last group data did not reach statistical significance. *Itga8* mRNA was significantly increased in cells growing on P2-alginate-coated scaffolds compared to control alginate scaffolds after 21 days of culture.

3.6   Gene expression of several osteoblast differentiation markers.

Figure 7 shows relative mRNA levels for several osteoblast differentiation marker genes. After 21 days of culture, osterix mRNA levels were increased in cells growing on alginate-coated scaffolds (either with or without P2) compared to uncoated scaffolds. *Bmp-2* and *Il-6* mRNA levels were significantly increased in cells cultured on P2-alginate-coated scaffolds compared to both uncoated scaffolds and alginate-coated scaffolds after 21days of cell

10

culture. *Coll-I* mRNA levels, a marker related with cell proliferation [21], were significantly increased in cells cultured on P2-alginate-coated scaffolds compared to alginate-coated scaffolds after 7 days of cell culture. After 21 days of culture *Coll-I* was significantly increased in both alginate-coated scaffolds and P2-alginate-coated scaffolds compared to uncoated scaffolds. No significant differences were observed in *Opn, Bsp, Alp* and *Oc* mRNA expression levels among experimental groups at any of the time points studied.

3. DISCUSSION

In the present study, we have combined the improved reported biocompability and osteoconductivity of TiO_2 scaffolds with the suitability of alginate gel as a carrier for the delivery of a proline-rich peptide, for their use in load-bearing bone tissue applications to promote bone formation and mineralization. TiO_2 scaffolds have been reported to have strength up to 2.6 MPa in compressive strength [10] and showed excellent mechanical resistance in a pig *in vivo* study [12].

In bone tissue engineering, the structure of the scaffold must provide an optimal microenvironment for osteogenesis [10]. The scaffold porosity, pore network interconnectivity, the surface-area-to-volume ratio and the physico-chemical properties of the surface determines cell migration and differentiation, bone ingrowth, vascularization, and mass transfer between the cells and the environment [22]. The use of highly porous TiO_2 scaffolds using an agitated cell seeding method has proved to achieve a good attachment and distribution of mouse pre-osteoblastic cells [11]. In the present study, TiO_2 scaffolds coated with one layer of 2% alginate displayed a microstructure suitable for their use as scaffold for three-dimensional cell growth. Although a few pores remained blocked right after the coating process, almost all pores were unblocked after 7 days of incubation at 37ºC due to biodegradability properties of alginate [23], thus providing opening windows for cells to penetrate and migrate into the structure. In this study, no differences on cell viability were observed between coated and uncoated TiO_2 scaffolds, in agreement with previous reports showing cell safety and biocompatibility of TiO_2

11

scaffolds [7] and of alginate gels [18, 24-26]. Alginate has been widely used for delivery of bioactive molecules [25, 27] and constitute a suitable carrier for delivery of synthetic peptides at the local site [18]. We found a burst release of P2 during the first hours of incubation followed by progressive and sustained release during the 21-days period, following the same pattern as in alginate hydrogels alone (Rubert et al, submitted).

Consistent with previous studies [6, 9, 11], TiO_2 scaffolds provided an appropriate surface for osteoblasts to adhere, migrate and proliferate. Although the amount of cells into alginate-coated TiO_2 scaffolds was lower than in uncoated TiO_2 scaffolds, scaffolds coated with alginate supported cell progression and differentiation. These results are in accordance with previous studies reporting that the alginate is an innert substrate for cell attachment [28] and that synthetic peptides rich in proline sequences increase properties for cell attachment of the alginate hydrogel [18]. Thus, although not significantly, TiO_2 scaffolds coated with 2% alginate containing synthetic peptide 2 showed a trend to improve cell attachment (+32 %) after 7 days compared to alginate-coated TiO_2 scaffolds.

It has been reported that biomaterial composition regulates cell attachment and cytoskeletal organization with long-term effects on osteoblast cell maturation and mineralization [29]. In accordance to the efficiency in cell attachment observed by SEM and DNA quantification onto the different groups, *Itgb1* mRNA levels were decreased in cells growing on alginate-coated TiO_2 scaffolds compared to those growing on uncoated scaffolds. Further, *Itgb3* and *Fn1* mRNA levels (which are highly expressed at early stages of osteogenesis and reduced through the cellular maturation process [11, 30, 31]) were significantly increased in cells growing into alginate-coated TiO_2 scaffolds compared to the uncoated scaffolds after 21 days of culture. Moreover, expression of *Itga8*, an integrin that plays a role during the mineralization stage through the binding to osteopontin, was induced by P2-alginate-coated scaffolds compared to alginate-coated scaffolds, suggesting that P2 might influence mineralization processes, as previously reported with the increased mineralization in MC3T3-E1 and hUCMSCs after P2 treatment [15]. Integrins are not only involved in the attachment of cells to

12

the material surface [32-36] but also mediate signal transduction pathways inducing bone formation and mineralization [31, 37]. Interestingly, expression of genes like *Itgb3, Fn1, Coll-I* and *Osx* that are related to early stages of osteoblast differentiation, and which are normally upregulated at short term and downregulated thereafter, were increased in the later time point studied (21 days) in cells grown into alginate-coated TiO_2 scaffolds compared to cells growing on uncoated scaffolds. It is possible that the temporal sequence of early markers related to osteoblast differentiation varies when MC3T3-E1 cells are growing on uncoated scaffolds or on alginate-coated scaffolds, so that cells growing onto alginate-coated surfaces showed an improved cell differentiation over proliferation compared to uncoated TiO_2 scaffolds, probably due to the initial difficulties of cell adhesion onto the alginate. Although alginate coating seems to impair cell adhesion and proliferation on the scaffolds, the acquisition of a mature and organized matrix (ECM) competent for mineralization was confirmed by a marked increase in *Alp* and *Bsp* mRNA levels from day 7 to 21 days for any of the groups. Once the synthesis, organization and maturation of the ECM has finalized, *Oc* expression is upregulated leading to mineralization [38, 39]. Our results showed a slight increase in *Oc* mRNA levels after 21 days of culture, therefore, we can conclude that cells were just at the beginning of the mineralization process. Moreover, in accordance to our results with gene expression levels of *Opn* and *Bsp*, the increased relation Bsp/Opn mRNA in osteoblastic cells could be indicative for the stimulation of ECM mineralization, as previously reported with MC3T3-E1 cells seeded on uncoated TiO_2 scaffolds [11].

It is important to highlight that the addition of P2 to alginate improved the properties for cell proliferation and differentiation compared to alginate-coated scaffolds, as it can be appreciated by the amount of cells measured by DNA content and the higher expression levels of *Bmp2, Coll-I* and *Il-6*. So far the synthetic peptides rich in polyproline sequences have repetitively shown an increase in osteocalcin mRNA levels, both *in vitro* [15, 16] and in *in vivo* studies where titanium implants were coated with the peptide [17], and further when loaded into an alginate hydrogel for their use as a carrier for local delivery [18]. Thus, taken together our

13

previous studies and the results from the present study, this allows us to suggest that P2-alginate-coated scaffolds would promote higher cell differentiation and mineralization in an *in vivo* environment.

4. CONCLUSION

In conclusion, our results demonstrate that alginate-coated TiO$_2$ scaffolds can act as a matrix for delivery of synthetic peptide rich in proline sequences inducing osteoblast cell differentiation. The combination of the physical and osteoconductive properties of TiO$_2$ scaffolds with the osteogenic effects of synthetic proline-rich peptides on bone formation and mineralization may represent a new strategy for bone tissue regeneration in load-bearing applications.

6. REFERENCES

[1] Jokinen M, Patsi M, Rahiala H, Peltola T, Ritala M, Rosenholm JB. Influence of sol and surface properties on in vitro bioactivity of sol-gel-derived TiO2 and TiO2-SiO2 films deposited by dip-coating method. Journal of biomedical materials research 1998;42:295-302.

[2] Lee N, Oh H, Hong C, Suh H, Hong S. Comparison of the synthetic biodegradable polymers, polylactide (PLA), and polylactic-co-glycolic acid (PLGA) as scaffolds for artificial cartilage. Biotechnology and Bioprocess Engineering 2009;14:180-6.

[3] Thonmson RC, Shung AK, Yaszemski MJ, Mikos AG. Scaffolds processing. In: R. Lanza R-LaJV, editor. Principles of tissue engineering. San Diego: Academic Press; 2000. p. 252-9.

[4] Bueno Rde B, Adachi P, Castro-Raucci LM, Rosa AL, Nanci A, Oliveira PT. Oxidative nanopatterning of titanium surfaces promotes production and extracellular accumulation of osteopontin. Braz Dent J 2011;22:179-84.

[5] Khan Y, Yaszemski MJ, Mikos AG, Laurencin CT. Tissue Engineering of Bone: Material and Matrix Considerations. J Bone Joint Surg Am 2008;90 Sippl 1:36-42.

[6] Fostad G, Hafell B, FÃ¸rde A, Dittmann R, Sabetrasekh R, Will J, et al. Loadable TiO2 scaffolds-A correlation study between processing parameters, micro CT analysis and mechanical strength. Journal of the European Ceramic Society 2009;29:2773-81.

[7] Nygren H, Tengvall P, Lundstrom I. The initial reactions of TiO2 with blood. Journal of biomedical materials research 1997;34:487-92.

[8] Rincon JC, Xiao Y, Young WG, Bartold PM. Enhanced proliferation, attachment and osteopontin expression by porcine periodontal cells exposed to Emdogain. Archives of oral biology 2005;50:1047-54.

[9] Sabetrasekh R, Tiainen H, Reseland JE, Will J, Ellingsen JE, Lyngstadaas SP, et al. Impact of trace elements on biocompatibility of titanium scaffolds. Biomed Mater 2010;5:15003.

[10] Tiainen H, Lyngstadaas SP, Ellingsen JE, Haugen HJ. Ultra-porous titanium oxide scaffold with high compressive strength. J Mater Sci Mater Med 2010;21:2783-92.

[11] Gómez-Florit M, Rubert M, Ramis JM, Haugen HJ, Lyngstadaas SP, Monjo M. Homogeneous seeding and differentiation of MC3T3-E1 cells on TiO$_2$ scaffolds. Submitted.

[12] Tiainen H, Wohlfahrt JC, Verket A, Lyngstadaas SP, Haugen HJ. Bone formation in TiO2 bone scaffolds in extraction sockets of minipigs. Acta Biomater 2012;8:2384-91.

[13] Ball LJ, Kuhne R, Schneider-Mergener J, Oschkinat H. Recognition of proline-rich motifs by protein-protein-interaction domains. Angew Chem Int Ed Engl 2005;44:2852-69.

[14] Jin T, Ito Y, Luan X, Dangaria S, Walker C, Allen M, et al. Elongated polyproline motifs facilitate enamel evolution through matrix subunit compaction. PLoS Biol 2009;7:e1000262.

[15] Rubert M, Ramis JM, Vondrasek J, Gayà A, Lyngstadaas SP, Monjo M. Synthetic peptides analogue to enamel proteins promote osteogenic differentiation of MC3T3-E1 and mesenchymal stem cells. J Biomater Tissue Eng 2011;1:198-209.

[16] Ramis JM, Rubert M, Vondrasek J, Gayà A, Lyngstadaas SP, Monjo M. Effect of enamel matrix derivative and of proline-rich synthetic peptides on the differentiation of human mesenchymal stem cells towards the osteogenic lineage. Tissue Eng Part A 2012;18:1-11.

[17] Petzold C, Monjo M, Rubert M, Reinholt FP, Gomez-Florit M, Ramis JM, et al. Effect of coated titanium implants with a proline-rich synthetic peptide on bone healing. Oral Craniofac Tissue Eng 2012;2:35-43.

[18] Rubert M, Monjo M, Lyngstadaas SP, Ramis JM. Effect of alginate hydrogel containing polyproline-rich peptides on osteoblast differentiation. Submitted.

[19] Takahashi Y, Tabata Y. Homogeneous seeding of mesenchymal stem cells into nonwoven fabric for tissue engineering. Tissue Eng 2003;9:931-8.

[20] Rage R, Mitchen J, Wilding G. DNA fluorometric assay in 96-well tissue culture plates using Hoechst 33258 after cell lysis by freezing in distilled water. Anal Biochem 1990;191:31-4.

[21] Stein GS, Lian JB, Stein JL, Van Wijnen AJ, Montecino M. Transcriptional control of osteoblast growth and differentiation. Physiological reviews 1996;76:593-629.

[22] Hutmacher DW. Scaffolds in tissue engineering bone and cartilage. Biomaterials 2000;21:2529-43.

[23] Rowley JA, Madlambayan G, Mooney DJ. Alginate hydrogels as synthetic extracellular matrix materials. Biomaterials 1999;20:45-53.

[24] Barbetta A, Barigelli E, Dentini M. Porous alginate hydrogels: synthetic methods for tailoring the porous texture. Biomacromolecules 2009;10:2328-37.

[25] Lee JY, Choo JE, Park HJ, Park JB, Lee SC, Jo I, et al. Injectable gel with synthetic collagen-binding peptide for enhanced osteogenesis in vitro and in vivo. Biochemical and biophysical research communications 2007;357:68-74.

[26] Rubert M, Alonso-Sande M, Monjo M, Ramis JM. Evaluation of alginate and hyaluronic acid for their use in bone tissue engineering. Submitted.

[27] Kolambkar YM, Dupont KM, Boerckel JD, Huebsch N, Mooney DJ, Hutmacher DW, et al. An alginate-based hybrid system for growth factor delivery in the functional repair of large bone defects. Biomaterials 2011;32:65-74.

[28] Alsberg E, Anderson KW, Albeiruti A, Franceschi RT, Mooney DJ. Cell-interactive alginate hydrogels for bone tissue engineering. Journal of dental research 2001;80:2025-9.

[29] Shah AK, Lazatin J, Sinha RK, Lennox T, Hickok NJ, Tuan RS. Mechanism of BMP-2 stimulated adhesion of osteoblastic cells to titanium alloy. Biol Cell 1999;91:131-42.

[30] Cheng S-L, Lai C-F, Blystone SD, Avioli LV. Bone Mineralization and Osteoblast Differentiation Are Negatively Modulated by Integrin $\alpha v \beta 3$. J Bone Miner Res 2001;16:277-88.

[31] Moursi AM, Globus RK, Damsky CH. Interactions between integrin receptors and fibronectin are required for calvarial osteoblast differentiation in vitro. J Cell Sci 1997;110:2187-96.

[32] El-Amin SF, Attawia M, Lu HH, Shah AK, Chang R, Hickok NJ, et al. Integrin expression by human osteoblasts cultured on degradable polymeric materials applicable for tissue engineered bone. J Orthop Res 2002;20:20-8.

[33] Gronowicz G, McCarthy MB. Response of human osteoblasts to implant materials: Integrin-mediated adhesion. J Orthop Res 1996;14:878-87.

[34] Lynch MP, Stein JL, Stein GS, Lian JB. The influence of type I collagen on the development and maintenance of the osteoblast phenotype in primary and passaged rat calvarial

osteoblasts: modification of expression of genes supporting cell growth, adhesion, and extracellular matrix mineralization. Exp Cell Res 1995;216:35-45.

[35] Siebers MC, ter Brugge PJ, Walboomers XF, Jansen JA. Integrins as linker proteins between osteoblasts and bone replacing materials. A critical review. Biomaterials 2005;26:137-46.

[36] Steele JG, Dalton BA, Johnson G, Underwood PA. Polystyrene chemistry affects vitronectin activity: an explanation for cell attachment to tissue culture polystyrene but not to unmodified polystyrene. Journal of biomedical materials research 1993;27:927-40.

[37] Hynes RO. Integrins: Versatility, modulation, and signaling in cell adhesion. Cell 1992;69:11-25.

[38] Sodek J, Chen J, Nagata T, Kasugai S, Todescan R, Jr., Li IW, et al. Regulation of osteopontin expression in osteoblasts. Ann N Y Acad Sci 1995;760:223-41.

[39] McKee MD, Nanci A. Osteopontin and the Bone Remodeling Sequence. Ann N Y Acad Sci 1995;760:177-89.

7. TABLES

Table 1. *Primer sequences of osteoblast markers related genes used in the real-time PCR.*

Gene	Primer sequence
18S	S 5'-GTAACCCGTTGAACCCCATT-3'
	A 5'- CCATCCAATCGGTAGTAGCG-3'
Gapdh	S 5'-ACCCAGAAGACTGTG-GATGG-3'
	A 5'-CACATTGGG-GGTAGGAACAC-3'
Itgb1	S 5'- AGCAGGCGTGGTTGCTGGAA -3'
	A 5'- TTTCACCCGTGTCCCACTTGGC -3'
Itgb3	S 5'- AGGGGAGATGTGTTCCGGCCA -3'
	A 5'- ACACACAGCTGCCGCACTCG -3'
Fn1	S 5'- GCTGCCAGGAGACAGCCGTG -3'
	A 5'- GTCTTGCCGCCCTTCGGTGG -3'
Itga8	S 5'- TCGCCTGGGAGGAGGCGAAA -3'
	A 5'- TCTTAACCGCTGTGCTCCCCG -3'
Osx	S 5' - ACTGGCTAG GTGGTGGTCAG- 3'
	A 5' - GGTAGGGAGCTGGGTTAAGG- 3'
Bmp2	S 5'- GCTCCACAAACGAGAAAAG-C-3'
	A 5'- AGCAAGGGGAAAAG-GACACT-3'
Coll-I	S 5'- AGAGC-ATGACCGATGGATTC -3'
	A 5'- CCTTCTTGAGGTTGCCAGTC -3'
Il-6	S 5'- ACTTCCATCCAGTTGCCTTC- 3'
	A 5' -TTTCCACGATTT CCCAGAGA- 3'
Bsp	S 5'-GAAAATGGAGACGGCGATAG-3'
	A 5'-ACCCGAGAGTGTGGAAAGTG-3'
Alp	S 5'-AACCCAGACACAAGCATT-CC-3'
	A 5'- GAGAGCGAAGGGTC-AGTCAG-3'
Oc	S 5'- CCGGGAGCAG-TGTGAGCTTA-3'
	A 5'-TAGATGC-GTTTGTAGGCGGTC -3'
Opn	S 5'-TCTGCGGCAGGCATTCTCGG-3'
	A 5'-GTCACTTTCACCGGGAGGGAGGA-3'

8.

Figure 1. Release profile of peptide 2 from P2-alginate-coated scaffolds after 21 days of incubation at 37ºC. Bar graph show the amount of peptide released after each time point. Line graph represents cumulative amount of peptide released up to 21 days. Values represent mean $\pm$ SD.

Figure 2. LDH activity measured from culture media collected after 48 h of culture. Values represent the mean $\pm$ SEM. Mann-Whitney test ($p \leq 0.05$): (a) versus regular scaffold (SC) and (b) versus control alginate scaffold (-).

Figure 3. SEM visualization of 2% alginate-coated TiO_2 scaffolds (control alginate scaffold) at 10kV and 40Pa. Figures A and B show the microstructure of TiO_2 scaffolds right after the coating process with one layer of 2% alginate gel at 50x (A) and 300x (B) of magnification. Figures C and D show cells cultured on control alginate scaffolds after 7 days of culture at 50x (C) and 300x (D) of magnification.

Figure 4. SEM visualization of MC3T3-E1 cells growing on regular scaffolds (A and B), control alginate scaffolds (C and D) and P2-alginate-coated scaffolds (E and F) after 7 (A, C and E) and 21 (B, D and F) days of culture. Scaffolds were observed by SEM at 10kV, 40Pa and x50 of magnification.

Figure 5. Number of cells growing on the scaffolds after 7 days of culture. DNA content was analyzed by Hoechst fluorescence staining and correlated to a linear standard curve. Values represent the mean $\pm$ SEM. Values represent the mean $\pm$ SEM. Mann-Whitney test: (a) $p \leq 0.05$ versus regular scaffold (SC) and (b) versus control alginate scaffold (-).

Figure 6. Relative mRNA expression levels of *Itgb1*(A), *Itgb3* (B), *Fn1*(C) and *Itga8* (D) in MC3T3-E1 cells cultured on TiO_2 scaffolds for 7 (□) and 21 days (■). Regular scaffolds (SC) were used as reference group. Data represent fold changes of target genes normalized with reference genes (*Gapdh* and *18S*), expressed as a percentage of cells cultured on regular

scaffolds (SC) at day 7, which were set to 100%. Values represent the mean ± SEM. Student t-test: (a) p≤ 0.05 versus regular scaffold (SC) and (b) versus control alginate scaffold (-).

Figure 7. Relative mRNA expression levels of (A) osterix (*Osx*), (B) bone morphogenetic protein 2 (*Bmp2*), (C) collagen-I (*Coll-I*), (D) interleukin 6 (*Il-6*), (E) osteopontin (*Opn*), (F) bone sialoprotein *(Bsp),* (G) alkaline phosphatase (*Alp*) and (H) osteocalcin (*Oc*) in MC3T3-E1 cells cultured on TiO2 scaffolds for 7 (□) and 21 days (▣). Regular scaffolds (SC) were used as reference group. Data represent fold changes of target genes normalized with reference genes (*Gapdh* and *18S*), expressed as a percentage of cells cultured on regular scaffolds (SC) at day 7, which were set to 100%. Values represent the mean ± SEM. Student t- test: (a) p≤ 0.05 versus regular scaffold (SC) and (b) versus control alginate scaffold (-).

Paper 7

Effect of proline-rich synthetic peptide–coated titanium implants

on bone healing in a rabbit model.

Petzold, C.; Monjo, M.; Rubert, M.; Gómez-Florit, M.; Ramis, J.M.; Ellingsen, J.E.;

Lyngstadaas, S.P.

Effect of Proline-Rich Synthetic Peptide–Coated Titanium Implants on Bone Healing in a Rabbit Model

Christiane Petzold, MSc[1]/Marta Monjo, PhD[2]/Marina Rubert, MSc[3]/Finn P. Reinholt, MD, PhD[4]/
Manuel Gomez-Florit, MSc[3]/Joana Maria Ramis, PhD[5]/Jan Eirik Ellingsen, DDS, PhD[6]/
S. Petter Lyngstadaas, DDS, PhD[7]

Purpose: *Previous studies have demonstrated the capacity of a designed proline-rich synthetic peptide to stimulate osteoblast differentiation and biomineralization in vitro. Therefore, the aim of the present study was to evaluate the osseointegration capacity of titanium (Ti) implants coated with these peptides in a rabbit model.* **Materials and Methods:** *Four calibrated defects were prepared in the tibiae of three New Zealand rabbits, and the defects were randomized into a test group (peptide-modified machined Ti implant) and a control group (unmodified machined Ti implant). The performance in vivo was investigated after 4 weeks of implantation by real-time reverse transcriptase polymerase chain reaction of bone and inflammatory markers, microcomputed tomographic analysis of mineralized bone, and histologic examination.* **Results:** *The peptides adsorbed in agglomerates on Ti and underwent a change in secondary structure upon adsorption, which induced an increase in surface wettability. Gene expression markers indicated that peptide-coated Ti implants had significantly decreased mRNA levels of tartrate-resistant acid phosphatase. A trend toward increased osteocalcin in the peri-implant bone tissue was also seen. Bone morphometric and histologic parameters did not show significant differences, although the peptide group showed a higher percentage of new bone histologically.* **Conclusions:** *Proline-rich peptides have potential as a biocompatible coating for promoting osseointegration of Ti implants by reducing bone resorption.* ORAL CRANIOFAC TISSUE ENG 2012;2:35–43

Key words: *dental implants, gene expression, histology, microcomputed tomography, osseointegration, proline-rich peptide*

[1]Doctoral Candidate, Department of Biomaterials, Institute of Clinical Dentistry, Faculty of Dentistry, University of Oslo, Norway.

[2]Ramon y Cajal Researcher, Department of Fundamental Biology and Health Sciences, Research Institute on Health Sciences (IUNICS), University of Balearic Islands, Spain.

[3]Doctoral Candidate, Department of Fundamental Biology and Health Sciences, IUNICS, University of Balearic Islands, Spain.

[4]Professor, Department of Pathology, University of Oslo, Oslo University Hospital Rikshospitalet, Oslo, Norway.

[5]Postdoctoral Researcher, Department of Fundamental Biology and Health Sciences, IUNICS, University of Balearic Islands, Spain.

[6]Professor, Head of Oral Research Laboratory, Faculty of Dentistry, University of Oslo, Norway.

[7]Professor, Head of Department of Biomaterials, University of Oslo, Norway.

Correspondence to: Dr Marta Monjo, Department of Fundamental Biology and Health Sciences, IUNICS, University of Balearic Islands, Cra. De Valldemossa, km 7.5 (E-07122), Palma de Mallorca, Spain. Fax: +34-971-173184. Email: marta.monjo@uib.es

A large body of research in the biomaterials field is focused on the production of innovative surfaces that can promote a more favorable biologic response to implant material at the bone-implant interface and accelerate osseointegration.[1] Several surface modifications have been proposed to promote osseointegration of titanium (Ti) implants. Among the strategies used, the deposition of bioactive coatings has been employed to improve adhesion between the implant and bone.[2,3]

Bone mineralization is mediated by a magnitude of proteins regulating the deposition of calcium and phosphorus ions to form hydroxyapatite crystals and direct crystal growth. Among the extracellular proteins that regulate biomineralization are several molecules that exhibit proline-rich regions, such as collagens, amelogenins, ameloblastin, and sialoproteins.[4] Various forms of amelogenin-containing or amelogenin

peptide products, such as porcine enamel matrix derivative (EMD),[5] recombinant murine amelogenin,[6] leucine-rich amelogenin peptide,[7] recombinant amelogenin polypeptides,[8] and osteoinductive fractions of enamel extracts,[9] have been applied successfully for induction of bone regeneration in vitro and in vivo.[10,11]

Given the described role of polyproline-rich proteins in the control of the assembly of biologic apatites,[4] an artificial consensus peptide has been designed based on the common characteristics of the proline-rich regions in hard tissue extracellular matrix proteins to find new molecules for induction of bone formation and biomineralization.[12] Previous studies demonstrated the capacity of the designed synthetic peptides to stimulate osteoblast differentiation and biomineralization in vitro in both mouse preosteoblastic cells (MC3T3-E1) and in human umbilical cord–derived mesenchymal stem cells (hUCMSCs).[12] The selected variant of the peptide improved cell viability, induced stronger gene expression of bone formation markers compared to EMD, and increased mineral deposition in MC3T3-E1 cells after 28 days of treatment in a similar manner to EMD.[12] Moreover, the synthetic peptide showed an osteopromotive effect in combination with osteogenic supplements after long-term treatment in hUCMSCs (unpublished results).

Peptide fragments can be physically adsorbed onto a Ti surface, since negatively charged carboxylic groups show a strong affinity for metal oxide surfaces and can therefore directly interact with the Ti surface.[13] In the present study, the best variant of the designed consensus peptide tested earlier in vitro was selected to functionalize implant surfaces to favor osseointegration. The peptide was used to coat Ti implants, and its bone-forming abilities were investigated in an animal in vivo model after 4 weeks of healing. After implant detachment, tissue fluid from the implant site was collected for measurement of lactate dehydrogenase (LDH) and alkaline phosphatase (ALP) activity, as well as total protein content. The peri-implant bone tissue attached to the extracted implants was used to analyze gene expression of osteoblast markers (type 1 collagen [col-1], runx2, osteocalcin [OC]), osteoclast markers (tartrate-resistant alkaline phosphatase [TRAP]), and inflammatory markers (tumor necrosis factor-alpha [TNF-α], interleukin 6 [IL-6], IL-10) in peri-implant bone tissue using real-time reverse transcriptase polymerase chain reaction (RT-PCR). In addition, the morphometry of the peri-implant cortical bone tissue was evaluated by microcomputed tomography (micro-CT) and histology.

MATERIALS AND METHODS

Preparation of Titanium Disks
Commercially pure machined Ti implants with a diameter of 6.25 mm and a height of 1.95 mm were cleaned and sterilized before use, as described elsewhere.[14] Before they were coated, the implants were washed for 10 seconds each in autoclaved deionized water, acetone/water (50:50 by volume), and 100% acetone; air dried; and packed individually in microcentrifuge sterile tubes.

Preparation of Peptide Solution
The synthetic peptide (H2N-PLV PSQ PLV PSQ PLV PSQ PQP PLP P-COOH) was purchased from Eurogentec and dissolved in phosphate-buffered saline (PBS) with a pH of 7.4 at a concentration of 20 mg/mL. This solution was further dissolved in PBS to a final concentration of 100 μg/mL.

Adsorption of Peptide to Ti Implants
The peptide solution (10 μL of 100 μg/mL) was applied to the surface of the Ti implant and incubated for 24 hours at 37°C. Subsequently, the Ti implants were rinsed with sterile deionized water, dried in a desiccator, packed, and stored at 4°C. The final concentration of peptides was 1 μg peptide/surface or 0.033 μg/mm^2, which equals $7.52 \times 1,014$ molecules/mm^2. Control implants were treated with 10 μL of PBS without the peptide.

Characterization of Peptide-Modified Ti Implants
Surface analysis of the Ti implants after coating with the peptide was performed using a blue light profilometer (Sensofar Plμ 2300) at a magnification of ×150.

Peptide-modified Ti implants and the peptide solution in PBS (2 mg/mL) were also analyzed with Fourier transform infrared (FTIR) spectroscopy (Spectrum 100, PerkinElmer) to verify the presence of attached peptides on the surfaces of Ti and to analyze structural changes upon adsorption. Physically attached peptide was measured after drying on Ti with the diffuse reflectance unit, and the spectra of peptide in PBS were collected with attenuated total reflectance spectroscopy with a resolution of 4 cm^{-1}. Eight spectra were averaged per final spectrum. The spectra were baseline corrected, deconvoluted ($\gamma = 1.5$, length = 75%), and normalized with Spectrum (version 6.3.2.0151, Perkin Elmer). Fitting and measurement of the curves were done with CasaXPS (version 2.3.15, Casa Software Ltd).

Finally, the water contact angles of the surfaces of the different Ti implants were measured using a video-based contact angle system (OCA 20, DataPhysics Instruments) with deionized water.

Animal Study

Three female New Zealand White rabbits, all 6 months old and weighing 3.0 to 3.5 kg, were used in this study (ESF-Produkter, Estuna). The animals were housed together in one cage before surgery and during the healing period. The room was lightened from 8 AM to 8 PM; temperature was regulated to 19°C ± 1°C with a humidity of 55% ± 10%. The animals were fed 160 g pelleted rabbit food (B&K Universal AS) each day, in addition to 15 g of autoclaved hay. Untreated tap water was available ad libitum. The microbiologic status of the rabbits was determined according to a program by The Microbiological Laboratories, London, United Kingdom. The experiment was approved by the Norwegian Animal Research Council and was in compliance with the Animal Welfare Act of December 20th, 1974, No. 73, Chapter VI, Sections 20–22 and the Regulation on Animal Experimentation of January 15th, 1996.[15]

Four Ti implants were inserted in the tibiae of each rabbit, two on the left side and two on the right side, according to a predetermined randomization protocol. Six implants per group were analyzed. The surgical method was based on a standardized and validated model that had been established for studying bone attachment to Ti implant surfaces.[16] Four weeks after surgery, the animals were sacrificed and the performance of the peptide-modified Ti implants was evaluated.

Tissue Fluid Analyses

LDH and ALP activity as well as total protein were analyzed in the tissue fluid collected from the implant site following a 4-week healing period. After the implants had been removed, two filter papers of the same size as the implants were applied for 1 minute in each drilled defect (proximal and distal) to absorb the tissue fluid. They were transferred to microcentrifuge tubes containing 200 μL of PBS and placed on ice until analyses were performed later that same day.

The presence of LDH activity in the tissue fluid was used as an indirect measure of tissue necrosis.[17] LDH activity was determined spectrophotometrically after 30 minutes of incubation of 50 μL of tissue fluid and 50 μL of the reaction mixture at 25°C, by measuring the oxidation of nicotinamide adenine dinucleotide at 490 nm in the presence of pyruvate, according to the manufacturer's instructions (Cytotoxicity Detection Kit, Roche Diagnostics).

An aliquot of 10 μL of tissue fluid in duplicate was assayed for ALP activity by measuring the cleavage of 100 μL of p-nitrophenyl phosphate (Sigma). After 30 minutes in the dark, 50 μL of 3 mol/L sodium hydroxide were added, and the absorbance of the stopped reaction was read at 405 nm. A standard curve with calf

intestinal ALP (1 IU/μL) (Promega) was made by mixing 1 μL from the calf intestinal ALP with 5 mL of ALP buffer (1:5,000 dilution) and then making 1:5 serial dilutions.

Total protein content in the tissue fluid for each sample was determined using a bicinchoninic acid protein assay kit (Pierce).

Determination of Bone Marker Expression

Total RNA content was isolated from peri-implant bone tissue attached to the extracted implants using Trizol reagent (Invitrogen Life Technologies) according to the manufacturer's protocol. Total RNA was quantified at 260 nm using a Nanodrop spectrophotometer (NanoDrop Technologies).

From the RNA isolated from peri-implant bone tissue attached to each implant, 1 μg was reverse transcribed to cDNA at 42°C for 60 minutes using the iScript cDNA Synthesis Kit (BioRad) containing both oligo(dT) and random hexamers. Each cDNA was diluted 1:10 and aliquots were stored at −20°C until the PCR reactions were carried out. Real-time PCR was performed in the iCycler (BioRad) using SYBR green detection.

Real-time PCR was done for three housekeeping genes—18S ribosomal RNA (18S rRNA), glyceraldehyde-3-phosphate dehydrogenase (GAPDH) and β-actin—and seven target genes: col-1, runx2, OC, TRAP, IL-6, IL-10, and TNF-α. The primer sequences and reaction conditions used for PCR analysis are detailed elsewhere.[18]

The crossing point readings for each of the unknown samples were used to calculate the amount of either the target or reference genes relative to the standard curve. Relative mRNA levels were calculated as the ratio of concentration of the target genes relative to that of the mean between the three reference genes (18S rRNA, GAPDH, and β-actin). Values were expressed as a percentage of the control implants, which were assigned a value of 100%.

Micro-CT Bone Morphometric Analysis of Bone Architecture

The Ti implants were removed from the defects and the tibiae were dissected. The bone blocks were submerged in a 4% neutral buffered formalin solution, which was changed once after 24 hours, and subsequently kept in 70% ethanol. The samples were wrapped in Parafilm (Pechiney Plastic Packaging) before scanning with a SkyScan 1172 tabletop μCT scanner (SkyScan). The samples were scanned with a voltage of 100 kV, a current of 100 μA, and an aluminum filter of 0.5 mm with a voxel size of 8.033 μm. The rotational velocity for the 360-degree scan was 0.4 degrees, with three pictures averaged for each
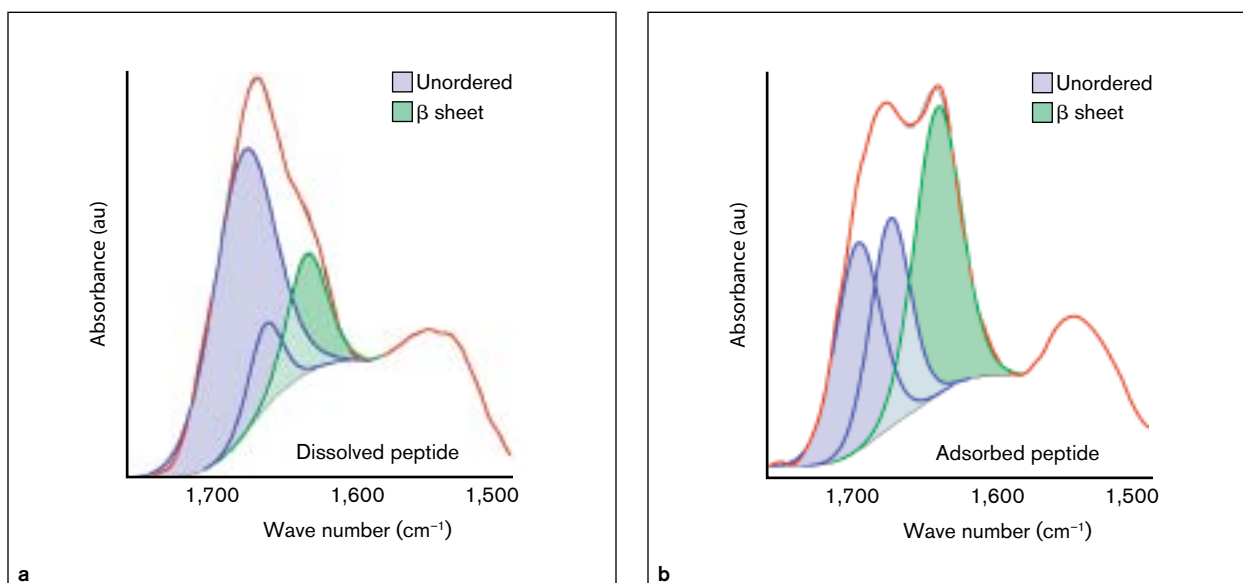
Fig 1 FTIR spectra of dissolved and adsorbed peptide with peaks fitted for unordered and β sheet secondary structures.

position. Scans were reconstructed using manufacturer-provided software (NRecon, SkyScan) with the following parameters: smoothing: 1; beam hardening correction: 40%; ring artefact reduction: 12; output: 0 to 0.05.

The same volume of interest was chosen for analysis of each sample: a cylinder with a volume of 14.04 mm³ starting from the outer cortical bone defect. According to the analogous morphologic parameters for trabecular and cortical bone proposed by Cooper et al,[19] the parameters analyzed were volumetric bone mineral density (vBMD), percentage of cortical porosity, canal surface, ratio of canal surface to tissue volume, canal diameter, and canal separation. To determine the vBMD, calibration of the standard unit of x-ray CT density (Hounsfield units) was performed by converting the density of air and two calcium hydroxyapatite phantoms (d = 8 mm, ρ = 0, 0.25, and 0.75 g/cm³, respectively) into Hounsfield units, followed by conversion into vBMD. The thresholds applied were 1 to 255 for vBMD and 86 to 255 for bone parameters. Calculation of the bone parameters was made with the program CTAn (version 1.10.0.1, SkyScan).

Histologic Preparation and Analyses

After removal, the bone samples were stored in formalin until decalcification in 7% by volume ethylenediaminetetraacetic acid at pH 7 for 40 days and embedding in paraffin. Four sections per defect for each of the six defects per group were stained with hematoxylin and eosin, coded, and subjected to semiquantitative light microscopic analysis. A set of parallel lines was projected on the images with random start (see Fig 5), and the crossing point with the bone-to-implant interface was evaluated for the presence of bone, new bone, and fibrous tissue at the interface. The ratios of bone, newly formed bone, and fibrous tissue were expressed as percentages, with 100% being the total count of all tissue types per group.

Statistical Analysis

All data are presented as means ± standard deviations (SDs). Differences between groups were assessed by paired t test or Student t test using the program SPSS for Windows, version 14.0. Results were considered statistically significant at the $P < .05$ level.

RESULTS

Secondary Structure of Dissolved and Adsorbed Peptides

Detailed FTIR analysis of the shape of the amide 1 peak (~1,740 to 1,580 cm⁻¹) of proteins and polypeptides allowed for analysis of its secondary structure.[20] The amide 1 peak obtained by FTIR spectra showed the changes that occurred in the secondary structure of the peptide upon adsorption to the Ti implant (Fig 1). The spectrum of the dissolved peptide showed a maximum at ~1,673 cm⁻¹ and a shoulder at ~1,645 cm⁻¹, whereas the spectrum of the adsorbed and dried peptide had two maxima: at ~1,683 cm⁻¹ and at ~1,630 cm⁻¹. Both the dissolved and the adsorbed peptide showed two peaks of unordered structure and one β sheet[21]:
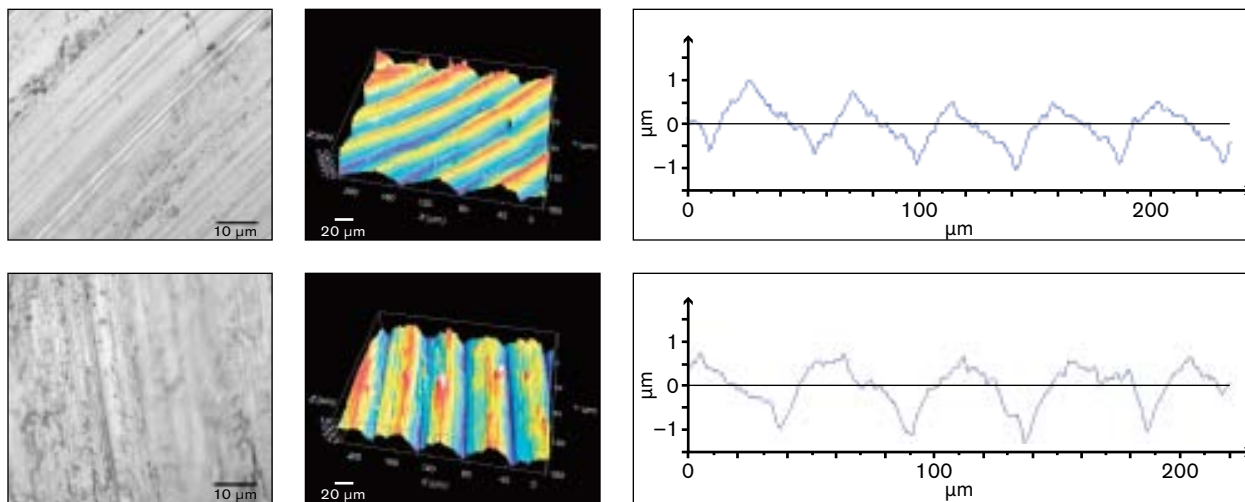
Fig 2 Profilometric analysis of machined Ti implants. *Above:* Uncoated; *below:* coated with peptides.
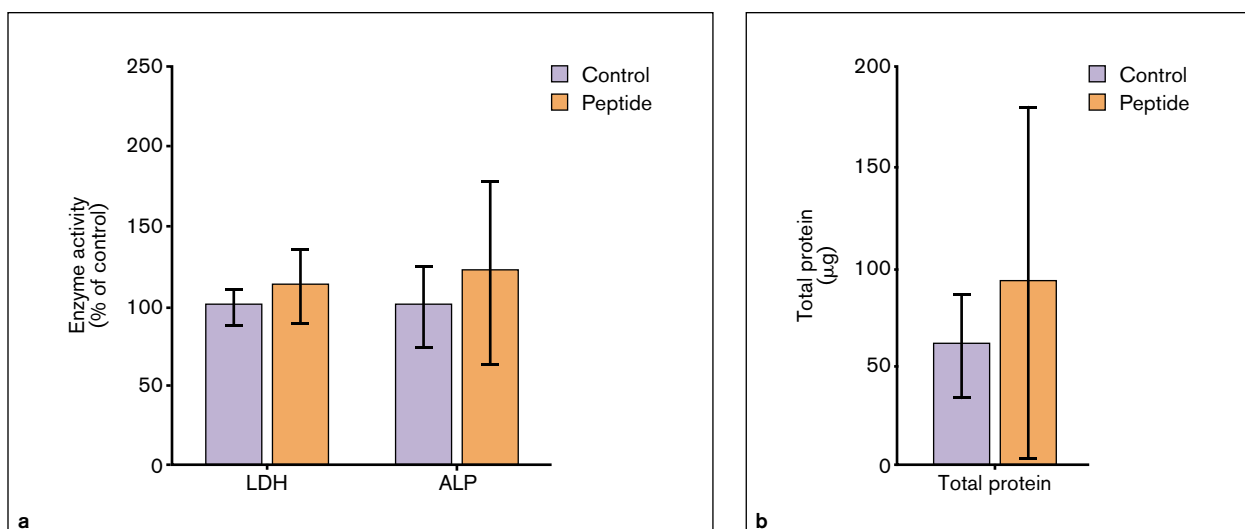

Fig 3 LDH activity, ALP activity, and total protein content measured in the tissue fluid in the bottom of the defect after implant removal (medians and quartiles shown) collected from the implant sites after 4 weeks of healing. LDH and ALP activity are expressed as a percentage of that seen on control samples at 4 weeks, and values represent means ± SDs (n = 6). *P < .05; significant differences between control versus peptide-modified Ti implants (paired *t* test).

81.2% of unordered structure and 18.8% β sheet for the dissolved peptide and 57.1% unordered structure plus 42.9% β sheet for the adsorbed peptide.

Surface Coating Observations

The mean contact angle (± SD) of polished Ti surfaces decreased significantly upon peptide coating, from 72.0 ± 1.3 degrees (n = 10 control disks) to 59.9 ± 1.5 degrees (n = 12 peptide-coated disks) (P = .0001; Student *t* test). Moreover, surface irregularities appeared, as observed with profilometry after the machined implant surfaces were coated with the peptide solution (Fig 2).

Tissue Fluid Observations

LDH and ALP activity and total protein content in the tissue fluid collected from the implant site were studied following the 4-week healing period (Fig 3). The release of LDH is a sensitive marker for tissue necrosis,[17] while ALP activity has been proposed to play an important role in the mineralization process around Ti implants.[22] No significant differences in LDH activity, ALP activity, or total protein content were observed between peptide-covered and control implants after 4 weeks of healing.
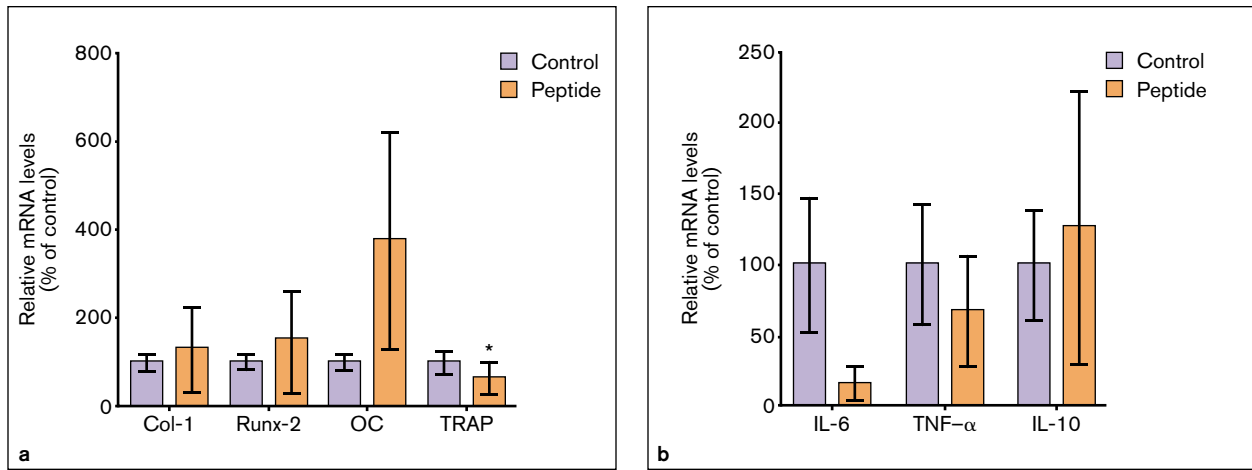
Fig 4 In vivo gene expression of bone markers in the peri-implant bone tissue attached to the modified Ti implants after 4 weeks of healing. (a) Bone formation markers col-1, runx2, and OC and the osteoclast marker TRAP; (b) inflammation markers TNF-α, IL-6, and IL-10. Data represent fold changes of target genes normalized with housekeeping genes (rRNA, GAPDH, β-actin), expressed as a percentage of control samples, which were set to 100%. Values represent means ± SDs (n = 6). *P < .05; significant differences between control and peptide-modified Ti implants (paired t test).

Table 1 Micro-CT Bone Parameters			
Parameter	Control	Peptide	P
vBMD (g/cm³)	1.04 ± 0.10	1.02 ± 0.06	NS
Ca.V/TV (%)	24.1 ± 10.6	31.2 ± 11.2	NS
Ca.S (mm²)	168 ± 56	180 ± 39	NS
Ca.S/TV (1/mm)	1.16 ± 0.47	1.38 ± 0.46	NS
Ca.Dm (mm)	0.173 ± 0.067	0.145 ± 0.031	NS
Ca.Sp (mm)	0.280 ± 0.026	0.270 ± 0.020	NS

vBMD = volumetric bone mineral density; Ca.V/TV = % cortical porosity; Ca.S = canal surface; Ca.S/TV = canal surface to tissue volume; Ca.Dm = canal diameter; Ca.Sp = canal separation. Data were analyzed by Student t test. NS = not significant.

Gene Expression at the Bone-Implant Interface

Figure 4 shows the expression levels of seven genes related to bone formation, resorption, and inflammation that were analyzed at the bone-implant interface. Relative mRNA levels for bone formation–related genes (col-1, runx2, and OC) were higher for the peptide-coated implants, although the differences did not reach statistical significance. Moreover, the mRNA levels of the marker for osteoclasts and bone resorption (TRAP) were significantly reduced for the peptide-coated implants.

Gene expression profiles of proinflammatory (TNF-α and IL-6) and anti-inflammatory (IL-10) cytokines were also investigated. Peptide-modified implants showed a trend toward reduced expression of the proinflammatory cytokines, while IL-10 mRNA levels appeared increased, but these differences were not statistically significant.

Bone Morphometric Parameters

The micro-CT parameters and values measured from the histologic specimens are shown in Table 1. No changes were observed in vBMD and the morphometric parameters analyzed for the bone adjacent to the control and peptide-modified implants (Table 1).

The histologic analysis showed similar bone thickness adjacent to the implants, with 54.9 ± 29.4 μm and 53.9 ± 11.4 μm for the control and peptide groups, respectively (Fig 5). However, with respect to the percentages of bone, new bone, and fibrous tissue (Fig 6), slightly (but not significantly) more new bone and fibrous tissue were measured around the peptide-modified implants. The majority of histologic specimens showed close bone-to-implant contact.

DISCUSSION

In this study, a polyproline synthetic peptide was used to coat the surface of Ti implants, and its effect on the bone-to-implant interface was evaluated in an animal model using standardized Ti disks, as previously described.[16,18] The modified Ti surface was characterized and the effect on implant osseointegration of the surface modification was evaluated.

Modification of Ti implant surfaces by adsorption of the proline-rich synthetic peptide resulted in the formation of peptide clusters on the surfaces, as evidenced by profilometric analysis. Such agglomeration of the polar peptides on the Ti surfaces was expected as a consequence of energy minimization. In addition, peptide-modified Ti implants showed increased wettability, as revealed by contact angle measurements.
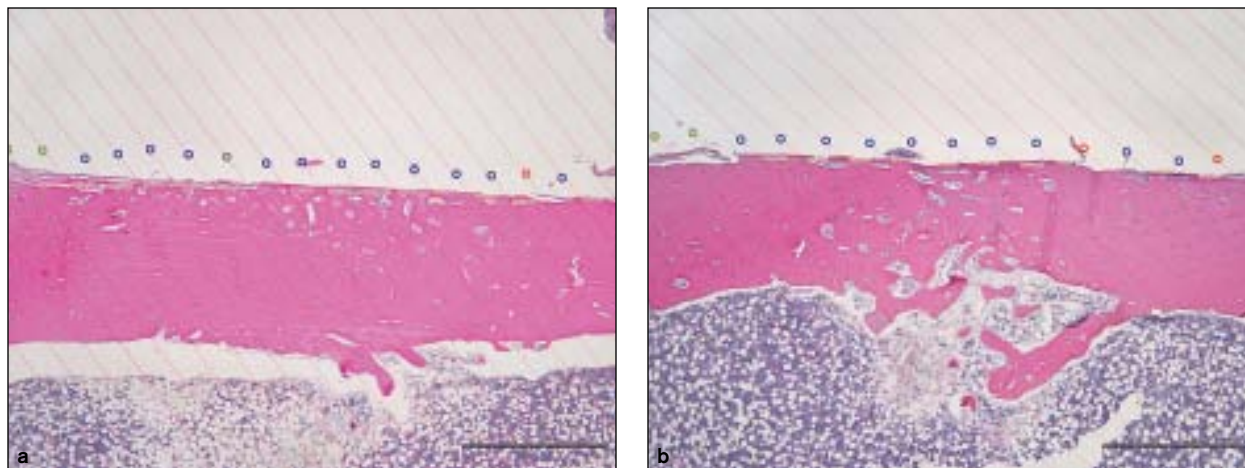
Fig 5 Micrographs of histologic sections of the decalcified bone tissue defects after 4 weeks of implantation. Parallel lines have been superimposed on the micrographs for analysis of the bone-to-implant interface. *(a)* Bone specimen in which the control implant had been in close contact with the bone tissue; *(b)* Corresponding micrograph from a bone-to-implant interface after placement of a peptide-containing implant. Green circle = fibrous tissue; blue circle = newly formed bone; red circle = original bone. Scale bars = 1 mm.

Fig 6 Percentage of bone, new bone, and fibrous tissue in the histologic sections at the bone-to-implant interface, with 100% being the total of all tissue types per group. Data were analyzed by Student *t* test.
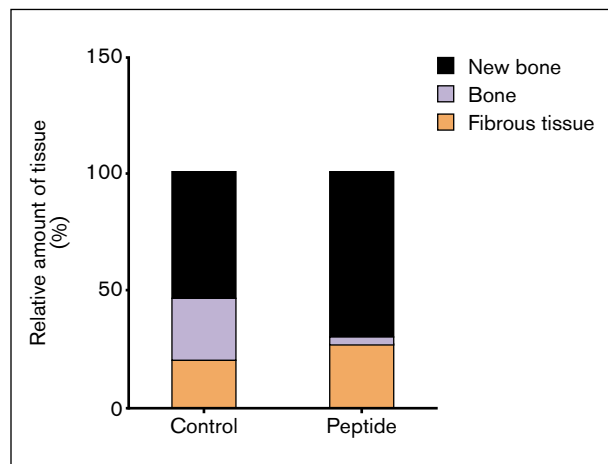
Previous in vitro studies have shown that cells preferentially adhere to surfaces with a contact angle of about 50 degrees,[23,24] which is in range with the characteristics shown by the peptide-modified Ti implants. Although cell adhesion was not evaluated in the present study, hydrophilicity of the modified Ti implants could have played a role in the initial contact after implant placement.

The structural properties of the peptides were analyzed by FTIR spectroscopy to examine conformational changes upon adsorption. The spectrum of the dissolved peptide was typical for a disordered secondary structure,[21] most likely caused by the rich content of prolines in the amino acid chain,[25] in agreement with the simulated structural model previously reported.[12] After adsorption, the peptide secondary structure mainly comprised antiparallel β sheets,[26] as has been reported also for lyophilization of proteins.[27] Those structural changes have been observed to be reversible,[28] and thus might not have changed the effect of the peptide upon rehydration of the peptide in the bone defect.

Analysis of the tissue fluid collected at the implant sites indicated that the peptide coating did not induce an adverse tissue response upon implantation, as evidenced by LDH activity. Previous in vitro studies have demonstrated the safety of this polyproline-rich peptide in concentrations up to 50 μg/mL in both mouse preosteoblastic cells and in hUCMSCs.[12]

The formation of mineralized bone near the implant surface requires colonization of the surface by cells of osteoblastic lineage, followed by the proliferation and

differentiation of these cells.[29] Here, the authors analyzed gene expression levels of three different markers of bone formation: the transcription factor runx2, which is considered the master regulator of osteoblast differentiation[30]; the early bone formation marker col-1[31]; and OC, one of the most specific markers for mature and mineralizing osteoblasts.[32] Higher levels of the three bone formation markers analyzed in the peri-implant bone attached to the extracted implants were indicated, but the differences were not statistically significant versus untreated implants. Runx2 and col-1 mRNA levels appeared slightly higher in the peptide group than in the control group, while the expression of OC was enhanced by more than threefold, indicating the presence of more mature osteoblasts adjacent to the peptide-coated implants compared to those of plain Ti. In addition to bone formation markers, mRNA levels of TRAP, a marker of osteoclasts that is commonly used as an indicator of bone resorption, were also analyzed.[33] It was found that peptide modification of Ti implants significantly decreased the expression of TRAP after 4 weeks of healing. Thus, the results indicate that the modified surface reduces bone resorption at the implant interface. These results correlate with the expression profile obtained for the cytokines analyzed, since a modification in the expression profile of proinflammatory (IL-6 and TNF-α) versus anti-inflammatory (IL-10) cytokines in the peri-implant cortical bone was noted. The proinflammatory cytokines TNF-α and IL-6 stimulate osteoclast differentiation, while IL-10 is an anti-inflammatory cytokine that plays a major role in suppressing the inflammatory response and TNF-α and IL-6 secretion by monocytes/macrophages; in addition, IL-10 may also contribute to extracellular matrix synthesis.[34–36]

Bone morphometric and histologic parameters did not show significant differences in peri-implant tissue between coated and control implants in the present study. This could be a result of the duration of the healing period or the dose of the peptide used. A longer healing period may be needed for differences in bone morphometric parameters to become apparent, as peri-implant bone is still immature, with a low degree of mineralization, after 4 weeks.[18] However, a higher rate of new bone formation was observed in the peptide group.

CONCLUSION

The present study showed that polyproline peptide adsorbs to titanium implant surfaces as agglomerates and enhances surface wettability. Further, the results suggest that proline-rich peptides have potential as a biocompatible and bioactive coating for promoting osseointegration of titanium implants in the longer term by reducing bone resorption.

ACKNOWLEDGMENTS

REFERENCES

1. Ellingsen JE, Thomsen P, Lyngstadaas SP. Advances in dental implant materials and tissue regeneration. Periodontol 2000 2006;41:136–156.
2. Liu XY, Chu PK, Ding CX. Surface modification of titanium, titanium alloys, and related materials for biomedical applications. Mater Sci Eng R Rep 2004;47:49–121.
3. Yang Y, Oh N, Liu Y, et al. Enhancing osseointegration using surface-modified titanium implants. JOM (1989) 2006;58:71–76.
4. Jin T, Ito Y, Luan X, et al. Elongated polyproline motifs facilitate enamel evolution through matrix subunit compaction. PLoS Biol 2009;7:e1000262.
5. Lyngstadaas SP, Lundberg E, Ekdahl H, Andersson C, Gestrelius S. Autocrine growth factors in human periodontal ligament cells cultured on enamel matrix derivative. J Clin Periodontol 2001;28:181–188.
6. Du C, Schneider GB, Zaharias R, et al. Apatite/amelogenin coating on titanium promotes osteogenic gene expression. J Dent Res 2005;84:1070–1074.
7. Le TQ, Gochin M, Featherstone JD, Li W, DenBesten PK. Comparative calcium binding of leucine-rich amelogenin peptide and full-length amelogenin. Eur J Oral Sci 2006;114(suppl 1):320–326.
8. Veis A, Tompkins K, Alvares K, et al. Specific amelogenin gene splice products have signaling effects on cells in culture and in implants in vivo. J Biol Chem 2000;275:41263–41272.
9. Nagano T, Oida S, Suzuki S, et al. Porcine enamel protein fractions contain transforming growth factor-beta1. J Periodontol 2006;77:1688–1694.
10. Lyngstadaas SP, Wohlfahrt JC, Brookes SJ, et al. Enamel matrix proteins: Old molecules for new applications. Orthod Craniofac Res 2009;12:243–253.
11. Rathe F, Junker R, Chesnutt BM, Jansen JA. The effect of enamel matrix derivative (Emdogain) on bone formation: A systematic review. Tissue Eng Part B Rev 2009;15:215–224.
12. Rubert M, Ramis JM, Vondrasek J, et al. Synthetic peptides analogue to enamel proteins promote osteogenic differentiation of MC3T3-E1 and mesenchymal stem cells. J Biomater Tissue Eng 2011;1:198–209.

13. Imamura K, Kawasaki Y, Nagayasu T, Sakiyama T, Nakanishi K. Adsorption characteristics of oligopeptides composed of acidic and basic amino acids on titanium surface. J Biosci Bioeng 2007;103:7–12.

14. Petzold C, Rubert M, Lyngstadaas SP, Ellingsen JE, Monjo M. In vivo performance of titanium implants functionalized with eicosapentaenoic acid and UV irradiation. J Biomed Mater Res A 2011;96:83–92.

15. Animal Welfare Act website. http://oslovet.norecopa.no/act.html. Accessed 31 January 2012.

16. Rønold HJ, Ellingsen JE. The use of a coin shaped implant for direct in situ measurement of attachment strength for osseointegrating biomaterial surfaces. Biomaterials 2002;23:2201–2209.

17. Williams DL, Marks V (eds). Biochemistry in Clinical Practice. London: William Heineman Medical Books, 1983.

18. Monjo M, Lamolle SF, Lyngstadaas SP, Ronold HJ, Ellingsen JE. In vivo expression of osteogenic markers and bone mineral density at the surface of fluoride-modified titanium implants. Biomaterials 2008;29:3771–3780.

19. Cooper DM, Turinsky AL, Sensen CW, Hallgrimsson B. Quantitative 3D analysis of the canal network in cortical bone by micro-computed tomography. Anat Rec B New Anat 2003;274:169–179.

20. Barth A. Infrared spectroscopy of proteins. Biochim Biophys Acta 2007;1767:1073–1101.

21. Fu K, Griebenow K, Hsieh L, Klibanov AM, Langer R. FTIR characterization of the secondary structure of proteins encapsulated within PLGA microspheres. J Control Release 1999;58:357–366.

22. Piattelli A, Scarano A, Piattelli M. Detection of alkaline and acid phosphatases around titanium implants: A light microscopical and histochemical study in rabbits. Biomaterials 1995;16:1333–1338.

23. Lee JH, Lee JW, Khang G, Lee HB. Interaction of cells on chargeable functional group gradient surfaces. Biomaterials 1997;18:351–358.

24. Webb K, Hlady V, Tresco PA. Relative importance of surface wettability and charged functional groups on NIH 3T3 fibroblast attachment, spreading, and cytoskeletal organization. J Biomed Mater Res 1998;41:422–430.

25. Bhattacharyya R, Chakrabarti P. Stereospecific interactions of proline residues in protein structures and complexes. J Mol Biol 2003;331:925–940.

26. Chirgadze YN, Shestopalov BV, Venyaminov SY. Intensities and other spectral parameters of infrared amide bands of polypeptides in the beta- and random forms. Biopolymers 1973;12:1337–1351.

27. Griebenow K, Klibanov AM. Lyophilization-induced reversible changes in the secondary structure of proteins. Proc Nat Acad Sci U S A 1995;92:10969–10976.

28. Souillac PO, Middaugh CR, Rytting JH. Investigation of protein/carbohydrate interactions in the dried state. 2. Diffuse reflectance FTIR studies. Int J Pharm 2002;235:207–218.

29. Albrektsson T, Johansson C. Osteoinduction, osteoconduction and osseointegration. Eur Spine J 2001;10(suppl 2):S96–101.

30. Ducy P. Cbfa1: A molecular switch in osteoblast biology. Dev Dyn 2000;219:461–471.

31. Aubin JE. Advances in the osteoblast lineage. Biochem Cell Biol 1998;76:899–910.

32. Jiang DK, Xu FH, Liu MY, et al. No evidence of association of the osteocalcin gene HindIII polymorphism with bone mineral density in Chinese women. J Musculoskelet Neuronal Interact 2007;7:149–154.

33. Minkin C. Bone acid phosphatase: Tartrate-resistant acid phosphatase as a marker of osteoclast function. Calcif Tissue Int 1982;34:285–290.

34. Tamura T, Udagawa N, Takahashi N, et al. Soluble interleukin-6 receptor triggers osteoclast formation by interleukin 6. Proc Natl Acad Sci USA 1993;90:11924–11928.

35. Tan KS, Qian L, Rosado R, Flood PM, Cooper LF. The role of titanium surface topography on J774A.1 macrophage inflammatory cytokines and nitric oxide production. Biomaterials 2006;27:5170–5177.

36. Thomsen P, Gretzer C. Macrophage interactions with modified material surfaces. Curr Opin Solid State Mater Sci 2001;5:163–176.

4. General discussion & Future perspectives

4. General discussion & Future perspectives

The research of this doctoral thesis was undertaken with the aim to find new treatments for bone regeneration. For that purpose, we first designed artificial peptides based on the common characteristics of the proline-rich region in hard tissue extracellular matrix proteins and tested their effect on both preosteoblasts and mesenchymal stem cells. Then, different biomaterials (hydrogels, scaffolds and endosseous titanium implants) were coated with the artificial peptides, and their effect was investigated both *in vitro* and *in vivo*.

Proline-rich proteins regulate the initiation, growth and deposition of mineral crystals (Weiner et al., 2005). The well defined mobile and semi-flexible structure of proline-rich proteins has led to hypothesize that such proteins may function as mineral binding domains, protein-protein interaction domains or internal molecular spacers during the formation of biological minerals and other biocomposites (Jin et al., 2009). Amelogenins and ameloblastin are two enamel proteins that contain proline-rich regions. Both amelogenin and ameloblastin are involved in tissue mineralization. In this thesis, six different variants of synthetic peptides rich in proline regions have been designed and their osteogenic effects were compared to the commercially available EMD, a purified acid extract of proteins from pig enamel matrix that are mainly composed by amelogenins. The results of this thesis show that, although treatment with both EMD or synthetic peptide 2 increased mineral depositions, only cells treated with synthetic peptides induce expression of markers related to later stages of osteoblast differentiation. It is of interest to point out that the proline-rich peptides have repetitively shown an increase in osteocalcin mRNA levels, suggesting that cells treated with synthetic peptides are at a more mature stage of the differentiation process. The relevance of this marker in bone regeneration has been demonstrated in a recent *in vivo* study (Monjo et al., 2012), where osteocalcin was the best predictive marker for osseointegration of titanium among all the markers investigated. Moreover, even though synthetic peptides did not induce cell proliferation after direct administration into the cell culture media, synthetic peptides improved alginate properties for cell attachment, suggesting that they may act as a receptor for cell interaction improving cell attachment and, in consequence, cell proliferation and differentiation.

In addition, though all synthetic peptides induced cell differentiation, some functional differences were observed among the different peptides. Although all peptides (1) are 25 aminoacids length mainly composed of hydrophobic aminoacids and with a high prevalence of prolines, (2) are characterized by compact and well-packed structures without any secondary structure, as expected due to the rich content of prolines and (3) share exposition of the C-terminal, they differ in the non-proline aminoacid composition, thus affecting to the topology of the peptide. Therefore, differences in the topology of the different peptides might be related to the accessibility of the PPLPP sequences present at the C-terminal, which might probably affect on its function.

Taking all together, the results derived from this thesis suggest a more specific mechanism of action for the synthetic proline-rich peptides than for EMD, possibly involving intracellular signalling pathways for osteogenic differentiation of pre-osteoblastic cells. In contrast, and as it has earlier been proposed (Lyngstadaas et al., 2009), EMD being a mix of mostly amelogenin derived peptides, is less specific in its actions combining the effect of several peptides, both proline-rich and not, that influences several processes including cell growth, inflammatory responses and repair mechanisms and also works as a modulator of crystal deposition and growth. Consequently, while EMD would mainly act as a nucleator agent for growth of hydroxyapatite crystal in the extracellular matrix (Figure 22A), synthetic peptides might involve interaction with a receptor capable of influencing intracellular signaling cascades at the initial states of cell differentiation to finally stimulate osteoblast differentiation. The accessibility and structural rigidity of this short consensus sequence (PPXPP) may be of importance in the signaling activity of the synthetic peptides. We hypothesize that the peptides could bind to the integrins expressed on cell surface, which first could increase the osteoblast attachment on the biomaterial surface and secondly modulate the expression of genes related with mature osteoblast phenotype (Figure 22B).
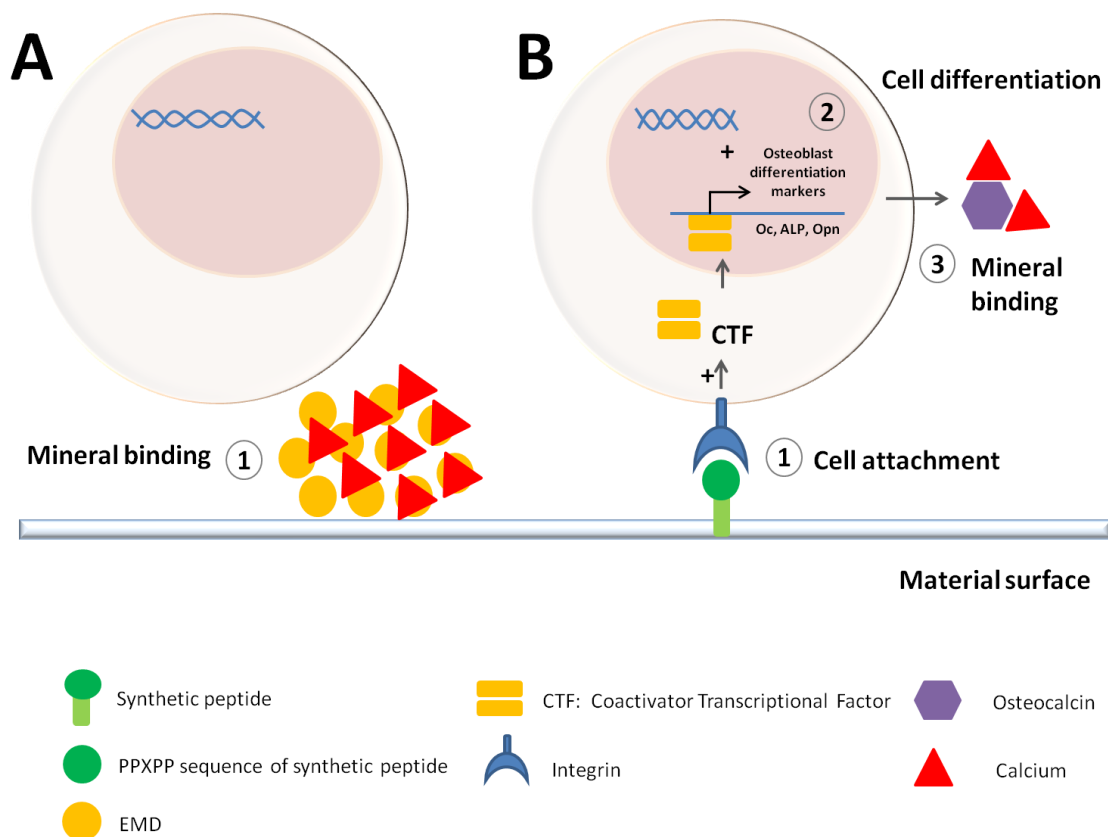

Figure 22. Schematic diagram showing the different mechanisms of action hypothesized for EMD (A) and synthetic proline-rich peptides (B).

In order to go any depth, the study of the osteocalcin gene promoter and specific transcriptional factors could constitute a new line of research that would provide a direct understanding of the effects

of synthetic peptides on tissue-specific transcriptional mechanisms in bone. Other question opened remains on peptide primary and secondary structure for effect optimization, and the isolation and characterization of possible receptors for polyproline motifs. Those studies would be useful to first confirm that the structural features are directly responsible for the effect of the peptides and second for the characterization of the possible receptors to clarify the biological importance of this intriguing molecule family in the development, growth and repair of hard tissues. Bioinformatics methods available at EBI (Proteins Functional Analysis) have been used to analyze the sequences of our synthetic peptides in order to find their cellular analogs or counterparts (Finger-PRINT), and to identify putative functional sites identified by patterns (ELM). It could be useful then to perform reporter gene assays of the protein receptors identified by bioinformatics methods to evaluate the effect of synthetic peptides on regulation of the specific genes. Localization of synthetic peptides labeled with a fluorophore (e.g FITC) could also contribute to a better understanding of their mechanism of action.

Furthermore, the use of synthetic peptides is versatile since they can be applied to modify different biomaterials, including injectable hydrogels or hydrogels for coating bone implants, scaffolds to fill bone defects or Ti implants for replacement of a dental or a bone structure, depending on the specific requirements of the site to be repaired. In fact, results derived from this thesis have demonstrated that synthetic peptides improve the osteogenic properties of those biomaterials either *in vitro* (alginate hydrogel, alginate-coated TiO_2 scaffolds) or *in vivo* (Ti implants). More specifically, synthetic peptides have shown to improve alginate properties for cell adhesion and, in consequence, cell proliferation and differentiation of cells cultured either onto an alginate hydrogel or alginate-coated TiO_2 scaffolds, showing in both cases enhanced OC mRNA levels in accordance with the previous results. However, some differences on the effect of the synthetic peptides on gene expression of the different markers were found among the different biomaterials tested, which may be due to the fact that material properties modulate the expression of certain integrins. In accordance with the proposed mechanism of action of the synthetic peptides, the expression of different integrins in cell surface might influence the interaction of the PPXPP sequence of the peptide, and, consequently cause a different signaling pathway which, in turn, will affect the progression in the sequential stages of osteoblast differentiation. In addition, cells expressed different osteoblast markers when growing on a 2D surface or on a 3D structure. While P2 could influence more on the expression of markers related to early stages of differentiation like BMP2 and Coll-I in a 3D system, the administration of P2 into the solution modulated the expression of later markers like osteocalcin. Differences between these studies could be related to the observation that temporal gene expression is retarded when cells grow in a 3D structure and is affected by the influence of the alginate properties.

In vivo, synthetic peptide 2 improved osseointegration of Ti implant as evidenced by a reduction in bone resorption; although Oc mRNA levels were not increased significantly after 4 weeks of surgery, a trend to increased osteocalcin in the peri-implant bone tissue was also observed. In addition, although no differences were observed for bone mineral density and morphometric parameters, the peptide group showed a higher percentage of new bone histologically. Thus, for further studies we could

General discussion & Future perspectives

consider longer healing periods for detecting differences in bone morphometric parameters as the peri-implant bone after 4 weeks is still immature with a low degree of mineralization (Monjo et al., 2008).

Future work could be the improvement of the functionalization of each specific biomaterial with the synthetic proline-rich peptides. Covalent binding of the peptides on Ti implants could also be performed and bioactivity compared to current results obtained with the peptide physically adsorbed on Ti implants. In the same way, osteopromotive effects of the synthetic peptides coated on TiO_2 scaffolds either physically adsorbed or covalently bound could also be studied. Further studies using modified alginate systems that incorporate a tethered ECM protein, such as RGD peptide, to the synthetic peptides could overcome the limitation of alginate as regards to its poor cell adhesion.

The work derived from this thesis has allowed the design and identification of the most promising proline-rich synthetic peptide, which may represent a new bone regeneration treatment for different applications.

4

General discussion & Future perspectives

5. Conclusions

5. Conclusions

I. Synthetic proline-rich peptides have no toxic effects and stimulate osteoblast differentiation in vitro either in MC3T3-E1 cells or in hUCMSCs. Among the different synthetic peptides tested, P2 shows the best structural and biological activity.

II. Osteocalcin, the most specific marker of fully differentiated osteoblasts, is induced in vitro in MC3T3-E1 cells and in hUCMSCs by treatment with synthetic proline-rich peptides, suggesting that these peptides enhance osteoblast differentiation. Additionally, synthetic proline-rich peptides may act as a receptor for adhesion molecules possibly involving intracellular signaling pathways for osteogenic differentiation.

III. Unmodified alginate hydrogels support osteoblast differentiation better than hyaluronic acid hydrogels, suggesting that alginates are more suitable for bone biomaterial applications. Moreover, 2% of alginate gel is a suitable formulation for the local delivery of synthetic proline-rich peptides, inducing integrin alpha8, osteopontin and osteocalcin expression in MC3T3-E1 cells. These peptide-modified alginate hydrogels may represent a new generation of injectable carriers with bioactive molecules for bone regeneration.

IV. TiO_2 scaffolds have shown to sustain MC3T3-E1 growth towards a mature and differentiated state. In addition, alginate-coated TiO_2 scaffolds can act as a matrix for delivery of synthetic proline-rich peptides inducing osteoblast cell differentiation. The combination of the physical and osteoconductive properties of TiO_2 scaffolds with the osteogenic effects of synthetic proline-rich peptides on bone formation and mineralization may represent a new strategy for bone tissue regeneration in load-bearing applications.

V. Proline-rich peptide 2 adsorbs to Ti implant surfaces as agglomerates and enhances surface wettability. In vivo results show that surface coating of Ti implants with proline-rich peptides is biocompatible and promotes osseointegration by reducing bone resorption.

VI. All in all, synthetic proline-rich peptides are osteopromotive when used in combination with alginate hydrogels, when contained into alginate-coated TiO_2 scaffolds or when coated on titanium implant surfaces.

5

Conclusions

6.References

6. References

Acero, J., Calderon, J., Salmeron, J. I., Verdaguer, J. J., Concejo, C., Somacarrera, M. L., 1999. The behaviour of titanium as a biomaterial: microscopy study of plates and surrounding tissues in facial osteosynthesis. J Craniomaxillofac Surg. 27, 117-123.

Alsberg, E., Anderson, K. W., Albeiruti, A., Franceschi, R. T., Mooney, D. J., 2001. Cell-interactive alginate hydrogels for bone tissue engineering. J Dent Res. 80, 2025-9.

Anselme, K., 2000. Osteoblast adhesion on biomaterials. Biomaterials. 21, 667-81.

Baker, J. B., Barsh, G. S., Carney, D. H., Cunningham, D. D., 1978. Dexamethasone modulates binding and action of epidermal growth factor in serum-free cell culture. Proc Natl Acad Sci U S A. 75, 1882-6.

Baksh, D., Boland, G. M., Tuan, R. S., 2007. Cross-talk between Wnt signaling pathways in human mesenchymal stem cells leads to functional antagonism during osteogenic differentiation. J.Cell Biochem. 101, 1109-1124.

Baleani, M., Viceconti, M., Toni, A., 2000. The effect of sandblasting treatment on endurance properties of titanium alloy hip prostheses. Artif Organs. 24, 296-9.

Ballini, A., Cantore, S., Capodiferro, S., Grassi, F. R., 2009. Esterified hyaluronic acid and autologous bone in the surgical correction of the infra-bone defects. Int J Med Sci. 6, 65-71.

Barbetta, A., Barigelli, E., Dentini, M., 2009. Porous alginate hydrogels: synthetic methods for tailoring the porous texture. Biomacromolecules. 10, 2328-37.

Barnes, D. M., Gillet, C. E., 1995. Determination of cell proliferation. Clin Mol Pathol. 48, M2-M5.

Baroli, B., 2009. From natural bone grafts to tissue engineering therapeutics: Brainstorming on pharmaceutical formulative requirements and challenges. J Pharm Sci. 98, 1317-75.

Baron, R., Anatomy and biology of bone matrix and cellular elements. Primer on the metabolic bone disease and disorders of mineral metabolism. The American Society for bone and mineral research, 2003.

Barth, A., 2007. Infrared spectroscopy of proteins. Biochim Biophys Acta. 1767, 1073-101.

Bartold, P. M., Xiao, Y., Lyngstaadas, S. P., Paine, M. L., Snead, M. L., 2006. Principles and applications of cell delivery systems for periodontal regeneration. Periodontol 2000. 41, 123-35.

Bashutski, J. D., Wang, H. L., 2009. Periodontal and endodontic regeneration. J Endod. 35, 321-8.

Bergman, K., Engstrand, T., Hilborn, J., Ossipov, D., Piskounova, S., Bowden, T., 2009. Injectable cell-free template for bone-tissue formation. J Biomed Mater Res A. 91A, 1111-1118.

Bernhardt, A., Despang, F., Lode, A., Demmler, A., Hanke, T., Gelinsky, M., 2009. Proliferation and osteogenic differentiation of human bone marrow stromal cells on alginate-gelatine-hydroxyapatite scaffolds with anisotropic pore structure. J Tissue Eng Regen Med. 3, 54-62.

Bhatnagar, R. S., Qian, J. J., Wedrychowska, A., Sadeghi, M., Wu, Y. M., Smith, N., 1999. Design of biomimetic habitats for tissue engineering with P-15, a synthetic peptide analogue of collagen. Tissue Eng. 5, 53-65.

Biedermannova, L., E Riley, K., Berka, K., Hobza, P., Vondrasek, J., 2008. Another role of proline: stabilization interactions in proteins and protein complexes concerning proline and tryptophane. Phys Chem Chem Phys. 10, 6350-9.

Bielby, R., Jones, E., McGonagle, D., 2007. The role of mesenchymal stem cells in maintenance and repair of bone. Injury. 38, S26-S32.

Biesalski, M. A., Knaebel, A., Tu, R., Tirrell, M., 2006. Cell adhesion on a polymerized peptide-amphiphile monolayer. Biomaterials. 27, 1259-69.

Blumer, M. J., Hausott, B., Schwarzer, C., Hayman, A. R., Stempel, J., Fritsch, H., 2012. Role of tartrate-resistant acid phosphatase (TRAP) in long bone development. Mechanisms of Development. 129, 162-76.

Bobis, S., Jarocha, D., Majka, M., 2006. Mesenchymal stem cells: characteristics and clinical applications. Folia Histochem Cytobiol. 44, 215-30.

Bochicchio, B., Tamburro, A. M., 2002. Polyproline II structure in proteins: identification by chiroptical spectroscopies, stability, and functions. Chirality. 14, 782-92.

Boeckel, D. G., Shinkai, R. S., Grossi, M. L., Teixeira, E. R., 2012. Cell Culture-Based Tissue Engineering as an Alternative to Bone Grafts in Implant Dentistry: A Literature Review. J Oral Implantol. doi:10.1563/AAID-JOI-D-11-00197.1.

Bonass, W. A., Robinson, P. A., Kirkham, J., Shore, R. C., Robinson, C., 1994. Molecular cloning and DNA sequence of rat amelogenin and a comparative analysis of mammalian amelogenin protein sequence divergence. Biochem Biophys Res Commun. 198, 755-63.

Bose, S., Roy, M., Bandyopadhyay, A., 2012. Recent advances in bone tissue engineering scaffolds. Trends Biotechnol. 30, 546-54.

Boskey, A. L., Gadaleta, S., Gundberg, C., Doty, S. B., Ducy, P., Karsenty, G., 1998. Fourier transform infrared microspectroscopic analysis of bones of osteocalcin-deficient mice provides insight into the function of osteocalcin. Bone. 23, 187-196.

Boyce, B. F., Li, P., Yao, Z., Zhang, Q., Badell, I. R., Schwarz, E. M., O'Keefe, R. J., Xing, L., 2005. TNF-alpha and pathologic bone resorption. Keio J Med. 54, 127-31.

Brama, M., Rhodes, N., 2007. Effect of titanium carbide coating on the osseointegration response in vitro and in vivo. Biomaterials. 28, 595-608.

Bronner, F., Farach-Carson, M. C., 2004. Bone formation. Springer, London.

Bueno Rde, B., Adachi, P., Castro-Raucci, L. M., Rosa, A. L., Nanci, A., Oliveira, P. T., 2011. Oxidative nanopatterning of titanium surfaces promotes production and extracellular accumulation of osteopontin. Braz Dent J. 22, 179-84.

Buser, D., Nydegger, T., Oxland, T., Cochran, D. L., Schenk, R. K., Hirt, H. P., Snetivy, D., Nolte, L. P., 1999. Interface shear strength of titanium implants with a sandblasted and acid-etched surface: a biomechanical study in the maxilla of miniature pigs. J Biomed Mater Res. 45, 75-83.

Bustin, S. A., 2000. Absolute quantification of mRNA using real-time reverse transcription polymerase chain reaction assays. J Mol Endocrinol. 25, 169-93.

Bustin, S. A., Benes, V., Garson, J. A., Hellemans, J., Huggett, J., Kubista, M., Mueller, R., Nolan, T., Pfaffl, M. W., Shipley, G. L., Vandesompele, J., Wittwer, C. T., 2009. The MIQE guidelines: minimum information for publication of quantitative real-time PCR experiments. Clin Chem. 55, 611-22.

Bustin, S. A., Benes, V., Nolan, T., Pfaffl, M. W., 2005. Quantitative real-time RT-PCR--a perspective. J Mol Endocrinol. 34, 597-601.

Clift, M. D., Gehr, P., Rothen-Rutishauser, B., 2011. Nanotoxicology: a perspective and discussion of whether or not in vitro testing is a valid alternative. Arch Toxicol. 85, 723-731.

6

References

Coelho, M. J., Cabral, A. T., Fernande, M. H., 2000. Human bone cell cultures in biocompatibility testing. Part I: osteoblastic differentiation of serially passaged human bone marrow cells cultured in alpha-MEM and in DMEM. Biomaterials. 21, 1087-94.

Corle, T. R., Kino, G. S., 1996. Confocal Scanning Optical Microscopy and Related Imaging Systems Academic Press, London.

Cornell, W. D., Cieplak, P., Bayly, C. I., Gould, I. R., Merz, K. M., Ferguson, D. M., Spellmeyer, D. C., Fox, T., Caldwell, J. W., Kollman, P. A., 1995. A Second Generation Force Field for the Simulation of Proteins, Nucleic Acids, and Organic Molecules. J Am Chem. 117, 5179-5197.

Currey, J. D., 2002. Bones. Structure and mechanics. Princeton University Press, New Jersey.

Czekanska, E. M., Stoddart, M. J., Richards, R. G., Hayes, J. S., 2012. In search of an osteoblast cell model for in vitro research. Eur Cell Mater. 24, 1-17.

Cheng, S.-L., Lai, C.-F., Blystone, S. D., Avioli, L. V., 2001. Bone Mineralization and Osteoblast Differentiation Are Negatively Modulated by Integrin $\alpha v \beta 3$. J Bone Miner Res. 16, 277-288.

Chetty, A., Steynberg, T., Moolman, S., Nilen, R., Joubert, A., Richter, W., 2008. Hydroxyapatite-coated polyurethane for auricular cartilage replacement: an in vitro study. J Biomed Mater Res A. 84, 475-82.

Chung, T. W., Yang, J., Akaike, T., Cho, K. Y., Nah, J. W., Kim, S. I., Cho, C. S., 2002. Preparation of alginate/galactosylated chitosan scaffold for hepatocyte attachment. Biomaterials. 23, 2827-2834.

Daculsi, G., Pilet, P., Cottrel, M., Guicheux, G., 1999. Role of fibronectin during biological apatite crystal nucleation: ultrastructural characterization. J Biomed Mater Res. 47, 228-33.

Davis, E. K., Zou, Y., Ghosh, A., 2008. Wnts acting through canonical and noncanonical signaling pathways exert opposite effects on hippocampal synapse formation. Neural Dev. 3, 1-17.

De Jonge, H. J., Fehrmann, R. S., de Bont, E. S., Hofstra, R. M., Gerbens, F., Kamps, W. A., de Vries, E. G., van der Zee, A. G., te Meerman, G. J., ter Elst, A., 2007. Evidence based selection of housekeeping genes. PLoS One. 2, e898.

Denda, S., Reichardt, L. F., Müller, U., 1998. Identification of Osteopontin as a Novel Ligand for the Integrin $\alpha 8 \beta 1$ and Potential Roles for This Integrin–Ligand Interaction in Kidney Morphogenesis. Mol Biol Cell 9, 1425-1435.

Deschaseaux, F., Sensebe, L., Heymann, D., 2009. Mechanisms of bone repair and regeneration. Trends Mol Med. 15, 417-29.

Deutsch, D., Haze-Filderman, A., Blumenfeld, A., Dafni, L., Leiser, Y., Shay, B., Gruenbaum-Cohen, Y., Rosenfeld, E., Fermon, E., Zimmermann, B., Haegewald, S., Bernimoulin, J. P., Taylor, A. L., 2006. Amelogenin, a major structural protein in mineralizing enamel, is also expressed in soft tissues: brain and cells of the hematopoietic system. Eur J Oral Sci. 114 Suppl 1, 183-9; discussion 201-2, 381.

Dimitriou, R., Jones, E., McGonagle, D., Giannoudis, P. V., 2011. Bone regeneration: current concepts and future directions. BMC Med. 9, 66.

Dinopoulos, H., Dimitriou, R., Giannoudis, P. V., 2012. Bone graft substitutes: What are the options? The Surgeon. 10, 230-239.

Dominici, M., Le Blanc, K., Mueller, I., Slaper-Cortenbach, I., Marini, F., Krause, D., Deans, R., Keating, A., Prockop, D., Horwitz, E., 2006. Minimal criteria for defining multipotent mesenchymal stromal cells. The International Society for Cellular Therapy position statement. Cytotherapy. 8, 315-7.

References

Donachie, M. J., 2000. Titanium: A Technical Guide. ASM International.

Drury, J. L., Mooney, D. J., 2003. Hydrogels for tissue engineering: scaffold design variables and applications. Biomaterials. 24, 4337-51.

Duranti, F., Salti, G., Bovani, B., Calandra, M., Rosati, M. L., 1998. Injectable hyaluronic acid gel for soft tissue augmentation. A clinical and histological study. Dermatol Surg. 24, 1317-25.

Eastoe, J. E., 1965. The Chemical Composition of Bone and Tooth. Advances in Fluorine Research and Dental Caries Prevention. 21, 5-17.

Einhorn, T. A., 1995. Enhancement of fracture-healing. J Bone Joint Surg Am. . 77, 940-956.

Elias, C. N., Lima, J. H. C., Valiev, R., Meyers, M. A., 2008. Biomedical applications of titanium and its alloys. JOM. 60, 46-49.

Ellingsen, J. E., Thomsen, P., Lyngstadaas, S. P., 2006. Advances in dental implant materials and tissue regeneration. Periodontol 2000. 41, 136-56.

Fincham, A. G., Moradian-Oldak, J., Simmer, J. P., Sarte, P., Lau, E. C., Diekwisch, T., Slavkin, H. C., 1994. Self-assembly of a recombinant amelogenin protein generates supramolecular structures. J Struct Biol. 112, 103-9.

Fiorito, S., Magrini, L., Goalard, C., 2003. Pro-inflammatory and anti-inflammatory circulating cytokines and periprosthetic osteolysis. J Bone Joint Surg Br. . 85, 1202-1206.

Fleisch, H., 2000. Bone and mineral metabolism. From the Laboratory to the Patient. Academic press, Switzerland.

Fong, C. D., Cerny, R., Hammarstrom, L., Slaby, I., 1998. Sequential expression of an amelin gene in mesenchymal and epithelial cells during odontogenesis in rats. Eur J Oral Sci. 106 Suppl 1, 324-30.

Fostad, G., Hafell, B., FÃ¸rde, A., Dittmann, R., Sabetrasekh, R., Will, J., Ellingsen, J. E., Lyngstadaas, S. P., Haugen, H. J., 2009a. Loadable TiO_2 scaffolds-A correlation study between processing parameters, micro CT analysis and mechanical strength. Journal of the European Ceramic Society. 29, 2773-2781.

Fostad, G., Hafell, B., Førde, A., Dittmann, R., Sabetrasekh, R., Will, J., Ellingsen, J. E., Lyngstadaas, S. P., Haugen, H. J., 2009b. Loadable TiO_2 scaffolds-A correlation study between processing parameters, micro CT analysis and mechanical strength. J Eur Ceram Soc. 29, 2773-2781.

Ganss, B., Kim, R. H., Sodek, J., 1999. Bone sialoprotein. Crit Rev Oral Biol Med. 10, 79-98.

George, M., Abraham, T. E., 2006. Polyionic hydrocolloids for the intestinal delivery of protein drugs: alginate and chitosan--a review. J Control Release. 114, 1-14.

Giancotti, F. G., Ruoslahti, E., 1999. Integrin signaling. Science. 285, 1028-32.

Giannoudis, P. V., Dinopoulos, H., Tsiridis, E., 2005. Bone substitutes: An update. Injury. 36, S20-S27.

Gibson, C. W., Golub, E. E., Abrams, W. R., Shen, G., Ding, W., Rosenbloom, J., 1992. Bovine amelogenin message heterogeneity: alternative splicing and Y-chromosomal gene transcription. Biochemistry. 31, 8384-8.

Gkioni, K., Leeuwenburgh, S. C. G., Douglas, T. E. L., Mikos, A. G., Jansen, E. J., 2010. Mineralization of hydrogels for bone regeneration. Tissue Eng Part B. 16, 577-585.

Goh, C. H., Heng, P. W. S., Chan, L. W., 2011. Alginates as a useful natural polymer for microencapsulation and therapeutic applications. Carbohydrate Polymers. 88, 1-12.

Golub, E. E., Harrison, G., Taylor, A. G., Camper, S., Shapiro, I. M., 1992. The role of alkaline phosphatase in cartilage mineralization. Bone and Mineral. 17, 273-8.

6

References

Gomes, S., Leonor, S. B., Mano, J. F., Reis, R. L., Kaplan, D. L., 2011. Spider silk-bone sialoprotein fusion proteins for bone tissue engineering. Soft Matter. 7, 4964-4973.

Gregory, C. A., Gunn, W. G., Peister, A., Prockop, D. J., 2004. An Alizarin red-based assay of mineralization by adherent cells in culture: comparison with cetylpyridinium chloride extraction. Anal Biochem. 329, 77-84.

Gronowicz, G., McCarthy, M. B., 1996. Response of human osteoblasts to implant materials: Integrin-mediated adhesion. J Orthop Res. 14, 878-887.

Guida, L., Annunziata, M., Carinci, F., Di Feo, A., Passaro, I., Oliva, A., 2007. In vitro biologic response of human bone marrow stromal cells to enamel matrix derivative. J Periodontol. 78, 2190-6.

Gutowska, A., Jeong, B., Jasionowski, M., 2001. Injectable gels for tissue engineering. Anatomical Record. 263, 342-9.

Habibovic, P., Woodfield, T., Groot de, K., Blitterswijk van, C., Predictive Value of In Vitro and In Vivo Assays in Bone and Cartilage Repair -What do They Really Tell Us about the Clinical Performance? In: J. P. Fisher, (Ed.), Tissue Engineering. Springer, New York, 2007, pp. 327-360.

Hale, L. V., Ma, Y. F., Santerre, R. F., 2000. Semi-quantitative fluorescence analysis of calcein binding as a measurement of in vitro mineralization. Calcif Tissue Int. 67, 80-84.

Hammarstrom, L., 1997. Enamel matrix, cementum development and regeneration. J Clin Periodontol. 24, 658-68.

Hanks, C. T., 1979. Insulin and hydrocortisone influences on cultured rat tongue epithelium. Arch Oral Biol. 24, 765-76.

Haugen, H. J., Monjo, M., Rubert, M., Verket, A., Lyngstadaas, S. P., Ellingsen, J. E., Ronold, H. J., Wohlfahrt, J. C., 2012. Porous Ceramic Titanium Dioxide Scaffolds Promote Bone Formation in Rabbit Peri-Implant Cortical Defect Model. Acta Biomater. doi:10.1016/j.actbio.2012.09.009.

Haugen, H. v., Will, J., Kohler, A., Hopfner, U., Aigner, J., Wintermantel, E., 2004. Ceramic TiO_2-foams: characterisation of a potential scaffold. J Eur Ceram Soc. 24, 661-668.

Haze, A., Taylor, A. L., Blumenfeld, A., Rosenfeld, E., Leiser, Y., Dafni, L., Shay, B., Gruenbaum-Cohen, Y., Fermon, E., Haegewald, S., Bernimoulin, J. P., Deutsch, D., 2007. Amelogenin expression in long bone and cartilage cells and in bone marrow progenitor cells. Anat Rec (Hoboken). 290, 455-60.

He, J., Jiang, J., Safavi, K. E., Spangberg, L. S., Zhu, Q., 2004. Emdogain promotes osteoblast proliferation and differentiation and stimulates osteoprotegerin expression. Oral Surg Oral Med Oral Pathol Oral Radiol Endod. 97, 239-45.

Heijl, L., Heden, G., Svardstrom, G., Ostgren, A., 1997. Enamel matrix derivative (EMDOGAIN) in the treatment of intrabony periodontal defects. J Clin Periodontol. 24, 705-14.

Henry, P. J., 1987. Comparative surface analysis of two osseointegrated implant systems. International Journal of Oral and Maxillofacial Implants. 2, 23-7.

Hoemann, C. D., El-Gabalawy, H., McKee, M. D., 2009. In vitro osteogenesis assays: influence of the primary cell source on alkaline phosphatase activity and mineralization. Pathol Biol (Paris). 57, 318-23.

Hornak, V., Abel, R., Okur, A., Strockbine, B., Roitberg, A., Simmerling, C., 2006. Comparison of multiple Amber force fields and development of improved protein backbone parameters. Proteins. 65, 712-25.

References

Hughes, F. J., Aubin, J. E., Culture of cells of the osteoblast lineage Methods in bone biology. Chapman & Hall, 1998.

Hutmacher, D. W., 2000. Scaffolds in tissue engineering bone and cartilage. Biomaterials. 21, 2529-43.

Hutmacher, D. W., Schantz, J. T., Lam, C. X., Tan, K. C., Lim, T. C., 2007. State of the art and future directions of scaffold-based bone engineering from a biomaterials perspective. J Tissue Eng Regen Med. 1, 245-60.

Ichikawa, F., Sato, K., Nanjo, M., Nishii, Y., Shinki, T., Takahashi, N., Suda, T., 1995. Mouse Primary Osteoblasts Express Vitamin D3 25-Hydroxylase mRNA and Convert 1alpha-Hydroxyvitamin D3 into 1alpha,25-Dihydroxyvitamin D3. Bone. 16, 129-135.

Issa, J. P. M., Tiossi, R., Pitol, D. L., Mello, A. S. d. S., 2006. TGF-beta and New Bone Formation. International Journal of Morphology. 24, 399-405.

Iwasaki, Y., Tojo, Y., Kurosaki, T., Nakabayashi, N., 2003. Reduced adhesion of blood cells to biodegradable polymers by introducing phosphorylcholine moieties. J Biomed Mater Res A. 65, 164-9.

Izumikawa, M., Hayashi, K., Polan, M. A. A., Tang, J., Saito, T., 2012. Effects of amelogenin on proliferation, differentiation, and mineralization of rat bone marrow mesenchymal stem cells in vitro. ScientificWorldJournal. 2012, 8.

Jaiswal, N., Haynesworth, S. E., Caplan, A. I., Bruder, S. P., 1997. Osteogenic differentiation of purified, culture-expanded human mesenchymal stem cells in vitro. J Cell Biochem. 64, 295-312.

Janicki, P., Schmidmaier, G., 2011. What should be the characteristics of the ideal bone graft substitute? Combining scaffolds with growth factors and/or stem cells. Injury. 42, S77-81.

Jensen, E. D., Gopalakrishnan, R., Westendorf, J. J., 2010. Regulation of Gene Expression in Osteoblasts. Biofactors. 36, 25-32.

Jiang, J., Fouad, A. F., Safavi, K. E., Spangberg, L. S., Zhu, Q., 2001. Effects of enamel matrix derivative on gene expression of primary osteoblasts. Oral Surg Oral Med Oral Pathol Oral Radiol Endod. 91, 95-100.

Jin, T., Ito, Y., Luan, X., Dangaria, S., Walker, C., Allen, M., Kulkarni, A., Gibson, C., Braatz, R., Liao, X., Diekwisch, T. G., 2009. Elongated polyproline motifs facilitate enamel evolution through matrix subunit compaction. PLoS Biol. 7, e1000262.

Jorgensen, W. L., Chandrasekhar, J., Madura, J. D., Impey, R. W., Klein, M. L., 1983. Comparison of simple potential functions for simulating liquid water. The Journal of Chemical Physics. 79, 926-935.

Kalmar, L., Homola, D., Varga, G., Tompa, P., 2012. Structural disorder in proteins brings order to crystal growth in biomineralization. Bone. 51, 528-34.

Kamegai, A., Tanabe, T.-i., Mori, M., 1994. Laminin and fibronectin in bone formation induced by bone morphogenetic protein (BMP) in mouse muscle tissue. J Bone Miner Met. 12, 31-41.

Karageorgiou, V., Kaplan, D., 2005. Porosity of 3D biomaterial scaffolds and osteogenesis. Biomaterials. 26, 5474-91.

Kasemo, B., 1983. Biocompatibility of titanium implants: surface science aspects. J Prosthet Dent. 49, 832-7.

References

Kawana, F., Sawae, Y., Sahara, T., Tanaka, S., Debari, K., Shimizu, M., Sasaki, T., 2001. Porcine enamel matrix derivative enhances trabecular bone regeneration during wound healing of injured rat femur. Anat Rec. 264, 438-46.

Kawase, T., Okuda, K., Momose, M., Kato, Y., Yoshie, H., Burns, D. M., 2001. Enamel matrix derivative (EMDOGAIN®) rapidly stimulates phosphorylation of the MAP kinase family and nuclear accumulation of smad2 in both oral epithelial and fibroblastic human cells. J Periodontal Res. 36, 367-376.

Keila, S., Nemcovsky, C. E., Moses, O., Artzi, Z., Weinreb, M., 2004. In vitro effects of enamel matrix proteins on rat bone marrow cells and gingival fibroblasts. J Dent Res. 83, 134-8.

Kempen, D. H., Creemers, L. B., Alblas, J., Lu, L., Verbout, A. J., Yaszemski, M. J., Dhert, W. J., 2010. Growth factor interactions in bone regeneration. Tissue Eng Part B Rev. 16, 551-66.

Kim, H. D., Valentini, R. F., 2002. Retention and activity of BMP-2 in hyaluronic acid-based scaffolds in vitro. J Biomed Mater Res. 59, 573-84.

Kim, H. K., Kim, K., Byun, Y., 2005. Preparation of a chemically anchored phospholipid monolayer on an acrylated polymer substrate. Biomaterials. 26, 3435-44.

Klein-Nulend, J., Bonewald, L. F., 2008. Osteocyte. Academic Press Inc., Melbourne.

Komori, T., Yagi, H., Nomura, S., Yamaguchi, A., Sasaki, K., Deguchi, K., Shuimizu, Y., Bronson, R. T., Gao, Y.-H., Inada, M., Sato, M., Okamoto, R., Kitamura, Y., Yoshiki, S., Kishimoto, T., 1997. Targeted disruption of Cbfa1 results in a complete lack of bone formation owing to maturational arrest of osteoblasts. Cell. 89, 755-764.

Krinsley, D. H., Pye, K., Boggs, S. J., Tovey, N. K., 1998. Backscattered scanning electron microscopy and image analysis of sediments. Cambridge University Press.

Lai, C.-F., Cheng, S.-L., 2005. αvβ Integrins Play an Essential Role in BMP-2 Induction of Osteoblast Differentiation. J Bone Miner Res. 20, 330-340.

Lakowicz, J. R., 2006. Principles of Fluorescence Spectroscopy. Springer.

Lamolle, S. F., Monjo, M., Lyngstadaas, S. P., Ellingsen, J. E., Haugen, H. J., 2009. Titanium implant surface modification by cathodic reduction in hydrofluoric acid: surface characterization and in vivo performance. J Biomed Mater Res A. 88, 581-8.

Lang, C., 2006. Proteinas de la matriz del esmalte (amelogeninas). Rev Cient Ondontol. 1 (1), 27-35.

Larsson, C., Thomsen, P., Aronsson, B. O., Rodahl, M., Lausmaa, J., Kasemo, B., Ericson, L. E., 1996. Bone response to surface-modified titanium implants: studies on the early tissue response to machined and electropolished implants with different oxide thicknesses. Biomaterials. 17, 605-16.

Larsson, C., Thomsen, P., Lausmaa, J., Rodahl, M., Kasemo, B., Ericson, L. E., 1994. Bone response to surface modified titanium implants: studies on electropolished implants with different oxide thicknesses and morphology. Biomaterials. 15, 1062-74.

Lau, E. C., Simmer, J. P., Bringas, P., Jr., Hsu, D. D., Hu, C. C., Zeichner-David, M., Thiemann, F., Snead, M. L., Slavkin, H. C., Fincham, A. G., 1992. Alternative splicing of the mouse amelogenin primary RNA transcript contributes to amelogenin heterogeneity. Biochem Biophys Res Commun. 188, 1253-60.

Lee, J. H., Lee, J. W., Khang, G., Lee, H. B., 1997. Interaction of cells on chargeable functional group gradient surfaces. Biomaterials. 18, 351-8.

6

References

Lee, J. Y., Choo, J. E., Park, H. J., Park, J. B., Lee, S. C., Jo, I., Lee, S. J., Chung, C. P., Park, Y. J., 2007. Injectable gel with synthetic collagen-binding peptide for enhanced osteogenesis in vitro and in vivo. Biochem Biophys Res Commun. 357, 68-74.

Lee, K. Y., Bouhadir, K. H., Mooney, D. J., 2000. Degradation behavior of covalently cross-linked poly(aldehyde guluronate) hydrogels. Macromolecules. 33, 97-101.

Lee, S. H., Shin, H., 2007. Matrices and scaffolds for delivery of bioactive molecules in bone and cartilage tissue engineering. Adv Drug Deliv Rev. 59, 339-59.

Lee, Y.-L., Chen, C.-Y., 2003. Surface wettability and platelet adhesion studies on Langmuir-Blodgett films. Applied Surface Science. 207, 51-62.

Leeuwenburgh, S. C. G., Wolke, J. G. C., Siebers, M. C., Schoonman, J., Jansen, J. A., 2006. In vitro and in vivo reactivity of porous, electrosprayed calcium phosphate coatings. Biomaterials. 27, 3368-3378.

Lekic, P., Sodek, J., McCulloch, C. A., 1996. Osteopontin and bone sialoprotein expression in regenerating rat periodontal ligament and alveolar bone. Anatomical Record. 244, 50-8.

Li, Z., Ramay, H. R., Hauch, K. D., Xiao, D., Zhang, M., 2005. Chitosan-alginate hybrid scaffolds for bone tissue engineering. Biomaterials. 26, 3919-28.

Liew, C. V., Chan, L. W., Ching, A. L., Heng, P. W. S., 2006. Evaluation of sodium alginate as drug release modifier in matrix tablets. Int J Pharm. 309, 25-37.

Lim, J. Y., Hansen, J. C., Siedlecki, C. A., Hengstebeck, R. W., Cheng, J., Winograd, N., Donahue, H. J., 2005. Osteoblast adhesion on poly(l-lactic acid)/polystyrene demixed thin film blends: effect of nanotopography, surface chemistry, and wettability. Biomacromolecules. 6, 3319-3327.

Lin, C. C., Metters, A. T., 2006. Hydrogels in controlled release formulations: network design and mathematical modeling. Adv Drug Deliv Rev. 58, 1379-408.

Ling, L., Nurcombe, V., Cool, S. M., 2009. Wnt signaling controls the fate of mesenchymal stem cells. Gene. 433, 1-7.

Lisignoli, G., Zini, N., Remiddi, G., Piacentini, A., Puggioli, A., Trimarchi, C., Fini, M., Maraldi, N. M., Facchini, A., 2001. Basic fibroblast growth factor enhances in vitro mineralization of rat bone marrow stromal cells grown on non-woven hyaluronic acid based polymer scaffold. Biomaterials. 22, 2095-2105.

Liu, X., Chu, P. K., Ding, C., 2004. Surface modifiaction of titanium, titanium alloys, and related materials for biomedical applications. Material Science and Engineering R. 47, 49-121.

Lucchini, J. P., Aurelle, J. L., Therin, M., Donath, K., Becker, W., 1996. A pilot study comparing screw-shaped implants. Surface analysis and histologic evaluation of bone healing. Clinical Oral Implants Research. 7, 397-404.

Lutolf, M. P., Weber, F. E., Schmoekel, H. G., Schense, J. C., Kohler, T., Muller, R., Hubbell, J. A., 2003. Repair of bone defects using synthetic mimetics of collagenous extracellular matrices. Nat Biotech. 21, 513-518.

Lyngstadaas, S. P., Lundberg, E., Ekdahl, H., Andersson, C., Gestrelius, S., 2001. Autocrine growth factors in human periodontal ligament cells cultured on enamel matrix derivative. J Clin Periodontol. 28, 181-8.

Lyngstadaas, S. P., Risnes, S., Nordbø, H., Flønes, A. G., 1990. Amelogenin gene similarity in vertebrates: DNA sequences encoding amelogenin seem to be conserved during evolution. J Comp Physiol B. 160, 469-472.

Lyngstadaas, S. P., Wohlfahrt, J. C., Brookes, S. J., Paine, M. L., Snead, M. L., Reseland, J. E., 2009. Enamel matrix proteins; old molecules for new applications. Orthod Craniofac Res. 12, 243-53.

Mackiewicz, Z., Niklińska, W. E., Kowalewska, J., Chyczewski, L., 2011. Bone as a source of organism vitality and regeneration. Folia Histochem Cytobiol. . 49, 558-569.

Maes, C., Coenegrachts, L., Stockmans, I., Daci, E., Luttun, A., Petryk, A., Gopalakrishnan, R., Moermans, K., Smets, N., Verfaillie, C. M., Carmeliet, P., Bouillon, R., Carmeliet, G., 2006. Placental growth factor mediates mesenchymal cell development, cartilage turnover, and bone remodeling during fracture repair. J Clin Invest. 116, 1230-42.

Maharjan, A. S., Pilling, D., Gomer, R. H., 2011. High and low molecular weight hyaluronic acid differentially regulate human fibrocyte differentiation. PLoS One. 6, e26078.

Mandalunis, P. M., 2006. Remodelación ósea. Actualizaciones en osteologia. 2, 16-18.

Mann, B. K., 2003. Biologic gels in tissue engineering. Clin Plast Surg. 30, 601-9.

Marchi, J., Ussui, V., Delfino, C. S., Bressiani, A. H., Marques, M. M., 2010. Analysis in vitro of the cytotoxicity of potential implant materials. I: Zirconia-titania sintered ceramics. J Biomed Mater Res B Appl Biomater. 94, 305-11.

Martinez-Sanz, E., Ossipov, D. A., Hilborn, J., Larsson, S., Jonsson, K. B., Varghese, O. P., 2011. Bone reservoir: Injectable hyaluronic acid hydrogel for minimal invasive bone augmentation. J Control Release. 152, 232-40.

Maupetit, J., Derreumaux, P., Tuffery, P., 2009. PEP-FOLD: an online resource for de novo peptide structure prediction. Nucleic Acids Res. 37, W498-503.

Mazzey, G., Balbontin, J., Villavicencio, J. J., 2006. Systematic review of histologic periodontal regeneration in humans when using proteins derived from the matrix of enamel (Emdogain R). Rev Chil Periodon Oseoint. 3(1), 9-18.

McKee, M. D., Nanci, A., 1995. Osteopontin and the Bone Remodeling Sequence. Ann N Y Acad Sci. 760, 177-189.

Minkin, C., 1982. Bone acid phosphatase: tartrate-resistant acid phosphatase as a marker of osteoclast function. Calcified Tissue International. 34, 285-90.

Mix, P. E., 2010. Introduction to Nondestructive Testing: A training guide. Wiley-Interscience, New Jersey.

Mizuno, M., Imai, T., Fujisawa, R., Tani, H., Kuboki, Y., 2000. Bone sialoprotein (BSP) is a crucial factor for the expression of osteoblastic phenotypes of bone marrow cells cultured on type I collagen matrix. Calcif Tissue Int. 66, 388-396.

Mohamad Yunos, D., Bretcanu, O., Boccaccini, A., 2008. Polymer-bioceramic composites for tissue engineering scaffolds. J Mater Sci. 43, 4433-4442.

Monjo, M., Lamolle, S. F., Lyngstadaas, S. P., Ronold, H. J., Ellingsen, J. E., 2008. In vivo expression of osteogenic markers and bone mineral density at the surface of fluoride-modified titanium implants. Biomaterials. 29, 3771-80.

Monjo, M., Ramis, J. M., Rønold, H. J., Taxt-Lamolle, S. F., Ellingsen, J. E., Lyngstadaas, S. P., 2012. Correlation between molecular signals and bone bonding to titanium implants. Clin Oral Implants Res. 16.

Monjo, M., Rubert, M., Ellingsen, J. E., Lyngstadaas, S. P., 2010a. Rosuvastatin promotes osteoblast differentiation and regulates SLCO1A1 transporter gene expression in MC3T3-E1 cells. Cell Physiol Biochem. 26, 647-56.

Monjo, M., Rubert, M., Wohlfahrt, J. C., Ronold, H. J., Ellingsen, J. E., Lyngstadaas, S. P., 2010b. In vivo performance of absorbable collagen sponges with rosuvastatin in critical-size cortical bone defects. Acta Biomater. 6, 1405-12.

Moradian-Oldak, J., Wen, H. B., Schneider, G. B., Stanford, C. M., 2006. Tissue engineering strategies for the future generation of dental implants. Periodontol 2000. 41, 157-76.

Moursi, A. M., Globus, R. K., Damsky, C. H., 1997. Interactions between integrin receptors and fibronectin are required for calvarial osteoblast differentiation in vitro. J Cell Sci. 110, 2187-2196.

Muller, U., Bossy, B., Venstrom, K., Reichardt, L. F., 1995. Integrin a8f31 Promotes Attachment, Cell Spreading and Neurite Outgrowth on Fibronectin. Molecular Biology of the Cell. 6, 433-448.

Murad, S., Grove, D., Lindberg, K. A., Reynolds, G., Sivarajah, A., Pinnell, S. R., 1981. Regulation of collagen synthesis by ascorbic acid. Proc Natl Acad Sci U S A. 78, 2879-82.

Murashita, T., Nakayama, Y., Hirano, T., Ohashi, S., 1996. Acceleration of granulation tissue ingrowth by hyaluronic acid in artificial skin. British Journal of Plastic Surgery. 49, 58-63.

Nagano, T., Oida, S., Suzuki, S., Iwata, T., Yamakoshi, Y., Ogata, Y., Gomi, K., Arai, T., Fukae, M., 2006. Porcine enamel protein fractions contain transforming growth factor-beta1. J Periodontol. 77, 1688-94.

Niinomi, M., 1998. Mechanical properties of biomedical titanium alloys. Materials Science and Engineering: A. 243, 231-236.

Novak, S., Druce, J., Chen, Q., Boccaccini, A. R., 2009. TiO2 foams with poly-(d,l-lactic acid) (PDLLA) and PDLLA/Bioglass® coatings for bone tissue engineering scaffolds. J Mater Sci. 44, 1442-1448.

Nygren, H., Eriksson, C., Lausmaa, J., 1997a. Adhesion and activation of platelets and polymorphonuclear granulocyte cells at TiO2 surfaces. J Lab Clin Med. 129, 35-46.

Nygren, H., Tengvall, P., Lundstrom, I., 1997b. The initial reactions of TiO2 with blood. J Biomed Mater Res. 34, 487-92.

Ono, K., Saito, Y., Yura, H., Ishikawa, K., Kurita, A., Akaike, T., Ishihara, M., 2000. Photocrosslinkable chitosan as a biological adhesive. J Biomed Mater Res. 49, 289-295.

Orsini, G., Assenza, B., Scarano, A., Piattelli, M., Piattelli, A., 2000. Surface analysis of machined versus sandblasted and acid-etched titanium implants. Int J Oral Maxillofac Implants. 15, 779-84.

Palioto, D. B., Rodrigues, T. L., Marchesan, J. T., Beloti, M. M., de Oliveira, P. T., Rosa, A. L., 2011. Effects of enamel matrix derivative and transforming growth factor-beta1 on human osteoblastic cells. Head Face Med. 7, 13.

Park, D.-J., Choi, B.-H., Zhu, S.-J., Huh, J.-Y., Kim, B.-Y., Lee, S.-H., 2005. Injectable bone using chitosan-alginate gel/mesenchymal stem cells/BMP-2 composites. J Craniomaxillofac Surg. 33, 50-54.

Park, J. B., Lakes, R. S., 1992. Biomaterials an introduction. Plenum Press.

Patterson, J., Siew, R., Herring, S. W., Lin, A. S., Guldberg, R., Stayton, P. S., 2010. Hyaluronic acid hydrogels with controlled degradation properties for oriented bone regeneration. Biomaterials. 31, 6772-81.

Pavón, J., Galvis, O., Echeverría, F., Castaño, J. G., Echeverry, M., Robledo, S., Jiménez-Piqué, E., Mestra, A., Anglada, M., 2012. Anodic oxidation of titanium for implants and prosthesis: processing, characterization and potential improvement of osteointegration.

6

References

Peterson, W. J., Tachiki, K. H., Yamaguchi, D. T., 2004. Serial passage of MC3T3-E1 cells down-regulates proliferation during osteogenesis in vitro. Cell Prolif. 37, 325-36.

Petite, H., Viateau, V., Bensaid, W., Meunier, A., de Pollak, C., Bourguignon, M., Oudina, K., Sedel, L., Guillemin, G., 2000. Tissue-engineered bone regeneration. Nat Biotechnol. 18, 959-63.

Pischon, N., Zimmermann, B., Bernimoulin, J. P., Hagewald, S., 2006. Effects of an enamel matrix derivative on human osteoblasts and PDL cells grown in organoid cultures. Oral Surg Oral Med Oral Pathol Oral Radiol Endod. 102, 551-7.

Potijanyakul, P., Sattayasansakul, W., Pongpanich, S., Leepong, N., Kintarak, S., 2010. Effects of enamel matrix derivative on bioactive glass in rat calvarium defects. J Oral Implantol. 36, 195-204.

Price, R. D., Myers, S., Leigh, I. M., Navsaria, H. A., 2005. The role of hyaluronic acid in wound healing: assessment of clinical evidence. Am J Clin Dermatol. 6, 393-402.

Rammelt, S., Illert, T., Bierbaum, S., Scharnweber, D., Zwipp, H., Schneiders, W., 2006. Coating of titanium implants with collagen, RGD peptide and chondroitin sulfate. Biomaterials. 27, 5561-71.

Rao, J., Otto, W. R., 1992. Fluorimetric DNA assay for cell growth estimation. Anal Biochem. 207, 186-92.

Rault, I., Frei, V., Herbage, D., Abdul-Malak, N., Huc, A., 1996. Evaluation of different chemical methods for cros-linking collagen gel, films and sponges. J Mater Sci Mater Med. 7, 215-221.

Reimer, L., 1998. Scanning electron microscopy: physics of image formation and microanalysis Springer, New York.

Reseland, J. E., Reppe, S., Larsen, A. M., Berner, H. S., Reinholt, F. P., Gautvik, K. M., Slaby, I., Lyngstadaas, S. P., 2006. The effect of enamel matrix derivative on gene expression in osteoblasts. Eur J Oral Sci. 114 Suppl 1, 205-11; discussion 254-6, 381-2.

Rezwan, K., Chen, Q. Z., Blaker, J. J., Boccaccini, A. R., 2006. Biodegradable and bioactive porous polymer/inorganic composite scaffolds for bone tissue engineering. Biomaterials. 27, 3413-31.

Rincon, J. C., Xiao, Y., Young, W. G., Bartold, P. M., 2005. Enhanced proliferation, attachment and osteopontin expression by porcine periodontal cells exposed to Emdogain. Arch Oral Biol. 50, 1047-54.

Ronold, H. J., Ellingsen, J. E., 2002. The use of a coin shaped implant for direct in situ measurement of attachment strength for osseointegrating biomaterial surfaces. Biomaterials. 23, 2201-9.

Rønold, H. J., Ellingsen, J. E., 2002. The use of a coin shaped implant for direct in situ measurement of attachment strength for osseointegrating biomaterial surfaces. Biomaterials. 23, 2201-2209.

Rønold, H. J., Lyngstadaas, S. P., Ellingsen, J. E., 2003. A study on the effect of dual blasting with TiO2 on titanium implant surfaces on functional attachment in bone. J Biomed Mater Res A. 67, 524-30.

Sabetrasekh, R., Tiainen, H., Lyngstadaas, S. P., Reseland, J., Haugen, H., 2011. A novel ultra-porous titanium dioxide ceramic with excellent biocompatibility. J Biomater Appl. 25, 559-80.

Sabetrasekh, R., Tiainen, H., Reseland, J. E., Will, J., Ellingsen, J. E., Lyngstadaas, S. P., Haugen, H. J., 2010. Impact of trace elements on biocompatibility of titanium scaffolds. Biomed Mater. 5, 15003.

Salgado, A. J., Coutinho, O. P., Reis, R. L., 2004. Bone tissue engineering: state of the art and future trends. Macromol Biosci. 4, 743-65.

6

References

Sambrook J, Fritsch EF, T, M., 1989. Molecular Cloning: A Laboratory Manual. New York: Cold Spring Harbor Laboratory Press.

Sauer, M., Hofkens, J., Enderlein, J., 2011. Handbook of Fluorescence Spectroscopy and Imaging: From Ensemble to Single Molecules. Wiley VCH.

Sawae, Y., Sahara, T., Kawana, F., Sasaki, T., 2002. Effects of enamel matrix derivative on mineralized tissue formation during bone wound healing in rat parietal bone defects. Journal of Electron Microscopy. 51, 413-23.

Sculean, A., Donos, N., Windisch, P., Brecx, M., Gera, I., Reich, E., Karring, T., 1999. Healing of human intrabony defects following treatment with enamel matrix proteins or guided tissue regeneration. J Periodontal Res. 34, 310-22.

Scheideler L, Rupp F, Wendel HP, Sathe S, J., G.-G., 2007. Photocoupling of fibronectin to titanium surfaces influences keratinocyte adhesion, pellicle formation and thrombogenicity. Dent. Mater. 23, 469-478.

Schindeler, A., McDonald, M. M., Bokko, P., Little, D. G., 2008. Bone remodeling during fracture repair: The cellular picture. Semin Cell Dev Biol. 19, 459-66.

Schmut, O., Hofmann, H., 1982. Preparation of gels from hyaluronate solutions. Graefes Arch Clin Exp Ophthalmol. 218, 311-4.

Schwartz, Z., Carnes, D. L., Jr., Pulliam, R., Lohmann, C. H., Sylvia, V. L., Liu, Y., Dean, D. D., Cochran, D. L., Boyan, B. D., 2000. Porcine fetal enamel matrix derivative stimulates proliferation but not differentiation of pre-osteoblastic 2T9 cells, inhibits proliferation and stimulates differentiation of osteoblast-like MG63 cells, and increases proliferation and differentiation of normal human osteoblast NHOst cells. J Periodontol. 71, 1287-96.

Schweitzer, P. A., 2007. Titanium. CRC Press, New York.

Sela, J. J., Bab, I. A., Cellular and molecular aspects of bone repair. In: S. Jona J, B. Itai A, Eds.), Principles of bone regeneration. Springer, Jerusalem, 2012.

Shah, A. K., Lazatin, J., Sinha, R. K., Lennox, T., Hickok, N. J., Tuan, R. S., 1999. Mechanism of BMP-2 stimulated adhesion of osteoblastic cells to titanium alloy. Biology of the Cell. 91, 131-142.

Shi, D., 2006. Introduction to biomaterials. World Scientific, Singapore.

Shimokawa, H., Ogata, Y., Sasaki, S., Sobel, M. E., McQuillan, C. I., Termine, J. D., Young, M. F., 1987. Molecular cloning of bovine amelogenin cDNA. Advances in Dental Research. 1, 293-7.

Sila-Asna, M., Bunyaratvej, A., Maeda, S., Kitaguchi, H., Bunyaratavej, N., 2007. Osteoblast differentiation and bone formation gene expression in strontium-inducing bone marrow mesenchymal stem cell. Kobe Journal of Medical Sciences. 53, 25-35.

Simonian, M. H., 2002. Current Protocols in Food Analytical Chemistry John Wiley & Sons, Inc.

Skoug, J. W., Mikelsons, M. V., Vigneron, C. N., Stemm, N. L., 1993. Qualitative evaluation of the mechanism of release of matrix sustained release dosage forms by measurement of polymer release. Journal of Controlled Release. 27, 227-245.

Smith, B. C., 2011. Fundamentals of Fourier Transform Infrared Spectroscopy. CRC Press, USA.

Snead, M. L., Zeichner-David, M., Chandra, T., Robson, K. J., Woo, S. L., Slavkin, H. C., 1983. Construction and identification of mouse amelogenin cDNA clones. Proc Natl Acad Sci U S A. 80, 7254-8.

Sodek, J., Chen, J., Nagata, T., Kasugai, S., Todescan, R., Jr., Li, I. W., Kim, R. H., 1995. Regulation of osteopontin expression in osteoblasts. Ann N Y Acad Sci. 760, 223-41.

Sommer, B., Bickel, M., Hofstetter, W., Wetterwald, A., 1996. Expression of matrix proteins during the development of mineralized tissues. Bone. 19, 371-80.

Spahr, A., Lyngstadaas, S. P., Slaby, I., Pezeshki, G., 2006. Ameloblastin expression during craniofacial bone formation in rats. Eur J Oral Sci. 114, 504-11.

Stapley, B. J., Creamer, T. P., 1999. A survey of left-handed polyproline II helices. Protein Sci. 8, 587-95.

Stein, G. S., Lian, J. B., Stein, J. L., Van Wijnen, A. J., Montecino, M., 1996. Transcriptional control of osteoblast growth and differentiation. Physiol Rev. 76, 593-629.

Stern, R., Asari, A. A., Sugahara, K. N., 2006. Hyaluronan fragments: an information-rich system. Eur J Cell Biol. 85, 699-715.

Sul, Y. T., 2003. The significance of the surface properties of oxidized titanium to the bone response: special emphasis on potential biochemical bonding of oxidized titanium implant. Biomaterials. 24, 3893-907.

Sul, Y. T., Johansson, C. B., Jeong, Y., Wennerberg, A., Albrektsson, T., 2002. Resonance frequency and removal torque analysis of implants with turned and anodized surface oxides. Clin Oral Implants Res. 13, 252-9.

Sutherland, D. S., Forshaw, P. D., Allen, G. C., Brown, I. T., Williams, K. R., 1993. Surface analysis of titanium implants. Biomaterials. 14, 893-9.

Svedhem, S., Dahlborg, D., Ekeroth, J., Kelly, J., Hook, F., Gold, J., 2003. In situ peptide-modified supported lipid bilayers for controlled cell attachment. Langmuir. 19, 6730-3736.

Taguchi, Y., Yamamoto, M., Yamate, T., Lin, S. C., Mocharla, H., DeTogni, P., Nakayama, N., Boyce, B. F., Abe, E., Manolagas, S. C., 1998. Interleukin-6-type cytokines stimulate mesenchymal progenitor differentiation toward the osteoblastic lineage. Proc Assoc Am Physicians. 110, 559-74.

Takagi, T., Suzuki, M., Baba, T., Minegishi, K., Sasaki, S., 1984. Complete amino acid sequence of amelogenin in developing bovine enamel. Biochem Biophys Res Commun. 121, 592-7.

Taki, K., Sakatsume, T., Takahashi, K., Shindo, T., Kenoko, M., Characteristics of high-corrosion resistant titanium alloy TICOREX and its applications. Nippon steel technical report, 2002.

Tamburstuen, M. V., Reseland, J. E., Spahr, A., Brookes, S. J., Kvalheim, G., Slaby, I., Snead, M. L., Lyngstadaas, S. P., 2010. Ameloblastin expression and putative autoregulation in mesenchymal cells suggest a role in early bone formation and repair. Bone. 48, 406-13.

Tamura, T., Udagawa, N., Takahashi, N., Miyaura, C., Tanaka, S., Yamada, Y., Koishihara, Y., Ohsugi, Y., Kumaki, K., Taga, T., et al., 1993. Soluble interleukin-6 receptor triggers osteoclast formation by interleukin 6. Proc Natl Acad Sci U S A. 90, 11924-8.

Tan, H., Chu, C. R., Payne, K. A., Marra, K. G., 2009. Injectable in situ forming biodegradable chitosan-hyaluronic acid based hydrogels for cartilage tissue engineering. Biomaterials. 30, 2499-506.

Tan, H., Li, H., Rubin, J. P., Marra, K. G., 2011. Controlled gelation and degradation rates of injectable hyaluronic acid-based hydrogels through a double crosslinking strategy. J Tissue Eng Regen Med. 5, 790-797.

Tegoulia, V. A., Rao, W., Kalambur, A. T., Rabolt, J. F., Cooper, S. L., 2001. Surface Properties, Fibrinogen Adsorption, and Cellular Interactions of a Novel Phosphorylcholine-Containing Self-Assembled Monolayer on Gold. Langmuir. 17, 4396-4404.

6

References

Thorwarth, M., Schultze-Mosgau, S., Wehrhan, F., Srour, S., Wiltfang, J., Neukam, F. W., Schlegel, K. A., 2005. Enhanced bone regeneration with a synthetic cell-binding peptide--in vivo results. Biochem Biophys Res Commun. 329, 789-95.

Thurner, P. J., Chen, C. G., Ionova-Martin, S., Sun, L., Harman, A., Porter, A., Ager, J. W., Ritchie, R. O., Alliston, T., 2010. Osteopontin Deficiency Increases Bone Fragility but Preserves Bone Mass. Bone. 46, 1564-1573.

Tiainen, H., Lyngstadaas, S. P., Ellingsen, J. E., Haugen, H. J., 2010. Ultra-porous titanium oxide scaffold with high compressive strength. J Mater Sci Mater Med. 21, 2783-92.

Tilg, H., Trehu, E., Atkins, M., Dinarello, C., Mier, J., 1994. Interleukin-6 (IL-6) as an anti-inflammatory cytokine: induction of circulating IL-1 receptor antagonist and soluble tumor necrosis factor receptor p55. Blood. 83, 113-118.

Tu, Q., Valverde, P., Chen, J., 2006. Osterix enhances proliferation and osteogenic potential of bone marrow stromal cells. Biochem Biophys Res Commun. 341, 1257-65.

Ungefroren, H., Ergun, S., Krull, N. B., Holstein, A. F., 1995. Expression of the small proteoglycans biglycan and decorin in the adult human testis. Biol Reprod. 52, 1095-105.

Urist, M. R., 1965. Bone: formation by autoinduction. Science. 150, 893-9.

van den Dolder, J., Vloon, A. P., Jansen, J. A., 2006. The effect of Emdogain on the growth and differentiation of rat bone marrow cells. J Periodontal Res. 41, 471-6.

Van Tienhoven, E. A., Korbee, D., Schipper, L., Verharen, H. W., De Jong, W. H., 2006. In vitro and in vivo (cyto)toxicity assays using PVC and LDPE as model materials. J Biomed Mater Res A. 78, 175-82.

Van Vlasselaer, P., Borremans, B., van Gorp, U., Dasch, J. R., De Waal-Malefyt, R., 1994. Interleukin 10 inhibits transforming growth factor-beta (TGF-beta) synthesis required for osteogenic commitment of mouse bone marrow cells. J Cell Biol. 124, 569-577

Vercruysse, K. P., Marecak, D. M., Marecek, J. F., Prestwich, G. D., 1997. Synthesis and in vitro degradation of new polyvalent hydrazide cross-linked hydrogels of hyaluronic acid. Bioconjug Chem. 8, 686-94.

Verrier, S., Meury, T. R., Kupcsik, L., Heini, P., Stoll, T., Alini, M., 2010. Platelet-released supernatant induces osteoblastic differentiation of human mesenchymal stem cells: potential role of BMP-2. Eur Cell Mater. 20, 403-14.

Viguet-Carrin, S., Garnero, P., Delmas, P. D., 2006. The role of collagen in bone strength. Osteoporos Int. 17, 919-336.

Vitale, R. F., Ribeiro, F. A., 2007. The role of tumor necrosis factor-alpha (TNF-alpha) in bone resorption present in middle ear cholesteatoma. Braz J Otorhinolaryngol. 73, 117-21.

Waddington, R. J., Roberts, H. C., Sugars, R. V., Schonherr, E., 2003. Differential roles for small leucine-rich proteoglycans in bone formation. Eur Cell Mater. 6, 12-21; discussion 21.

Warotayanont, R., Zhu, D., Snead, M. L., Zhou, Y., 2008. Leucine-rich amelogenin peptide induces osteogenesis in mouse embryonic stem cells. Biochem Biophys Res Commun. 367, 1-6.

Watson, R., 1985. Tissue-integrated protheses. Br. J Oral Maxillofac Surg. 23, 463-463.

Weiner, S., Sagi, I., Addadi, L., 2005. Structural biology. Choosing the crystallization path less traveled. Science. 309, 1027-8.

Weishaupt, P., Bernimoulin, J. P., Trackman, P., Hagewald, S., 2008. Stimulation of osteoblasts with Emdogain increases the expression of specific mineralization markers. Oral Surg Oral Med Oral Pathol Oral Radiol Endod. 106, 304-8.

Willems, E., Mateizel, I., Kemp, C., Cauffman, G., Sermon, K., Leyns, L., 2006. Selection of reference genes in mouse embryos and in differentiating human and mouse ES cells. Int. J. Dev. Biol. 50, 627-635.

Williamson, M. P., 1994. The structure and function of proline-rich regions in proteins. Biochem J. 297 249-60.

Willumeit, R., Feyerabend, F., Kamusewitz, H., Schossig, M., Clemens, H., 2003. Biological Multi-layer Systems as Implant Surface Modification. Mater Sci Eng Tech. 34, 1084-1093.

Wu, Q., Merchant, F., Castleman, K. R., 2008. Elsevier Inc.

Xiao, G., Gopalakrishnan, R., Jiang, D., Reith, E., Benson, M. D., Franceschi, R. T., 2002. Bone morphogenetic proteins, extracellular matrix, and mitogen-activated protein kinase signaling pathways are required for osteoblast-specific gene expression and differentiation in MC3T3-E1 cells. J Bone Miner Res. 17, 101-10.

Yamaguchi, A., Komori, T., Suda, T., 2000. Regulation of Osteoblast Differentiation Mediated by Bone Morphogenetic Proteins, Hedgehogs, and Cbfa1. Endocrine Reviews. 21, 393-411.

Yoneda, S., Itoh, D., Kuroda, S., Kondo, H., Umezawa, A., Ohya, K., Ohyama, T., Kasugai, S., 2003. The effects of enamel matrix derivative (EMD) on osteoblastic cells in culture and bone regeneration in a rat skull defect. J Periodontal Res. 38, 333-42.

Zhang, J., Tu, Q., Chen, J., 2009. Applications of transgenics in studies of bone sialoprotein. J Cell Physiol. 220, 30-4.

Zhao, J. M., Tsuru, K., Hayakawa, S., Osaka, A., 2008. Modification of Ti implant surface for cell proliferation and cell alignment. J Biomed Mater Res A. 84, 988-93.